

## INFORMATION TO USERS

This manuscript has been reproduced from the microfilm master. UMI films the text directly from the original or copy submitted. Thus, some thesis and dissertation copies are in typewriter face, while others may be from any type of computer printer.

**The quality of this reproduction is dependent upon the quality of the copy submitted.** Broken or indistinct print, colored or poor quality illustrations and photographs, print bleedthrough, substandard margins, and improper alignment can adversely affect reproduction.

In the unlikely event that the author did not send UMI a complete manuscript and there are missing pages, these will be noted. Also, if unauthorized copyright material had to be removed, a note will indicate the deletion.

Oversize materials (e.g., maps, drawings, charts) are reproduced by sectioning the original, beginning at the upper left-hand corner and continuing from left to right in equal sections with small overlaps. Each original is also photographed in one exposure and is included in reduced form at the back of the book.

Photographs included in the original manuscript have been reproduced xerographically in this copy. Higher quality 6" x 9" black and white photographic prints are available for any photographs or illustrations appearing in this copy for an additional charge. Contact UMI directly to order.

# UMI

A Bell & Howell Information Company  
300 North Zeeb Road, Ann Arbor MI 48106-1346 USA  
313/761-4700 800/521-0600



## **NOTE TO USERS**

**The original manuscript received by UMI contains pages with slanted print. Pages were microfilmed as received.**

**This reproduction is the best copy available**

**UMI**



# Dynamics of Flexible Mobile Manipulator Structures

by

UNYIME OKON AKPAN

A Thesis Submitted to the

Faculty of Engineering

in Partial Fulfillment of the Requirements

for the Degree of

DOCTOR OF PHILOSOPHY

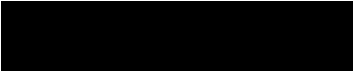
Major Subject: Mechanical Engineering

APPROVED:

  
\_\_\_\_\_  
Professor M. R. Kujath

  
\_\_\_\_\_  
Professor C. R. Hazell

  
\_\_\_\_\_  
Professor C. R. Baird

  
\_\_\_\_\_  
Dr. H. G. Davies  
University of New Brunswick  
External Examiner

TECHNICAL UNIVERSITY OF NOVA SCOTIA

Halifax, Nova Scotia

1996



National Library  
of Canada

Acquisitions and  
Bibliographic Services

395 Wellington Street  
Ottawa ON K1A 0N4  
Canada

Bibliothèque nationale  
du Canada

Acquisitions et  
services bibliographiques

395, rue Wellington  
Ottawa ON K1A 0N4  
Canada

*Your file Votre référence*

*Our file Notre référence*

The author has granted a non-exclusive licence allowing the National Library of Canada to reproduce, loan, distribute or sell copies of this thesis in microform, paper or electronic formats.

The author retains ownership of the copyright in this thesis. Neither the thesis nor substantial extracts from it may be printed or otherwise reproduced without the author's permission.

L'auteur a accordé une licence non exclusive permettant à la Bibliothèque nationale du Canada de reproduire, prêter, distribuer ou vendre des copies de cette thèse sous la forme de microfiche/film, de reproduction sur papier ou sur format électronique.

L'auteur conserve la propriété du droit d'auteur qui protège cette thèse. Ni la thèse ni des extraits substantiels de celle-ci ne doivent être imprimés ou autrement reproduits sans son autorisation.

0-612-31515-0

**Canada**

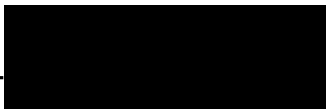
TECHNICAL UNIVERSITY OF NOVA SCOTIA

"AUTHORITY TO DISTRIBUTE MANUSCRIPT THESIS"

TITLE: DYNAMICS OF FLEXIBLE MOBILE MANIPULATOR STRUCTURES

The above library may make available or authorize another library to make available individual photo/microfilm copies of this thesis without restriction

Full name of Author UNYIME OKON AKPAN

Signature of Author \_\_\_\_\_  


Date: 26th, August, 1996

# TABLE OF CONTENTS

TABLE OF CONTENTS .....	iii
LIST OF TABLES.....	x
LIST OF FIGURES.....	xii
NOMENCLATURE .....	xxi
ACKNOWLEDGMENTS.....	xxv
ABSTRACT.....	xxvi
1. INTRODUCTION .....	1
1.1. BACKGROUND AND MOTIVATION .....	1
1.2. SCOPE OF THE THESIS .....	2
1.3. OBJECTIVES OF THE THESIS.....	4
1.4. LAYOUT OF THE THESIS.....	4
1.5. SUMMARY AND CONCLUDING REMARKS.....	6
2. LITERATURE REVIEW.....	13
2.1. DYNAMICS OF MANIPULATORS AND VEHICLES.....	13
2.1.1. BASIC DEFINITIONS.....	13
2.1.2. NON-MOBILE FLEXIBLE MANIPULATOR.....	14
2.1.3. WHEELED MOBILE RIGID MANIPULATORS.....	16
2.1.4. NON-WHEELED MOBILE RIGID MANIPULATORS.....	17
2.1.5. DYNAMICS OF WHEELED VEHICLES .....	17
2.1.6. RANDOM DYNAMICS OF SIMPLE SYSTEMS .....	18



<b>2.2. IDENTIFICATION OF MANIPULATOR PARAMETERS.....</b>	<b>19</b>
2.2.1. IDENTIFICATION OF KINEMATIC PARAMETERS.....	19
2.2.2. IDENTIFICATION OF DYNAMIC PARAMETERS.....	20
<b>2.3. LAGRANGE PRINCIPLE OF DYNAMICS.....</b>	<b>21</b>
<b>2.4. SINGULAR VALUE DECOMPOSITION OF A MATRIX.....</b>	<b>23</b>
<b>2.5. THE CONCEPT OF MANIPULATOR JACOBIAN.....</b>	<b>24</b>
<b>2.6. SUMMARY AND CONCLUDING REMARKS.....</b>	<b>25</b>
<b>3. NON-WHEELED MOBILE MANIPULATOR, ANALYSIS.....</b>	<b>26</b>
3.1. INTRODUCTION.....	26
3.2. BASE EXCITATION MODELS.....	27
3.3. EQUATION OF MOTION.....	28
3.4. COVARIANCE TENSOR OF THE JOINT RESPONSES.....	30
3.4.1. STATIONARY RESPONSES.....	30
3.4.2. NONSTATIONARY RESPONSE.....	36
3.5. COVARIANCE TENSORS OF THE TIP RESPONSES.....	40
3.6. SUMMARY AND CONCLUDING REMARKS.....	43
<b>4. NON-WHEELED MOBILE MANIPULATOR, EXAMPLES.....</b>	<b>46</b>
4.1. INTRODUCTION.....	46
4.2. EXAMPLES OF EXCITATION MODELS.....	47
4.3. EXAMPLE 1: SINGLE LINK FLEXIBLE MANIPULATOR.....	47
4.4. EXAMPLE 2: TWO LINK FLEXIBLE MANIPULATOR.....	51
4.5. NUMERICAL SIMULATION.....	55

4.5.1. JOINT RESPONSE .....	55
4.5.2. TIP RESPONSE .....	58
4.6. SUMMARY AND CONCLUDING REMARKS.....	59
<b>5. WHEELED MOBILE MANIPULATOR, ANALYSIS .....</b>	<b>77</b>
5.1. INTRODUCTION.....	77
5.2. MODEL ASSUMPTIONS .....	77
5.3. EQUATION OF MOTION.....	78
5.4. DETERMINISTIC RESPONSE.....	79
5.5. STOCHASTIC RESPONSE .....	80
5.5.1. JOINT RESPONSE .....	80
5.5.2. CONSTANT VELOCITY OF THE MOBILE BASE .....	84
5.5.2.1. State Space Approach .....	85
5.5.2.2. Power Spectral Density Approach .....	85
5.5.3. TIP RESPONSE.....	87
5.6. SUMMARY AND CONCLUDING REMARKS.....	88
<b>6. WHEELED MOBILE MANIPULATOR, EXAMPLE.....</b>	<b>90</b>
6.1. EXAMPLE: TWO LINK MANIPULATOR.....	90
6.2. SURFACE PROFILE REPRESENTATION .....	96
6.2.1. RELATION BETWEEN CORRELATION AND SPECTRAL REPRESENTATION.....	96
6.2.2. POWER SPECTRUM REPRESENTATION AND AUTOREGRESSIVE EQUATION .....	101
6.3. NUMERICAL SIMULATION .....	103
6.3.1. CASE 1. MANIPULATOR ON AN ACCELERATING MOBILE BASE.....	103
6.3.2. CASE 2. MANIPULATOR ON A CONSTANT VELOCITY MOBILE BASE .....	104
6.4. RESULTS AND DISCUSSIONS .....	104

6.4.1. CASE 1. MANIPULATOR ON AN ACCELERATING MOBILE BASE.....	104
6.4.2. CASE 2. MANIPULATOR ON A CONSTANT VELOCITY MOBILE BASE.....	107
6.5. SUMMARY AND CONCLUDING REMARKS.....	108
<b>7. MULTIPLE-WHEELED MOBILE MANIPULATOR, ANALYSIS.....</b>	<b>128</b>
7.1. INTRODUCTION.....	128
7.2. MODEL ASSUMPTIONS.....	128
7.3. EQUATION OF MOTION.....	129
7.4. STOCHASTIC RESPONSE.....	130
7.4.1. JOINT RESPONSE.....	130
7.4.2. CONSTANT VELOCITY OF THE MOBILE BASE.....	137
7.4.3. TIP RESPONSE.....	137
7.5. SUMMARY AND CONCLUDING REMARKS.....	138
<b>8. MULTIPLE-WHEELED MOBILE MANIPULATOR, EXAMPLE.....</b>	<b>140</b>
8.1. EXAMPLE: TWO LINK MANIPULATOR.....	140
8.2. SURFACE PROFILE REPRESENTATION.....	150
8.3. NUMERICAL SIMULATION.....	151
8.3.1. CASE 1. MANIPULATOR ON AN ACCELERATING MOBILE BASE.....	151
8.4. RESULTS AND DISCUSSION.....	152
8.4.1. CASE 1. MANIPULATOR ON AN ACCELERATING MOBILE BASE.....	152
8.4.2. CASE 2. MANIPULATOR ON A CONSTANT VELOCITY MOBILE BASE.....	154
8.5. SUMMARY AND CONCLUDING REMARKS.....	155
<b>9. IDENTIFICATION OF MOBILE MANIPULATORS, ANALYSIS.....</b>	<b>170</b>
9.1. INTRODUCTION.....	170

9.2. MODEL ASSUMPTIONS .....	170
9.3. EQUATION OF MOTION.....	171
9.4. IDENTIFICATION MODEL .....	173
9.5. ESTIMATION OF THE DYNAMIC PARAMETER DEVIATION.....	176
9.6. IDENTIFIABILITY AND EXCITABILITY OF THE PARAMETER VECTOR.....	179
9.7. ESTIMATE ERROR AND IMPROVEMENT OF ESTIMATED PARAMETER.....	183
9.9. PRACTICAL APPLICATION OF THE PROPOSED MODEL.....	184
9.10. SUMMARY AND CONCLUDING REMARKS.....	185
<b>10. IDENTIFICATION OF MOBILE MANIPULATORS, EXAMPLE .....</b>	<b>187</b>
10.1. EXAMPLE: TWO LINK MANIPULATOR.....	187
10.2. NUMERICAL SIMULATION .....	191
10.3. SUMMARY AND CONCLUDING REMARKS.....	192
<b>11. CONCLUSIONS.....</b>	<b>202</b>
11.1. FINAL REMARKS.....	202
11.2. MAJOR CONTRIBUTION AND CONCLUSIONS.....	204
11.3. RECOMMENDATIONS FOR FUTURE WORK .....	206
<b>REFERENCES .....</b>	<b>208</b>
<b>APPENDIX A: FUNDAMENTALS OF RANDOM PROCESS.....</b>	<b>226</b>
A1. TERMINOLOGY OF STOCHASTIC PROCESS.....	226
A1.1. PROBABILITY STRUCTURE OF RANDOM PROCESSES.....	227

A1.2. STATISTICAL PROPERTIES OF A RANDOM PROCESS.....	228
A1.3. STATISTICAL PROPERTIES OF TWO RANDOM PROCESSES .....	229
<b>A2. DEFINITIONS OF NONSTATIONARY AND STATIONARY RANDOM PROCESSES...</b>	<b>230</b>
<b>APPENDIX B: LONG DERIVATIONS OF EQUATIONS OF MOTION.....</b>	<b>235</b>
<b>B1. INTRODUCTION.....</b>	<b>235</b>
<b>B2. TWO-LINK NON-WHEELED MOBILE MANIPULATOR.....</b>	<b>235</b>
<b>B3.. TWO-LINK WHEELED MOBILE MANIPULATOR .....</b>	<b>237</b>
<b>B4. TWO-LINK TWO-WHEELED MOBILE MANIPULATOR.....</b>	<b>239</b>
<b>APPENDIX C: DERIVATION OF ROTATION AND JACOBIAN MATRICES. 242</b>	
<b>C1. INTRODUCTION.....</b>	<b>242</b>
<b>C2. NON-WHEELED MOBILE MANIPULATOR.....</b>	<b>242</b>
C2.1 SINGLE-LINK MANIPULATOR.....	242
C2.1.1. Jacobian Matrix in the Base Frame.....	243
C2.1.2. Transformation of Jacobian Matrix Between Cartesian Frames.....	244
C2.2. TWO-LINK MANIPULATOR.....	245
C2.2.1. Jacobian Matrix in the Base Frame.....	246
<b>C3. WHEELED MOBILE MANIPULATOR.....</b>	<b>248</b>
C3.1. TWO-LINK MANIPULATOR.....	248
C3.1.1. Jacobian Matrix in the Vehicle Frame .....	249
<b>C4. TWO- WHEELED MOBILE MANIPULATOR.....</b>	<b>250</b>
C4.1. TWO-LINK MANIPULATOR.....	250
C4.1.1. Jacobian Matrix in the Vehicle Frame .....	251
<b>APPENDIX D: CONTOUR INTEGRALS USED FOR THE STATIONARY</b>	
<b>RESPONSES .....</b>	<b>254</b>

<b>D1. INTRODUCTION</b> .....	<b>254</b>
D1.1. COMMON NOTATIONS .....	254
<b>D2. NON-WHEELED MOBILE MANIPULATOR</b> .....	<b>255</b>
D2.1. COVARIANCE OF MODAL RESPONSES .....	255
<b>D3. WHEELED MOBILE MANIPULATOR</b> .....	<b>260</b>
D3.1 COVARIANCE OF MODAL RESPONSES).....	260
<b>D4. DEFINITION OF SYMBOLS USED IN APPENDIX D</b> .....	<b>270</b>
<b>APPENDIX E: SPECIAL INTEGRALS USED FOR THE NONSTATIONARY RESPONSE</b> .....	<b>274</b>
<b>APPENDIX F: SOME PROPERTIES OF THE DIRAC DELTA FUNCTION</b> .....	<b>275</b>
<b>F.1. THE DELTA FUNCTION UNDER A CHANGE OF VARIABLE</b> .....	<b>275</b>
<b>F.2. THE DELTA FUNCTION OCCURRING AT THE LIMIT OF INTEGRATION</b> .....	<b>277</b>

## LIST OF TABLES

Table 10.1. Nominal and actual values of Parameters Used for Simulation	194
Table10.2. Configuration Used for Simulation	195
Table 10.3. Identifiability Index, Number of Measurements and Estimation Error for Case 1 to Case 5.	197
Table10.4a. Actual and Estimated Parameters for Case 1	197
Table10.4b. Actual and Estimated Parameters for Case 2	198
Table10.4c. Actual and Estimated Parameters for Case 3	198
Table10.4d. Actual and Estimated Parameters for Case 4	199
Table10.4e. Actual and Estimated Parameters for Case 5	199
Table 10.5. Values of individual identifiability indices for Case 1 to Case 5	200
Table10.6a. Actual and Estimated Parameters for Case 6	200
Table10.6b. Actual and Estimated Parameters for Case 7	201

**Table 10.7. Identifiability Index, Number of Measurements and Estimation  
Error for Case 6 and Case 7.**

201



## LIST OF FIGURES

Figure 1.1. Model of a Non-wheeled Mobile Manipulator	7
Figure 1.2. Model of a Single-wheeled Mobile Manipulator	8
Figure 1.3. Model of a Multiple-wheeled Mobile Manipulator	9
Figure 1.4. The Reference Zero- Configuration of the Mobile Manipulator	10
Figure 1.5. Single Link Non-wheeled Mobile Manipulator	11
Figure 1.6. Two-Link Non-wheeled Mobile Manipulator	11
Figure 1.7. Two-Link Wheeled Mobile Manipulator	12
Figure 1.8. Two-Link Multiple-wheeled Mobile Manipulator	12
Figure 3.1. Model of a Non-wheeled Mobile Manipulator	45
Figure 4.1. Model of a Single Link Non-wheeled Mobile Manipulator	62
Figure 4.2. Model of a Two Link Non-wheeled Mobile Manipulator	63

Figure 4.3. Plot of the Deterministic Modulating Function Used for Simulating the Nonstationary Stochastic Dynamics of a Non-wheeled Mobile Manipulator.

64

Figure 4.4. Variance of Joint-1  $R_{q_1q_1}$  for specified values of  $\Theta_2$  and  $\pm 180^\circ$  range of  $\Theta_1$  of Non-wheeled Mobile Manipulator. The damping factor  $\xi = 0.001$ . (a) Stationary Response (b) Nonstationary Response at  $t = 20$ .

65

Figure 4.5. Variance of the Joint-2  $R_{q_2q_2}$  for specified values of  $\Theta_2$  and  $\pm 180^\circ$  range of  $\Theta_1$  of Non-wheeled Mobile Manipulator. The damping factor  $\xi = 0.001$ . (a) Stationary Response (b) Nonstationary Response at  $t = 20$

66

Figure 4.6. Covariance of Joint-1 and Joint-2  $R_{q_1q_2}$  for specified values of  $\Theta_2$  and  $\pm 180^\circ$  range of  $\Theta_1$  of Non-wheeled Mobile Manipulator. The damping factor  $\xi = 0.001$  (a) Stationary Response (b) Nonstationary Response at  $t = 20$

67

Figure 4.7. Motion of the Manipulator Joints at  $\Theta_2 = 131.81^\circ$  (a) First Mode (b) Second Mode

68

Figure 4.8. Sensitivity of the Major Principal Variance of the Tip Response to Changes in  $\Theta_1$  of Non-wheeled Mobile manipulator. The damping

factor  $\xi = 0.001$ . (a) Stationary Response (b) Nonstationary Response at  $t = 20$ .

69

Figure 4.9. Influence of the Relative Length of the Links on the Major Principal Variance of the Tip Response of Non-Wheeled Mobile Manipulator. The damping factor  $\xi = 0.001$  (a) Stationary Response (b) Nonstationary Response

70

Figure 4.10. Effect of Damping on the Major Principal Variance of the Tip Response of Non-wheeled Mobile Manipulator

71

Figure 4.11. Magnitude and Orientation of the normalized principal tip displacement variance of a Non-wheeled mobile Manipulator for five configurations. (a) Stationary Response (b) Nonstationary Response

72

Figure 4.12. Effect of Cross Coupling of Modal Covariance on Major Principal Variance of the Tip Response of Non-wheeled Mobile Manipulator. (a) Stationary Response (b) Nonstationary Response

73

Figure 4.13. Comparison of the Nonstationary Tip Response of Non wheeled Mobile Manipulator Obtained Using the Presented Method and that Obtained Using The Evolutionary Spectrum Method (To, 1984)

74

Figure 4.14. Flow Chart of the Program Used for Simulating the Stationary Stochastic Dynamics of a Non-wheeled Mobile Manipulator.	75
Figure 4.15. Flow Chart of the Program Used for Simulating the Nonstationary Stochastic Dynamics of a Non-wheeled Mobile Manipulator	76
Figure 5.1. Model of a Wheeled Mobile Manipulator .	89
Figure 6.1. Model of a Two Link Wheeled Mobile Manipulator	111
Figure 6.2. Sample of a Surface Profile	112
Figure 6.3. Flow Chart of the Program Used for Simulating the Deterministic Dynamics of a Wheeled Mobile Manipulator.	113
Figure 6.4. Flow Chart of the Program Used for Simulating the Nonstationary Stochastic Dynamics of a Wheeled Mobile Manipulator.	114
Figure 6.5. Sensitivity of the Principal Variance and the Square of the Deterministic Tip Response of Accelerating Wheeled Mobile Manipulator to Configuration Changes (a) Nonstationary Stochastic (b) Deterministic	115

Figure 6.6. Influence of Damping on the Principal Tip Displacement Variance and Square of the Deterministic Tip Response of a Wheeled Mobile Manipulator	(a) Nonstationary Stochastic (b) Deterministic.	116
Figure 6.7. Effect of the Base Horizontal acceleration on the Square of the Deterministic Tip Response of a Wheeled Mobile Manipulator.		117
Figure 6.8. Effect of the Base Horizontal Acceleration and Surface Roughness Coefficient on the Normalized Principal Tip Displacement Variance of a Wheeled Mobile Manipulator.		118
Figure 6.9. Magnitude and Orientation of the Normalized Principal Tip Displacement Variance of a Wheeled Mobile Manipulator for Six Configurations.		119
Figure 6.10. Flow Chart of the Program Used for Simulating the Stationary Stochastic Dynamics of a Wheeled Mobile Manipulator Using the Power Spectral Density approach.		120
Figure 6.11. Flow Chart of the Program Used for Simulating the Stationary Stochastic Dynamics of a Wheeled Mobile Manipulator Using the State Space approach.		121

Figure 6.12. Comparison of the Stationary Principal Variance of Tip Response Obtained Using the State Space Representation and the Power Spectral Density Representation for a Wheeled Mobile Manipulator on a Constant Horizontal Velocity base	122
Figure 6.13. Sensitivity of the Stationary Principal Tip Displacement Variance of a Wheeled Mobile Manipulator to Configuration Changes.	123
Figure 6.14. Effect of Damping on the Normalized Stationary Principal Tip Displacement Variance of a Wheeled Mobile Manipulator Moving with a Constant Base Velocity	124
Figure 6.15. Effect of Surface Roughness Coefficient on the Normalized Principal Tip Displacement Variance of a Wheeled Mobile Manipulator Moving with a Constant Base Velocity	125
Figure 6.16. Effect of Links Length on the Normalized Principal Tip Displacement Variance of a Wheeled Mobile Manipulator Moving with a Constant Base Velocity	126
Figure 6.17. Magnitude and Orientation of the Normalized Principal Tip Displacement Variance of a Wheeled Mobile Manipulator on a Base Moving with Constant Velocity for six configurations.	127

Figure 7.1. Model of a Multiple-Wheeled Mobile Manipulator	139
Figure 8.1. Model of a Two Link Two-wheeled Mobile Manipulator	157
Figure 8.2. Flow Chart of the Program Used for Simulating the Deterministic Dynamics of a Manipulator on a Two-wheeled Mobile Base	158
Figure 8.3. Flow Chart of the Program Used for Simulating the Nonstationary Stochastic Dynamics of a Two-wheeled Mobile Manipulator	159
Figure 8.4. Sensitivity of the principal variance and the square of the deterministic tip response of a two-wheeled mobile manipulator on an accelerating base to configuration (a) Nonstationary Stochastic (b) Deterministic	160
Figure 8.5. Influence of joint stiffness on the principal tip displacement variance and square of the deterministic tip response of a two-wheeled mobile manipulator (a) Nonstationary Stochastic (b) Deterministic	161
Figure 8.6. Influence of damping on the principal tip displacement variance and square of the deterministic tip response of a two-wheeled mobile manipulator (a) Nonstationary Stochastic (b) Deterministic	162

Figure 8.7. Influence of links length on the principal tip displacement variance and square of the deterministic tip response of a two-wheeled mobile manipulator (a) Nonstationary Stochastic (b) Deterministic	163
Figure 8.8. Effect of the base horizontal acceleration on the square of the deterministic tip response of a two-wheeled mobile manipulator.	164
Figure 8.9. Effect of the base horizontal acceleration and surface roughness coefficient on the normalized principal tip displacement variance of a two-wheeled mobile manipulator.	165
Figure 8.10. Flow Chart of the Program Used for Simulating the Stationary Stochastic Dynamics of a Two-wheeled Mobile Manipulator Using the State Space approach.	166
Figure 8.11. Sensitivity of the Stationary Principal Variance of a Constant Velocity Two-Wheeled Mobile Manipulator to Configuration Changes.	167
Figure 8.12. Effect of Damping on the Principal Tip Displacement Variance of a Two-wheeled Mobile Manipulator Moving with a Constant Base Velocity.	168



Figure 8.13. Sensitivity of the Principal Tip Displacement Variance of a Two-wheeled Mobile Manipulator Moving with a Constant Velocity to the Length of Links.	169
Figure A.1. Sample of a Deterministic Process	22
Figure A.2. Realization of a random Process	232
Figure A.3. Records of Realizations of a random Process	233
Figure A.4. Classifications of Processes	234

# NOMENCLATURE

The aim here is to present nomenclature which have recurrent meaning throughout the report. Every use of a particular symbol is not listed here but no ambiguity should occur since each re-definition of a symbol is explained in the text. In general upper case bold face letters denote matrices and lower case bold face letters denote vectors.

$a_i$	ith inertia term
$\bar{C}$	dimensionless damping matrix
$C$	damping matrix
$\cos(\cdot)$	cosine of .
$D$	inertia matrix
$\bar{D}$	dimensionless inertia matrix
$c_n$	combined damping of link-n and joint-n
$\det(\cdot)$	determinant of .
$\text{diag}(\cdot)$	diagonal matrix
$dx$	perturbation of the tip motion vector
$E\{\cdot\}$	expectation operator
$\bar{f}$	dimensionless excitation vector
$H_i$	frequency response function of mode-i
$i$	$\sqrt{-1}$
$I$	identity matrix
$I_i$	centroidal moment of inertia of link-i
$J$	Jacobian matrix

<b>K</b>	stiffness matrix
$\bar{\mathbf{K}}$	dimensionless stiffness matrix
$k_i$	combined stiffness of link-i and joint-i
$L$	lagrangian of system
$l_{ci}$	axial coordinate of the centroid of link-i
$l_i$	length of link-i
$m_i$	mass of link-i
<b>P</b>	parameter deviations propagation matrix
PSD	power spectral density
<b>q</b>	elastic joint coordinate
$\ddot{\mathbf{q}}_0$	random base excitation input vector
<b>R</b>	Rayleigh dissipation function
$\mathbf{R}_{\dot{\mathbf{x}}\dot{\mathbf{x}}}(t)$	nonstationary covariance tensor of tip velocities
$\mathbf{R}_{\dot{\mathbf{x}}\dot{\mathbf{x}}}(0)$	stationary covariance tensor of tip velocities
$\mathbf{R}_{\dot{\mathbf{q}}\dot{\mathbf{q}}}(0)$	stationary covariance tensor of joints velocities
$\mathbf{R}_{\dot{\mathbf{q}}\dot{\mathbf{q}}}(t)$	nonstationary covariance tensor of joints velocities
$R_{\dot{q}_n\dot{q}_m}(0)$	n m element of $\mathbf{R}_{\dot{\mathbf{q}}\dot{\mathbf{q}}}(0)$
$R_{\dot{q}_n\dot{q}_m}(t)$	n m element of $\mathbf{R}_{\dot{\mathbf{q}}\dot{\mathbf{q}}}(t)$
$R_{q_nq_m}(0)$	n m element of $\mathbf{R}_{\mathbf{q}\mathbf{q}}(0)$
$R_{q_nq_m}(\tau)$	n m element of $\mathbf{R}_{\mathbf{q}\mathbf{q}}(\tau)$
$R_{q_nq_m}(t)$	n m element of $\mathbf{R}_{\mathbf{q}\mathbf{q}}(t)$
$\mathbf{R}_{\mathbf{q}\mathbf{q}}(0)$	stationary covariance tensor of joints displacements
$\mathbf{R}_{\mathbf{q}\mathbf{q}}(t)$	nonstationary covariance tensor of joints displacements
$\mathbf{R}_{\mathbf{q}\mathbf{q}}(\tau)$	stationary correlation tensor of joints displacements
$\mathbf{R}_{\mathbf{x},\mathbf{x}}(0)$	stationary principal variance tensor of tip displacements

$\mathbf{R}_{\mathbf{x},\mathbf{x}}(t)$	nonstationary principal variance tensor of tip displacements
$\mathbf{R}_{\mathbf{xx}}(0)$	stationary covariance tensor of tip displacements
$\mathbf{R}_{\mathbf{xx}}(t)$	nonstationary covariance tensor of tip displacements
$Re(\cdot)$	real value of
$Res(\cdot)$	residue of
$\mathbf{Rot}$	rotation matrix
$S_{0y}$	intensity of white noise
$\sin(\cdot)$	sine of .
$S_{q_n q_m}(\omega)$	n m element of $S_{qq}(\omega)$
$S_{qq}(\omega)$	PSD matrix of joints displacements
$T$	kinetic energy
$t$	time variable
$\bar{t}$	dimensionless time variable
$U$	modal matrix
$U$	mass normalized modal matrix
$\omega_{dr}$	damped natural frequency of mode-r
$\mathbf{x}^A$	actual values of the tip displacement vector
$\mathbf{x}^N$	nominal values of the tip displacement vector
*	asterisk indicates complex conjugate
$\alpha$	surface roughness coefficient
$\delta$	Dirac delta
$\delta_{ij}$	kronecker tensor
$\boldsymbol{\varepsilon}^A$	actual values of the dynamic parameter vector
$\boldsymbol{\varepsilon}^E$	estimated values of the dynamic parameter vector
$\boldsymbol{\varepsilon}^N$	nominal values of the dynamic parameter vector

$\Phi(t, t_0)$	system transition matrix
$\Theta_i$	kinematic configuration of link i
$\tau$	dimensionless time lag
$\Omega(t, t_0)$	deterministic modulating function
$\omega_r$	natural frequency of mode-r
$\xi_r$	damping factor of mode-r

## ACKNOWLEDGMENTS

I am highly indebted to several people who motivated and encouraged me in this work. My thanks goes, first and foremost, to the Almighty God through His son Jesus Christ (my saviour and my Lord) for bearing me up every inch of the journey, indeed He was there all the time.

Much thanks goes to Dr. Marek Kujath, my supervisor, who introduced me to the subject of robotics. The work bears testimony to his keen mind and careful scrutiny. I am also grateful for the friendship that I have enjoyed with him. Thanks also to members of my committee, Dr. C. R. Hazell and Dr. C. R. Baird, for their encouragement.

I benefited immensely from Dr. I. R. Orisamolu who introduced me to the subject of Random Vibration, Dr. G. Fenton who taught me how to carry out efficient numerical simulation and Dr. Kefu Liu who introduced me to the concept of state space.

The saints of the Christian Fellowship Group and Northbrook Bible Chapel and the IVCU brethren both past and present laboured with me in prayers and I pray that the Lord will reward their labour of love and ministrations (physical and spiritual).

Many thanks to my wife, Simi, for her unfailing support and to my son, Ukeme, for ensuring that I took short breaks at regular intervals during the course of the work. I also wish to acknowledge my indebtedness to my father Elder Okon Akpan, and my mother Mrs A. O Akpan who taught me the virtue of hardwork and diligence, and to my in-laws, 'Seni and Victoria Fagade and other members of our extended families for their support.

I also wish to thank all the staff of the Mechanical Engineering Department at TUNS for their friendship and support and everybody who contributed in one way or another to this work.

## ABSTRACT

The topic of this thesis is the dynamics of mobile manipulators. To streamline the study and to facilitate systematic analysis mobile manipulators are divided into two broad categories: the wheeled and the non-wheeled systems. A non-wheeled mobile manipulator has a base which is much more massive than the manipulator structure and the dynamics of the manipulator does not affect the base dynamics. The wheeled mobile manipulator has a base mounted on wheels and the base dynamics is of the same order of magnitude as the manipulator and they are dynamically coupled with each other.

In non-wheeled mobile manipulators the base motion is modeled as a random process. The responses of the joints and the tip of the manipulator are studied as stationary and nonstationary random processes. Expressions for the covariance tensors of the joint and the tip responses are developed. Single link and two-link manipulators are used to demonstrate the proposed analysis.

Two different models are used to study wheeled manipulators: the so-called quarter-car and the half-car models. The horizontal motion of the base is assumed, deterministic and known. The response of the wheeled manipulator system results from the motion on an irregular surface. The surface is modeled as a stochastic spatial field. Two cases of forward motion of the manipulator have been explored: uniform with constant speed and accelerated. The uniform forward motion produces purely stationary stochastic response while the accelerated motion produces nonstationary response in addition to a decaying deterministic

component. Expressions for the covariance of the tip and the joints responses of the wheeled mobile manipulators are derived. Examples of two link manipulators mounted on quarter-car and half-car models are fully investigated.

In all mobile manipulator models studied in the thesis, the Singular Value Decomposition technique is used to derive expressions for the principal variance of the tip responses. The sensitivity of the principal variance of the tip responses to system parameters and configuration changes is investigated. It is shown that the principal variance of the tip motion is almost unidirectional and highly configuration dependent. To minimise the vibration of the manipulator tip it is suggested that: the “lower” links should be longer than the “upper” links; the damping efforts should be concentrated in the “lower” joints in addition to suspension damping; the “lower” joints should be stiffer than the “upper” joints. Therefore, it is suggested that for minimal tip vibration most of the design and control efforts should be focused on the “lower links and joints.”

The Singular Value Decomposition technique is used to derive computation models for identification of the dynamic parameters of flexible mobile manipulators as well. Optimization criteria which can be used to set the manipulator configuration and excitation for efficient testing are proposed. Numerical simulations are discussed to validate the ideas.



# Chapter One

## INTRODUCTION

### 1.1. Background and Motivation

Robotics technology has been successfully applied in industry for manufacturing automation since the early sixties. The need for application of this technology in other areas has been reported in the literature (Murray et al., 1994). These areas include medical applications for the physically-challenged, agriculture, nuclear plant toxic waste clean-up, forestry, mining, construction, remote maintenance, fire fighting, space and sea explorations. These new applications will require mobile manipulators mounted on vehicles, marine vessels, and spaceships. A manipulator is an open loop mechanism which is composed of a number of connected bodies. Unlike conventional industrial manipulators which are structured for a specific tasks, the environments in which the mobile manipulators are expected to operate are highly unstructured. Manipulators mounted on vehicles, spaceships, and marine vessels experience random motion resulting from the vehicle's interaction with the traction surface, normal operation activities of the spaceships, and waves and wind affecting the marine vessels respectively.

Most industrial manipulators are rigid and depend on bulky designs. This rigidity results from design requirements to passively minimize the amplitude of structural deflections and vibration. Such manipulators typically handle only

objects that weigh less than five percent of the manipulator's weight (Choi et al., 1995). The bulky design results in high energy consumption, therefore, future light weight and slender manipulators will result in more efficient energy usage.

The slender mobile manipulators will be subjected to base-induced stochastic excitation. The stochastic vibration will result in fatigue, excursion failures, and undesirable paths of motion of the tools attached to the manipulator tip. To reduce and eliminate these undesirable effects an understanding of the manipulator dynamics is crucial for the motion control and for the structural design development. To the best knowledge of the author, no studies have been reported on the stochastic dynamics of mobile manipulators. In addition, very few reports are available on identification of structural parameters of flexible manipulators. These two areas are the focus of this thesis.

## **1.2. Scope of the Thesis**

This study deals with the vibration of manipulator structures excited from the base. The base motion comes from traction vehicles, marine vessels, spaceships, and foundation motion. Because the bases of the manipulators are not stationary but moving, therefore, they are referred to as mobile manipulators. Two classes of mobile manipulator dynamics are considered. In the first category it is assumed that the mass of the base to which the manipulator structure is mounted is so large, compared to that of the manipulator, that the motion of the manipulator does not (practically) influence the base. Figure 1.1 shows a model of the first type of mobile manipulator structure studied. In this thesis, the manipulators of this

category will be referred to as non-wheeled by analogy to manipulators mounted on large ships.

The second class of manipulator dynamics discussed includes the base to which the manipulator is attached and the manipulator influences the motion of the vehicle significantly. Models of the second family of mobile manipulator systems are shown in Figures 1.2 and 1.3. In this thesis, this category of manipulators will be referred to as wheeled manipulators.

For the two versions of manipulator systems studied, it is assumed that: the manipulator is flexible and the flexibility is concentrated at the joints: the kinematic configuration of the links of the manipulator can be represented as  $\Theta = [\Theta_1, \Theta_2, \dots, \Theta_n]^T$  and this configuration is assumed invariant when the system vibration is studied; the horizontal alignment of the x-axes is the reference zero-configuration (see Figure 1.4); the motion coordinate vector  $q = [q_1, q_2, \dots, q_n]^T$  represents the elastic motion about a kinematic configuration; the vector  $q$  is assumed very small such that the non-linear terms in the equation of motion can be neglected; the system damping is viscous, below critical value, concentrated at the joints, and invariant with respect to changes of the kinematic configuration; the effect of gravity is neglected.

The thesis does not consider the vibration of spatial mobile manipulators and walking manipulators. It is limited to the dynamics of planar mobile manipulators.

### **1.3. Objectives of the Thesis**

The objectives of the thesis are as follows:

1. To review published studies on structural dynamics of flexible manipulators;
2. To systematically advance knowledge on structural dynamics of flexible mobile manipulators;
3. To review studies on estimation of dynamic parameters of manipulators and to develop optimal estimation techniques for mobile manipulators.

### **1.4. Layout of the Thesis**

The thesis may be roughly divided into four parts. The first part is contained in the material up to Chapter two. It contains the introductions and the literature review of studies on the dynamics of manipulators and parameter estimation techniques. In Chapter two a number of useful mathematical concepts are reviewed as well. The second part of the report explores the stochastic dynamics of mobile manipulators. This is presented in Chapters three through eight. Estimation of the dynamic parameters of flexible mobile manipulators is studied in the third part of the thesis which is collected in Chapters nine and ten. The last part of the thesis embodies the thesis conclusions in Chapter eleven, references and a number of appendices dealing with long derivations.

Chapter two of the thesis begins with definitions and the term manipulator is explained. Published studies on the dynamics of manipulators and vehicles are summarized. Basic definitions relevant to the study of random dynamics are

discussed: they serve as foundation for studying the random vibration of mobile manipulators. The distinction between the manipulator kinematics and the dynamic parameters is explained. The reports on estimation of kinematics and dynamic parameters of manipulators are then reviewed. Summaries of useful and recurrent mathematical concepts and helpful background information on manipulators are presented as well.

In Chapters three through eight various models of multi-degree of freedom, articulated, and mobile manipulator systems are developed. These models are employed for the study of the stochastic dynamics of mobile manipulators. In Chapter three methods for studying the stochastic dynamics of manipulators mounted on very large and massive mobile bases are developed (Figure 1.1). This model of motion is applicable to spaceships, marine vessels, and foundations of buildings during an earthquake. Numerical examples involving the models shown in Figures 1.5 and 1.6 are presented in Chapter four to demonstrate the application of the ideas discussed in Chapter three.

The stochastic dynamics of manipulators mounted on wheeled bases (vehicles) are explored in Chapter five. A wheeled base such as a car can be represented by the quarter car model (see Figure 1.2). Chapter six is used to illustrate the applications of the ideas presented in Chapter five. The example considered in Chapter six is shown in Figure 1.7. A study of manipulator dynamics involving multiple wheels (Figure 1.3) is explored and an example demonstrating the method are given in Chapters seven and eight respectively. The model considered in Chapter eight is shown in Figure 1.8.

The third part of the thesis, contained in Chapters nine and ten, focuses on the estimation of the dynamic parameters of mobile manipulators. Algorithms for updating the nominal parameters of the manipulators, optimization of the manipulator configurations for testing, and optimization of the excitations for dynamic testing are presented in Chapter nine. Numerical validation of the proposed model is discussed in Chapter ten.

Chapter eleven contains final remarks, major contribution and conclusions of the thesis and the recommendations for further research. Bibliography is then cited fully. Long derivations and useful background information are given in the Appendices.

## **1.5. Summary and Concluding Remarks**

In this chapter the motivation for the thesis is outlined. The various models and the general assumptions used in the study have been discussed. Summaries of the objectives and the layout of the thesis have been presented. In the next chapter, the literature on the dynamics of manipulators and parameter estimation are reviewed.

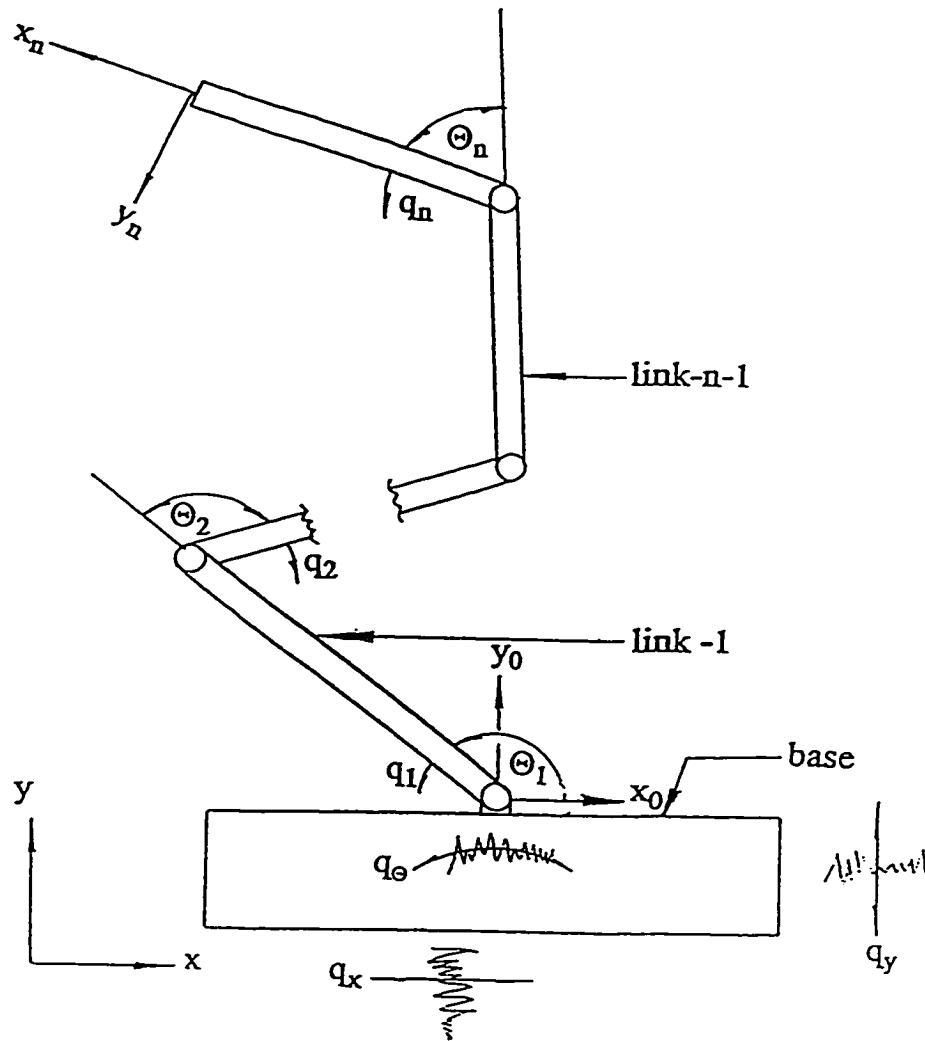


Figure 1.1. Model of a Non-wheeled Mobile Manipulator

- $\Theta_i$      $i$ -th kinematic configuration
- $q_i$      $i$ -th elastic motion variable
- $(x, y)_i$     Cartesian coordinate frame attached to the  $i$ -th link

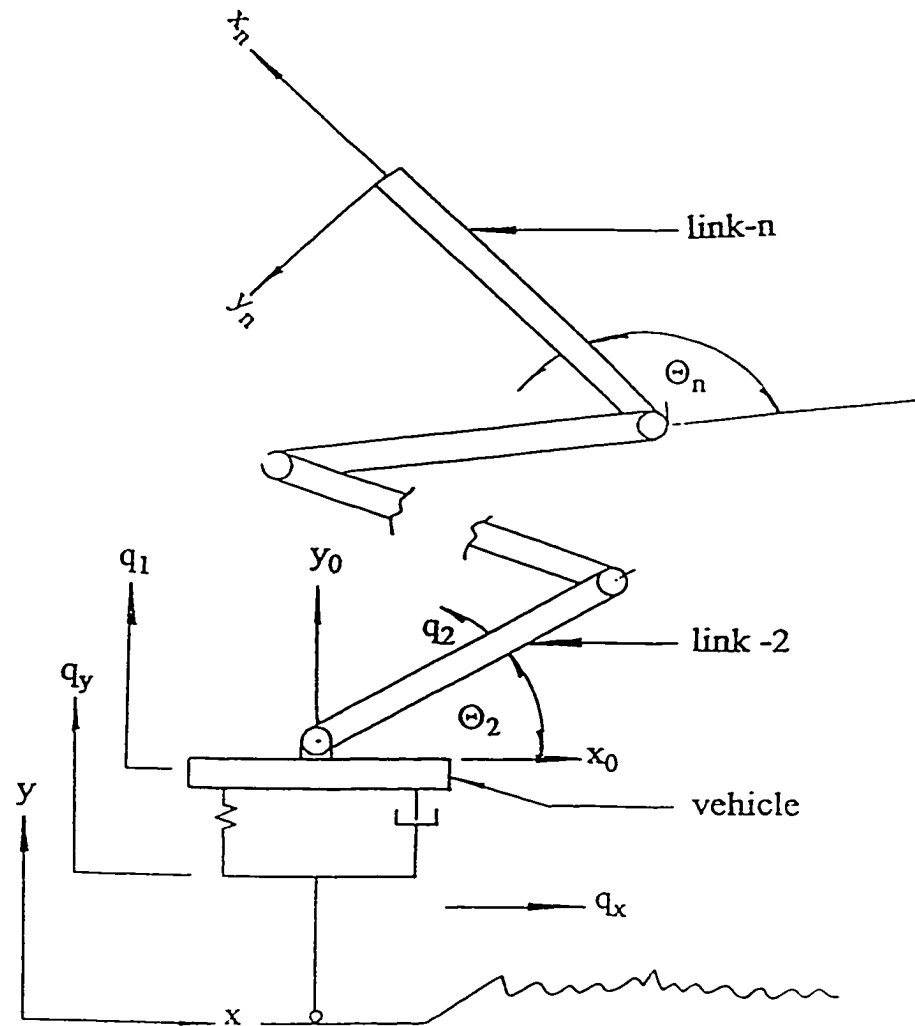


Figure 1.2. Model of a Single-wheeled Mobile Manipulator

- $\Theta_i$      $i$ -th kinematic configuration
- $q_i$      $i$ -th elastic motion variable
- $(x,y)_i$     Cartesian coordinate frame attached to the  $i$ -th link



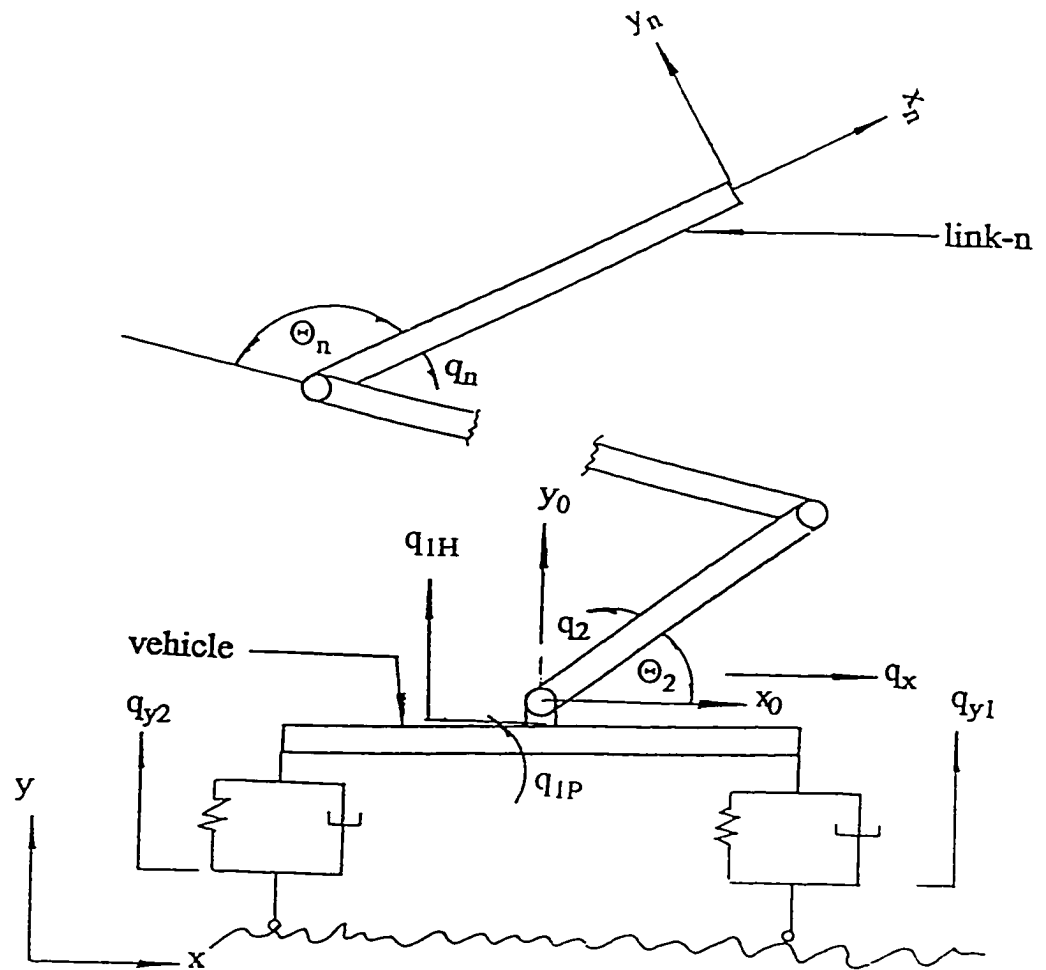


Figure 1.3. Model of a Multiple-wheeled Mobile Manipulator

- $\Theta_i$      $i$ -th kinematic configuration
- $q_i$      $i$ -th elastic motion variable
- $(x,y)_i$     Cartesian coordinate frame attached to the  $i$ -th link

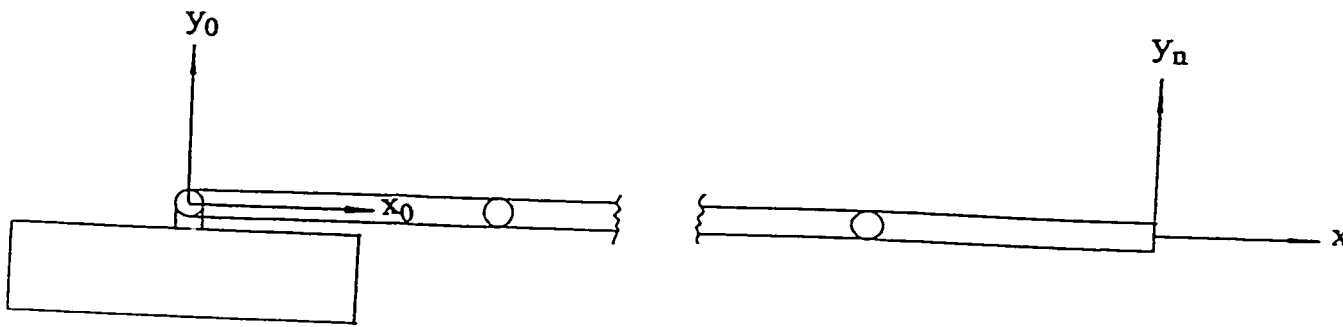


Figure 1.4. The Reference Zero-Configuration of the Mobile Manipulator.

$$\Theta_i = 0 \text{ for } i = 1, 2, \dots, n$$

$(x,y)_i$  Cartesian coordinate frame attached to the  $i$ -th link.

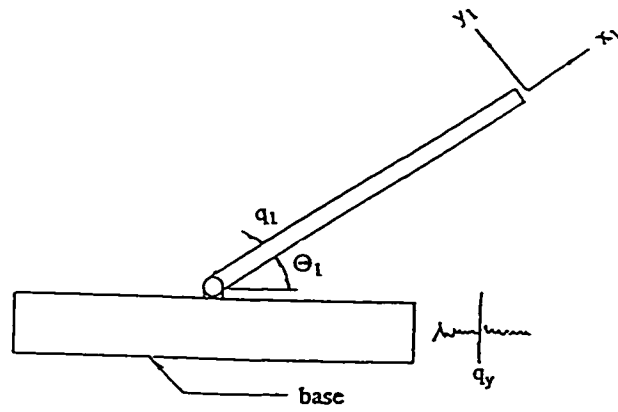


Figure 1.5. Single Link Non-wheeled Mobile Manipulator.

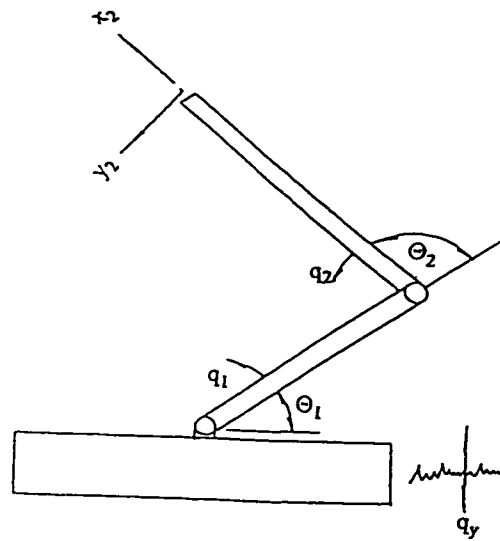


Figure 1.6. Two-Link Non-wheeled Mobile Manipulator.

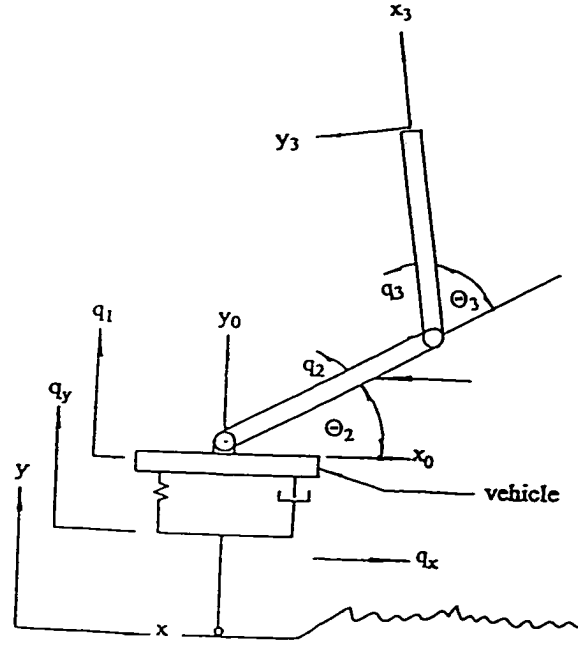


Figure 1.7. Two-Link Wheeled Mobile Manipulator.

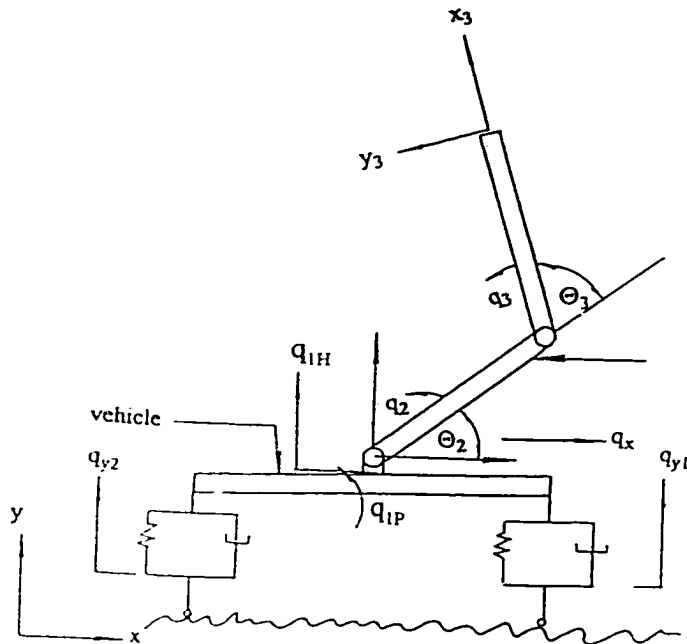


Figure 1.8. Two-Link Multiple-wheeled Mobile Manipulator.

## **Chapter Two**

### **LITERATURE REVIEW**

#### **2.1. Dynamics of Manipulators and Vehicles**

##### **2.1.1. Basic Definitions**

In this study the term manipulator refers to an open loop mechanism which is composed of a number of connected bodies. The bodies, which could be rigid or flexible, are referred to as links. The links are connected through joints. Each joint can be either prismatic (sliding or telescopic) or revolute (pin or hinge). The tool or end-effector is attached to the last link. The first link is the base which could be fixed or moving.

A moving base is referred to as a vehicle or a mobile base. There are basically two types of vehicles -non-wheeled and wheeled vehicles. The non-wheeled mobile base include the foundation of buildings, spaceships and marine vessels. The non-wheeled base is usually so massive compared to the manipulator that the motion of the manipulator does not affect the dynamics of the base. Further, the non-wheeled base may be subjected to motion (excitation) by interaction with its environment. Examples of such interactions include motion of the foundation of a building subjected to earthquake, vibration of marine vessel due to hydrodynamic sea waves and winds, and flexural motion of spaceship due to normal operation activities.

The second type of mobile manipulators move on wheels. These include cars and trains. The base is of commensurate dimension with the manipulator structure, therefore the dynamics of the manipulator affects the base. Further, the wheeled mobile manipulator is subjected to excitation due to the motion of its wheels on a rough surface. In this report manipulators mounted on wheeled mobile base are called wheeled mobile manipulators and manipulators mounted on non-wheeled mobile base are referred to as non-wheeled mobile manipulators. Manipulators mounted on a fixed base are called non-mobile manipulators.

### **2.1.2. Non-Mobile Flexible Manipulators**

The past studies on the dynamics of manipulators considered only deterministic joint excitation and assumed that the arms are rigid and that there is no elastic deformation at joints. Under this assumption the manipulator's equation of motion established by methods such as Hamilton principle are basically a description of the relationship between the input joint torque and the output motion (Asada and Slotine, 1986). The necessity for light manipulators has already been pointed out in the introduction, therefore flexibility effects must be considered both in the design and control process.

The need to consider flexibility of robotic manipulators first came from the interest in better control system design (Book et al., 1975; Book, 1984; Chalhoub and Ulsoy, 1986; Singh and Schy, 1986). These studies were intended to find suitable control schemes to track desired trajectories as well as to regulate the system position by recognizing the flexible nature of the structures and considering

oscillation induced by elastic deformation. Books et al. (1975, 1984) studied the control of a planar, two link manipulator including distributed mass and elasticity effects. This system was composed of simple straight beams in fixed configurations. Chalhoub and Ulsoy (1986) studied the controller design for a lead screw-driven flexible robot arm. The dynamic model for the robot included the effect of the distributed mass and the elasticity of the last link. The assumed modes method was used to approximate the dynamics of the infinite dimensional link. The study showed that by including the flexible motion in the controller design the positional accuracy of the tool could be improved significantly. Singh and Schy (1986) studied the control of elastic robotic systems by nonlinear inversion and modal damping.

Several researchers have used the finite element techniques to describe the elastic deformations of manipulators (Sunada and Dubowsky, 1983; Turcic and Midha, 1984; Usoro et al, 1986; Smaili, 1993). Others have used global methods such as the assumed modes method, Rayleigh-Ritz method and the two-coordinate method (Anderson, 1985; Streit et al 1986, 1989; Krishnamurthy, 1989; Sasiadek and Srinivasan, 1989; Rivin, 1988; Liu, 1992).

The two-coordinate method describes the position of a flexible manipulator by two distinct coordinates. The first set of coordinates represents the kinematic configuration of the manipulator while the second set of coordinates represents the small vibration about the kinematic configuration. Anderson (1985) employed this method to study the stability of a manipulator subjected to a compressive force at its free end. Streit et al (1986) applied this method to develop a dynamic model of a two degree-of-freedom robotic system composed of one prismatic joint and one

revolute joint. The model was then used to study the parametric stability when a manipulator performs a repetitive task. Liu (1992) used a similar model to study parametric stability of a two degree-of-freedom manipulator with revolute joints performing repetitive tasks. Liu and Kujath (1994) used the same model to optimize the trajectory for a two link flexible manipulator. The authors -Liu and Kujath- illustrated that the two coordinate model has an advantage over the assumed mode and the finite element representations since the resulting equations of motion are simpler and transparent without a compromise on accuracy.

In general it can be noted that all the studies that have been reported on the dynamics of flexible manipulators have been focused on deterministic loading. None of the aforementioned studies have addressed the crucial issue of stochastic loading of flexible manipulators.

### **2.1.3. Wheeled Mobile Rigid Manipulators**

Jacobs and Canny (1989) and later Yun-Hui and Suguru (1991) studied wheeled mobile manipulators as simple vehicles without dynamics. They focused on map building of unknown environments and motion planning algorithm. The limited studies on the dynamics of wheeled mobile manipulators [Dubowsky and Vance, 1989; Hootsman and Dubowsky, 1991; Hootsman, 1992] treated the manipulators as rigid links on wheeled mobile vehicles. The excitation of the manipulators due to the motion of the vehicle on a surface was assumed to be a deterministic process. A more realistic model for the system excitation is a stochastic process since the surface on which the vehicle is moving is in general



irregular and uneven. None of the aforementioned studies addressed the issue of stochastic excitation.

#### **2.1.4. Non-Wheeled Mobile Rigid Manipulators**

A limited number of scattered studies exist on the dynamics of non-wheeled mobile rigid manipulators under random loading. The dynamics of the simplest manipulator -a simple rigid pendulum- subjected to stationary stochastic base excitation was reported by Bogdanoff and Citron (1965). Chang and Young (1989) later studied the dynamics of a two degree-of-freedom rigid manipulator under stationary random base and deterministic tip loading. Both studies focused on the stochastic dynamics of the rigid manipulator joint motion. In practical applications, however, the motion of the tip of a manipulator is very important since the tool is attached there. These studies did not address the crucial issue of the stochastic dynamics of the manipulator tip.

#### **2.1.5. Dynamics of Wheeled Vehicles**

Some research has been devoted to the stochastic motion of vehicles that traverse uneven surfaces. Virchis and Robsin (1971) considered the vehicle as a linear, time invariant, second order, single degree of freedom system running over a spatially homogenous rough ground. The authors used the impulse response function of the vehicle together with the autocorrelation function of the spatial excitation to express the autocorrelation function of the vehicle. Sobczyk and Macvean (1976) obtained a closed form solution for the variance of the response

for simple velocity profiles. Yadav and Nigam (1978) transformed the dynamic system to a pair of uncoupled equations using a spatial domain formulation. Since the excitation was spatially stationary and the system coefficient space dependent, the solution admitted an evolutionary spectral form. Hammond and Harrison (1981) used the state space formulation in which the excitation could be represented as a shaping filter for the vehicle problem represented by a linear, time invariant, second order single degree of freedom system.

#### **2.1.6. Random Dynamics of Simple Systems**

The random vibration of systems like beams, plates and axisymmetric shells with simple boundary conditions have been studied by To (1983, 1984, 1986), To and Wang (1993), To and Orisamolu (1987), and Iwan and Hou (1989). The expressions for evolutionary spectra and cross spectra density functions were derived by To (1983). The time dependent variance and covariance of displacement were obtained using the evolutionary spectrum approach. The time dependent responses of axisymmetric shell structure and plates were computed by To and Wang (1993), and To and Orisamolu (1987) respectively. The response of a single degree of freedom system was studied using the state space approach by Iwan and Hou (1989).

It can be observed from all the reported studies that the stochastic dynamics of flexible mobile manipulator subjected to stationary and nonstationary excitation have not been addressed. This thesis will tackle this issue in subsequent chapters. In order to set the background for the study of the stochastic dynamics of mobile

manipulators basic terminology and properties of stochastic process have been reviewed in Appendix A.

## **2.2. Identification of Manipulator Parameters**

The design of controllers for manipulators to position the tip of the end-effector at a specified point in the world coordinate require a mathematical model relating the tool location and orientation with reference to the joint positions. The goal of identification in robotics is either to derive, estimate, improve or verify the parameters of the mathematical model.

Models for manipulator parameter estimation could be either kinematic or dynamic. Kinematic models focus on the identification of only the geometric parameters such as length and orientation of the manipulator links. Dynamic models on the other hand are used for the identification of such parameters as compliance, friction, and inertia of the manipulator links and joints.

### **2.2.1. Identification of Kinematic Parameters**

A common method of representing the kinematic relationship between two consecutive link coordinate frames is the convention defined by Denavit and Hartenberg (1955). The representation uses four kinematic parameters to completely describe the kinematic relationship for two consecutive links namely length, offset, orientation and twist (Spong and Vidyasagar, 1989). Parameter deviation errors in estimating the geometry of the manipulator structure will

produce corresponding errors in the Denavit Hartenberg [DH] kinematic parameters. Kumar and Waldron (1981) developed a kinematic model for the tool positioning error as a function of the joint variable error. Wu (1983a, 1983b, 1984) developed a kinematic model for the tool positioning error as a function of the errors in all four of the DH link parameters. Several other authors have addressed the problem of kinematic models for tool positioning due to joint axis misalignment (Veitschegger and Wu, 1987; Mooring, 1983; Hayati, 1983).

Whitney et al. (1984) devised a method for correcting both the geometric and non-geometric parameter deviation for rigid manipulators and verified the method experimentally on a PUMA 560. Chen et al (1985) proposed a kinematic model for estimating geometric errors in the manipulator structure using six parameter deviations per link plus three for the tool.

Menq et al. (1989) developed a kinematic model to address the problem of identifiability of a set of kinematic parameters deviation for rigid manipulators and later extended the work (Borm and Menq, 1991) to determine optimal measurement configurations for identifying the basis set of kinematic parameters. Other authors (Khalil et al., 1991) also addressed the issue of observability and configuration optimization for measurement of the kinematic parameters.

### **2.2.2. Identification of Dynamic Parameters**

Several methods for identifying the inertia parameters of rigid manipulators have been presented in the literature. Mukerjee and Ballard (1985) suggested an

identification procedure for rigid manipulators to deduce the inertial and friction parameters from the measured reaction forces at the joint by incorporating force-torque sensors in the robot inputs. Kshola (1988) presented an algorithm for identifying the inertia properties of rigid manipulators. An experimental method to estimate the inertia parameters of the manipulator links using rigid body model and measured motor current, positions, velocities and acceleration has been discussed by Atkeson et al. (1990). Seeger and Leonard (1989) presented an off-line procedure to estimate friction forces and inertial parameters in small sets, using test motions that allows the reduction of the general model to a few identifiable parameters. Behi and Tesar (1991) discussed a technique for identifying the stiffness and the inertia parameters of a manipulator using experimental modal analysis. The foregoing studies addressed only non-mobile rigid manipulators and have not addressed the issue of identifiability and optimization procedures for the estimation of the dynamic parameters of mobile flexible manipulators. This topic will be addressed in a later part of this report.

### 2.3. Lagrange Principle of Dynamics

This is an energy principle that can be used to derive the equation of motion of dynamic systems (Meirovitch, 1990). Consider a dynamic system with a set of generalized (independent) coordinates  $q = [q_1, q_2, \dots, q_n]^T$ . Let the kinetic energy for the system be given as

$$T = T(q_i, \dot{q}_i) \quad \text{for } i = 1, 2, \dots, n \quad (2.1)$$

The potential energy be given as

$$V = V(q_i) \quad \text{for } i = 1, 2, \dots, n. \quad (2.2)$$

The Lagrangian  $L$  for the system can be defined as

$$L = T - V \quad (2.3)$$

If the Rayleigh dissipation function  $R$  (representing non-conservation damping force) is

$$R = R(\dot{q}_i) \quad \text{for } i = 1, 2, \dots, n \quad (2.4)$$

and the generalized force acting on the system is

$$F_i \quad \text{for } i = 1, 2, \dots, n. \quad (2.5)$$

Then, the equation of motion for the system can be derived using Lagrange energy equation (Meirovitch, 1990) as

$$\frac{d}{dt} \left( \frac{\partial L}{\partial \dot{q}_i} \right) - \frac{\partial L}{\partial q_i} = F_i - \frac{\partial R}{\partial \dot{q}_i} \quad \text{for } i = 1, 2, \dots, n. \quad (2.6)$$

In particular for the robotic system considered in this report, the generalized coordinates vector  $q$  is the elastic motion of the manipulator joints.

## 2.4. Singular Value Decomposition of a Matrix

This is a unique property of matrices. Consider any rectangular real  $m \times n$  matrix  $\mathbf{W}$ , from linear algebra, the matrix  $\mathbf{W}$  can be decomposed into (Golub and Van Loan, 1990)

$$\mathbf{W} = \mathbf{U}\mathbf{\Sigma}\mathbf{V}^T \quad (2.7)$$

where the columns of the  $m \times m$  matrix  $\mathbf{U}$  are the orthonormal eigenvectors of  $\mathbf{W}\mathbf{W}^T$  and are called the left singular vectors of  $\mathbf{W}$ ; the columns of the  $n \times n$  matrix  $\mathbf{V}$  are the orthonormal eigenvectors of  $\mathbf{W}^T\mathbf{W}$  and are called the right singular vectors of  $\mathbf{W}$ ;  $\mathbf{\Sigma}$  is a diagonal matrix with non-negative elements on its main diagonal which are called the singular values of  $\mathbf{W}$ . The singular values are the non-negative square roots of the eigenvalues of  $\mathbf{W}^T\mathbf{W}$  or  $\mathbf{W}\mathbf{W}^T$ .  $\mathbf{U}$  and  $\mathbf{V}$  are orthonormal matrices i.e.

$$\mathbf{U}^T\mathbf{U} = \mathbf{U}\mathbf{U}^T = \mathbf{I} \quad (2.8)$$

$$\mathbf{V}^T\mathbf{V} = \mathbf{V}\mathbf{V}^T = \mathbf{I} \quad (2.9)$$

$$\mathbf{U}^T = \mathbf{U}^{-1} \quad (2.10)$$

$$\mathbf{V}^T = \mathbf{V}^{-1} \quad (2.11)$$

where  $\mathbf{I}$  is the identity matrix.

If the matrix  $\mathbf{W}$  is symmetric and positive definite, the singular values are the eigenvalues of  $\mathbf{W}$ . The columns of the matrix  $\mathbf{U}$  are the

orthonormal eigenvectors of  $\mathbf{W}$ . Further, the matrix  $\mathbf{V}$  is the transpose of  $\mathbf{U}$  i.e.

$$\mathbf{V} = \mathbf{U}^T \quad (2.12)$$

and

$$\mathbf{UV} = \mathbf{V}^T\mathbf{U}^T = \mathbf{I} \quad (2.13)$$

## 2.5. The Concept of Manipulator Jacobian

The velocity of any robotic manipulator system can be represented, in either the relative joint coordinates  $\mathbf{q}$  or the absolute Cartesian coordinates  $\mathbf{x}$ . The manipulator Jacobian matrix  $\mathbf{J}$  provides the relationship between the joint velocities  $\dot{\mathbf{q}}$  and the tip Cartesian velocities  $\dot{\mathbf{x}}$ . In particular

$$\dot{\mathbf{x}} = \mathbf{J}\dot{\mathbf{q}} \quad (2.14)$$

where

$$\mathbf{J} = \frac{\partial \mathbf{x}}{\partial \mathbf{q}} \quad (2.15)$$

$\mathbf{x}$  is the position vector of the manipulator tip in the Cartesian coordinate, while  $\mathbf{q}$  is the joint coordinate. For very small motion of the joint  $\mathbf{q}$  it can be shown that (see Appendix C for details and examples)

$$\mathbf{x} = \mathbf{J}\mathbf{q} \quad (2.16)$$



## **2.6. Summary and Concluding Remarks**

In this chapter, fundamental terms used in the thesis have been defined. A literature review on the dynamics of manipulator and vehicles has been abridged. A summary of review works on the identification of the parameters of manipulators has been undertaken. The basic terminology of stochastic processes have been discussed. Useful concepts, singular value decomposition, Lagrangian principle and manipulator Jacobian have been summarised. In the next chapter a method for studying the stochastic dynamics of non-wheeled flexible mobile manipulator is presented.

## **Chapter Three**

# **NON-WHEELED MOBILE MANIPULATOR, ANALYSIS**

### **3.1. Introduction**

This chapter contains an original contribution of the author. Components of this chapter have been accepted for publication in Kujath and Akpan, (1996a). The originality is in the modeling of the joint and the tip covariance tensors of responses of the flexible manipulator structure to the non-wheeled random base motion. A selection and composition of known analytical tools such as Lagrange principle, modal analysis and the state space procedure have been used in the formulation.

The basic model of the manipulator structure used in this chapter is shown in Figure 3.1. It is assumed that the base on which the manipulator structure is mounted is so much more massive than the manipulator that the dynamics of the structure does not practically influence the base. This type of base can be found in large spaceships, marine vessels, and foundations of buildings. Such a base is referred to as a non-wheeled mobile base. The non-wheeled mobile base is subjected to motion (excitation) by interaction with its environment; examples are the foundation of a building subjected to earthquake, interaction of the marine vessel with hydrodynamic sea waves and winds, and flexural motion of the spaceship due to normal operation activities. The base motion is assumed random

and it couples kinematically as excitations into the dynamics of the manipulator structure. This coupling involves the acceleration vector of the base motion. Models have to be developed for the base excitations.

### 3.2. Base Excitation Models

Consider the manipulator of Figure 3.1. The base motion vector  $\mathbf{q}_0 = [q_x, q_y, q_\theta]^T$  relative to the inertia frame  $x_I y_I$  is assumed to be composed of zero mean uncorrelated stochastic processes i.e.

$$E\{q_i(t)\} = 0, \quad i = x, y, \theta \quad (3.1)$$

$$E\{q_i(t_1)q_j(t_2)\} = 0 \quad i \neq j \quad (3.2)$$

where  $E\{.\}$  is the expectation operator. Two representations of the base acceleration are used in this chapter.

#### Case I - Stationary Representation:

It is assumed that the base acceleration vector  $\mathbf{q}_0$  can be modeled as random processes with power spectral density

$$S_{\ddot{q}_i \ddot{q}_i} = S_i(\omega), \quad i = x, y, \theta \quad (3.3)$$

where  $\omega$  is the frequency of the excitation spectrum.

### Case II -Nonstationary Representation:

In this case, it is assumed that the base excitation can be represented as a modulated white noise i.e.

$$\ddot{q}_i(t) = \Omega_i(t) \varpi_i(t), \quad i = x, y, \theta \quad (3.4)$$

$$E\{\varpi_i(t)\} = 0, \quad i = x, y, \theta \quad (3.5)$$

$$E\{\varpi_i(t_1)\varpi_i(t_2)\} = S_{0i}\delta_i(t_2 - t_1), \quad i = x, y, \theta \quad (3.6)$$

where  $\Omega_i(t)$  is a deterministic modulating function and  $\varpi_i(t)$  is a stationary white noise with intensity  $S_{0i}$  ( $i = x, y, \theta$ ).

### 3.3. Equation of Motion

Application of the Lagrange principle leads to the equation of motion

$$\mathbf{D}\ddot{\mathbf{q}}(t) + \mathbf{C}\dot{\mathbf{q}}(t) + \mathbf{K}\mathbf{q}(t) = -\mathbf{f}_1\ddot{q}_x(t) - \mathbf{f}_2\ddot{q}_y(t) - \mathbf{f}_3\ddot{q}_\theta(t) \quad (3.7)$$

$\mathbf{f}_1$  -dynamic coupling vector between  $\mathbf{q}$  and  $\ddot{q}_x$

$\mathbf{f}_2$  -dynamic coupling vector between  $\mathbf{q}$  and  $\ddot{q}_y$

$\mathbf{f}_3$  -dynamic coupling vector between  $\mathbf{q}$  and  $\ddot{q}_\theta$

$\ddot{q}_x$ ,  $\ddot{q}_y$ , and  $\ddot{q}_\theta$  are small stochastic vibrations of the massive base,  $\mathbf{q}$  is the joint motion vector. Chapter four contains examples of detailed derivations of the equation of motion for specific manipulator structures. Equation (3.7) can be decoupled by employing the technique of modal analysis. With a knowledge of the natural frequencies and the mode shapes, the mass normalized modal matrix  $\mathbf{U}$  is defined as

$$\mathbf{U} = \frac{\mathbf{U}}{\sqrt{d_{jj}}}|_j, \quad j = 1, 2, 3, \dots, n. \quad (3.8)$$

where the term  $\mathbf{U}$  is the modal matrix of the system given by equation (3.7), the term  $d_{jj}$  is a diagonal element of the matrix  $\mathbf{U}^T \mathbf{D} \mathbf{U}$  and the symbol  $|_j$  denotes division of column  $j$  of matrix  $\mathbf{U}$  by the term  $\sqrt{d_{jj}}$ . Introducing the transformation

$$\mathbf{q} = \mathbf{U} \mathbf{z}(t) \quad (3.9)$$

where  $\mathbf{z}(t)$  represents the vector of normal coordinates, substituting  $\mathbf{q} = \mathbf{U} \mathbf{z}$  into equation (3.7) and premultiplying it throughout by matrix  $\mathbf{U}^T$  the following results

$$\mathbf{U}^T \mathbf{D} \mathbf{U} \dot{\mathbf{z}} + \mathbf{U}^T \mathbf{C} \mathbf{U} \dot{\mathbf{z}} + \mathbf{U}^T \mathbf{K} \mathbf{U} \mathbf{z} = -\mathbf{U}^T (\mathbf{f}_1 \ddot{q}_x(t) + \mathbf{f}_2 \ddot{q}_y(t) + \mathbf{f}_3 \ddot{q}_z(t)) \quad (3.10)$$

$$\mathbf{U}^T \mathbf{D} \mathbf{U} = \mathbf{I}, \quad \mathbf{U}^T \mathbf{C} \mathbf{U} = [2\xi_r \omega_r], \quad \mathbf{U}^T \mathbf{K} \mathbf{U} = [\omega_r^2] \quad (3.11)$$

$[2\xi_r \omega_r]$  is a diagonal matrix with the terms  $2\xi_r \omega_r$  on the diagonal,

$[\omega_r^2]$  is a diagonal matrix with the terms  $\omega_r^2$  on the diagonal.

Equation (3.10) reduces to the uncoupled set of equations

$$\ddot{z}_r + 2\xi_r\omega_r\dot{z}_r + \omega_r^2 z_r = f_r(t), \quad r = 1, 2, \dots, n \quad (3.12)$$

where

$$f_r(t) = f_{r1}\ddot{q}_x(t) + f_{r2}\ddot{q}_y(t) + f_{r3}\ddot{q}_\theta(t), \quad (3.13)$$

$$f_{r1} = -\mathbf{u}_r^T \mathbf{f}_1, \quad (3.14)$$

$$f_{r2} = -\mathbf{u}_r^T \mathbf{f}_2, \quad (3.15)$$

$$f_{r3} = -\mathbf{u}_r^T \mathbf{f}_3. \quad (3.16)$$

The term  $\mathbf{u}_r^T$  represents the transpose of the r-th column of the mass normalized modal matrix  $\mathbf{U}$ . From linear system theory, it is known that a stationary stochastic excitation will produce stationary responses while a nonstationary random excitation will produce nonstationary responses.

### 3.4. Covariance Tensor of the Joint Responses

#### 3.4.1. Stationary Responses

Consider the modal equation (3.12), using the Duhamel integral the displacement response of mode-r is obtained as

$$z_r = \int_{-\infty}^{\infty} h_r(\tau) f_r(t - \tau) d\tau, \quad r = 1, 2, \dots, n \quad (3.17)$$

$$h_r = u(t) \frac{1}{\omega_{dr}} e^{-\xi_r \omega_r t} \sin(\omega_{dr} t), \quad \omega_{dr} = \omega_r \sqrt{1 - \xi_r^2}. \quad (3.18)$$

The displacement response  $q_p(t_1)$  of joint-p at time  $t_1$  can be computed using the relationship given in equation (3.9) as

$$q_p(t_1) = \sum_{r=1}^n U_{pr} z_r(t_1) \quad (3.19)$$

Application of equation (3.17) in equation (3.19) gives

$$q_p(t_1) = \sum_{r=1}^n U_{pr} \int_{-\infty}^{\infty} h_r(\tau_1) f_r(t_1 - \tau_1) d\tau_1 \quad (3.20)$$

Similarly the response of joint-m is given as

$$q_m(t_2) = \sum_{r=1}^n U_{mr} \int_{-\infty}^{\infty} h_r(\tau_2) f_r(t_2 - \tau_2) d\tau_2 \quad (3.21)$$

Taking the ensemble average of  $q_p(t_1)$  and  $q_m(t_2)$  the crosscorrelation of the displacements of joint-p and joint-m is given as

$$R_{q_p q_m}(t_1, t_2) = E\{q_p(t_1) q_m(t_2)\}$$

$$\begin{aligned}
&= E\left\{ \sum_{r=1}^n \sum_{k=1}^n U_{pr} U_{mk} \int_{-\infty}^{\infty} h_r(\tau_1) f_r(t_1 - \tau_1) \int_{-\infty}^{\infty} h_k(\tau_2) f_k(t_2 - \tau_2) d\tau_2 d\tau_1 \right\} \\
&= \sum_{r=1}^n \sum_{k=1}^n U_{pr} U_{mk} \int_{-\infty}^{\infty} \int_{-\infty}^{\infty} E\{f_k(t_2 - \tau_2) f_r(t_1 - \tau_1)\} h_r(\tau_1) h_k(\tau_2) d\tau_2 d\tau_1. \quad (3.22)
\end{aligned}$$

The following relations can be obtained from equation (3.13)

$$f_r(t_1 - \tau_1) = f_{r1} \ddot{q}_x(t_1 - \tau_1) + f_{r2} \ddot{q}_y(t_1 - \tau_1) + f_{r3} \ddot{q}_\theta(t_1 - \tau_1) \quad (3.23)$$

$$f_k(t_2 - \tau_2) = f_{k1} \ddot{q}_x(t_2 - \tau_2) + f_{k2} \ddot{q}_y(t_2 - \tau_2) + f_{k3} \ddot{q}_\theta(t_2 - \tau_2). \quad (3.24)$$

Application of equations (3.2), (3.23) and (3.24) in equation (3.22) gives the crosscorrelation of the displacement of joint-p and joint-m as

$$\begin{aligned}
R_{q_p q_m}(t_1, t_2) &= \\
&\sum_{r=1}^n \sum_{k=1}^n U_{pr} U_{mk} f_{r1} f_{k1} \int_{-\infty}^{\infty} \int_{-\infty}^{\infty} E\{\ddot{q}_x(t_2 - \tau_2) \ddot{q}_x(t_1 - \tau_1)\} h_r(\tau_1) h_k(\tau_2) d\tau_2 d\tau_1 \\
&+ \sum_{r=1}^n \sum_{k=1}^n U_{pr} U_{mk} f_{r2} f_{k2} \int_{-\infty}^{\infty} \int_{-\infty}^{\infty} E\{\ddot{q}_y(t_2 - \tau_2) \ddot{q}_y(t_1 - \tau_1)\} h_r(\tau_1) h_k(\tau_2) d\tau_2 d\tau_1 \\
&+ \sum_{r=1}^n \sum_{k=1}^n U_{pr} U_{mk} f_{r3} f_{k3} \int_{-\infty}^{\infty} \int_{-\infty}^{\infty} E\{\ddot{q}_\theta(t_2 - \tau_2) \ddot{q}_\theta(t_1 - \tau_1)\} h_r(\tau_1) h_k(\tau_2) d\tau_2 d\tau_1
\end{aligned} \quad (3.25)$$



If the process is stationary then the crosscorrelation is a function of the time difference  $t_1 - t_2 = \tau$ . Equation (3.25) can be rewritten as

$$\begin{aligned}
R_{q_p q_m}(t_1 - t_2) = & \\
& \sum_{r=1}^n \sum_{k=1}^n U_{pr} U_{mk} f_{r1} f_{k1} \int_{-\infty}^{\infty} \int_{-\infty}^{\infty} R_{q_x q_x}(t_1 - \tau_1 - t_2 + \tau_2) h_r(\tau_1) h_k(\tau_2) d\tau_2 d\tau_1 \\
& + \sum_{r=1}^n \sum_{k=1}^n U_{pr} U_{mk} f_{r2} f_{k2} \int_{-\infty}^{\infty} \int_{-\infty}^{\infty} R_{q_y q_y}(t_1 - \tau_1 - t_2 + \tau_2) h_r(\tau_1) h_k(\tau_2) d\tau_2 d\tau_1 \\
& + \sum_{r=1}^n \sum_{k=1}^n U_{pr} U_{mk} f_{r3} f_{k3} \int_{-\infty}^{\infty} \int_{-\infty}^{\infty} R_{q_\theta q_\theta}(t_1 - \tau_1 - t_2 + \tau_2) h_r(\tau_1) h_k(\tau_2) d\tau_2 d\tau_1. \quad (3.26)
\end{aligned}$$

The Power Spectral Density of the displacements of joint-p and joint-m is determined by the Wiener Khinchine relation

$$S_{q_p q_m}(\omega) = \frac{1}{2\pi} \int_{-\infty}^{\infty} R_{q_p q_m}(\tau) e^{-i\omega\tau} d\tau. \quad (3.27)$$

Defining the variable

$$\kappa = \tau - \tau_1 + \tau_2 \quad (3.28)$$

Applying equations (3.28) and (3.26) in equation (3.27) gives

$$\begin{aligned}
S_{q_n q_m}(\omega) = & \\
& \sum_{r=1}^n \sum_{k=1}^n U_{pr} U_{mk} f_{r1} f_{k1} \frac{1}{2\pi} \int_{-\infty}^{\infty} R_{\ddot{q}_x \ddot{q}_x}(\kappa) e^{-i\omega \kappa} d\kappa \int_{-\infty}^{\infty} h_r(\tau_1) e^{-i\omega \tau_1} d\tau_1 \int_{-\infty}^{\infty} h_k(\tau_2) e^{i\omega \tau_2} d\tau_2 \\
& + \sum_{r=1}^n \sum_{k=1}^n U_{pr} U_{mk} f_{r2} f_{k2} \frac{1}{2\pi} \int_{-\infty}^{\infty} R_{\ddot{q}_y \ddot{q}_y}(\kappa) e^{-i\omega \kappa} d\kappa \int_{-\infty}^{\infty} h_r(\tau_1) e^{-i\omega \tau_1} d\tau_1 \int_{-\infty}^{\infty} h_k(\tau_2) e^{i\omega \tau_2} d\tau_2 \\
& + \sum_{r=1}^n \sum_{k=1}^n U_{pr} U_{mk} f_{r3} f_{k3} \frac{1}{2\pi} \int_{-\infty}^{\infty} R_{\ddot{q}_0 \ddot{q}_0}(\kappa) e^{-i\omega \kappa} d\kappa \int_{-\infty}^{\infty} h_r(\tau_1) e^{-i\omega \tau_1} d\tau_1 \int_{-\infty}^{\infty} h_k(\tau_2) e^{i\omega \tau_2} d\tau_2
\end{aligned} \tag{3.29}$$

By definition  $H_r(\omega)$  is

$$\int_{-\infty}^{\infty} h_r(\tau_1) e^{-i\omega \tau_1} d\tau_1 = H_r(\omega) \tag{3.30}$$

$$\int_{-\infty}^{\infty} h_k(\tau_2) e^{i\omega \tau_2} d\tau_2 = H_k^*(\omega) \tag{3.31}$$

where  $H_r = (\omega_r^2 - \omega^2 + 2i\xi_r \omega \omega_r)^{-1}$ ,  $i = \sqrt{-1}$ , and  $H_k^*(\omega)$  is the complex conjugate of  $H_k(\omega)$ . Further, using equation (3.3) and by definition we have

$$\frac{1}{2\pi} \int_{-\infty}^{\infty} R_{\ddot{q}_x \ddot{q}_x}(\kappa) e^{-i\omega \kappa} d\kappa = S_x(\omega) \tag{3.32}$$

$$\frac{1}{2\pi} \int_{-\infty}^{\infty} R_{\ddot{q}_y \ddot{q}_y}(\kappa) e^{-i\omega\kappa} d\kappa = S_y(\omega) \quad (3.33)$$

$$\frac{1}{2\pi} \int_{-\infty}^{\infty} R_{\ddot{q}_\theta \ddot{q}_\theta}(\kappa) e^{-i\omega\kappa} d\kappa = S_\theta(\omega) \quad (3.34)$$

Application of equations (3.33), (3.32), (3.31), (3.30) and (3.34) in equation (3.29) gives

$$\begin{aligned} S_{q_p q_m}(\omega) &= \sum_{r=1}^n \sum_{k=1}^n (f_{r1} S_x f_{k1} + f_{r2} S_y f_{k2} + f_{r3} S_\theta f_{k3}) U_{pr} U_{mk} H_r(\omega) H_k^*(\omega) \\ &= \sum_{r=1}^n \sum_{k=1}^n (\mathbf{u}_r^T \mathbf{f}_1 S_x \mathbf{u}_k^T \mathbf{f}_1 + \mathbf{u}_r^T \mathbf{f}_2 S_y \mathbf{u}_k^T \mathbf{f}_2 + \mathbf{u}_r^T \mathbf{f}_3 S_\theta \mathbf{u}_k^T \mathbf{f}_3) \\ &\quad (U_{pr} U_{mk} H_r(\omega) H_k^*(\omega)) \end{aligned} \quad (3.35)$$

Equations (3.35) can be used to construct the power spectral density matrix  $S_{qq}(\omega)$  of the joint displacements. The covariance matrix of the joint displacements is obtained as

$$\mathbf{R}_{qq}(0) = E\{\mathbf{q}\mathbf{q}^T\} = \int_{-\infty}^{\infty} S_{qq}(\omega) d\omega. \quad (3.36)$$

From the calculus of stationary random processes the covariance matrix of the joint velocities is obtained as

$$\mathbf{R}_{\dot{q}\dot{q}}(0) = \int_{-\infty}^{\infty} \omega^2 \mathbf{S}_{qq}(\omega) d\omega \quad (3.37)$$

Equations (3.36) and (3.37) can be integrated using the residue theorem.

### 3.4.2. Nonstationary Response

The spectral approach (frequency domain) used in the previous section for the stationary response cannot be easily applied to the nonstationary responses because of the time varying nature of the excitation. Therefore in this section, the state space approach (time domain) will be used. The state vector  $\mathbf{z}_r$  for mode  $r$  can be defined as

$$\mathbf{z}_r = \begin{bmatrix} z_r(t) \\ \dot{z}_r(t) \end{bmatrix} \quad (3.38)$$

Equation (3.12) can be reformulated in state space as

$$\dot{\mathbf{z}}_r = \mathbf{A}_r \mathbf{z}_r + \mathbf{b}_{r1}(t) + \mathbf{b}_{r2}(t) + \mathbf{b}_{r3}(t) \quad (3.39)$$

$$\mathbf{z}_r(0) = \mathbf{0}$$

$$\mathbf{A}_r = \begin{bmatrix} 0 & 1 \\ -\omega_r^2 & -2\xi_r \omega_r \end{bmatrix} \quad (3.40)$$

$$\mathbf{b}_{r1}(t) = -\mathbf{u}_r^T \mathbf{f}_1 \begin{bmatrix} 0 \\ 1 \end{bmatrix} \ddot{q}_x(t) \quad (3.41)$$

$$\mathbf{b}_{r2}(t) = -\mathbf{u}_r^T \mathbf{f}_2 \begin{bmatrix} 0 \\ 1 \end{bmatrix} \ddot{q}_y(t) \quad (3.42)$$

$$\mathbf{b}_{r3}(t) = -\mathbf{u}_r^T \mathbf{f}_3 \begin{bmatrix} 0 \\ 1 \end{bmatrix} \ddot{q}_\theta(t) \quad (3.43)$$

The transition matrix  $\Phi_r(t)$  for equation (3.39) can be obtained using the relationship found in Iwan and Ho (1989). The solution of equation (3.39) for the state  $\mathbf{z}_r$  is obtained as

$$\mathbf{z}_r = \int_0^t \Phi_r(t - \tau) (\mathbf{b}_{r1}(\tau) + \mathbf{b}_{r2}(\tau) + \mathbf{b}_{r3}(\tau)) d\tau \quad (3.44)$$

Using equations (3.44), the cross covariance matrix of the response of the state-r and the state-s is given as

$$\begin{aligned} \mathbf{R}_{rs}(t) &= E\{\mathbf{z}_r(t) \mathbf{z}_s^T(t)\} \\ &= \int_0^t \Phi_r(t - \tau) E\{[\mathbf{b}_{r1}(\tau) + \mathbf{b}_{r2}(\tau) + \mathbf{b}_{r3}(\tau)] [\mathbf{b}_{s1}(\tau) + \mathbf{b}_{s2}(\tau) + \mathbf{b}_{s3}(\tau)]^T\} \Phi_s^T(t - \tau) d\tau \end{aligned} \quad (3.45)$$

Application of equations (3.4), (3.5), (3.6), (3.41), (3.42), and (3.43) in equation (3.45) gives

$$\begin{aligned} & E\{[\mathbf{b}_{r1}(\tau)+\mathbf{b}_{r2}(\tau)+\mathbf{b}_{r3}(\tau)] [\mathbf{b}_{s1}(\tau) + \mathbf{b}_{s2}(\tau) + \mathbf{b}_{s3}(\tau)]^T\} \\ &= \mathbf{u}_r^T [\mathbf{f}_1 \mathbf{u}_s^T \mathbf{f}_1 \Omega_x^2(\tau) S_{0x} + \mathbf{f}_2 \mathbf{u}_s^T \mathbf{f}_2 \Omega_y^2(\tau) S_{0y} + \mathbf{f}_3 \mathbf{u}_s^T \mathbf{f}_3 \Omega_\theta^2(\tau) S_{0\theta}] \Psi \end{aligned} \quad (3.46)$$

where

$$\Psi = \begin{bmatrix} 0 & 0 \\ 0 & 1 \end{bmatrix}. \quad (3.47)$$

By algebraic manipulation, equation (3.45) can be written as

$$\mathbf{R}_{rs}(t) = \mathbf{L}_r \mathbf{G}_{rs}(t) \mathbf{L}_s^T \quad (3.48)$$

$$\begin{aligned} \mathbf{G}_{rs}(t) = & [\mathbf{u}_r^T (\mathbf{f}_1 \mathbf{u}_s^T \mathbf{f}_1 S_{0x} \int_0^t \Omega_x^2(t-\tau) + \mathbf{f}_2 \mathbf{u}_s^T \mathbf{f}_2 S_{0y} \int_0^t \Omega_y^2(t-\tau) + \mathbf{f}_3 \mathbf{u}_s^T \mathbf{f}_3 S_{0\theta} \int_0^t \Omega_\theta^2(t-\tau))] \\ & \mathbf{p}_r(\tau) \mathbf{p}_s^T(\tau) d\tau \end{aligned} \quad (3.49)$$

$$\mathbf{L}_s = \begin{bmatrix} 0 & \frac{1}{\omega_{ds}} \\ 1 & -\xi_s \frac{\omega_s}{\omega_{ds}} \end{bmatrix} \quad (3.50)$$

$$\mathbf{L}_r = \begin{bmatrix} 0 & \frac{1}{\omega_{dr}} \\ 1 & -\xi_r \frac{\omega_r}{\omega_{dr}} \end{bmatrix} \quad (3.51)$$

$$\mathbf{p}_s(t) = \begin{bmatrix} e^{-\xi_s \omega_s t} \cos(\omega_{ds} t) \\ e^{-\xi_s \omega_s t} \sin(\omega_{ds} t) \end{bmatrix} \quad (3.52)$$

$$\mathbf{p}_r(t) = \begin{bmatrix} e^{-\xi_r \omega_r t} \cos(\omega_{dr} t) \\ e^{-\xi_r \omega_r t} \sin(\omega_{dr} t) \end{bmatrix} \quad (3.53)$$

$$\omega_{ds} = \omega_s \sqrt{1 - \xi_s^2} \quad (3.54)$$

$$\omega_{dr} = \omega_r \sqrt{1 - \xi_r^2}. \quad (3.55)$$

The terms  $\mathbf{L}_s$  and  $\mathbf{L}_r$  are constant matrices which depend on the system parameters. The integrals involved in the computation of the elements of the matrix  $\mathbf{G}_{rs}(t)$  can be obtained from standard integration tables (Beyer, 1987). By replacing the subscript  $s$  in equation (3.48) by  $r$  the covariance matrix of state  $r$   $\mathbf{R}_{rr}(t) = E\{\mathbf{z}_r(t) \mathbf{z}_r^T(t)\}$  can be computed. The components of the state covariance matrices  $\mathbf{R}_{rr}(t)$ ,  $\mathbf{R}_{ss}(t)$ , and  $\mathbf{R}_{rs}(t)$  can be reassembled into the modal covariance matrices  $\mathbf{R}_{\underline{z}}(t)$ ,  $\mathbf{R}_{\underline{z}}(t)$ , and  $\mathbf{R}_{\underline{z}}(t)$ . The covariance matrices of the joint motion

vector  $\mathbf{q}$  defined as  $\mathbf{R}_{\mathbf{q}\mathbf{q}}(t)$  can be obtained using the modal transformation matrix  $\mathbf{U}$  (equation (3.9)) as

$$\mathbf{R}_{\mathbf{q}\mathbf{q}}(t) = E\{\mathbf{q}(t)\mathbf{q}^T(t)\} = E\{(\mathbf{U}\mathbf{z}(t))(\mathbf{U}\mathbf{z}(t))^T\} = \mathbf{U}\mathbf{R}_{\mathbf{z}\mathbf{z}}(t)\mathbf{U}^T \quad (3.56)$$

Similarly the covariance matrix of the joint velocities  $\dot{\mathbf{q}}$  is given as

$$\mathbf{R}_{\dot{\mathbf{q}}\dot{\mathbf{q}}}(t) = \mathbf{U}E\{\dot{\mathbf{z}}(t)\dot{\mathbf{z}}^T(t)\}\mathbf{U}^T = \mathbf{U}\mathbf{R}_{\dot{\mathbf{z}}\dot{\mathbf{z}}}(t)\mathbf{U}^T \quad (3.57)$$

### 3.5. Covariance Tensors of the Tip Responses

Before discussing the responses of the manipulator tip it is important to note that in this work each link of the manipulator structures can be assigned a Cartesian coordinate frame. The coordinate frame for each link should be attached to the end of that link (see for example the base and the tip link on Figure 3.1)

In the following discussion only the nonstationary response is presented. Details on how to obtain the stationary response is discussed at the end of the section. A Jacobian  $\mathbf{J}$  relating the joint motion  $\mathbf{q}$  to the tip motion vector  $\mathbf{x}$  can be applied to compute the latter, i.e.

$$\mathbf{x} = \mathbf{J}\mathbf{q} \quad (3.58)$$



The covariance matrix of the manipulator tip displacement can be expressed in any Cartesian coordinate frame (for example frame  $\mathbf{x}_0 = [x_0, y_0]$  attached to the base) through the Jacobian associated with this frame  $\mathbf{J}_0$  as

$$\mathbf{R}_{\mathbf{x}_0\mathbf{x}_0}(t) = E\{\mathbf{x}_0\mathbf{x}_0^T\} = \mathbf{J}_0 E\{\mathbf{q}(t)\mathbf{q}^T(t)\}\mathbf{J}_0^T = \mathbf{J}_0 \mathbf{R}_{\mathbf{q}\mathbf{q}}(t)\mathbf{J}_0^T \quad (3.59)$$

Similarly the covariance tensor of the manipulator tip velocities in the base frame is

$$\mathbf{R}_{\dot{\mathbf{x}}_0\dot{\mathbf{x}}_0} = E\{\dot{\mathbf{x}}_0\dot{\mathbf{x}}_0^T\} = \mathbf{J}_0 E\{\dot{\mathbf{q}}(t)\dot{\mathbf{q}}^T(t)\}\mathbf{J}_0^T = \mathbf{J}_0 \mathbf{R}_{\dot{\mathbf{q}}\dot{\mathbf{q}}}(t)\mathbf{J}_0^T. \quad (3.60)$$

The rotation matrix transforming the Cartesian base coordinate frame  $\mathbf{x}_0$  to the  $i$ -th frame  $\mathbf{x}_i$  is defined as  $\mathbf{Rot}_0^i$  and

$$\mathbf{J}_0 = \mathbf{Rot}_0^i \mathbf{J}_i. \quad (3.61)$$

By substituting equation (3.61) in equation (3.59) the covariance matrix of the tip displacement in the Cartesian frame  $\mathbf{x}_i$  can be obtained as

$$\mathbf{R}_{\mathbf{x}_i\mathbf{x}_i}(t) = (\mathbf{Rot}_0^i)^T \mathbf{R}_{\mathbf{x}_0\mathbf{x}_0}(t)\mathbf{Rot}_0^i \quad (3.62)$$

Similarly, the covariance matrix of the tip velocity in  $\mathbf{x}_i$  frame is given as

$$\mathbf{R}_{\dot{\mathbf{x}}_i\dot{\mathbf{x}}_i}(t) = (\mathbf{Rot}_0^i)^T \mathbf{R}_{\dot{\mathbf{x}}_0\dot{\mathbf{x}}_0}(t)\mathbf{Rot}_0^i \quad (3.63)$$

In particular, a rotated frame  $\mathbf{x}_*$  in which the covariance matrix of the tip displacement is diagonal can be used. This frame will be referred to as the

principal variance frame. The principal Jacobian matrix  $\mathbf{J}_*$  can be defined as the Jacobian associated with the principal variance frame i.e.

$$\mathbf{R}_{\mathbf{x},\mathbf{x}_*}(t) = \mathbf{J}_* \mathbf{R}_{\mathbf{q}\mathbf{q}}(t) \mathbf{J}_*^T \quad (3.64)$$

where  $\mathbf{R}_{\mathbf{x},\mathbf{x}_*}(t)$  is the principal variance matrix and it is a positive definite diagonal matrix. To compute the principal variance matrix  $\mathbf{R}_{\mathbf{x},\mathbf{x}_*}(t)$  singular value decomposition of the tip displacement covariance matrix in a known frame, for example  $\mathbf{R}_{\mathbf{x}_0\mathbf{x}_0}(t)$  is employed (see Section 2.4) and this process leads to

$$\mathbf{R}_{\mathbf{x}_0\mathbf{x}_0}(t) = (\mathbf{Rot}_0^*) \Sigma_{\mathbf{x}_0}(t) (\mathbf{Rot}_0^*)^T \quad (3.65)$$

where  $\mathbf{Rot}_0^*$  is an orthonormal matrix. The diagonal matrix  $\Sigma_{\mathbf{x}_0}$  contains the eigenvalues of  $\mathbf{R}_{\mathbf{x}_0\mathbf{x}_0}(t)$  and its elements represents the principal variance of the tip displacements  $\mathbf{R}_{\mathbf{x},\mathbf{x}_*}(t)$  i.e.

$$\mathbf{R}_{\mathbf{x},\mathbf{x}_*}(t) = \Sigma_{\mathbf{x}_0}(t) \quad (3.66)$$

The principal variance matrix of the tip displacement contains the maximum and the minimum variance of the tip displacement due to the nonstationary base excitation. The direction cosines of the principal variance of the nonstationary tip response -principal Cartesian coordinate- is given by the columns of orthonormal matrix  $\mathbf{Rot}_0^*$ .

Similar by applying the singular value decomposition theorem to the tip velocity in a known Cartesian frame, the principal variance of the nonstationary tip velocity can be obtained

$$\mathbf{R}_{\dot{\mathbf{x}},\dot{\mathbf{x}}}(t) = \Sigma_{\dot{\mathbf{x}}_0}(t) \quad (3.67)$$

A similar procedure as outline in this section can be used to develop expressions for the stationary random response of the manipulator tip displacement and velocity. In this case the time variable  $t$  is zero i.e.  $t = 0$ .

### 3.6. Summary and Concluding Remarks

In this chapter the equation of motion of a manipulator attached to a non-wheeled mobile base has been developed using the Lagrange's principle. The base on which the manipulator structure is mounted is assumed to be so much more massive than the manipulator that the dynamics of the structure does not practically influence the base. The base is subjected to stochastic motion which couples kinematically as excitations into the dynamics of the manipulator structure. This coupling involves the acceleration vector of the base motion.

Expressions for the covariance tensors of the joint motions have been derived. Further, by using the kinematic relation between the joint motion and the manipulator tip motion, expressions for the covariance matrices of the tip motion have been obtained. Transformations which can be used to relate the covariance

matrices in various coordinate frames have been derived. The singular value decomposition theorem has been used to develop expressions for the principal variances and principal coordinate directions of the tip motion. The above expressions have been developed for the stationary and the nonstationary responses. Two examples and numerical simulations are presented in the next chapter to illustrate the analysis discussed in this chapter.

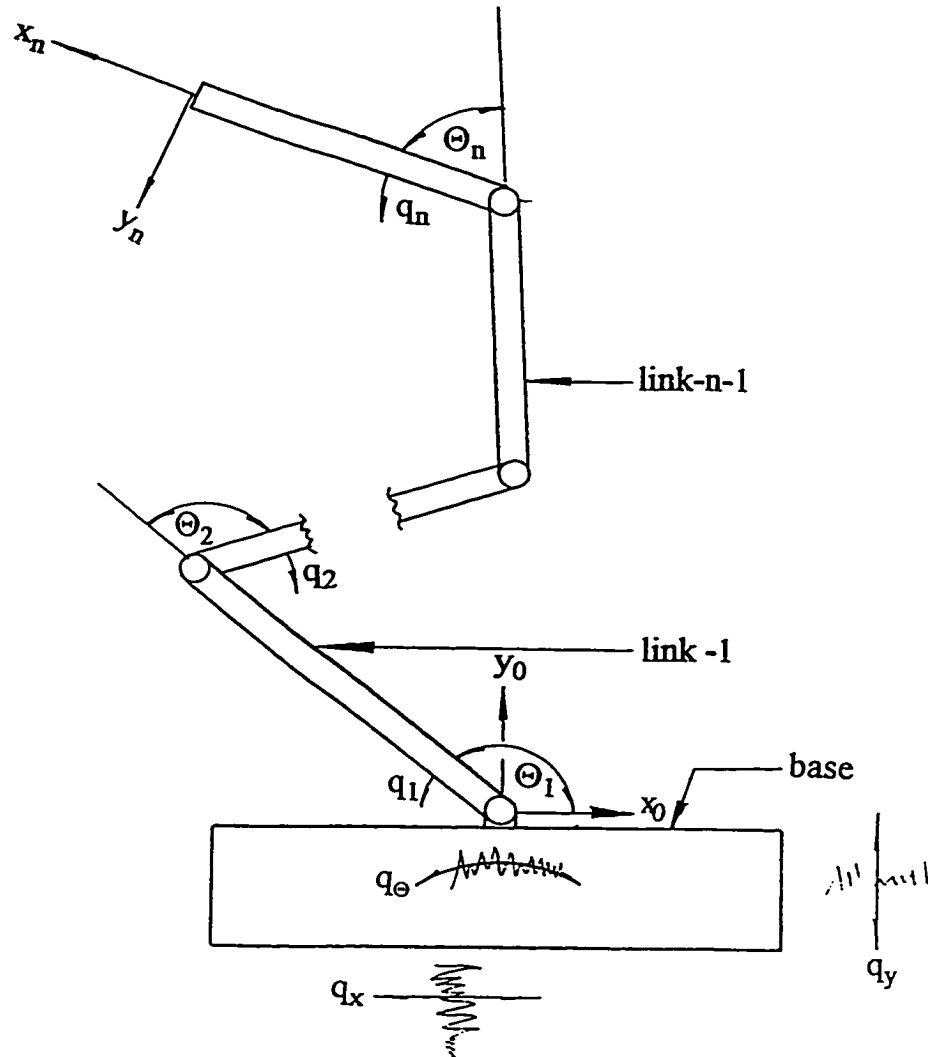


Figure 3.1. Model of a Non-wheeled Mobile Manipulator

- $\Theta_i$   $i$ -th kinematic configuration
- $q_i$   $i$ -th elastic motion variable
- $(x,y)_i$  Cartesian coordinate frame attached to the  $i$ -th link

## Chapter Four

### NON-WHEELED MOBILE MANIPULATOR, EXAMPLES

#### 4.1. Introduction

Two examples are presented in this chapter to illustrate the method discussed in chapter three. A dimensionless time  $\bar{t}$  is introduced to generalize the results where  $\bar{t}$  is defined as

$$t = \sqrt{\frac{a_i}{k_i}} \bar{t} \quad (4.1)$$

$$\frac{d}{dt} = \sqrt{\frac{k_i}{a_i}} \frac{d}{d\bar{t}} \quad (4.2)$$

$$\frac{d^2}{dt^2} = \frac{k_i}{a_i} \frac{d^2}{d\bar{t}^2} \quad (4.3)$$

$a_i$  and  $k_i$  are the  $i$ -th inertia and stiffness terms respectively. It is assumed that the massive base is excited only in the vertical direction i.e.  $\ddot{q}_0(t) = \ddot{q}_x(t) = 0$ .

## 4.2. Examples of Excitation Models

### Representation of the Stationary Base Excitation:

The power spectrum representation of the excitation used has the form as suggested by Chang and Young (1989)

$$S_{\ddot{q}_y \ddot{q}_y} = S_{0y} \quad (4.4)$$

where  $S_{0y}$  is a positive constant i.e.  $\ddot{q}_y(t)$  is a white noise.

### Representation of the Nonstationary Base Excitation:

The modulating function for the nonstationary base excitation model has the form as suggested by To (1986) i.e.

$$\Omega_y(t) = Wu(t) (e^{-\alpha_1 t} - e^{-\alpha_2 t}) \quad (4.5)$$

where  $W$ ,  $\alpha_1$ ,  $\alpha_2$  with  $\alpha_1 < \alpha_2$  are positive constants and  $u(t)$  is a unit step function.

## 4.3. Example 1: Single Link Flexible Manipulator

Consider the manipulator of Figure 4.1 excited by the base random motion  $q_y$ . The Lagrangian  $L$  and the Rayleigh dissipation function  $R$  for the system are

$$L = \frac{1}{2} (m_1) \dot{q}_y^2 + \frac{1}{2} a_1 \dot{q}_1^2 + a_2 \dot{q}_y \dot{q}_1 \cos(\Theta_1) - \frac{1}{2} k_1 q_1^2 \quad (4.6)$$

$$R = \frac{1}{2} c_1 \dot{q}_1^2 \quad (4.7)$$

$$a_1 = I_1 + m_1 l_{c1}^2 \quad (4.8)$$

$$a_2 = m_1 l_{c1} \quad (4.9)$$

Lagrangian principle (equation (2.6)) can be used to derive the equation of motion for the system (equation (3.7)). Introducing the dimensionless time  $\bar{t}$ , the equation of motion becomes

$$\ddot{q}_1(\bar{t}) + 2\xi\dot{q}_1(\bar{t}) + q_1(\bar{t}) = -\bar{a}_2 \cos(\Theta_1)\ddot{q}_y(\bar{t}) \quad (4.10)$$

$$2\xi = \frac{c_1}{\sqrt{a_1 k_1}} \quad (4.11)$$

$$\bar{a}_2 = \frac{a_1}{a_2}, \quad (4.12)$$

The Jacobian matrix relating the tip motion to the joint motion in the base frame is (see Appendix C)

$$\mathbf{J}_0 = \begin{bmatrix} -l_1 \sin(\Theta_1) \\ l_1 \cos(\Theta_1) \end{bmatrix} \quad (4.13)$$

### Stationary Response:

Using the procedure developed in Chapter three, and the excitation model defined in equation (4.4), the covariance matrices of the system displacements can be obtained:



Joint Variance (see equations 3.35 and 3.36)

$$\mathbf{R}_{q_1 q_1}(0) = S_{0y} \bar{a}_2^2 \frac{\pi}{2\xi} \cos^2(\Theta_1) \quad (4.14)$$

Tip Covariance Matrices:

The covariance matrix of the manipulator tip displacement in the Cartesian base frame  $\mathbf{x}_0 = [x_0, y_0]^T$  (see equations 3.59) is

$$\mathbf{R}_{\mathbf{x}_0 \mathbf{x}_0}(0) = l_1^2 \cos^2(\Theta_1) S_{0y} \bar{a}_2^2 \frac{\pi}{2\xi} \Delta(\Theta_1) \quad (4.15)$$

$$\Delta(\Theta_1) = \cos^2(\Theta_1) \begin{bmatrix} \sin^2(\Theta_1) & -\cos(\Theta_1)\sin(\Theta_1) \\ -\cos(\Theta_1)\sin(\Theta_1) & \cos^2(\Theta_1) \end{bmatrix} \quad (4.16)$$

The principal variance matrix of tip displacement can be obtained (see equation 3.66). This is done by taking the singular values of  $\Delta(\Theta_1)$  matrix.

$$\mathbf{R}_{\mathbf{x}, \mathbf{x}}(0) = l_1^2 \cos^2(\Theta_1) S_{0y} \bar{a}_2^2 \frac{\pi}{2\xi} \varphi(\Theta_1) \quad (4.17)$$

$$\varphi(\Theta_1) = \cos^2(\Theta_1) \begin{bmatrix} 0 & 0 \\ 0 & 1 \end{bmatrix} \quad (4.18)$$

**Nonstationary Response:**

Joint Variance (see equation 3.48)

$$\mathbf{R}_{q_1 q_1}(\bar{t}) = S_{0y} \bar{a}_2^2 \frac{1}{1-\xi^2} \cos^2(\Theta_1) \Lambda(\bar{t}) \quad (4.19)$$

where the expression  $\Lambda(\bar{t})$  is obtained using Bayer(198) and is given as

$$\begin{aligned}
\Lambda(\bar{t}) = & \frac{e^{-2\xi\bar{t}} - e^{-2\alpha_1\bar{t}}}{4(\alpha_1 - \xi)} + \frac{e^{-2\xi\bar{t}} - e^{-2\alpha_2\bar{t}}}{4(\alpha_2 - \xi)} - \left( \frac{e^{-2\xi\bar{t}} - e^{-(\alpha_1+\alpha_2)\bar{t}}}{\alpha_1 + \alpha_2 - 2\xi} \right) \\
& - \frac{e^{-2\xi\bar{t}}[(\sqrt{1-\xi^2})\sin(2(\sqrt{1-\xi^2})\bar{t}) + (\alpha_1-\xi)\cos(2(\sqrt{1-\xi^2})\bar{t})]}{4[\alpha_1^2 + 1 - 2\alpha_1\xi]} + \frac{e^{-2\alpha_1\bar{t}}[(\alpha_1-\xi)]}{4[\alpha_1^2 + 1 - 2\alpha_1\xi]} \\
& - \frac{e^{-2\xi\bar{t}}[(\sqrt{1-\xi^2})\sin(2(\sqrt{1-\xi^2})\bar{t}) + (\alpha_2-\xi)\cos(2(\sqrt{1-\xi^2})\bar{t})]}{4[\alpha_2^2 + 1 - 2\alpha_2\xi]} + \frac{e^{-2\alpha_2\bar{t}}[(\alpha_2-\xi)]}{4[\alpha_2^2 + 1 - 2\alpha_2\xi]} \\
& + \frac{e^{-2\xi\bar{t}}[(\sqrt{1-\xi^2})\sin(2(\sqrt{1-\xi^2})\bar{t}) + (\alpha_1 + \alpha_2 - 2\xi)\cos(2(\sqrt{1-\xi^2})\bar{t})]}{[\alpha_1^2 + \alpha_2^2 - 4(1 - \alpha_1\xi - \alpha_2\xi)]} \\
& - \frac{e^{-(\alpha_1+\alpha_2)\bar{t}}[(\alpha_1+\alpha_2-2\xi)]}{[\alpha_1^2 + \alpha_2^2 - 4(1 - \alpha_1\xi - \alpha_2\xi)]}. \tag{4.20}
\end{aligned}$$

### Tip Covariance Matrices:

The covariance Matrix of the manipulator tip displacement in the base frame  $\mathbf{x}_0 = [x_0, y_0]^T$  is

$$\mathbf{R}_{\mathbf{x}_0\mathbf{x}_0}(\bar{t}) = r_1^2 S_{0y} \bar{a}_2^{-2} \frac{1}{1-\xi^2} \cos^2(\Theta_1) \Lambda(\bar{t}) \Delta(\Theta_1) \tag{4.21}$$

$\Delta(\Theta_1)$  is defined in equation (4.15). The principal variance of tip displacement can be obtained (equation 3.66) as

$$\mathbf{R}_{x,x}(\bar{t}) = l^2 \cos^2(\Theta_1) S_{0y} \frac{a_2^2}{1-\xi^2} \Lambda(\bar{t}) \varphi(\Theta_1) \quad (4.22)$$

$\varphi(\Theta_1)$  is defined in equation (4.18). Using the method developed in Chapter three (section 3.5), it can be shown that for the stationary and the nonstationary tip displacements there is only one direction in which the maximum variance is reached. The direction cosine of this principal direction can be found as

$$\text{Rot}_0^* = \frac{1}{\sqrt{1+\tan^2(\Theta_1)}} \begin{bmatrix} \tan(\Theta_1) \\ 1 \end{bmatrix} \pm 180^\circ \quad (4.23)$$

The highest value of the principal variance of the tip displacement occurs at  $\Theta_1 = 0$ .

#### 4.4. Example 2: Two Link Flexible Manipulator

The Lagrangian for the two-link manipulator system of Figure 4.2 is

$$\begin{aligned} L = & \frac{1}{2} a_0 \dot{q}_y^2 + \frac{1}{2} a_1 \dot{q}_1^2 + \frac{1}{2} a_2 (\dot{q}_1 + \dot{q}_2)^2 + a_3 \dot{q}_1 (\dot{q}_1 + \dot{q}_2) \cos(\Theta_2 + q_2) \\ & + a_5 \dot{q}_y \dot{q}_1 \cos(\Theta_1 + q_1) + a_4 \dot{q}_y (\dot{q}_1 + \dot{q}_2) \cos(\Theta_1 + q_1 + \Theta_2 + q_2) \\ & - \frac{1}{2} k_1 q_1^2 - \frac{1}{2} k_2 q_2^2 \end{aligned} \quad (4.24)$$

$$a_0 = m_1 + m_2 + m_b \quad (4.25)$$

$$a_1 = I_1 + m_1(l_{c1})^2 + m_2(l_2)^2 + I_2 + m_2(l_{c2})^2 \quad (4.26)$$

$$a_2 = I_2 + m_2(l_{c2})^2 \quad (4.27)$$

$$a_3 = m_2(l_{c2}l_1) \quad (4.28)$$

$$a_5 = m_1(l_{c1}) + m_2(l_1) \quad (4.29)$$

$$a_4 = m_2(l_{c2}). \quad (4.30)$$

The Rayleigh dissipation function  $R$  for the system is given as

$$R = \frac{1}{2}c_1\dot{q}_1^2 + \frac{1}{2}c_2\dot{q}_2^2 \quad (4.31)$$

The detail derivation of the equation of motion using Lagrange principle is given in Appendix B. The elements of the resulting system matrices are given below.

#### Elements of the inertia matrix

$$\mathbf{D} = \begin{bmatrix} D_{11} & D_{12} \\ D_{21} & D_{22} \end{bmatrix}$$

$$D_{11} = a_1 + 2a_3 \cos(\Theta_2) \quad (4.32)$$

$$D_{12} = a_2 + a_3 \cos(\Theta_2) \quad (4.33)$$

$$D_{21} = a_2 + a_3 \cos(\Theta_2) \quad (4.34)$$

$$D_{22} = a_2 \quad (4.35)$$

#### Elements of the stiffness matrix

$$\mathbf{K} = \begin{bmatrix} K_{11} & K_{12} \\ K_{21} & K_{22} \end{bmatrix}$$

$$K_{11} = k_1 \quad (4.36)$$

$$K_{22} = k_2 \quad (4.37)$$

$$K_{ij} = 0 \quad \text{for } i \neq j \quad (4.38)$$

Elements of the damping matrix

$$\mathbf{C} = \begin{bmatrix} C_{11} & C_{12} \\ C_{21} & C_{22} \end{bmatrix}$$

$$C_{11} = c_1 \quad (4.39)$$

$$C_{22} = c_2 \quad (4.40)$$

$$C_{ij} = 0 \quad \text{for } i \neq j \quad (4.41)$$

Elements of the dynamic coupling vector

$$\mathbf{f}_2 = \begin{bmatrix} f_{21} \\ f_{22} \end{bmatrix}$$

$$f_{21} = a_5 \cos(\Theta_1) + a_4 \cos(\Theta_1 + \Theta_2) \quad (4.42)$$

$$f_{22} = a_4 \cos(\Theta_1 + \Theta_2) \quad (4.43)$$

The resulting dimensionless matrices (see section 4.1) are

$$\bar{\mathbf{D}} = \frac{1}{a_1} \mathbf{D} \quad (4.44)$$

$$\bar{\mathbf{C}} = \frac{1}{\sqrt{a_1 k_1}} \mathbf{C} \quad (4.45)$$

$$\bar{\mathbf{K}} = \frac{1}{k_1} \mathbf{K} \quad (4.46)$$

$$\bar{\mathbf{f}}_2 = \frac{1}{a_1} \mathbf{f}_2. \quad (4.47)$$

The Jacobian matrix of the tip motion in the base frame  $\mathbf{x}_0 = [x_0, y_0]^T$  is given as

$$\mathbf{J}_0 = \begin{bmatrix} J_{11} & J_{12} \\ J_{21} & J_{22} \end{bmatrix} \quad (4.48)$$

$$J_{11} = -l_1 \sin(\Theta_1) - l_2 \sin(\Theta_1 + \Theta_2) \quad (4.49)$$

$$J_{12} = -l_2 \sin(\Theta_1 + \Theta_2) \quad (4.50)$$

$$J_{21} = l_1 \cos(\Theta_1) + l_2 \cos(\Theta_1 + \Theta_2) \quad (4.51)$$

$$J_{22} = l_2 \cos(\Theta_1 + \Theta_2) \quad (4.52)$$

Detailed derivation of the elements of the Jacobian matrix  $\mathbf{J}_0$  is given in Appendix C. Using the procedure outlined in section 3.3 to section 3.5 the stationary and the nonstationary responses can be computed. The contour integrals required for computing the stationary responses (equations 3.36 and 3.37) using the white noise excitation (equation 4.4) are derived in Appendix D and are derived in Section D2 (equations (D.7), (D.18), (D.23) and (D.30)). The formulae required for obtaining the nonstationary responses (equation 3.48) using the modulated white noise excitation are given in Appendix E. The nonstationary and the stationary joint and tip responses have been computed numerically.

## 4.5. Numerical Simulation

Programs to simulate the random vibration of the joint and the tip motion of non-wheeled two-link mobile flexible manipulator under stochastic base excitation has been developed. The flow chart for the programs are shown at the end of the chapter (Figures 4.14 and 4.15). For the sake of simplicity in the simulation, it is assumed that the links of the manipulators are uniform cylinders of lengths  $l_1 = l_2 = 1$  m, masses  $m_1 = m_2 = m$  kg and stiffness  $k_1 = k_2 = k$  N/m, where  $k$  and  $m$  can have any arbitrary values. The parameters  $W$ ,  $\alpha_1$  and  $\alpha_2$  of the modulating function  $\Omega_y(\bar{t})$  used in the nonstationary responses have the values of 15, 0.1, and 0.5 respectively. Figure 4.3 displays a plot of the modulating function  $\Omega_y(\bar{t})$  used for simulation. The variance and covariances depicted in subsequent figures have been normalized by the intensity of the white noise  $S_0$ .

### 4.5.1. Joint Response

The statistical characteristics of a nonstationary response are time varying, therefore for the discussion in this section, the figures are made for a time instant of  $t = 20$ . Figure 4.4 is made for the specified values of  $\Theta_1$  and  $\Theta_2 \pm 180^\circ$  range of one degree incremental values of  $\Theta_2$ . It shows the variances of joint 1 displacements. The variances of joint 2 response is shown in Figure 4.5. It can be noticed that the smaller the value of  $\Theta_1$  the larger the variance of joint 1 and this is always greater than the variance of joint 2. The variances have zero values at the configuration  $\Theta_1 = 90^\circ$ ,  $\Theta_2 = 0^\circ$  since the manipulator moves as a rigid body at this configuration. The covariance of the joint displacement is shown in Figure 4.6. It is observed that at the configuration of  $\Theta_2$  of about  $\pm 130^\circ$  the covariance of the

joint displacement is zero. This result can be interpreted as follows. As the absolute value of the angle  $\Theta_2$  between the two links increases from zero and approaches  $130^\circ$ , at about this configuration a mode reversal takes place. Before  $130^\circ$ , at about  $126^\circ$  for example, the modal matrix  $U$  and the corresponding natural frequency vector  $\omega$  are given as

$$U = \begin{bmatrix} 1.109 & 0.106 \\ 0.059 & -2.004 \end{bmatrix} \quad (4.53)$$

$$\omega = \begin{bmatrix} 0.498 \\ 0.900 \end{bmatrix} \quad (4.54)$$

At about  $132^\circ$  the modal matrix  $U$  becomes diagonal and the mass normalized modal matrix  $U$  becomes a unit matrix (see equation (3.8)) i.e.

$$U = \begin{bmatrix} 1.0 & 0.0 \\ 0.0 & 1.0 \end{bmatrix} \quad (4.55)$$

$$\omega = \begin{bmatrix} 0.500 \\ 0.866 \end{bmatrix} \quad (4.56)$$

It has been discovered that, physically this means that in the first mode of motion joint 2 does not move and the whole manipulator moves as a rigid body about joint 1 (see Figure 4.7a). In the second mode joint 1 does not move therefore link 1 is stationary and only link 2 experiences motion about joint 2 (see Figure 4.7b). During a forced motion of the manipulator at this mode reversal configuration the



first normal coordinate  $z_1$  contributes only to the motion of joint 1, i.e., to the motion  $q_1$ ; and the second normal coordinate  $z_2$  contributes only to the motion of joint 2 i.e. to the motion  $q_2$ . It means that the joint coordinates  $q$  are now normal coordinates as well. Therefore the joint motion is decoupled. Hence in the equation of motion (3.7) the dynamic coupling terms vanish. For the chosen set of motion coordinates the coupling between the joint motion is manifested by the diagonal terms of the inertia matrix  $\mathbf{D}$ . Therefore the off diagonal terms of the inertia matrix become zero thus

$$D_{21} = D_{12} = a_2 + a_3 \cos(\Theta_2) = 0 \quad (4.57)$$

The solution of equation (4.57) provides an accurate value for the mode reversal angles as  $\Theta_2 = \pm 131.81^\circ$ . At the adjacent angles, to the mode reversal angle  $\Theta_2$  the modal parameters of each modal vector change their direction with respect to each other, for example at about  $136^\circ$

$$\mathbf{U} = \begin{bmatrix} 1.185 & 0.0 \\ -0.050 & 2.010 \end{bmatrix} \quad (4.58)$$

$$\boldsymbol{\omega} = \begin{bmatrix} 0.499 \\ 0.843 \end{bmatrix} \quad (4.59)$$

Therefore the covariance of the joint displacement change their signs.

### 4.5.2. Tip Response

In this section the response is plotted as an explicit function of time in order to show the time varying nature of the nonstationary response. Since, in practical applications, the maximum variance of the tip motion is of interest because it gives the highest effect of the excitation, the major principal variance of the tip motion will be discussed in this section (see equation 3.66). Figure 4.8 is made for the specified values of  $\Theta_1$  and  $\Theta_2 = 0^\circ$  and it shows the sensitivity of the tip response to changes in the manipulator configuration  $\Theta_1$ . It is observed that the more perpendicular the manipulator structure to the excitation, the higher the response to the excitation. Thus, the highest displacement occurs at  $\Theta_1 = \Theta_2 = 0^\circ$ . At this configuration the links of the manipulator are perpendicular to the stochastic base excitation  $q_v(t)$ . It is noted that the stochastic response at  $\Theta_1 = 90^\circ$  and  $\Theta_2 = 0^\circ$  is essentially zero since the links move as a rigid body. Subsequent plots are made for the configuration  $\Theta_1 = \Theta_2 = 0^\circ$ . The influence of the relative lengths of link-2 to link-1 on the response is shown in Figure 4.9. It can be observed that the longer the terminal link (link-2) compared to link-1, the higher the value of the tip response.

The sensitivity of the tip response to damping is shown in Figure 4.10. In both stationary and nonstationary cases the tip response can be reduced with the presence of damping. Figure 4.11 shows the computed and scaled values of the principal variance and their orientations for five configurations  $[\Theta_1, \Theta_2] = [0^\circ, 90^\circ], [45^\circ, 0^\circ], [45^\circ, 90^\circ], [90^\circ, 90^\circ]$  and  $[90^\circ, 0^\circ]$ . The principal variances are illustrated by the crossed line segments located at the manipulator tip. The major variance is very high compared to the minor variance i.e. the

stochastic motion of the manipulator tip is almost unidirectional though the direction is different for different configurations.

The effect of the cross coupling terms of the modal covariance  $\mathbf{R}_{rs}(t)$  of the normal modes on the tip response is shown in Figure 4.12. In the nonstationary case, for both low and high damping factors, there is no observable difference between the principal variance of tip motion, with and without the coupling terms. Thus, the coupling terms have no influence on the principal value of the tip response. On the other hand, for the stationary case, there is no observable difference at low damping, but there is a marked difference at high damping. Further, the nonstationary results obtained from the method developed in this thesis was compared with that obtained with the evolutionary spectrum method (To, 1984). The two methods yield the same results (Figure 4.13). The advantage of the presented method is its simplicity since it makes use of already existing standard integrals and yields both the velocity and displacement covariance simultaneously.

#### **4.6. Summary and Concluding Remarks**

To illustrate the ideas developed in Chapter three, the Lagrangian and the Rayleigh dissipation function for the single and the two links non-wheeled mobile manipulator have been developed. The Lagrangian principle has been used to develop the equation of motion for both systems. A dimensionless time variable has been introduced to generalize the results. For the single link manipulator,

closed form expressions for the covariance of the joint displacement and the covariance of the tip displacement in the base frame have been developed. Further, closed form expressions for the direction and magnitude of the principal variance of the tip displacements have been derived. It is noted that while the stationary response is time invariant the nonstationary response is time varying.

For the two link manipulator, numerical simulation has been undertaken to study the joint response and to evaluate the influence of the system parameters on the covariance of the tip response. For the joint response, it was noticed that the manipulator has a family of configurations at which a mode reversal takes place. The configurations are characterized by the mode reversal angle  $\Theta_2 = \pm 131.81^\circ$ . At these angles the covariance between the joint motion is zero since the joint motion is decoupled. Further, at the adjacent angles to the mode reversal angle the modal parameters of each modal vector change their direction with respect to each other therefore the covariance of the displacement changes sign.

Results from the sensitivity analysis of the tip motion show that the direction and the magnitude of the major motion varies significantly for different configurations and is almost unidirectional along the major principal variance axis. It can also be concluded that to minimize the maximum vibration of the tip motion the links must be damped. Further, the upper links should be shorter than the lower links.

It has been noted from the computed results that the cross coupling terms  $\mathbf{R}_{rs}$  of the modal response makes no significant contribution to the nonstationary

tip response. Therefore, to simplify computation, the cross coupling terms can be neglected. On the other hand, for the stationary tip response the cross coupling terms  $\mathbf{R}_{rs}$  should be included when the system has high damping. The technique developed in this thesis for the nonstationary response has been compared with the evolutionary spectrum technique (To, 1984). The results from both methods are the same, however, the presented method has the advantage of simplicity.

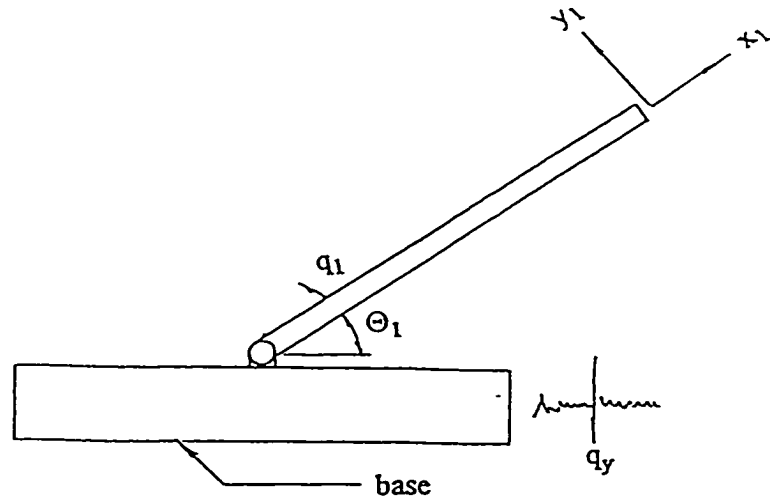


Figure 4.1. Single link Non-wheeled Mobile Manipulator

- $\Theta_1$  kinematic configuration of link 1
- $q_1$  elastic motion variable of link 1
- $(x,y)_1$  Cartesian coordinate frame attached to link 1

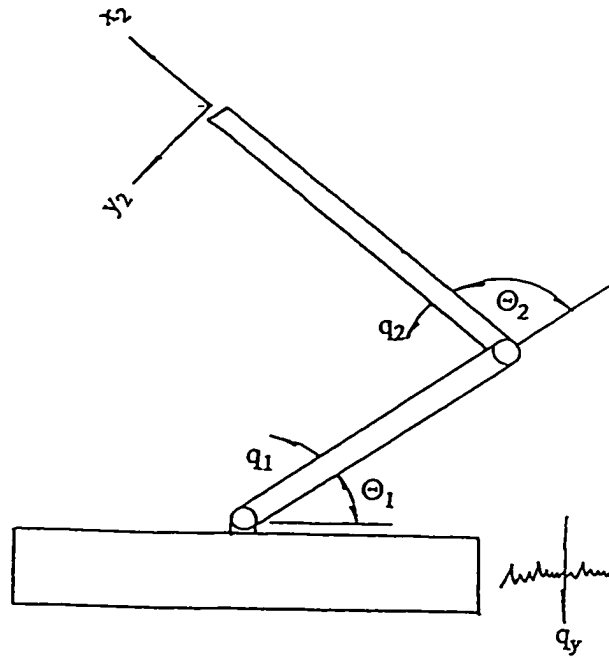


Figure 4.2. Two link Non-wheeled Mobile Manipulator

- $\Theta_1$  kinematic configuration of link 1
- $\Theta_2$  kinematic configuration of link 2
- $q_1$  elastic motion variable of link 1
- $q_2$  elastic motion variable of link 2
- $(x, y)_2$  Cartesian coordinate frame attached to link 2

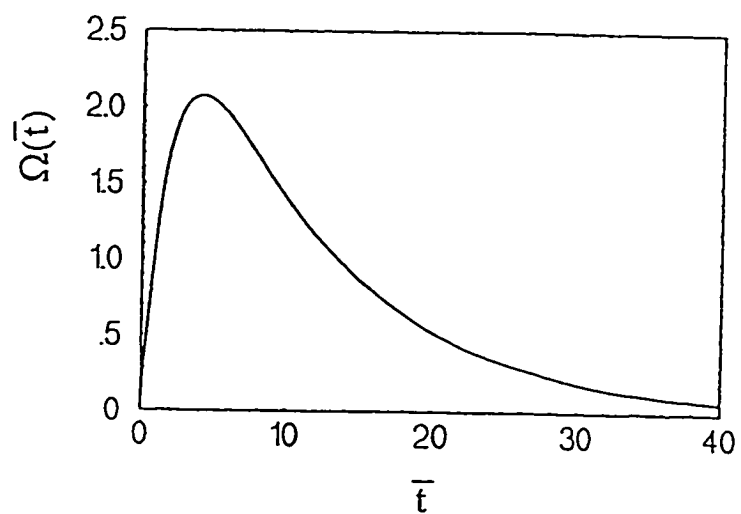
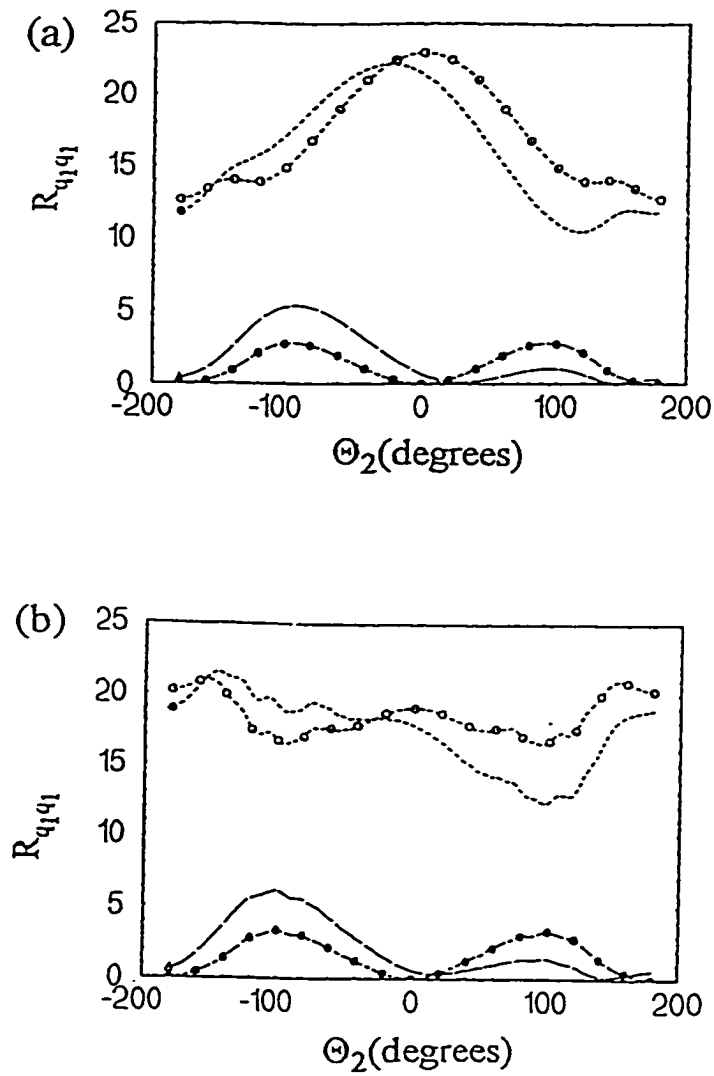


Figure 4.3. Plot of the Deterministic Modulating Function Used for Simulating the Nonstationary Stochastic Dynamics of a Non-wheeled Mobile Manipulator.





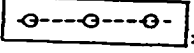



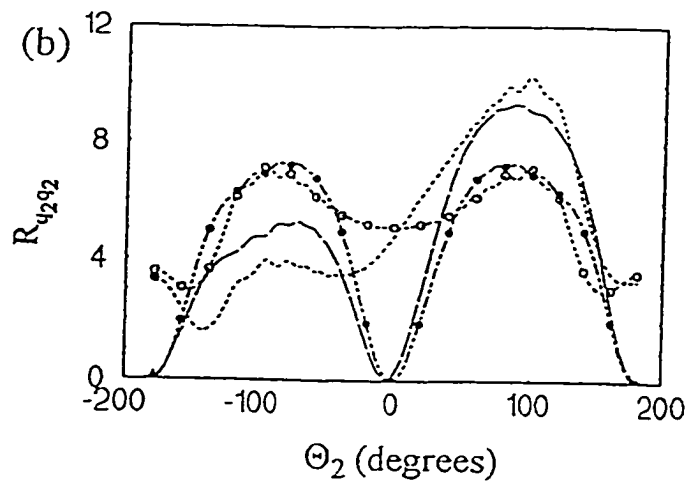
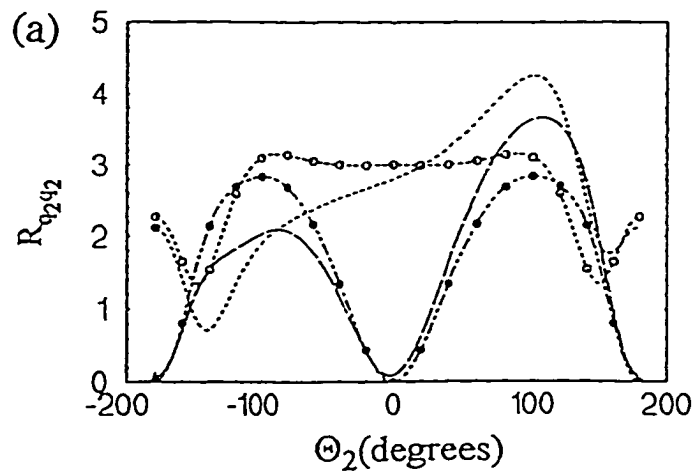
Legend for  $\Theta_1$ ,  $0^\circ$  ,  $15^\circ$  ,  $90^\circ$  ,  $80^\circ$  

Figure 4.4. Variance of the Joint-1  $R_{q_1 q_1}$  for specified values of  $\Theta_2$  and  $\pm 180^\circ$  range of  $\Theta_1$  of Non-wheeled Mobile Manipulator. The damping factor  $\xi = 0.001$ . (a) Stationary Response (b) Nonstationary Response at  $\bar{t} = 20$ .



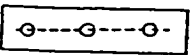
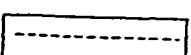
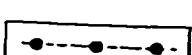
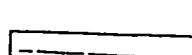
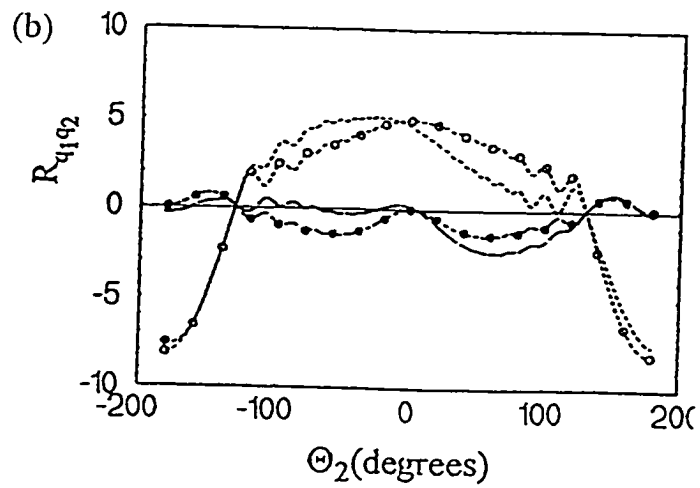
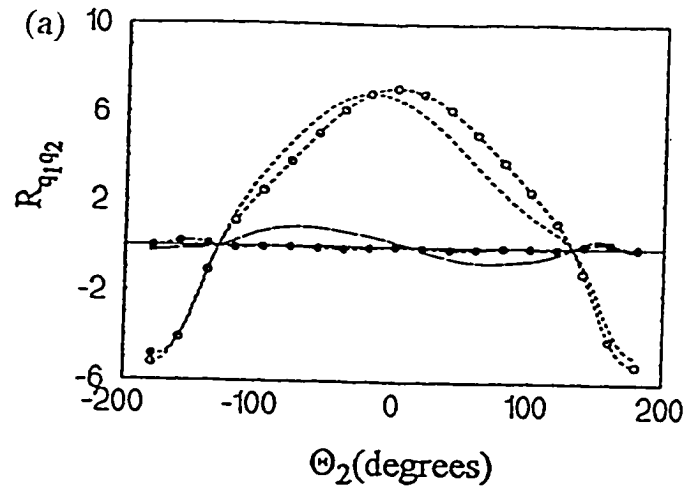
Legend for  $\Theta_1$ ,  $0^\circ$  ,  $15^\circ$  ,  $90^\circ$  ,  $80^\circ$  

Figure 4.5. Variance of the Joint-2  $R_{q_2q_2}$  for specified values of  $\Theta_2$  and  $\pm 180^\circ$  range of  $\Theta_1$  of Non-wheeled Mobile Manipulator. The damping factor  $\xi = 0.001$ . (a) Stationary Response (b) Nonstationary Response at  $\bar{t} = 20$ .



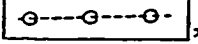


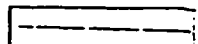
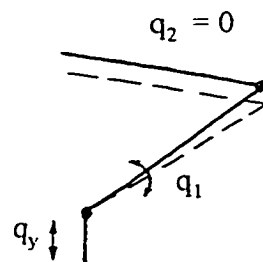
Legend for  $\Theta_1$ ,  $0^\circ$  ,  $15^\circ$  ,  $90^\circ$  ,  $80^\circ$  

Figure 4.6. Covariance of the Joint-1 and Joint-2  $R_{q_1 q_2}$  for specified values of  $\Theta_2$  and  $\pm 180^\circ$  range of  $\Theta_1$  of Non-wheeled Mobile Manipulator. The damping factor  $\xi = 0.001$ .

(a) Stationary Response (b) Nonstationary Response at  $\bar{t} = 20$ .

(a)



(b)

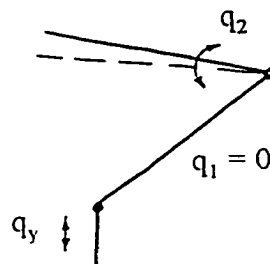


Figure 4.7. Motion of the Manipulator joints at  $\Theta_2 = 131.81^\circ$

(a) First Mode,  $\omega_1 = 0.5\text{rad/s}$  (b) Second Mode,  $\omega_2 = 0.866\text{rad/s}$

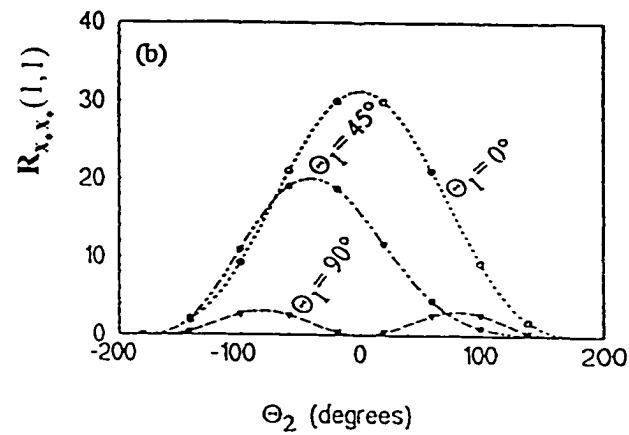
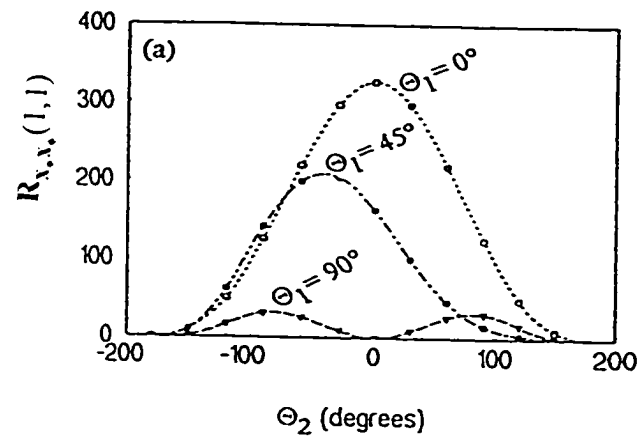


Figure 4.8. Sensitivity of the Major Principal Variance of the Tip Response to Changes in  $\Theta_1$  of Non-wheeled Mobile Manipulator. The damping factor  $\xi = 0.001$ . (a) Stationary Response (b) Nonstationary Response at  $\bar{t} = 20$ .

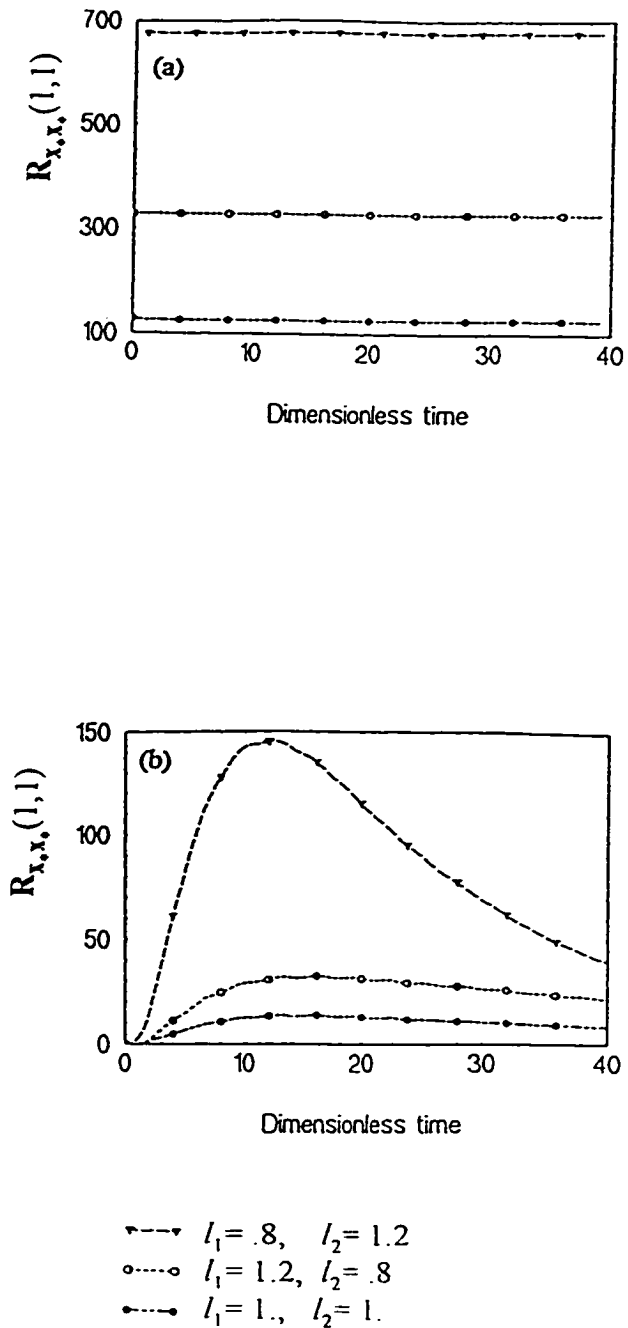


Figure 4.9. Influence of the Relative Length of the Links on the Major Principal Variance of the Tip Response of Non-Wheeled Mobile Manipulator. The damping factor  $\xi = 0.001$ .

(a) Stationary Response (b) Nonstationary Response

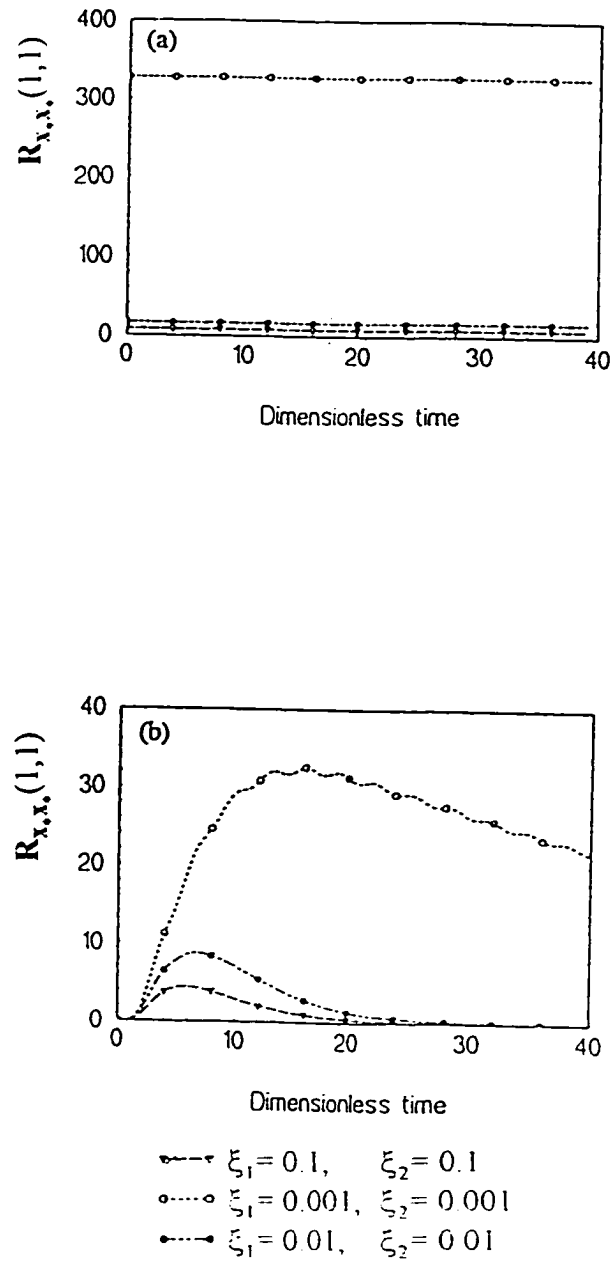


Figure 4.10. Effect of Damping on the Major Principal Variance of the Tip Response of Non-wheeled Mobile Manipulator.

(a) Stationary Response (b) Nonstationary Response

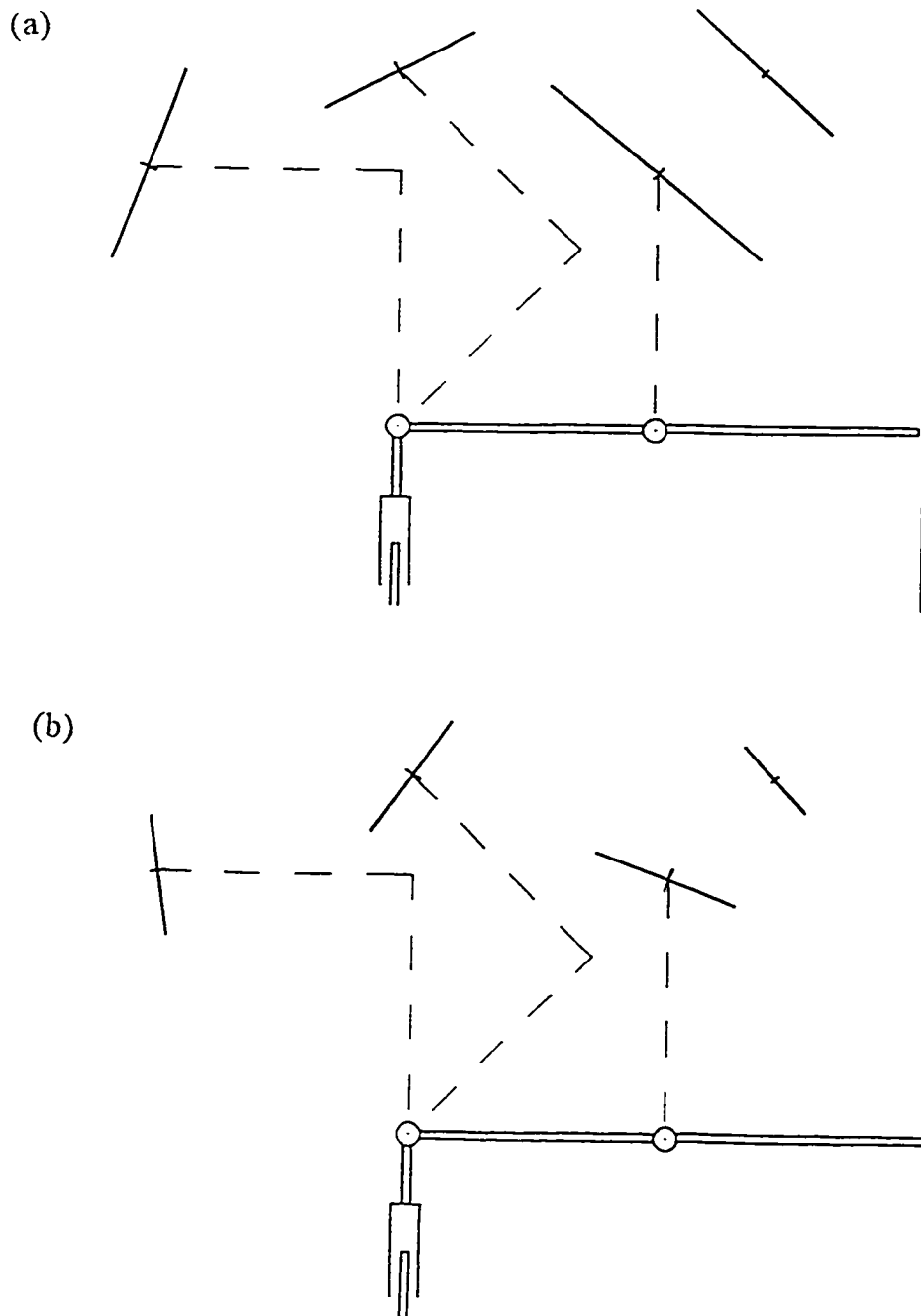
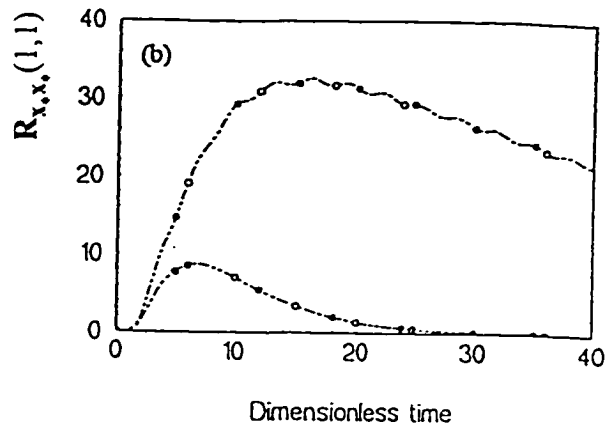
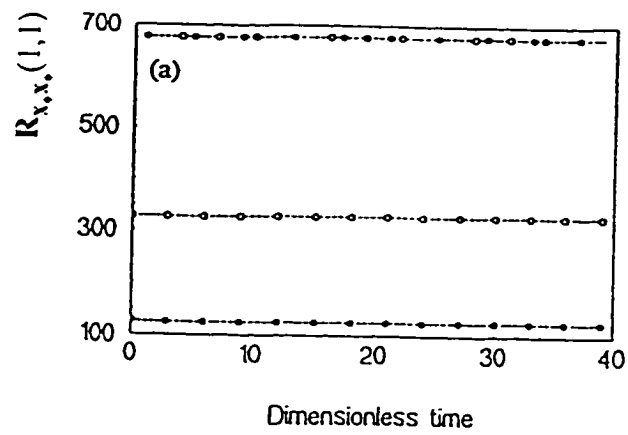


Figure 4.11. Magnitude and Orientation of the Normalized principal Tip Displacement Variance of a Non-wheeled Manipulator  
 (a) Stationary Response (b) Nonstationary Response.





●---●  $R_{rs}(t) = 0$   
 ○---○  $R_{rs}(t) \neq 0$

Figure 4.12. Effect of Cross Coupling of Modal Covariance on Major Principal Variance of the Tip Response of Non-wheeled Mobile Manipulator .  
 (a) Stationary Response (b) Nonstationary Response.

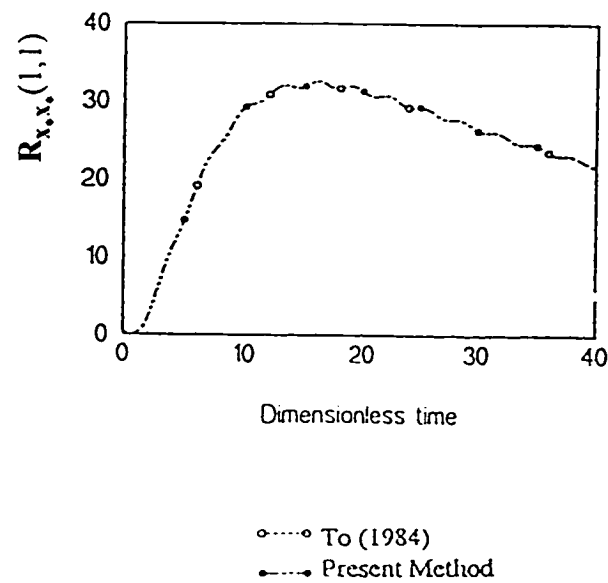


Figure 4.13. Comparison of the Nonstationary Tip Response of Non-wheeled Mobile Manipulator Obtained Using the Presented Method and that Obtained Using The Evolutionary Spectrum Method (To, 1984) .

(a) Stationary Response (b) Nonstationary Response

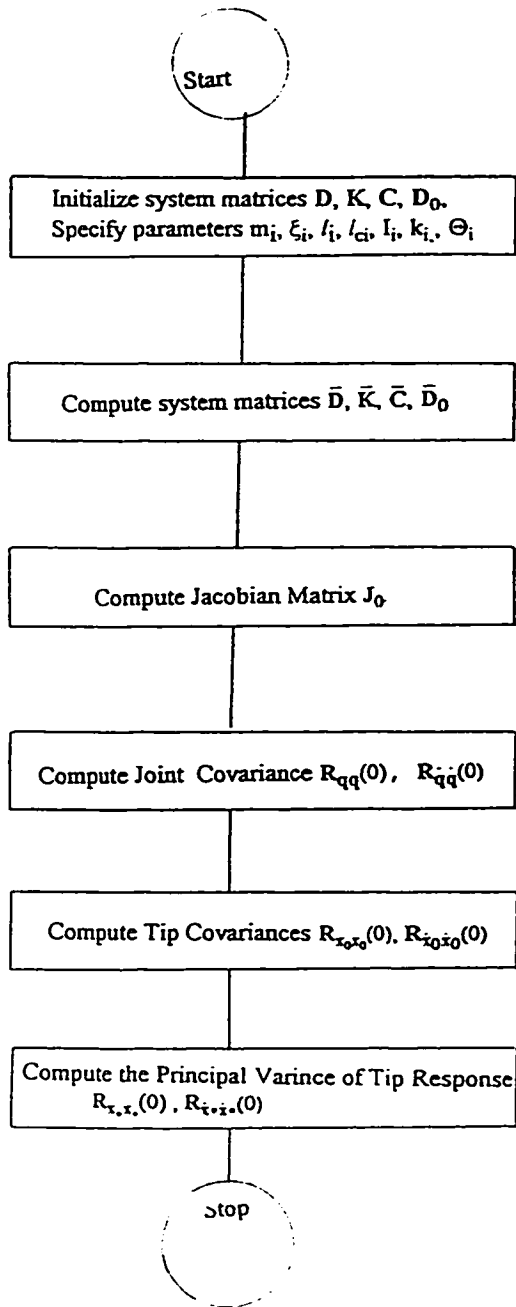


Figure 4.14. Flow Chart of the Program Used for Simulating the Stationary Stochastic Dynamics of a Non-wheeled Mobile Manipulator.

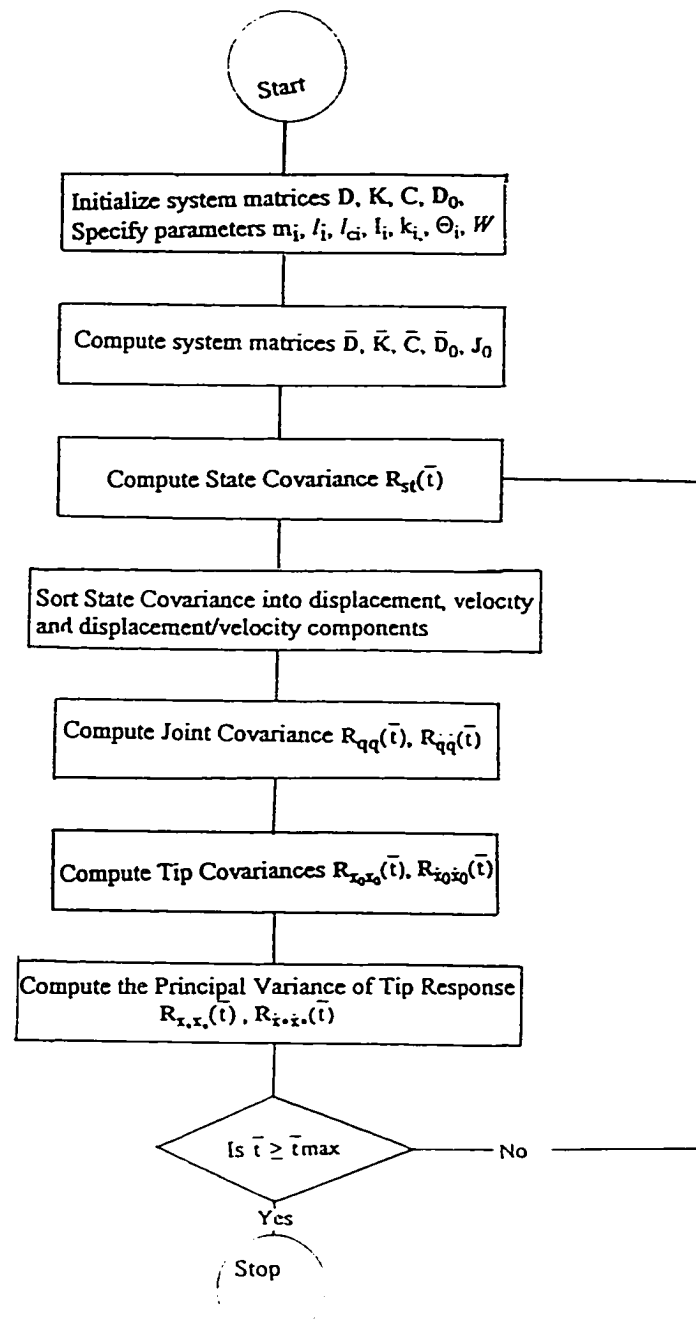


Figure 4.15. Flow Chart of the Program Used for Simulating the Nonstationary Stochastic Dynamics of a Non-wheeled Mobile Manipulator.

## Chapter Five

# WHEELED MOBILE MANIPULATOR, ANALYSIS

### 5.1. Introduction

The presentation in this chapter is an original contribution of the author. Components of this chapter have been accepted for publication in Akpan and Kujath, (1996b). The originality is in the modeling of the joint and the tip covariance responses of the flexible manipulator structure to the traction induced random base motion. A selection and composition of known analytical tools such as state space techniques and modeling of traction induced excitation have been used in the formulation.

### 5.2. Model Assumptions

The basic model of the manipulator structure used in this chapter is shown in Figure 5.1. The manipulator structure is mounted on a mobile base whose mass is of the same order of magnitude as that of the manipulator so that the manipulator dynamics affects the mobile base. Further, the mobile base mounted on wheels is supported by a suspension and it moves on a traction surface. The suspension of the base is modeled by a linear joint. It is assumed that the suspension motions  $q_y$  and  $q_x$  are known,  $q_x$  is the horizontal motion of the base which is taken as a deterministic function while  $q_y$  is the surface irregularities of

the traction surface and is assumed to be a random function. The random excitation (due to the motion of the manipulator base on a traction surface) is small and produces small responses. Also, the wheels maintains constant contact with the surface and there is no deformation of the surface during motion. It is noted that while for the non-wheeled mobile manipulator (Chapter 3)  $q_x$  and  $q_y$  are known oscillatory random motion, for the traction mobile manipulator  $q_y$  is an oscillatory random function and  $q_x$  is a deterministic function.

### 5.3. Equation of Motion

Application of the Lagrangian principle leads to the linear equation of motion

$$\mathbf{D}\ddot{\mathbf{q}}(t) + \mathbf{C}\dot{\mathbf{q}}(t) + \mathbf{K}\mathbf{q}(t) = \mathbf{f}_1 q_y(t) + \mathbf{f}_2 \dot{q}_y(t) + \mathbf{f}_3 \ddot{q}_x(t) \quad (5.1)$$

- $\mathbf{f}_1$  -coefficient vector of the stochastic excitation  $q_y(t)$ ,
- $\mathbf{f}_2$  -coefficient vector of the stochastic excitation  $\dot{q}_y(t)$ ,
- $\mathbf{f}_3$  -coefficient vector of the deterministic excitation  $\ddot{q}_x(t)$

A specific example of the components of equation (5.1) is given in Chapter six. Using the principle of superposition, equation (5.1) can be written as two equations

$$\mathbf{D}\ddot{\mathbf{q}}_d(t) + \mathbf{C}\dot{\mathbf{q}}_d(t) + \mathbf{K}\mathbf{q}_d(t) = \mathbf{f}_3 \ddot{q}_x(t) \quad (5.2)$$

and

$$\mathbf{D}\ddot{\mathbf{q}}_s(t) + \mathbf{C}\dot{\mathbf{q}}_s(t) + \mathbf{K}\mathbf{q}_s(t) = \mathbf{f}_1\mathbf{q}_y(t) + \mathbf{f}_2\dot{\mathbf{q}}_y(t) \quad (5.3)$$

where  $\mathbf{q} = \mathbf{q}_s + \mathbf{q}_d$ . Since in equation (5.2) the excitation term  $\mathbf{f}_3\ddot{\mathbf{q}}_x(t)$  is deterministic, then the response  $\mathbf{q}$  induced by it is also deterministic and has a mean value  $E\{\mathbf{q}_d\} = \mu_{\mathbf{q}} = \mathbf{q}_d$ . Further, its covariance matrix has only zero elements. On the other hand for equation (5.3) the excitation term  $\mathbf{f}_1\mathbf{q}_y(t) + \mathbf{f}_2\dot{\mathbf{q}}_y(t)$  is stochastic, therefore the response  $\mathbf{q}_s$  is stochastic and the associated covariance matrix  $E\{\mathbf{q}\mathbf{q}^T\} = \mathbf{R}_{\mathbf{q}\mathbf{q}}(t)$  has non zero elements. The deterministic and stochastic responses can be treated separately.

## 5.4. Deterministic Response

Assuming that  $\mathbf{q}$  has dimension  $n \times 1$  then the state variable  $\mathbf{z}$  ( $2n \times 1$ ) can be define as

$$\mathbf{z} = [\mathbf{q}^T, \dot{\mathbf{q}}^T]^T. \quad (5.4)$$

Application of equation (5.4), to equation (5.2) transforms it to

$$\dot{\mathbf{z}} = \mathbf{A}_z\mathbf{z} + \mathbf{F}_{3z} \quad (5.5)$$

$$\mathbf{A}_z = \begin{bmatrix} \mathbf{0} & \mathbf{I} \\ -\mathbf{D}^{-1}\mathbf{K} & -\mathbf{D}^{-1}\mathbf{C} \end{bmatrix} \quad (5.6)$$

$$\mathbf{f}_{3z} = \begin{bmatrix} \mathbf{0} \\ \mathbf{D}^{-1}\mathbf{f}_3(t) \end{bmatrix} \ddot{\mathbf{q}}_x(t) \quad (5.7)$$

$\mathbf{0}$  is an  $n \times n$  null matrix,  $\mathbf{I}$  is the  $n \times n$  identity matrix. Equation (5.5) can be solved for  $\mathbf{z}$  which can be reassembled into  $\mathbf{q}$  and  $\dot{\mathbf{q}}$ . The tip response can be computed in any moving coordinate frame attached either to the vehicle or any of the links. Since the vibration is small, (see Sections 2.5 and 3.5) a Jacobian  $\mathbf{J}$  relating the joint displacement vector  $\mathbf{q}$  to the tip displacement vector  $\mathbf{x}$  and the joint velocity vector  $\dot{\mathbf{q}}$  to the tip velocity vector  $\dot{\mathbf{x}}$  can be applied to compute the latter.

## 5.5. Stochastic Response

### 5.5.1. Joint Response

The excitation produced by the surface  $q_y(t)$  has a correlation  $R_{q_y q_y}$  which can be modeled as output of a shaping filter to a white noise expressed by (Narayanan and Raju, 1990)

$$\dot{q}_y(t) = f_y(t)q_y(t) + \mathbf{b}_y^T(t)\mathbf{w}(t) \quad (5.8)$$

where  $\mathbf{w}(t)$  is a vector of white noise with covariance matrix

$$E\{\mathbf{w}(t_1)\mathbf{w}^T(t_2)\} = \mathbf{Q}\delta(t_1 - t_2) \quad (5.9)$$

$\mathbf{Q}$  is the covariance matrix of the white noise;  $\delta$  is the Dirac delta function;  $f_y(t)$  is a function of time and  $\mathbf{b}_y(t)$  is a vector function of time. The augmented  $(2n+1) \times 1$  state vector  $\mathbf{y}$  can be defined as



$$\mathbf{y} = [\mathbf{z}^T, \mathbf{q}_y]^T. \quad (5.10)$$

Application of equation (5.10) to equation (5.8) and (5.3) gives

$$\dot{\mathbf{y}} = \mathbf{A}\mathbf{y} + \mathbf{B}\mathbf{w}(t) \quad (5.11)$$

$$\mathbf{A} = \begin{bmatrix} \mathbf{A}_z & \mathbf{D}^{-1}\mathbf{f}_1 + \mathbf{D}^{-1}\mathbf{f}_2\mathbf{f}_y(t) \\ \mathbf{0}_2^T & \mathbf{f}_y \end{bmatrix} \quad (5.12)$$

$$\mathbf{B} = \begin{bmatrix} \mathbf{0}_1 \\ \mathbf{D}^{-1}\mathbf{f}_2\mathbf{b}_y^T \\ \mathbf{b}_y^T \end{bmatrix}. \quad (5.13)$$

Assuming the dimension of the white noise vector is  $m \times 1$  then  $\mathbf{B}$  is  $2n \times n$  matrix.  $\mathbf{0}_1$  is  $m \times 1$  vector and  $\mathbf{0}_2$  is a  $2n \times 1$  vector. Now, with the white noise  $\mathbf{w}$  considered as a function of the space coordinate  $q_x$  (which in turn is a function of time) equation (5.11) can be written as

$$\dot{\mathbf{y}} = \mathbf{A}\mathbf{y} + \dot{q}_x(t)\mathbf{B}\mathbf{w}(q_x(t)), \quad \text{for } \dot{q}_x(t) \geq 0 \quad (5.14)$$

$$E\{\mathbf{w}(q_x(t_1))\mathbf{w}^T(q_x(t_2))\} = \mathbf{Q}\delta(q_x(t_1) - q_x(t_2)) \quad (5.15)$$

The solution of equation (5.14) is given as

$$\mathbf{y}(t) = \Phi(t, t_0) \mathbf{y}(t_0) + \int_{t_0}^t \Phi(t, t_1) \dot{\mathbf{q}}_x(t_1) \mathbf{B}(t_1) \mathbf{w}(q_x(t_1)) dt_1 \quad (5.16)$$

$\Phi(t, t_0)$  is the transition matrix of equation (5.16),  $t_0$  is the initial time and  $t_1$  is a dummy time variable. The zero-lag covariance matrix of the augmented state  $\mathbf{y}$  can be defined as

$$\mathbf{P} = E\{\mathbf{y}\mathbf{y}^T\} \quad (5.17)$$

so that

$$\dot{\mathbf{P}} = E\{\dot{\mathbf{y}}\mathbf{y}^T + \mathbf{y}\dot{\mathbf{y}}^T\} \quad (5.18)$$

Application of equations (5.17) and (5.16) in equation (5.18) leads to

$$\dot{\mathbf{P}} = \mathbf{A}\mathbf{P} + \mathbf{P}\mathbf{A}^T + \dot{\mathbf{q}}_x(t) \mathbf{B} E\{\mathbf{w}(q_x(t))\mathbf{y}^T\} + \dot{\mathbf{q}}_x(t) E\{\mathbf{y}\mathbf{w}^T(q_x(t))\} \mathbf{B}^T \quad (5.19)$$

To solve equation (5.19) the averages in the equation have to be evaluated. Considering the second average and application of equation (5.18) gives

$$\begin{aligned} E\{\mathbf{y}\mathbf{w}^T(q_x(t))\} &= \Phi(t, t_0) E\{\mathbf{y}(t_0) \mathbf{w}^T(q_x(t))\} \\ &+ \int_{t_0}^t \Phi(t, t_1) \dot{\mathbf{q}}_x(t_1) \mathbf{B}(t_1) E\{\mathbf{w}(q_x(t_1)) \mathbf{w}^T(q_x(t))\} dt_1 \end{aligned} \quad (5.20)$$

The first term in equation (5.20) is a zero vector since the initial state  $y(t_0)$  is uncorrelated with the excitation following  $t_0$ . To obtain the second average in equation (5.20) it is noted that

$$E\{\mathbf{w}(q_x(t_1))\mathbf{w}^T(q_x(t))\} = \mathbf{Q}(t_1)\delta(q_x(t_1) - q_x(t)) \quad (5.21)$$

The Dirac delta function  $\delta$  can be simplified by making use of a result from the theory of generalized function, namely that for a function  $f(t)$ , having simple zeros at  $f = f_i$ , it may be shown (see Appendix F) that

$$\delta(f(t)) = \frac{\delta(t - t_i)}{|\dot{f}(t_i)|} \quad (5.22)$$

which is simply a convenient notation expressing the generalized sifting property of delta functions. Equation (5.21) can be written as

$$E\{\mathbf{w}(q_x(t_1))\mathbf{w}^T(q_x(t))\} = \mathbf{Q}(t) \frac{\delta(t_1 - t)}{|\dot{q}_x(t)|} \quad (5.23)$$

Since  $\dot{q}_x(t) \geq 0$  the modulus operator may be dispensed with. By substituting equation (5.23) in (5.20) and utilizing the sifting property of the delta functions, and noting that the integrand is only defined at the upper limit of the integration (see Appendix F) then only one half of integration makes any contribution, yielding the final result

$$E\{\mathbf{y}\mathbf{w}^T(q_x(t))\} = \frac{1}{2}\mathbf{Q}\mathbf{B} \quad (5.24)$$

similarly the first expectation in equation (5.19) gives

$$E\{\mathbf{w}(q_x(t))\mathbf{y}^T\} = \frac{1}{2}\mathbf{QB}^T \quad (5.25)$$

Application of equations (5.25) and (5.24) in equation (5.19) leads to

$$\dot{\mathbf{P}} = \mathbf{AP} + \mathbf{PA}^T + \dot{q}_x(t)\mathbf{BQB}^T \quad (5.26)$$

Equation (5.26) is the Liapunov matrix differential equation for the manipulator joint motion. It can be solved for the covariance  $\mathbf{P} = E\{\mathbf{y}\mathbf{y}^T\}$  using a numeration integration algorithm.

### 5.5.2. Constant Velocity of the Mobile Base

The discussion presented in the preceding section applies to accelerating wheeled mobile manipulators. When the manipulator base has constant velocity i.e.  $\ddot{q}_x(t) = 0$ , the deterministic component of the excitation in equation (5.1) vanishes. Further, the equation for the system excitation (equation (5.8)) is time-invariant and the frequency domain technique can be used to compute the response. The two approaches -the state space (time) and the power spectral density (frequency) approaches, used in this thesis for computing the joint responses are presented below.

### 5.5.2.1. State Space Approach

Using the state space approach the Liapunov's differential equation for the joint response (equation 5.26) degenerates to the algebraic form

$$\mathbf{AP} + \mathbf{PA}^T = -\dot{\mathbf{q}}_x(t)\mathbf{BQB}^T \quad (5.27)$$

Equation (5.27) is the Liapunov matrix equation and can be solved using iterative techniques. Smith's algorithm (Smith, 1970) can be used to solve equation (5.27). Alternatively the elements of the symmetric matrix equation (5.27) can be expanded and solved as systems of linear equations. The second approach was adopted in this report.

### 5.5.2.2. Power Spectral Density Approach

Equation (5.10) is the state space representation of the excitation  $q_y(t)$  and is also the time domain description. When the base velocity  $\dot{q}_x(t)$  is constant, the system excitation  $q_y(t)$  is stationary and its power spectral density can be found as (see Chapter six for example)

$$\mathbf{S}_{q_y q_y} = \mathbf{S}(\omega, \dot{q}_x) \quad (5.28)$$

The power spectral density of the derivative  $\dot{q}_y(t)$  can be computed as

$$\mathbf{S}_{\dot{q}_y \dot{q}_y} = \omega^2 \mathbf{S}_{q_y q_y} \quad (5.29)$$

Equations (5.28) and (5.29) give the power spectral density representation of the excitation and these are the frequency domain presentations. The joint vector  $\mathbf{q}$  can be expressed in terms of the mass normalized modal matrix  $\mathbf{U}$  and the normal coordinate  $\mathbf{e}$  as

$$\mathbf{q}(t) = \mathbf{U}\mathbf{e}(t) \quad (5.30)$$

Equation (5.3) can be expressed in the decoupled form

$$\ddot{e}_r(t) + 2\xi_r\omega_r\dot{e}_r(t) + \omega_r^2 e_r(t) = \mathbf{u}_r^T(\mathbf{f}_1\mathbf{q}_y + \mathbf{f}_2\dot{\mathbf{q}}_y(t)) \quad (5.31)$$

where  $\mathbf{u}_r^T$  represents the transpose of the  $r$ -th column of  $\mathbf{U}$ . Using the Duhamel integral the displacement response of mode- $r$  is obtained as

$$e_r(t) = \int_{-\infty}^{\infty} h_r(t - \tau) \mathbf{u}_r^T(\mathbf{f}_1\mathbf{q}_y + \mathbf{f}_2\dot{\mathbf{q}}_y(t)) d\tau \quad (5.32)$$

$$h_r(t) = u(t) \frac{1}{\omega_{dr}} e^{-\xi_r\omega_r t} \sin(\omega_{dr}t) \quad (5.33)$$

$$\omega_{dr} = \omega_r \sqrt{1 - \xi_r^2} \quad (5.34)$$

The crosscorrelation of the displacements of joint- $v$  and joint- $m$  is obtained as

$$R_{q_v, q_m}(\tau) = E\{q_v(t) q_m(t+\tau)\} = \sum_{j=1}^n \sum_{k=1}^n U_{vj} U_{mk} E\{e_j(t) e_k(t+\tau)\} \quad (5.35)$$

The power spectral density of  $q_v$  and  $q_m$  can be obtained by the Wiener Khinchine relation (equation (3.27)) using equations (5.35), (5.32), (5.29), and (5.30) as

$$S_{q_v q_m}(\omega) = (\mathbf{u}_v^T \mathbf{f}_1 S_{q_y q_y}(\omega) \mathbf{u}_m^T \mathbf{f}_1 + \mathbf{u}_v^T \mathbf{f}_2 S_{q_y q_y}(\omega) \mathbf{u}_m^T \mathbf{f}_2) \sum_{j=1}^n \sum_{k=1}^n U_{vj} U_{mk} H_j H_k^* \quad (5.36)$$

where  $H_j = (\omega_j^2 - \omega^2 + 2i\zeta_j \omega \omega_j)^{-1}$ ,  $i = \sqrt{-1}$ . The covariance matrix of the joint displacements can be obtained as

$$\mathbf{R}_{qq}(0) = E\{\mathbf{q}\mathbf{q}^T\} = \int_{-\infty}^{\infty} \mathbf{S}_{qq}(\omega) d\omega. \quad (5.37)$$

The covariance matrix of the joint velocities  $\dot{\mathbf{q}}$  can be obtained as

$$\mathbf{R}_{\dot{q}\dot{q}}(0) = E\{\dot{\mathbf{q}}\dot{\mathbf{q}}^T\} = \int_{-\infty}^{\infty} \omega^2 \mathbf{S}_{qq}(\omega) d\omega. \quad (5.38)$$

The residue theorem can be used to solve equations (5.37) and (5.38).

### 5.5.3. Tip Response

The components of the covariance matrix  $\mathbf{P}$  obtained by using either equation (5.26) or equation (5.27) can be reassembled into the joint displacement and the joint velocity covariance matrices defined as;  $\mathbf{R}_{qq}(t) = E\{\mathbf{q}\mathbf{q}^T\}$  and  $\mathbf{R}_{\dot{q}\dot{q}}(t) = E\{\dot{\mathbf{q}}\dot{\mathbf{q}}^T\}$  respectively. The tip velocity and displacement responses can be computed using the method discussed in Section 3.5.

## 5.6. Summary and Concluding Remarks

In this chapter the equation of motion of a wheeled mobile manipulator attached to a traction mobile base has been developed using Lagrange principle. The manipulator base has been modeled using the quarter car representation. Two cases of the base motion have been considered.

- (a) The uniform velocity case.
- (b) The accelerating case.

In case (a), the mobile robotics system is subjected to only random excitation. Expressions for the covariance tensors of the dynamics of the joints and the tip of the mobile manipulator have been fully developed using the power spectral density (frequency domain) representation and the state space (time domain) representation.

For case (b) it has been seen that the system excitation is both stochastic and deterministic. Further, principles of superposition for linear systems has been applied to obtain the deterministic and stochastic responses separately. The deterministic part of the excitation leads to a mean response and expressions for this at the joints and the tip of the manipulator have been developed. The stochastic excitation is nonstationary. Expressions for this time-varying configuration dependent nonstationary covariance tensor of both the joints and tip responses have been derived.

To illustrate the ideas discussed in this chapter, a case study, and numerical simulation are presented in the next chapter.



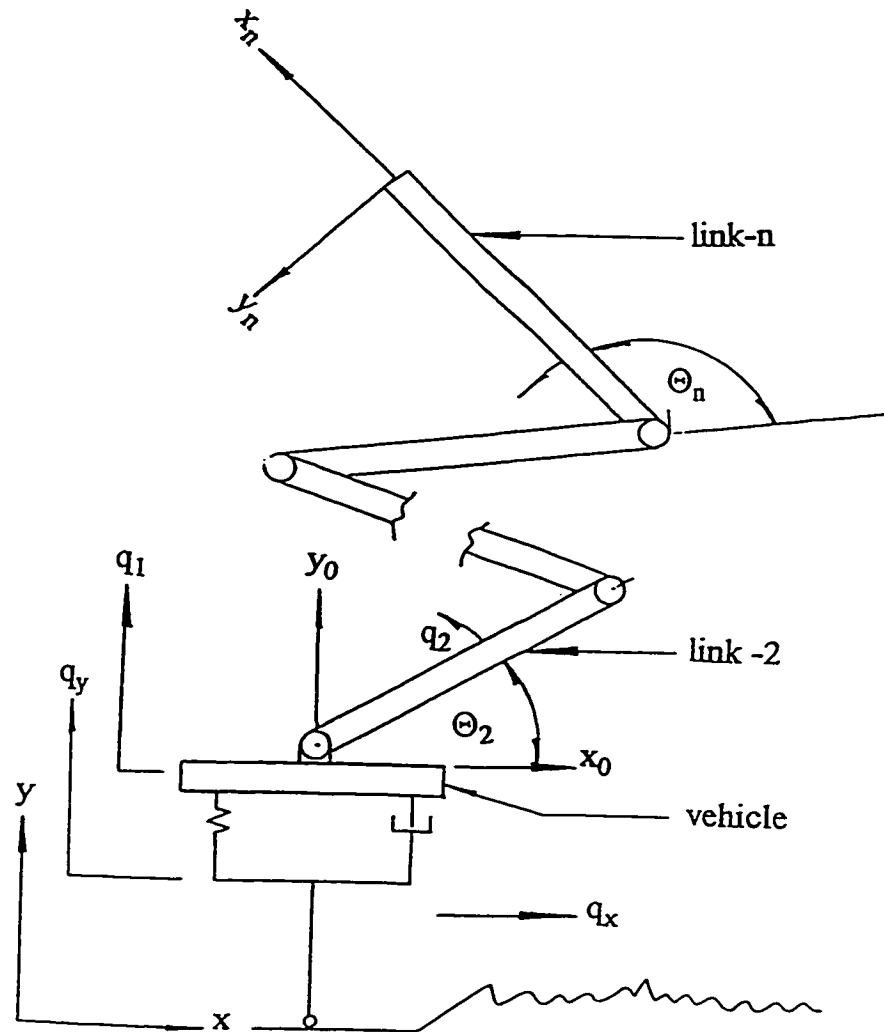


Figure 5.1. Model of a Wheeled Mobile Manipulator

- $\Theta_i$  i-th kinematic configuration
- $q_i$  i-th elastic motion variable
- $(x, y)_i$  Cartesian coordinate frame attached to the i-th link

## Chapter Six

### WHEELED MOBILE MANIPULATOR, EXAMPLE

#### 6.1. Example: Two Link Manipulator

A two link manipulator on a wheeled mobile base is used to illustrate the procedures presented in Chapter five (Figure 6.1). The total kinetic energy  $T$  for the mobile manipulator is

$$\begin{aligned}
 T = & \frac{1}{2} a_1 (\dot{q}_1^2 + \dot{q}_x^2) + \frac{1}{2} a_2 \dot{q}_2^2 + \frac{1}{2} a_3 (\dot{q}_2 + \dot{q}_3)^2 + a_4 \dot{q}_2 (\dot{q}_3 + \dot{q}_2) \cos(\Theta_3 + q_3) \\
 & + a_5 \dot{q}_1 \dot{q}_2 \cos(\Theta_2 + q_2) + a_6 \dot{q}_1 (\dot{q}_2 + \dot{q}_3) \cos(\Theta_2 + \Theta_3 + q_2 + q_3) \\
 & - a_5 \dot{q}_x \dot{q}_2 \sin(\Theta_2 + q_2) - a_6 \dot{q}_x (\dot{q}_2 + \dot{q}_3) \sin(\Theta_2 + \Theta_3 + q_2 + q_3) \quad (6.1)
 \end{aligned}$$

where

$$a_1 = m_1 + m_2 + m_3 \quad (6.2)$$

$$a_2 = I_2 + m_2(l_{c2})^2 + m_3(l_3)^2 \quad (6.3)$$

$$a_3 = I_3 + m_3(l_{c3})^2 \quad (6.4)$$

$$\mathbf{a}_4 = m_3 l_{c2} l_2 \quad (6.5)$$

$$\mathbf{a}_5 = m_2 l_{c2} + m_3 l_3 \quad (6.6)$$

$$\mathbf{a}_6 = m_3 l_{c3} \quad (6.7)$$

The potential energy,  $V$ , of the manipulator is

$$V = \frac{1}{2} k_1 (q_1 - q_y)^2 + \frac{1}{2} k_2 q_2^2 + \frac{1}{2} k_3 q_3^2 \quad (6.8)$$

The Lagrangian for the system can be found using equation (2.3). The Rayleigh dissipation function  $R$  is given as

$$R = \frac{1}{2} c_1 (\dot{q}_1 - \dot{q}_y)^2 + \frac{1}{2} c_2 \dot{q}_2^2 + \frac{1}{2} c_3 \dot{q}_3^2 \quad (6.9)$$

where

$\dot{q}_1$  absolute vertical motion of the vehicle

$m_1$  mass of the vehicle

$m_2$  mass of link-2

$m_3$  mass of link-3

$I_2$  centroidal moment of inertia of link-2

$I_3$  centroidal moment of inertia of link-3

Using the Lagrange equation (see section 2.5) the equation of motion can be obtained (see Appendix B for details). The inertia matrix is given as

$$\mathbf{D} = \begin{bmatrix} D_{11} & D_{12} & D_{13} \\ D_{21} & D_{22} & D_{23} \\ D_{31} & D_{32} & D_{33} \end{bmatrix} \quad (6.10)$$

$$D_{11} = a_1 \quad (6.11)$$

$$D_{12} = a_5 \cos(\Theta_2) + a_6 \cos(\Theta_2 + \Theta_3) \quad (6.12)$$

$$D_{21} = a_5 \cos(\Theta_2) + a_6 \cos(\Theta_2 + \Theta_3) \quad (6.13)$$

$$D_{13} = a_6 \cos(\Theta_2 + \Theta_3) \quad (6.14)$$

$$D_{31} = a_6 \cos(\Theta_2 + \Theta_3) \quad (6.15)$$

$$D_{22} = a_2 + a_3 + 2.0a_4 \cos(\Theta_3) \quad (6.16)$$

$$D_{23} = a_3 + a_4 \cos(\Theta_3) \quad (6.17)$$

$$D_{32} = a_3 + a_4 \cos(\Theta_3) \quad (6.18)$$

$$D_{33} = a_3 \quad (6.19)$$

The stiffness matrix is given as

$$\mathbf{K} = \begin{bmatrix} K_{11} & K_{12} & K_{13} \\ K_{21} & K_{22} & K_{23} \\ K_{31} & K_{32} & K_{33} \end{bmatrix} \quad (6.20)$$

$$K_{11} = k_1 \quad (6.21)$$

$$K_{22} = k_2 \quad (6.22)$$

$$K_{33} = k_3 \quad (6.23)$$

$$K_{ij} = 0 \quad \text{for } i \neq j \quad (6.24)$$

The damping matrix is given as

$$\mathbf{C} = \begin{bmatrix} C_{11} & C_{12} & C_{13} \\ C_{21} & C_{22} & C_{23} \\ C_{31} & C_{32} & C_{33} \end{bmatrix} \quad (6.25)$$

$$C_{11} = c_1 \quad (6.26)$$

$$C_{22} = c_2 \quad (6.27)$$

$$C_{33} = c_3 \quad (6.28)$$

$$C_{ij} = 0 \quad \text{for } i \neq j \quad (6.29)$$

$$\mathbf{f}_1 = \begin{bmatrix} k_1 \\ 0 \\ 0 \end{bmatrix} \quad (6.30)$$

$$\mathbf{f}_2 = \begin{bmatrix} c_1 \\ 0 \\ 0 \end{bmatrix} \quad (6.31)$$

$$\mathbf{f}_3 = \begin{bmatrix} 0 \\ a_5 \sin(\Theta_2) + a_6 \sin(\Theta_2 + \Theta_3) \\ a_6 \sin(\Theta_2 + \Theta_3) \end{bmatrix} \quad (6.32)$$

To generalize the results, a dimensionless time  $\bar{t}$  defined as in equation (4.1) can be introduced. The resulting dimensionless matrices are

$$\bar{\mathbf{D}} = \frac{1}{a_1} \mathbf{D} \quad (6.33)$$

$$\bar{\mathbf{C}} = \frac{1}{\sqrt{a_1 k_1}} \mathbf{C} \quad (6.34)$$

$$\bar{\mathbf{K}} = \frac{1}{k_1} \mathbf{K} \quad (6.35)$$

$$\bar{\mathbf{f}}_1 = \begin{bmatrix} 1 \\ 0 \\ 0 \end{bmatrix} \quad (6.36)$$

$$\bar{\mathbf{f}}_2 = \begin{bmatrix} \bar{c}_1 \\ 0 \\ 0 \end{bmatrix} \quad (6.37)$$

$$\bar{\mathbf{f}}_3 = \begin{bmatrix} 0 \\ \bar{a}_5 \sin(\Theta_2) + \bar{a}_6 \sin(\Theta_2 + \Theta_3) \\ \bar{a}_6 \sin(\Theta_2 + \Theta_3) \end{bmatrix} \quad (6.38)$$

$$\bar{c}_1 = \frac{c_1}{\sqrt{a_1 k_1}} \quad (6.39)$$

$$\bar{a}_5 = \frac{a_5}{a_1} \quad (6.40)$$

$$\bar{a}_6 = \frac{a_6}{a_1} \quad (6.41)$$

The Jacobian matrix of the tip motion in the vehicle frame  $\mathbf{x}_0 = [x_0, y_0]^T$  is given as

$$\mathbf{J}_0 = \begin{bmatrix} J_{11} & J_{12} & J_{13} \\ J_{21} & J_{22} & J_{23} \end{bmatrix} \quad (6.42)$$

$$J_{11} = 0 \quad (6.43)$$

$$J_{12} = -l_2 \sin(\Theta_2) - l_3 \sin(\Theta_2 + \Theta_3) \quad (6.44)$$

$$J_{12} = -l_3 \sin(\Theta_2 + \Theta_3) \quad (6.45)$$

$$J_{21} = 1 \quad (6.46)$$

$$J_{22} = l_2 \cos(\Theta_2) + l_3 \cos(\Theta_2 + \Theta_3) \quad (6.47)$$

$$J_{23} = l_3 \cos(\Theta_2 + \Theta_3) \quad (6.48)$$

Detailed derivation of the Jacobian matrix is given in Appendix C.

## 6.2. Surface Profile Representation

The wheeled mobile manipulator is assumed to move on a homogeneous spatial surface. Before stating the specific surface profile model used in this chapter the relationship between spatial and time correlation, spatial and time power spectrum and autoregressive model will be derived.

### 6.2.1. Relation Between Correlation and Power Spectral Representation

Consider the height  $q_y$  of the surface above a fixed horizontal datum plotted as a function of the horizontal position  $q_x$  (see Figure 6.2). The wave number  $\gamma$



which expresses the rate of change of  $q_y$  with respect to  $q_x$  can be defined. Assuming the vehicle speed  $\dot{q}_x$  is constant let the time when the vehicle is at position  $q_{x1}$  be  $t_1$  and the time when it is at position  $q_{x2}$  be  $t_2$ . The time lag can be defined as

$$\tau = t_2 - t_1 \quad (6.49)$$

and the spatial lag is given as

$$q_x = q_{x2} - q_{x1} \quad (6.50)$$

Further,

$$\dot{q}_x = \frac{q_x}{\tau} \quad (6.51)$$

Define the wave number (Newland, 1984) for the surface profile as

$$\gamma = \frac{2\pi}{\lambda} \quad (6.52)$$

where  $\lambda$  is the wavelength. Thus in the Fourier domain if a cycle of wavelength  $\lambda$  is covered in period  $T$ , then

$$T = \frac{\lambda}{\dot{q}_x} \quad (6.53)$$

and the time angular frequency is

$$\omega = \frac{2\pi}{T} = \frac{2\dot{q}_x\pi}{\lambda} \quad (6.54)$$

Application of equation (6.51) in (6.54) gives

$$\gamma = \frac{\omega}{\dot{q}_x} \quad (6.55)$$

In what follows it is shown that if the surface profile  $q_y(q_x)$  is spatially homogeneous and the vehicle speed is constant then the motion of the wheel  $q_y(t)$  is a stationary random process. The spatial autocorrelation function of the surface is defined as

$$\begin{aligned} E\{q_y(q_{x1})q_y(q_{x2})\} &= E\{q_y(q_{x1})q_y(q_{x1} + q_x)\} \\ &= R_{q_yq_y}(q_{x2}, q_{x1}) = R_{q_yq_y}(q_{x2}-q_{x1}) = R_{q_yq_y}(q_x) \end{aligned} \quad (6.56)$$

Since the surface is homogeneous. Using the Wiener Khinchine relation equation (6.56) becomes

$$R_{q_yq_y}(q_x) = \int_{-\infty}^{\infty} S_{q_yq_y}(\gamma) e^{i\gamma q_x} d\gamma \quad (6.57)$$

Application of equations (6.51) and (6.55) in equation (6.57) gives

$$R_{q_yq_y}(\dot{q}_x\tau) = \int_{-\infty}^{\infty} \frac{1}{\dot{q}_x} S_{q_yq_y}\left(\frac{\omega}{\dot{q}_x}\right) e^{i\omega\tau} d\omega \quad (6.58)$$

Since the vehicle velocity  $\dot{q}_x$  is constant then the spatial correlation function (equation 6.58) is essentially a function of the time lag  $\tau$ . From Wiener Khinchine relation in the spatial domain we have

$$S_{q_y q_y}(\gamma) = \frac{1}{2\pi} \int_{-\infty}^{\infty} R_{q_y q_y}(q_x) e^{-i\gamma q_x} dq_x \quad (6.59)$$

Also in the time domain we have

$$S_{q_y q_y}(\omega) = \frac{1}{2\pi} \int_{-\infty}^{\infty} R_{q_y q_y}(\tau) e^{-i\omega \tau} d\tau \quad (6.60)$$

Using equation (6.51), and (6.55) in equation (6.60) gives

$$S_{q_y q_y}(\omega = \dot{q}_x \gamma) = \frac{1}{2\pi} \int_{-\infty}^{\infty} \frac{1}{\dot{q}_x} R_{q_y q_y}(\tau = \frac{q_x}{\dot{q}_x}) e^{-i\gamma q_x} dq_x \quad (6.61)$$

Comparison of equation (6.61) and (6.59) gives

$$S_{q_y q_y}(\omega) = \frac{1}{\dot{q}_x} S_{q_y q_y}(\gamma) \quad (6.62)$$

Equation (6.62) gives the relationship between the spectrum of the surface profile expressed in the frequency (time) domain and that expressed in the wave number (spatial) domain. This expression is general and can be applied to any spatial correlation. In this study the spatial autocorrelation of the surface is assumed to be

of the form suggested by several authors (Narayana and Raju, 1991; Hac, 1985; Harrison, 1981).

$$R_{q_y q_y}(q_{x2}-q_{x1}) = \sigma^2 e^{-\alpha|q_{x2}-q_{x1}|} = \sigma^2 e^{-\alpha|q_x|} \quad (6.63)$$

Application of equation (6.63) in (6.59) gives the double sided spatial power spectrum of excitation as

$$S_{q_y q_y}(\gamma) = \frac{1}{2\pi} \int_{-\infty}^{\infty} \sigma^2 e^{-\alpha|q_x|} e^{-i\gamma q_x} dq_x \quad (6.64)$$

$$= \frac{1}{2\pi} \sigma^2 \left[ \int_{-\infty}^0 e^{\alpha q_x} e^{-i\gamma q_x} dq_x + \int_0^{\infty} e^{-\alpha q_x} e^{-i\gamma q_x} dq_x \right] \quad (6.65)$$

$$= \frac{\sigma^2 \alpha}{\pi(\gamma^2 + \alpha^2)} \quad (6.66)$$

Using equation (6.66) and the relationship defined in equation (6.62), then the double sided time power spectrum of excitation is

$$S_{q_y q_y}(\omega) = \frac{\sigma^2 \alpha}{\pi \dot{q}_x (\alpha^2 + \frac{\omega^2}{\dot{q}_x^2})}$$

$$= \frac{\sigma^2 \alpha \dot{q}_x}{\pi(\omega^2 + \alpha^2 \dot{q}_x^2)} \quad (6.67)$$

### 6.2.2. Power Spectrum Representation and Autoregressive Equation

The autoregressive model of the excitation represented in equations (6.67), (6.63) and (6.66) is given as

$$\frac{dq_y}{dq_x} + \alpha q_y = w(q_x) \quad (6.68)$$

$$E\{w(q_{x1})w(q_{x1} + q_x)\} = Q\delta(q_x) \quad (6.69)$$

where

$\sigma^2$  variance of the surface irregularity

$\alpha$  surface constant coefficient

$w(q_x)$  white noise with intensity  $Q = 2\alpha\sigma^2$

$\delta$  Dirac Delta function

It is observed that although equation (6.68), and the other related representations have been quoted in various references including the ones listed in Section 6.6.1, none of the references derives the relationship between them. For the purpose of this study this relationship will be derived. In the following discussion it is shown that equation (6.68) and the spatial power spectrum function given in equation (6.66) are equivalent. From the Wiener Khinchine relation the spectrum of the white noise  $w(q_x)$  in the wave number domain is

$$S_{ww}(\gamma) = \frac{1}{2\pi} \int_{-\infty}^{\infty} 2\alpha\sigma^2 \delta(q_x) dq_x = \frac{1}{\pi} \alpha\sigma^2 \quad (6.70)$$

The wave number response function  $H(\gamma)$  of equation (6.68) (equivalent to the frequency response function in the time domain) can be found. To this end let

$$w(q_x) = e^{i\gamma q_x}, \quad (6.71)$$

$$q_y(q_x) = H(\gamma)e^{i\gamma q_x}, \quad (6.72)$$

Application of equations (6.72) and (6.71) in equation (6.68) leads to

$$H(\gamma) = \frac{1}{i\gamma + \alpha} \quad (6.73)$$

The spectrum of the surface profile in the wave number domain is given as

$$S_{q_y q_y}(\gamma) = |H(\gamma)|^2 S_{ww}(\gamma) \quad (6.74)$$

Application of equations (6.70), and (6.73) in (6.74) gives

$$S_{q_y q_y}(\gamma) = \frac{\sigma^2 \alpha}{\pi(\gamma^2 + \alpha^2)} \quad (6.75)$$

From the above derivations it is seen that equations (6.75), (6.67), (6.63) and (6.68) are equivalent. Equation (6.68) can be used to represent the excitation in the state space approach. Before this can be done the equation has to be transformed to the time domain. The following transformation is introduced

$$\frac{d}{dq_x} = \frac{dt}{dq_x} \frac{d}{dt} = \frac{1}{\dot{q}_x} \frac{d}{dt} \quad (6.76)$$

Application of equation (6.76) to equation (6.68) transforms it to the time domain as

$$\dot{q}_y(t) = -\dot{q}_x(t)\alpha q_y(t) + \dot{q}_x(t) w(q_x(t)). \quad (6.77)$$

Equation (6.77) is an example of the general surface profile representation presented in equation (5.8). Therefore in equation (5.8)

$$f_y(t) = -\dot{q}_x(t)\alpha \quad (6.78)$$

$$b_y = \dot{q}_x(t) \quad (6.79)$$

Further equation (6.77) is general and applies to both constant and varying  $\dot{q}_x(t)$ . It is noted also apart from equation (6.77) all the other representation of the surface profile are applicable to constant  $\dot{q}_x(t)$ . Using the procedure outlined in Sections 5.4 and 5.5 the system response can be computed. This has been implemented numerically.

## 6.3. Numerical Simulation

### 6.31. Case 1. Manipulator on an Accelerating Wheeled Mobile Base

#### INITIAL CONDITIONS

#### Deterministic Response:

It is assumed that the vehicle starts from rest with uniform horizontal acceleration. To initiate the Runge Kutta integration algorithm for the deterministic response of equation (5.5), a set of initial values of the state  $z(0)$  have to be provided. Since the state vector  $z$  is normalized with the standard deviation of the surface profile  $\sigma$  and at time  $\bar{t} = 0$  there is no relative motion between the vehicle

$q_1$  and the suspension  $q_y$ , then  $z_1(0) = 1/\sigma$ . All other initial conditions are set to zero.

### Stochastic Response:

In order to initialize the Runge-Kuta integration routine for the stochastic response of equation (5.24) a set of initial values of the covariance matrix  $\mathbf{P}(0)$  entries is required. From the assumption of homogeneity of the surface profile, the variance of the suspension's motion is  $E\{q_y^2(\bar{t})\} = \sigma^2$ , and this implies  $P_{77}(0) = 1$ . Further, at  $\bar{t} = 0$ , there is no relative motion between the vehicle body  $q_1$  and the suspension  $q_y$ , therefore  $P_{11}(0) = P_{17}(0) = P_{77}(0)$ . All other initial conditions are set to zero.

### **6.32. Case 2. Manipulator on a Constant Velocity Mobile Base**

The spectrum of spatial excitation is given in equation (6.67) and the spectrum of the velocity  $\dot{q}_y$  is

$$S_{\dot{q}_y \dot{q}_y} = \omega^2 S_{q_y q_y} \quad (6.80)$$

## **6.4. Results and Discussion**

### **6.41. Case 1. Manipulator on an Accelerating Mobile Base**

Two programs have been developed to simulate the deterministic and nonstationary random response of the tip motion of a two degree of freedom flexible manipulator on an accelerating base respectively. The flow chart for the programs are given in Figure 6.3 and 6.4. In this discussion, the term stochastic response refers to the major principal variance of the tip displacement, while the



term deterministic response refers to the square of the magnitude of the tip deterministic displacement. Figure 6.5 shows the sensitivity of the tip response to the changes of the manipulator configuration for  $\Theta_3 = 0^\circ$ ,  $\alpha = .45$ , and  $\ddot{q}_x = 1$ . In general, it can be observed that the more perpendicular the manipulator to an excitation, the higher the response to that excitation. Thus, the highest stochastic response occurs at  $\Theta_2 = 0^\circ$ . At this configuration the links of the manipulator are perpendicular to the stochastic base excitations  $\dot{q}_y(t)$  and  $q_y(t)$ . Also, at this configuration the deterministic response is transient and depends only on the initial condition since the vector  $f_3 = 0$ . The highest deterministic response occurs at  $\Theta_2 = 90^\circ$  when the vector  $f_3$  reaches its maximum value. The stochastic response for  $\Theta_2 = 90^\circ$  and  $\Theta_3 = 0^\circ$  is only that of the wheeled mobile base since the dynamic coupling terms between the mobile base and the links are zero ( $D_{12} = D_{21} = D_{13} = D_{31} = 0$ ); therefore the mobile base moves with the links as a rigid body.

Subsequent plots for the deterministic and stochastic responses are for the configurations of maximum responses. Figure 6.6 shows the influence of the damping on the responses. The deterministic and the stochastic responses can be reduced by the presence of damping. But if only either joint or suspension damping is present, the stochastic response has low sensitivity to damping. The deterministic response, on the other hand, shows high sensitivity to the suspension damping in the absence of the manipulator joint damping and low sensitivity to the joint damping in the absence of the suspension damping. Further, at the beginning of motion the deterministic and stochastic responses show little sensitivity to damping.

Figure 6.7 shows the effect of the acceleration of the mobile base on the deterministic response. In general, the deterministic response increases with the increase of the acceleration of the mobile base except for the configurations when  $f_3 = 0$  i.e. when the excitation has no effect. Figure 6.8 shows the effects of the acceleration mobile base and surface roughness on the stochastic response. At the beginning of motion, the stochastic response is not sensitive to either surface roughness or acceleration. As the motion continues, for low acceleration  $\ddot{q}_x = .4$ , it is noted that the higher the surface roughness coefficient the higher the maximum value of the stochastic response; also the response under this condition is smooth. On the other hand, for high acceleration  $\ddot{q}_x = 4.$ , the surface with high roughness coefficient  $\alpha = .9$  produces uneven response with quick rise. The maximum value of the response is also low under this condition. The surface with low roughness coefficient  $\alpha = .15$  produces a smooth stochastic response with a slow rise and a high maximum value.

Figure 6.9 shows the computed and scaled values of the principal variance and their orientations for six configurations  $[\Theta_2, \Theta_3] = [0^\circ, 0^\circ], [0^\circ, 90^\circ], [45^\circ, 0^\circ], [45^\circ, 90^\circ], [90^\circ, 90^\circ]$  and  $[90^\circ, 0^\circ]$ . The principal variances are illustrated by the crossed line segments located at the manipulator tip. The major variance is very high compared to the minor variance i.e. the stochastic motion of the manipulator tip is almost unidirectional though the direction is different for different configurations.

### 6.42. Case 2. Manipulator on a Constant Velocity Mobile Base

Two general purpose programs to simulate the stationary random response of the tip motion of a two degree of freedom flexible manipulator on a constant velocity mobile base using the power spectral density approach and the state space approach have been developed. The flow chart for the programs are given in Figure 6.10 and 6.11. In the following discussion the term displacement refers to the major principal variance of the tip displacement.

Figures 6.12 and 6.13 are made for the specified values of  $\Theta_2$ , and for  $\pm 180^\circ$  range of  $\Theta_3$ ;  $\alpha = .45$ ;  $\dot{q}_x = 5$ . Figure 6.11 shows the displacements obtained using the power spectral density and the state space representations. It is noted that both representations yield the same displacements. The state space representation, however, has some advantages over the power spectral density representation since it can accommodate non-proportional damping. Also, unlike the power spectral density, the state space representation yields the displacements and velocities simultaneously (see equation (5.27)). Further, it avoids the contour integrals (see Appendix D, section D3) required for the power spectral density representation (equations (5.37) and (5.38)) and it can be used for very large degree of freedom systems.

Figure 6.14 shows the sensitivities of the displacements and velocities to changes in the manipulator configuration  $\Theta_2$ . It is observed that the more perpendicular the manipulator structure to the excitation, the higher the response. Thus, the highest response occurs at  $\Theta_2 = \Theta_3 = 0^\circ$ . At this configuration the links

of the manipulator are perpendicular to the stochastic base excitations  $\dot{q}_y(t)$  and  $q_y(t)$ .

The influence of the manipulator and the suspension damping on the displacement is shown in Figure 6.15. It is observed that the displacement can be reduced with the presence of damping. But if only the suspension damping  $c_1$  is present, the response has low sensitivity to damping. On the other hand, if only the manipulator joints are damped the response is very sensitive to damping.

Figure 6.16 shows the effect of the surface roughness coefficient  $\alpha$  on the responses for the configuration  $\Theta_2 = \Theta_3 = 0$ . The surface with high roughness coefficient  $\alpha = .9$  results in quick rise and very high responses. The influence of the relative lengths of link-1 to link-2 on the displacements and velocities is shown in Figure 6.17. It is noted that the longer the terminal link (link-2) compared to link-1, the higher the responses.

## 6.5. Summary and Concluding Remarks

In this chapter, the Lagrangian and the Rayleigh dissipation function for a two link wheeled mobile manipulator have been developed. The Lagrange principle has been used to derive the equation of motion for the manipulator mounted on an accelerating and a constant velocity mobile base. To generalize the results dimensionless time has been introduced. The ideas presented in chapter five have been employed to study the system.

For an accelerating wheeled mobile manipulator it has been observed that: the dominant system response (stochastic or deterministic) depends on the manipulator configuration, thus the more perpendicular the manipulator to an excitation, the higher the response to that excitation; the highest stochastic response occurs at  $\Theta_2 = \Theta_3 = 0^\circ$  and the highest deterministic response occurs at  $\Theta_2 = 90^\circ$  and  $\Theta_3 = 0^\circ$ ; the stochastic response of the manipulator tip is almost unidirectional along the major principal variance axis; the direction and magnitude of the principal variance differs significantly for different configurations; the deterministic response is generally more oscillatory compared to the stochastic response.

Sensitivity of the tip motion to the base acceleration, surface roughness coefficient, and damping have been investigated. In general, it has been observed that the higher the vehicle acceleration, the higher the deterministic response; the stochastic response is very quick and uneven when the base has high acceleration on a very rough surface. It can be concluded that the base suspension damping alone is not sufficient to minimize the stochastic vibration, damping has to be added to the manipulator joints.

For a constant velocity wheeled mobile manipulator two representations - the power spectral density and the state space- have been used to study the stationary response of the manipulator tip. It has been observed that: the responses obtained from the Power Spectral Density and the State Space representations are the same; the State Space representation is, however, recommended for practical

applications, because it gives the velocity and the displacement covariance simultaneously; also, the state space representation can accommodate non-proportional damping without computational complications and it avoids complex contour integration. From the sensitivity analysis it can be concluded that to minimize the stochastic vibration, damping has to be added to the manipulator joints. Further, the upper links of the manipulator should be shorter than the lower links. The analysis presented in chapter five and the example discussed in this chapter have been limited to single-wheeled mobile manipulator. In the next chapter procedures for studying the dynamics of multiple-wheeled mobile manipulators are developed.

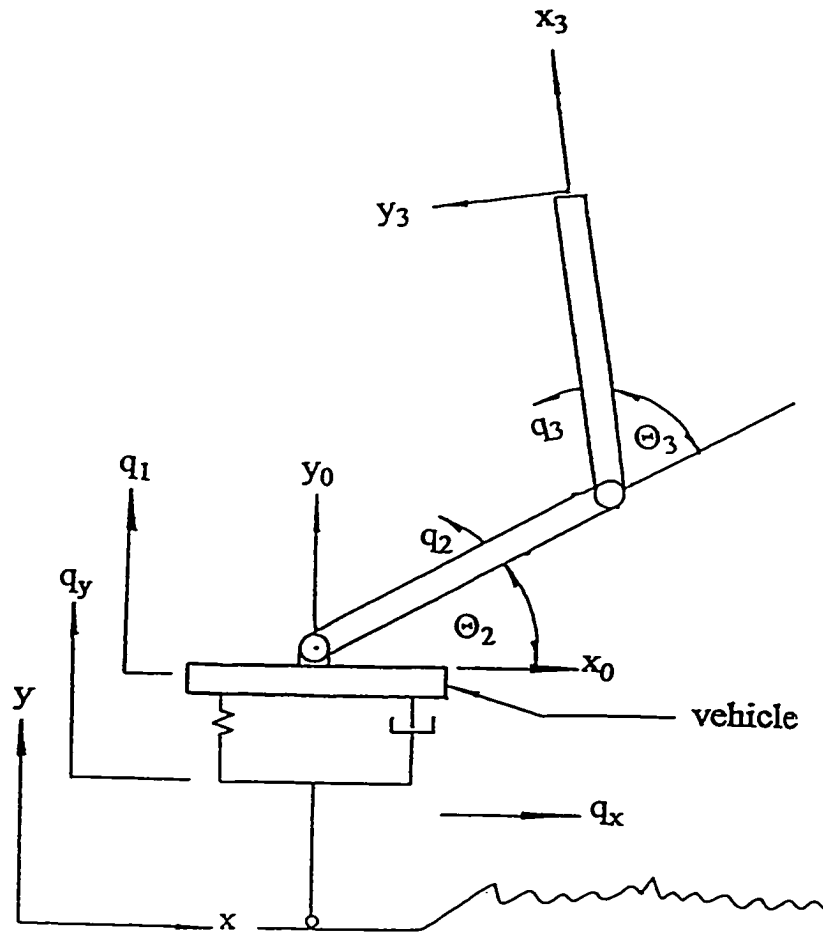


Figure 6.1. Two Link Wheeled Mobile Manipulator

- $\Theta_i$  kinematic configuration of link  $i$
- $q_i$  elastic motion variable of link  $i$
- $q_x$  vehicles horizontal motion
- $(x,y)_1$  Cartesian coordinate frame attached to link 1

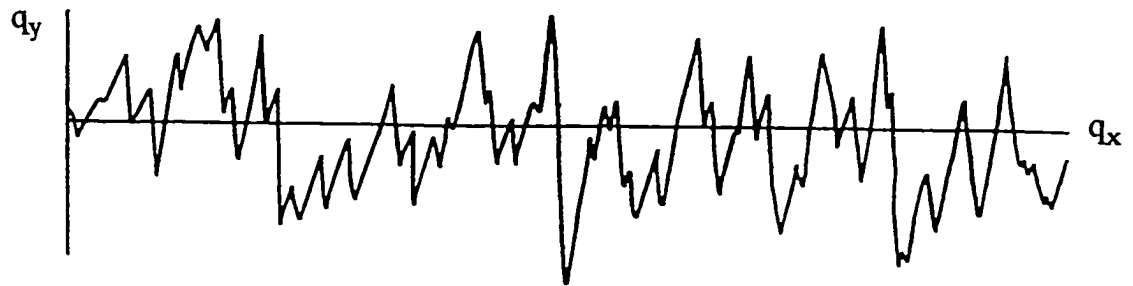


Figure 6.2. Sample of Surface Profile.



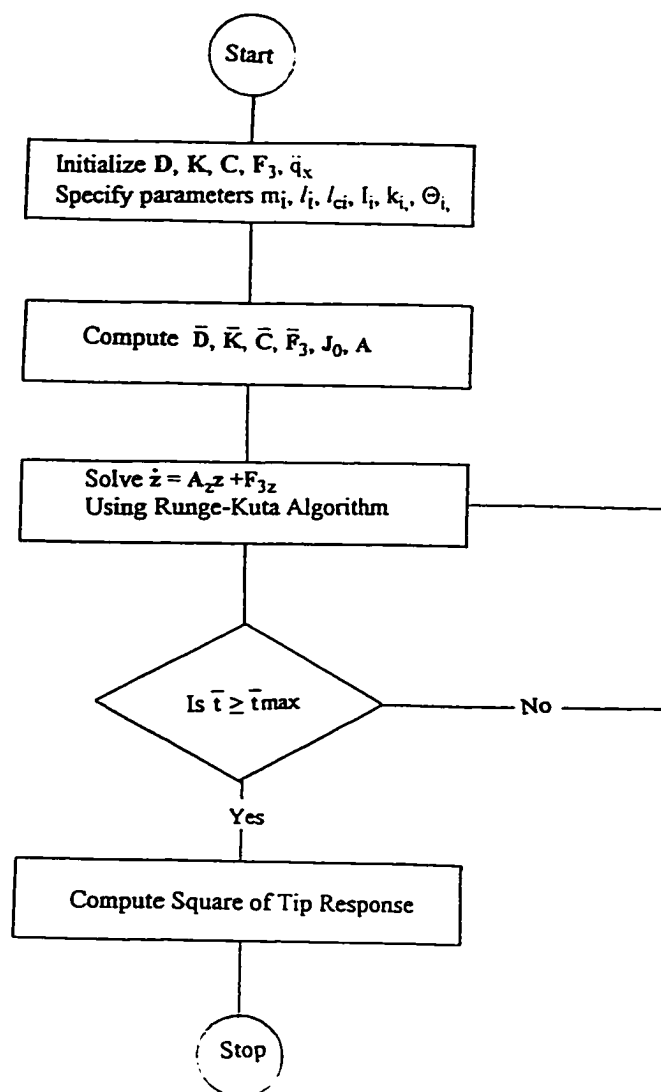


Figure 6.3. Flow Chart of the Program Used for Simulating the Deterministic Dynamics of a Wheeled Mobile Manipulator.

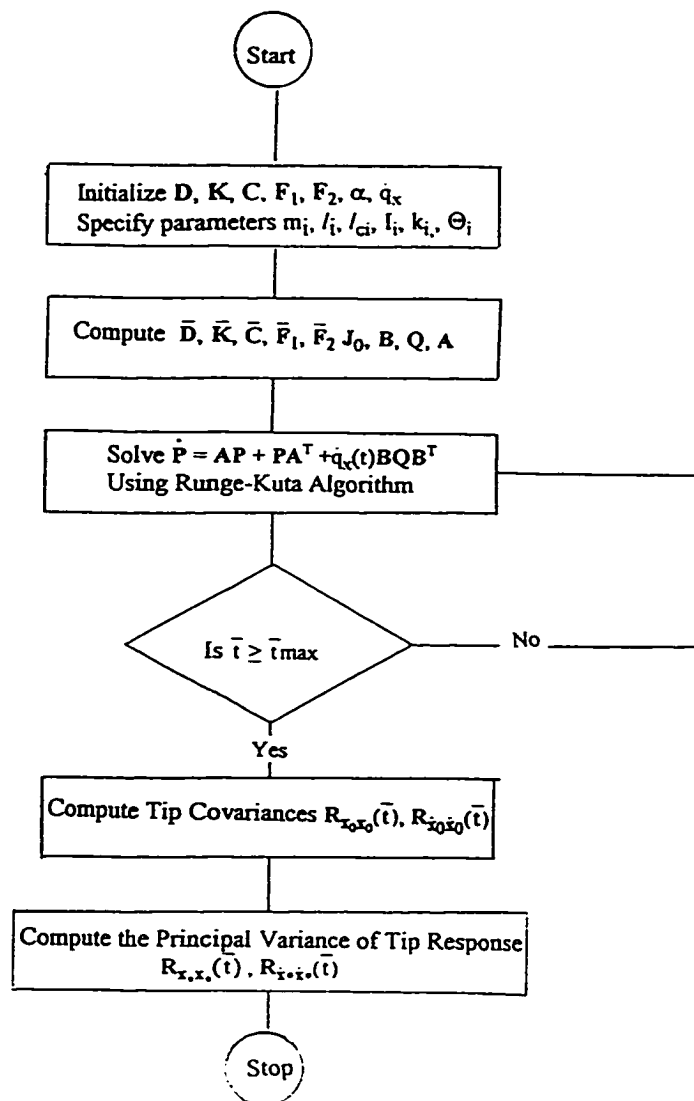


Figure 6.4. Flow Chart of the Program Used for Simulating the Nonstationary Stochastic Dynamics of a Wheeled Mobile Manipulator.

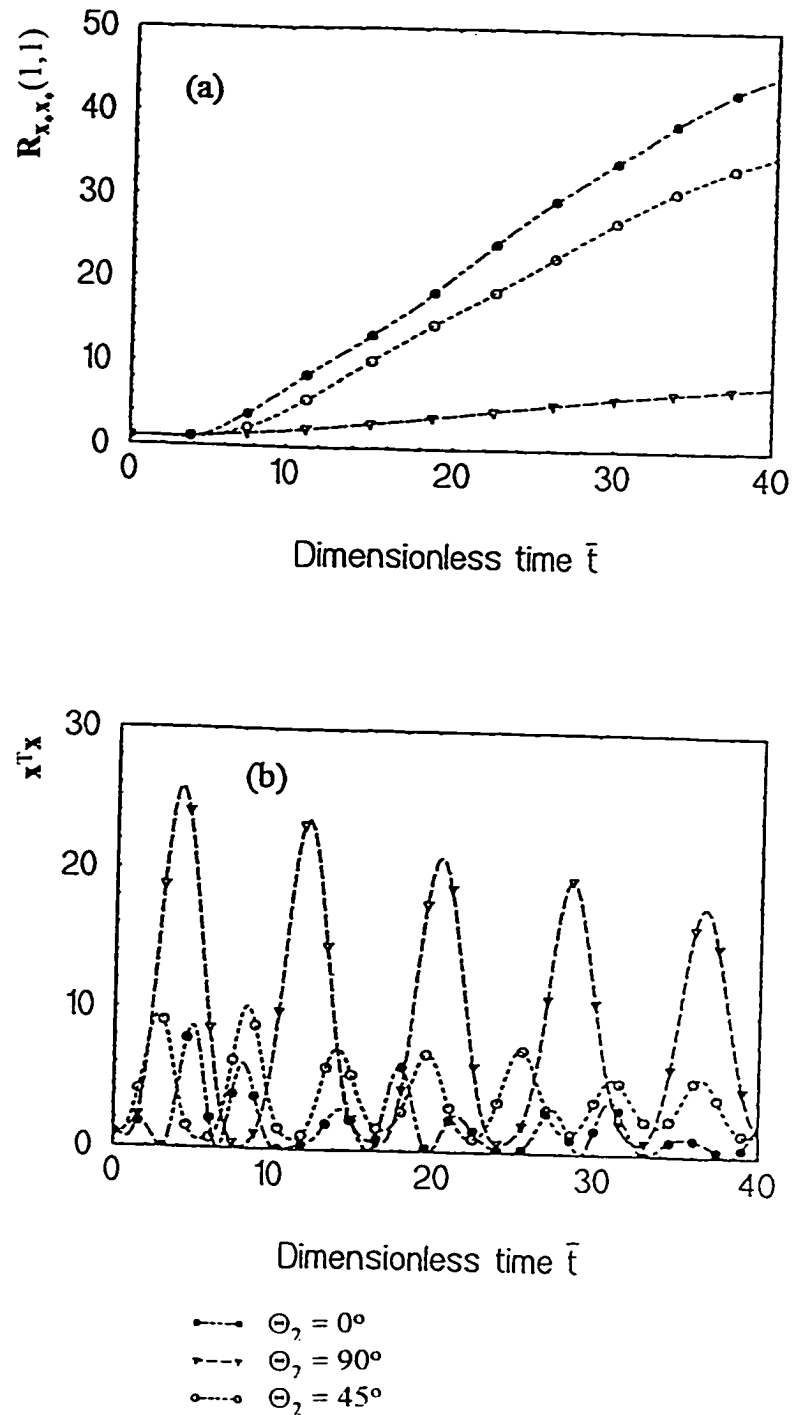


Figure 6.5. Sensitivity of the Principal Variance and the Square of the Deterministic Tip Response of Accelerating Wheeled Mobile Manipulator to Configuration Changes(a) Nonstationary Stochastic (b) Deterministic

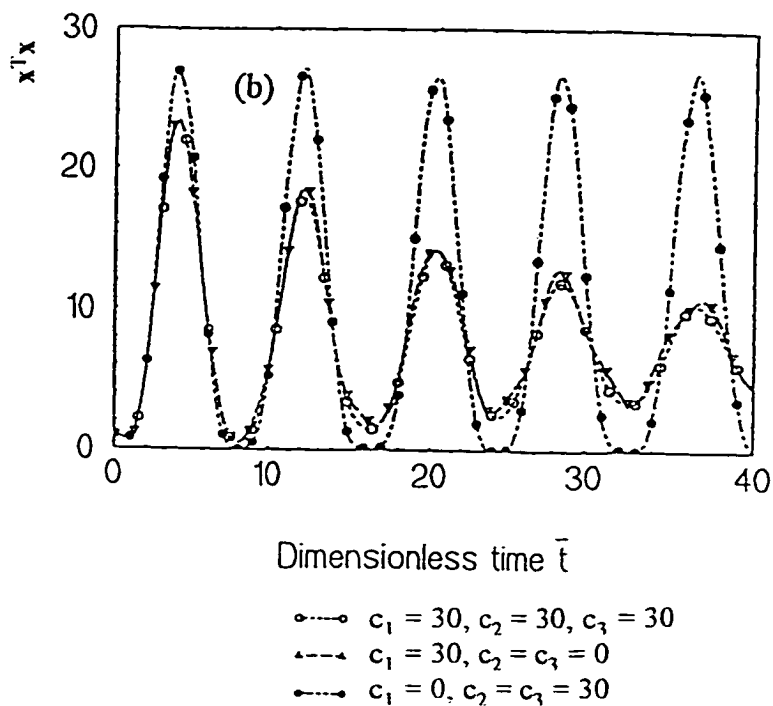
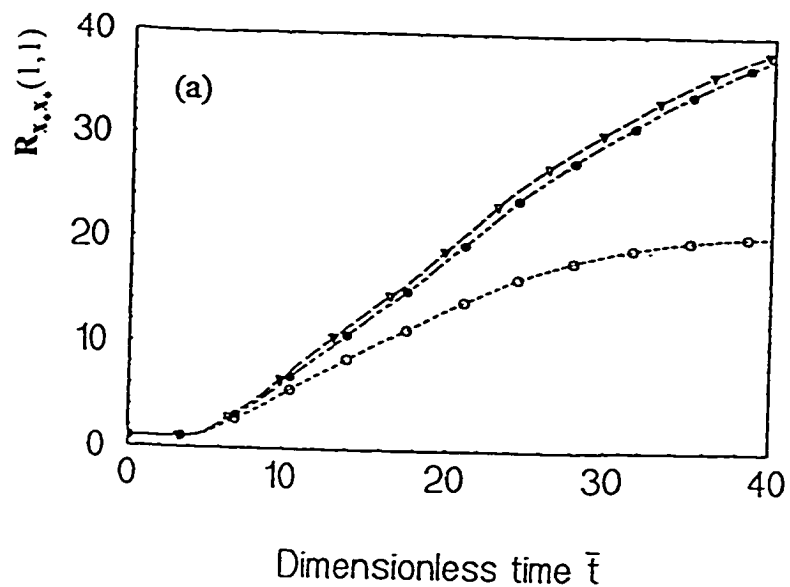


Figure 6.6. Influence of Damping on the Principal Tip Displacement Variance and Square of the Deterministic Tip Response of a Wheeled Mobile Manipulator (a) Nonstationary Stochastic (b) Deterministic.

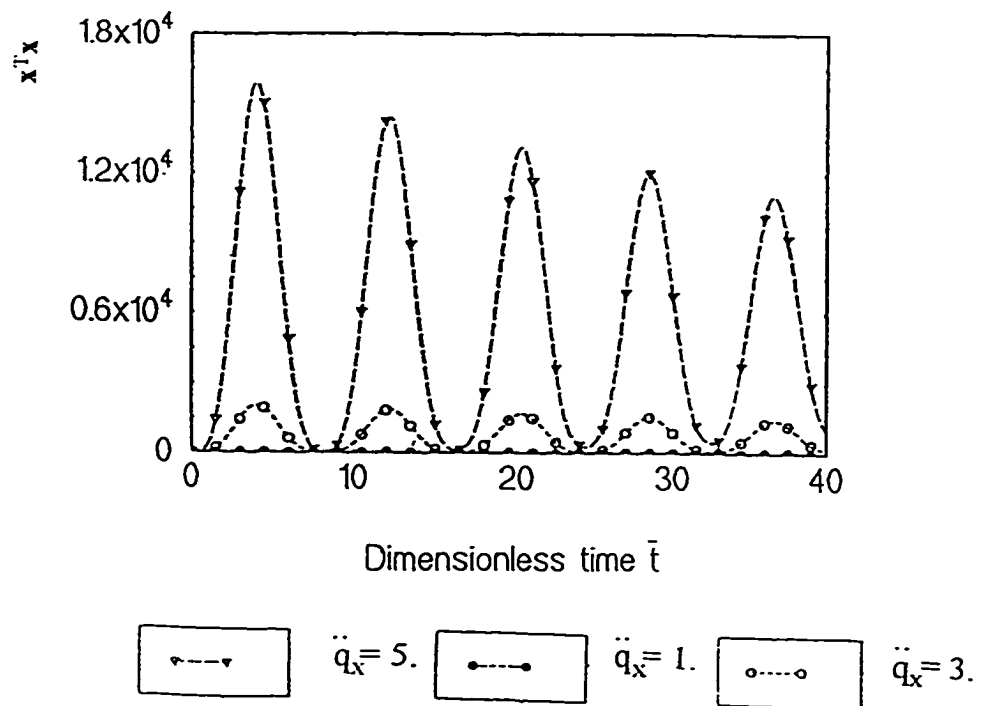


Figure 6.7. Effect of the Base Horizontal Acceleration on the Square of the Deterministic Tip Response of a Wheeled Mobile Manipulator.

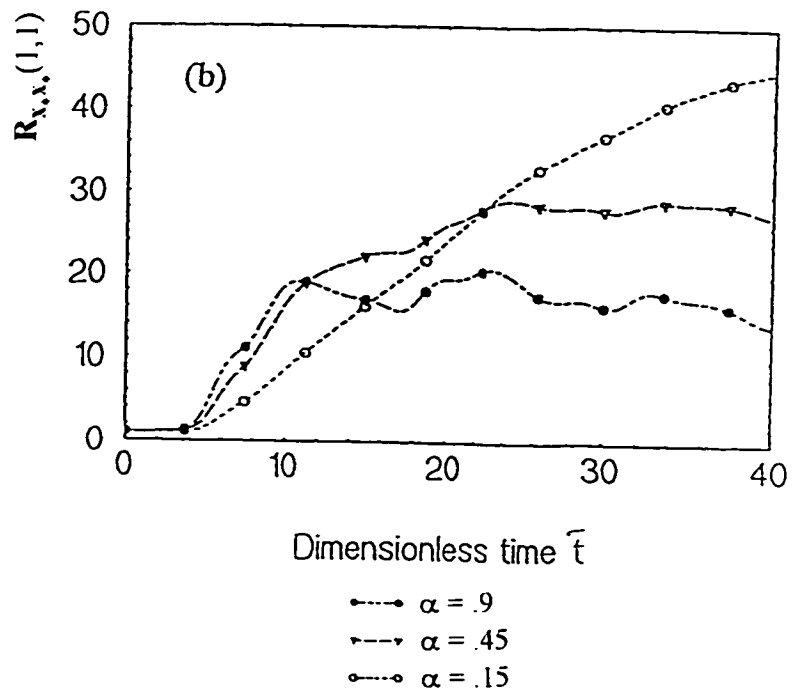
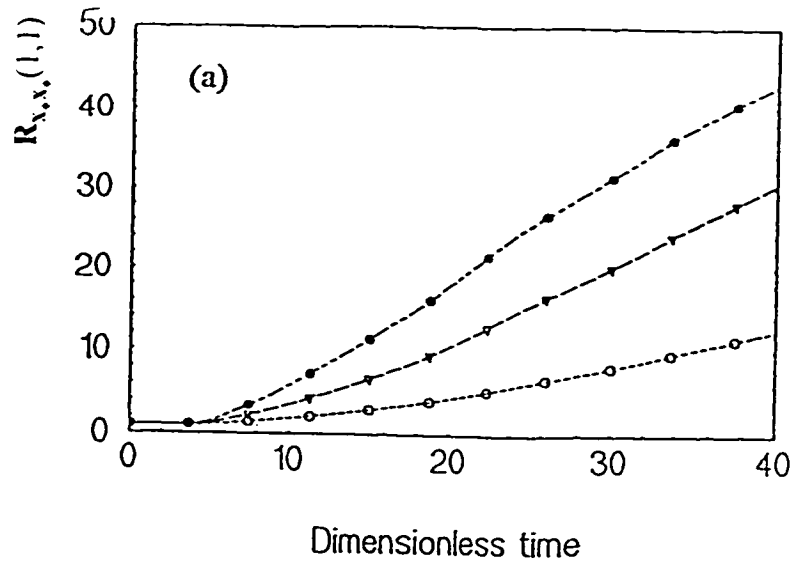


Figure 6.8. Effect of the Base Horizontal Acceleration and Surface Roughness Coefficient on the Normalized Principal Tip Displacement Variance of a Wheeled Mobile Manipulator.

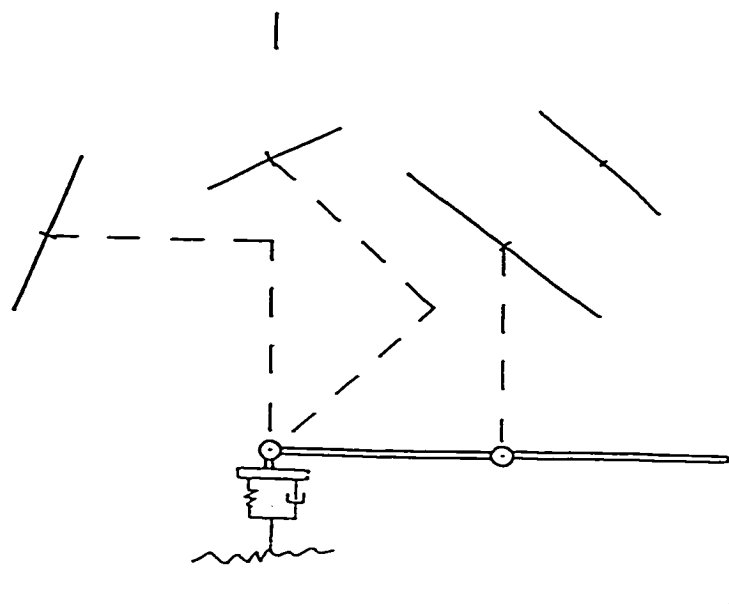


Figure 6.9. Magnitude and Orientation of the Normalized Principal Tip Displacement Variance of a Wheeled Mobile Manipulator for Six Configurations.

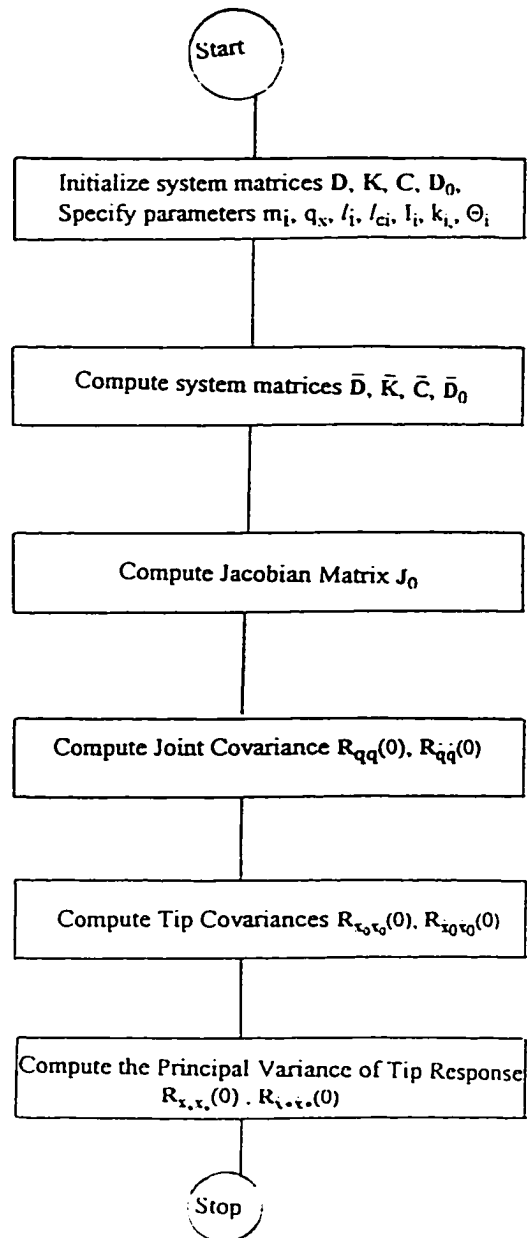


Figure 6.10. Flow Chart of the Program Used for Simulating the Stationary Stochastic Dynamics of a Wheeled Mobile Manipulator Using the Power Spectral Density Approach.



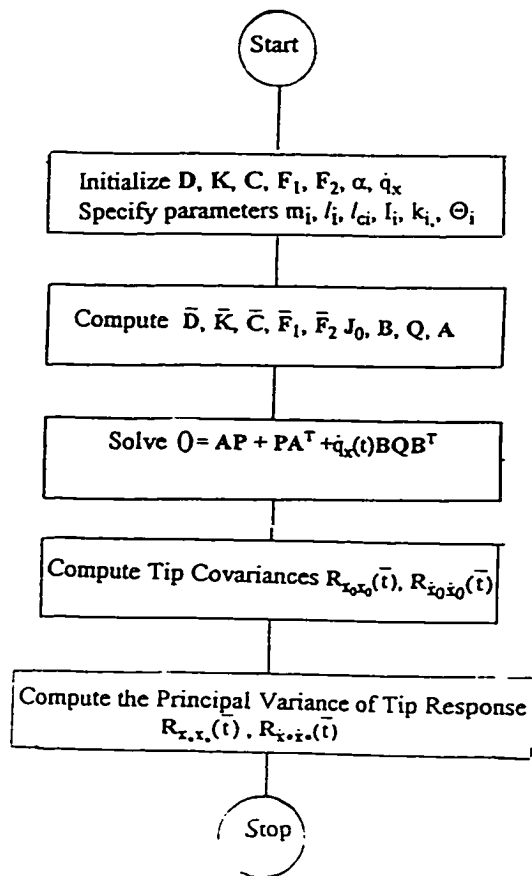


Figure 6.11. Flow Chart of the Program Used for Simulating the Stationary Stochastic Dynamics of a Wheeled Mobile Manipulator Using the State Space Approach.

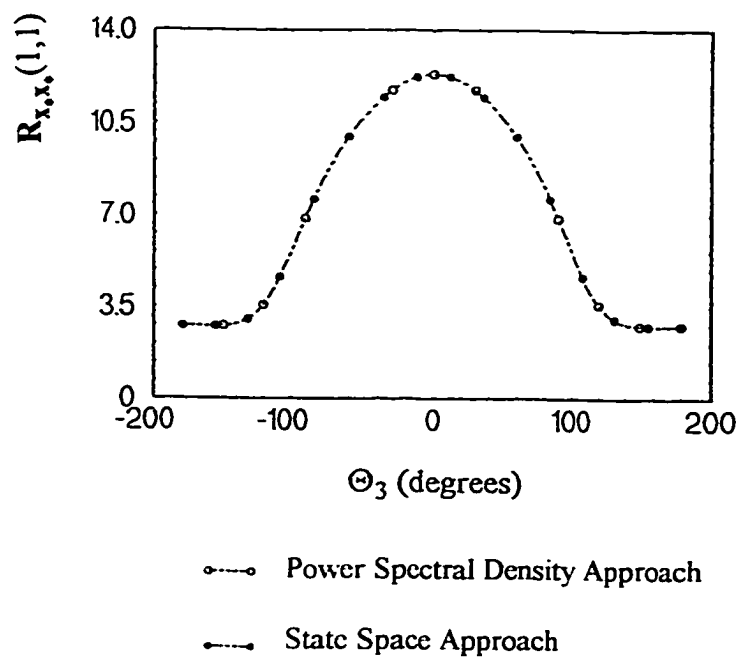


Figure 6.12. Comparison of the Stationary Principal Variance of Tip Response Obtained Using the State Space Representation and the Power Spectral Density Representation for a Wheeled Mobile Manipulator.

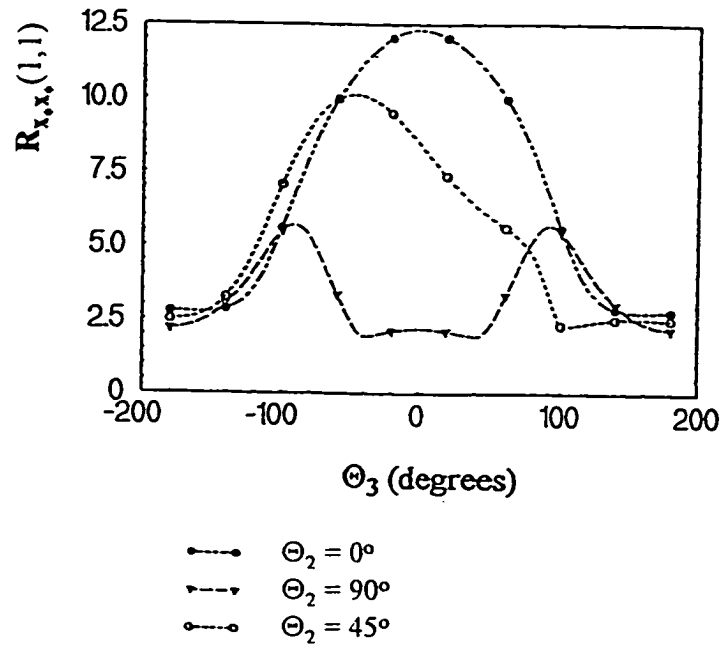


Figure 6.13. Sensitivity of the Stationary Principal Tip Displacement Variance of a Wheeled Mobile Manipulator to Configuration Changes.

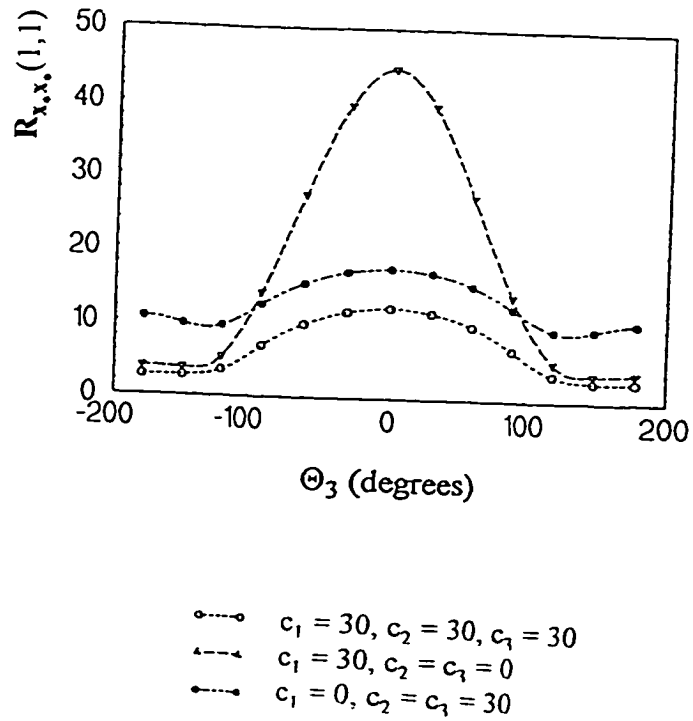


Figure 6.14. Effect of Damping on the Normalized Stationary Principal Tip Displacement Variance of a Wheeled Mobile Manipulator Moving with a Constant Base Velocity.

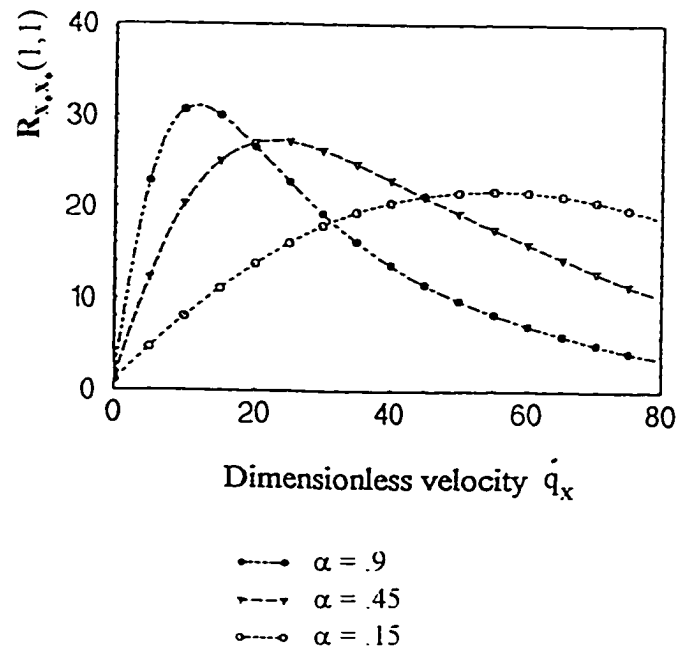


Figure 6.15. Effect of Surface Roughness Coefficient on the Normalized Stationary Principal Tip Displacement Variance of a Wheeled Mobile Manipulator Moving with a Constant Base Velocity.

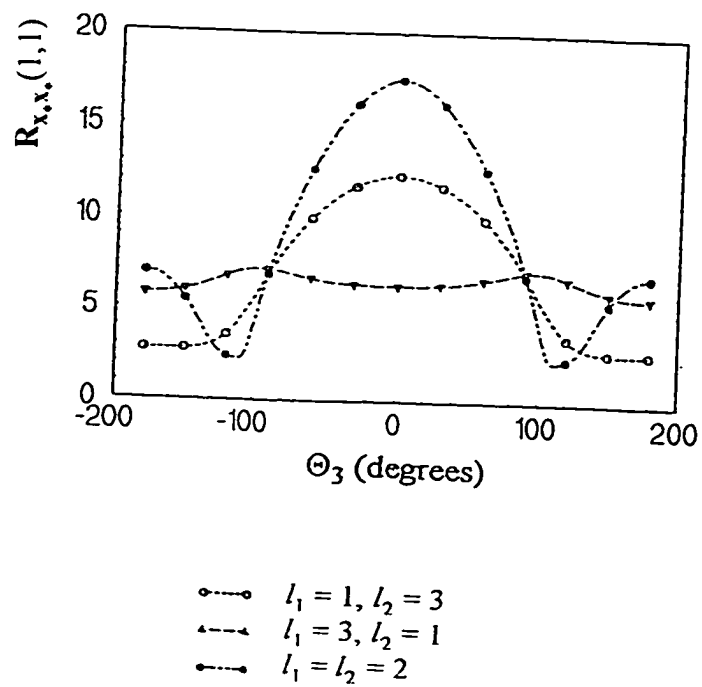


Figure 6.16. Effect of Links Length on the Normalized Principal Tip Displacement Variance of a Wheeled Mobile Manipulator Moving with a Constant Base Velocity.

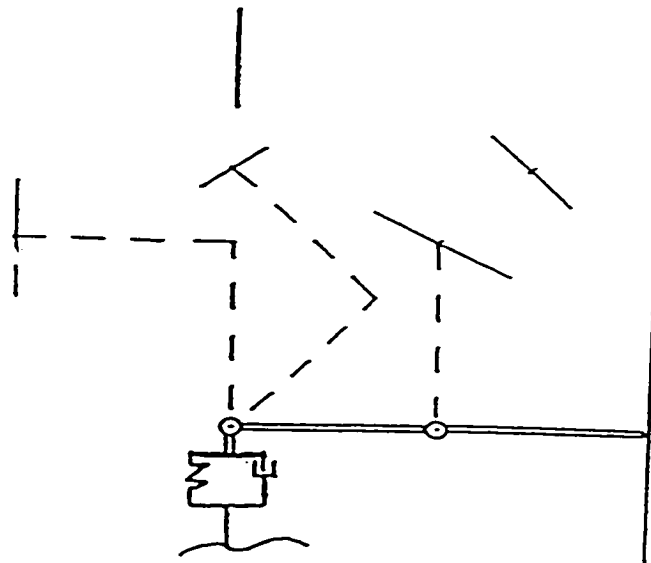


Figure 6.17. Magnitude and Orientation of the Normalized Stationary Principal Tip Displacement Variance of a Wheeled Mobile Manipulator for Six Configurations.

## Chapter Seven

# MULTIPLE-WHEELED MOBILE MANIPULATOR, ANALYSIS

### 7.1. Introduction

The formulation reported in this chapter is an original contribution of the author. Components of this chapter have been accepted for publication in Akpan and Kujath, (1996c). The originality is in the modeling of the joint and the tip covariance responses of the flexible manipulator structure to the traction induced multiple-wheel random base motion. Known analytical tools such as state space techniques and modeling of traction induced excitation have been used in the formulation.

### 7.2. Model Assumptions

In this chapter the wheeled mobile base is modeled as a beam on multiple suspensions. The suspensions are connected to the vehicle body by linear joints. The mobile base is modeled using a half car representation: there are two wheels which are longitudinally aligned (see Figure 7.1). The base moves horizontally and is subjected to heaving  $q_{1H}$  and pitching motion  $q_{1P}$ ; both the rear  $q_{y2}$  and the front  $q_{y1}$  wheel motions follow the ground profile; the second wheel follows exactly the



path of the first; the wheels maintain contact with the ground at all times; there is no deformation of the surface during motion; the distance between the front and the rear wheels does not change during motion.

### 7.3. Equation of Motion

Application of the Lagrangian principle leads to the linear equation of motion

$$D\ddot{\mathbf{q}}(t) + C\dot{\mathbf{q}}(t) + K\mathbf{q}(t) = \mathbf{f}_1\mathbf{q}_{y1}(t) + \mathbf{f}_2\dot{\mathbf{q}}_{y1}(t) + \mathbf{f}_4\mathbf{q}_{y2}(t) + \mathbf{f}_5\dot{\mathbf{q}}_{y2}(t) + \mathbf{f}_3\ddot{\mathbf{q}}_x(t) \quad (7.1)$$

where

- $\mathbf{f}_1$  coefficient vector of stochastic excitation  $\mathbf{q}_{y1}$ ,
- $\mathbf{f}_2$  coefficient vector of stochastic excitation  $\dot{\mathbf{q}}_{y1}$ ,
- $\mathbf{f}_4$  coefficient vector of stochastic excitation  $\mathbf{q}_{y2}$ ,
- $\mathbf{f}_5$  coefficient vector of stochastic excitation  $\dot{\mathbf{q}}_{y2}$ ,
- $\mathbf{f}_3$  coefficient vector of deterministic excitation  $\ddot{\mathbf{q}}_x(t)$ .

Equation (7.1) is an expanded version of equation (5.1) and the terms  $\mathbf{f}_4\mathbf{q}_{y2}(t) + \mathbf{f}_5\dot{\mathbf{q}}_{y2}(t)$  have been added to take into account the trailing wheels. Using the principle of superposition equation (7.1) can be separated into two equations - the deterministic and the stochastic motion respectively

$$D\ddot{\mathbf{q}}(t) + C\dot{\mathbf{q}}(t) + K\mathbf{q}(t) = \mathbf{f}_3\ddot{\mathbf{q}}_x(t) \quad (7.2)$$

and

$$\mathbf{D}\ddot{\mathbf{q}}(t) + \mathbf{C}\dot{\mathbf{q}}(t) + \mathbf{K}\mathbf{q}(t) = \mathbf{f}_1q_{y1}(t) + \mathbf{f}_2\dot{q}_{y1}(t) + \mathbf{f}_4q_{y2}(t) + \mathbf{f}_5\dot{q}_{y2}(t) \quad (7.3)$$

Equation (7.2) represents the deterministic part of the system while equation (7.3) represents the stochastic part of the system. The deterministic and the stochastic responses will be treated separately. The technique used in section (5.4) can be applied to compute the deterministic response. The procedure for the stochastic responses, however, is more complex since the second wheel experiences a time delayed excitation and it will be developed in the next section.

## 7.4. Stochastic Response

### 7.4.1. Joint Response

The excitation of the front wheel produced by the surface  $q_{y1}(t)$  can be modeled as output of a shaping filter to a white noise  $w(q_x(t))$  expressed by

$$\dot{q}_{y1}(t) = \mathbf{f}_y(t)q_{y1}(t) + \mathbf{b}_y^T(t)w(q_x(t)). \quad (7.4)$$

Since the two-wheeled configuration is used, then the shaping filter representation of the rear wheel is

$$\dot{q}_{y2}(t) = \mathbf{f}_y(t)q_{y2}(t) + \mathbf{b}_y^T(t)w(q_x(t) - l) \quad (7.5)$$

where  $l$  is the distance between the front and the rear wheel. The covariance matrix of the white noise vector for the two wheels is

$$E\{\mathbf{w}(q_x(t_1))\mathbf{w}_x^T(q_x(t_2))\} = \mathbf{Q}\delta(q_x(t_1) - q_x(t_2))$$

$$= \frac{\mathbf{Q}\delta(t_1 - t_2)}{\dot{q}_x(t_1)} \quad \text{for } \dot{q}_x(t_1) \geq 0. \quad (7.6)$$

See Appendix F. The term  $\delta$  is the Dirac Delta function. Assuming  $\mathbf{q}$  has dimension  $n \times 1$ , the augmented state variable  $\mathbf{y}$  can be defined as

$$\mathbf{y} = [\mathbf{z}^T, q_{y1}, q_{y2}]^T, \quad \mathbf{z} = [\mathbf{q}^T, \dot{\mathbf{q}}^T]^T. \quad (7.7)$$

where the state variable  $\mathbf{y}$  has dimension  $2(n+1) \times 1$ . Application of equation (7.7) to equations (7.2), (7.4) and (7.5) lead to

$$\dot{\mathbf{y}} = \mathbf{A}\mathbf{y} + \dot{q}_x(t)\mathbf{B}_1\mathbf{w}(q_x(t)) + \dot{q}_x(t)\mathbf{B}_2\mathbf{w}(q_x(t) - l) \quad (7.8)$$

$$\mathbf{A} = \begin{bmatrix} \mathbf{A}_z & \mathbf{D}^{-1}(\mathbf{f}_1 + \mathbf{f}_2\mathbf{f}_y) & \mathbf{D}^{-1}(\mathbf{f}_4 + \mathbf{f}_5\mathbf{f}_y) \\ \mathbf{0}_2^T & \mathbf{f}_y & \mathbf{0}_3 \\ \mathbf{0}_2^T & \mathbf{0}_3 & \mathbf{f}_y \end{bmatrix} \quad (7.9)$$

$$\mathbf{B}_1 = \begin{bmatrix} \mathbf{0}_1 \\ \mathbf{D}^{-1} \mathbf{f}_2 \mathbf{b}_y^T \\ \mathbf{b}_y^T \\ \mathbf{0}_1 \end{bmatrix} \quad (7.10)$$

$$\mathbf{B}_2 = \begin{bmatrix} \mathbf{0}_1 \\ \mathbf{D}^{-1} \mathbf{f}_4 \mathbf{b}_y^T \\ \mathbf{0}_1 \\ \mathbf{b}_y^T \end{bmatrix} \quad (7.11)$$

$$\mathbf{A}_z = \begin{bmatrix} \mathbf{0} & \mathbf{I} \\ -\mathbf{D}^{-1} \mathbf{K} & -\mathbf{D}^{-1} \mathbf{C} \end{bmatrix}. \quad (7.12)$$

Assuming the dimension of the white noise vector is  $m \times 1$  then  $\mathbf{B}_1$  and  $\mathbf{B}_2$  is  $2(n-1) \times m$  matrix.  $\mathbf{0}_1$  is  $m \times 1$  vector and  $\mathbf{0}_2$  is a  $2n \times 1$  vector.  $\mathbf{A}_z$  is matrix of dimension  $n \times n$ . The solution of equation (7.8) is given as

$$\mathbf{y} = \Phi(t, t_0) \mathbf{y}(t_0) + \int_{t_0}^t \Phi(t, t_1) \dot{\mathbf{q}}_x(t_1) (\mathbf{B}_1(t_1) \mathbf{w}(q_x(t_1)) + \mathbf{B}_2(t_1) \mathbf{w}(q_x(t_1) - l)) dt_1 \quad (7.13)$$

The term  $\Phi(t, t_0)$  is the transition matrix of equation (7.8),  $t_0$  is the initial time and  $t_1$  is a dummy time variable. The covariance matrix of the augmented state  $\mathbf{y}$  can be defined as

$$\mathbf{P} = E\{\mathbf{y}\mathbf{y}^T\} \quad (7.14)$$

so that

$$\dot{\mathbf{P}} = E\{\dot{\mathbf{y}}\mathbf{y}^T + \mathbf{y}\dot{\mathbf{y}}^T\}. \quad (7.15)$$

Application of equation (7.15) to equations (7.14) and (7.8) give

$$\begin{aligned} \dot{\mathbf{P}} = & \mathbf{A}\mathbf{P} + \mathbf{P}\mathbf{A}^T + \dot{\mathbf{q}}_x(t)E\{\mathbf{y}\mathbf{w}^T(\mathbf{q}_x(t))\}\mathbf{B}_1^T + \dot{\mathbf{q}}_x(t)E\{\mathbf{y}\mathbf{w}^T(\mathbf{q}_x(t) - l)\}\mathbf{B}_2^T \\ & + \dot{\mathbf{q}}_x(t)\mathbf{B}_1E\{\mathbf{w}(\mathbf{q}_x(t))\mathbf{y}^T\} + \dot{\mathbf{q}}_x(t)\mathbf{B}_2E\{\mathbf{w}(\mathbf{q}_x(t) - l)\mathbf{y}^T\} \end{aligned} \quad (7.16)$$

To solve equation (7.16) for the response covariance  $\mathbf{P}$  the averages  $E\{\cdot\}$  in the equation have to be defined. Considering the first average and using equation (7.13) gives

$$\begin{aligned}
E\{\mathbf{y}\mathbf{w}(\mathbf{q}_x(t))\} &= \Phi(t, t_0)E\{\mathbf{y}(t_0)\mathbf{w}^T(\mathbf{q}_x(t))\} \\
&+ \int_{t_0}^t \Phi(t, t_1)\dot{\mathbf{q}}_x(t_1)(\mathbf{B}_1(t_1)E\{\mathbf{w}(\mathbf{q}_x(t_1))\mathbf{w}^T(\mathbf{q}_x(t))\})dt_1 \\
&+ \int_{t_0}^t \Phi(t, t_1)\dot{\mathbf{q}}_x(t_1)(\mathbf{B}_1(t_1)E\{\mathbf{w}(\mathbf{q}_x(t_1) - l)\mathbf{w}^T(\mathbf{q}_x(t))\})dt_1
\end{aligned} \tag{7.17}$$

The three terms of the sum in equation (7.17) can be evaluated individually. Since the initial state  $\mathbf{y}(t_0)$  is uncorrelated with the excitation following  $t_0$ , then the first component of the sum is a zero vector. The second component of equation (7.17) can be obtained using equation (7.6) as

$$\int_{t_0}^t \Phi(t, t_1)\dot{\mathbf{q}}_x(t_1)(\mathbf{B}_1(t_1)E\{\mathbf{w}(\mathbf{q}_x(t_1))\mathbf{w}^T(\mathbf{q}_x(t))\})dt_1 = \frac{1}{2}\mathbf{B}_1\mathbf{Q} \tag{7.18}$$

To evaluate the third component in equation (7.17) note that

$$E\{\mathbf{w}(\mathbf{q}_x(t_1) - l)\mathbf{w}^T(\mathbf{q}_x(t))\} = \mathbf{Q}(t_1)\delta(\mathbf{q}_x(t_1) - l - \mathbf{q}_x(t)) \tag{7.19}$$

The zero of the expression  $(\mathbf{q}_x(t_1) - l - \mathbf{q}_x(t))$  can be located at time  $t_1 = \mathbf{q}_x^{-1}(\mathbf{q}_x(t) + l)$ . Since  $\dot{\mathbf{q}}_x(t) \geq 0$  and  $l \neq 0$ , then  $\mathbf{q}_x(t)$  is a non decreasing therefore  $t_1 > t$  for all  $t$ . Because  $t_1 \leq t$  and  $t_1 - \frac{l}{\dot{\mathbf{q}}_x}$  lags behind  $t_1$  therefore when  $t_1$

reaches the integration limit of  $t$  the rear wheel never reaches  $q_x(t)$ . It only reaches  $q_x(t) - l$ . Therefore the value of the third term of equation (7.17) is zero and so this term makes no contribution. Equation (7.17) becomes

$$E\{y\mathbf{w}^T(q_x(t))\} = \frac{l}{2}\mathbf{B}_1\mathbf{Q} \quad (7.20)$$

Considering the second expectation term  $E\{.\}$  in equation (7.16) gives

$$\begin{aligned} E\{y\mathbf{w}^T(q_x(t)-l)\} &= \Phi(t, t_0)E\{y(t_0)\mathbf{w}^T(q_x(t)-l)\} \\ &+ \int_{t_0}^t \Phi(t, t_1)\dot{q}_x(t_1)(\mathbf{B}_1(t_1)E\{\mathbf{w}(q_x(t_1))\mathbf{w}^T(q_x(t)-l)\})dt_1 \\ &+ \int_{t_0}^t \Phi(t, t_1)\dot{q}_x(t_1)(\mathbf{B}_2(t_1)E\{\mathbf{w}(q_x(t_1) - l)\mathbf{w}^T(q_x(t) - l)\})dt_1 \end{aligned} \quad (7.21)$$

Evaluation of the sum of the components in equation (7.21) results in the first term equal to zero since the initial state  $y(t_0)$  is uncorrelated with the excitation following  $t_0$ .

To evaluate the second term the zero of the expression  $(q_x(t_1) + l - q_x(t))$  is located at  $t_1 = q_x^{-1}(q_x(t) - l) = \bar{T}$ . Because  $\dot{q}_x(t) \geq 0$ , then  $q_x(t)$  is non decreasing. Since  $l \neq 0$ , then  $\bar{T} < t$  for all  $t$  but  $\bar{T}$  may also be less than  $t_0$ . This latter condition is the period during which the rear wheel has not yet begun to pass over the same

profile as the first. This is mathematically reflected by a zero contribution from the rear wheel so that the following result is obtained

$$\int_{t_0}^t \Phi(t, t_1) \dot{q}_x(t_1) (\mathbf{B}_1(t_1)) E \{ \mathbf{w}(q_x(t_1)) \mathbf{w}^T(q_x(t) - l) \} dt_1$$

$$= \begin{cases} 0 & q_x(t) - l < q_x(t_0) \\ \frac{1}{2} \Phi(t, t_0) \mathbf{B}_1(t_0) \mathbf{Q} & q_x(t) - l = q_x(t_0) \\ \Phi(t, \bar{T}) \mathbf{B}_1(\bar{T}) \mathbf{Q} & q_x(t) - l > q_x(t_0) \end{cases} \quad (7.22)$$

The third component of equation (7.21) is given as

$$\int_{t_0}^t \Phi(t, t_1) \dot{q}_x(t_1) (\mathbf{B}_2(t_1)) E \{ \mathbf{w}(q_x(t) - l) \mathbf{w}^T(q_x(t) - l) \} dt_1 = \frac{1}{2} \mathbf{B}_2 \mathbf{Q} \quad (7.23)$$

Equation (7.21) becomes

$$E \{ \mathbf{y} \mathbf{w}(q_x(t) - l) \} = \frac{1}{2} \mathbf{B}_2 \mathbf{Q}$$

$$+ \begin{cases} 0 & q_x(t) - l < q_x(t_0) \\ \frac{1}{2} \Phi(t, t_0) \mathbf{B}_1(t_0) \mathbf{Q} & q_x(t) - l = q_x(t_0) \\ \Phi(t, \bar{T}) \mathbf{B}_1(\bar{T}) \mathbf{Q} & q_x(t) - l > q_x(t_0) \end{cases} \quad (7.24)$$



Similar results can be obtained for the third and fourth expectations terms  $E\{.\}$  in equation (7.16) since they are transposes of the first and second terms respectively. Application of the results of the expectation evaluation in equation (7.16) gives

$$\dot{\mathbf{P}} = \mathbf{A}\mathbf{P} + \mathbf{P}\mathbf{A}^T + \dot{q}_x(t)[\mathbf{B}_1\mathbf{Q}\mathbf{B}_1^T + \mathbf{B}_2\mathbf{Q}\mathbf{B}_2^T + \mathbf{B}_2\mathbf{Q}\mathbf{B}_1^T\Phi^T(t, \bar{T}) + \Phi(t, \bar{T})\mathbf{B}_1\mathbf{Q}\mathbf{B}_2^T] \quad (7.25)$$

Equation (7.25) is the generalized Liapunov covariance matrix differential equation for the system. It can be solved for the covariance  $\mathbf{P}$  using numerical integration algorithm. In general, the covariance response  $\mathbf{P}$  is nonstationary.

#### 7.4.2. Constant Velocity of the Mobile Base

When the mobile base has constant velocity, i.e.,  $\ddot{q}_x(t) = 0$ , the deterministic component of the excitation in equation (7.1) vanishes. Further, the Liapunov's covariance differential equation (equation 7.25) degenerates to the algebraic form

$$\mathbf{A}\mathbf{P} + \mathbf{P}\mathbf{A}^T = -\dot{q}_x(t)[\mathbf{B}_1\mathbf{Q}\mathbf{B}_1^T + \mathbf{B}_2\mathbf{Q}\mathbf{B}_2^T + \mathbf{B}_2\mathbf{Q}\mathbf{B}_1^T\Phi^T(\tau) + \Phi(\tau)\mathbf{B}_1\mathbf{Q}\mathbf{B}_2^T] \quad (7.26)$$

where the time delay ( $\tau$ ) is given by  $\tau = \frac{l}{\dot{q}_x(t)}$  and the function  $\bar{T} = t - \frac{l}{\dot{q}_x(t)}$ . The Liapunov matrix algebraic equation can be solved for  $\mathbf{P}$  using appropriate numerical schemes. The responses in this case are stationary.

#### 7.4.3. Tip Response

The components of the covariance matrix  $\mathbf{P}$  can be reassembled into the joint displacement and the joint velocity covariance matrices defined as;

$R_{\mathbf{q}\mathbf{q}}(t) = E\{\mathbf{q}\mathbf{q}^T\}$  and  $R_{\dot{\mathbf{q}}\dot{\mathbf{q}}}(t) = E\{\dot{\mathbf{q}}\dot{\mathbf{q}}^T\}$  respectively. The tip velocity and displacement responses can be computed using the method discussed in Section 3.5.

## 7.5. Summary and Concluding Remarks

In this chapter the equation of motion for a manipulator wheeled mobile base has been developed. The mobile base has longitudinally aligned multiple wheels. This results in time delayed stochastic excitations. Two cases of the mobile base motion have been fully explored

- (a) The accelerating case.
- (b) The uniform velocity case.

For case (a) -the manipulator with an accelerating base- it has been seen that the system excitation is both stochastic and deterministic. Further, the deterministic part of the excitation leads to a mean response and expressions for this at the joints and the tip of the manipulator have been developed. The stochastic excitation is seen to be nonstationary. Expressions for this time-varying configuration dependent nonstationary covariance tensor of both the joints and tip responses have been derived. It is noted that no assumptions have been made about the nature of the base acceleration or the surface.

In modeling case (b), it was discussed that the mobile robotics system is subjected to only random excitation. Expressions for the covariance tensors of the dynamics of the joints and tip of the mobile manipulator have been fully developed.

To illustrate the procedures discussed in this chapter, a case study and numerical example are presented in the next chapter.

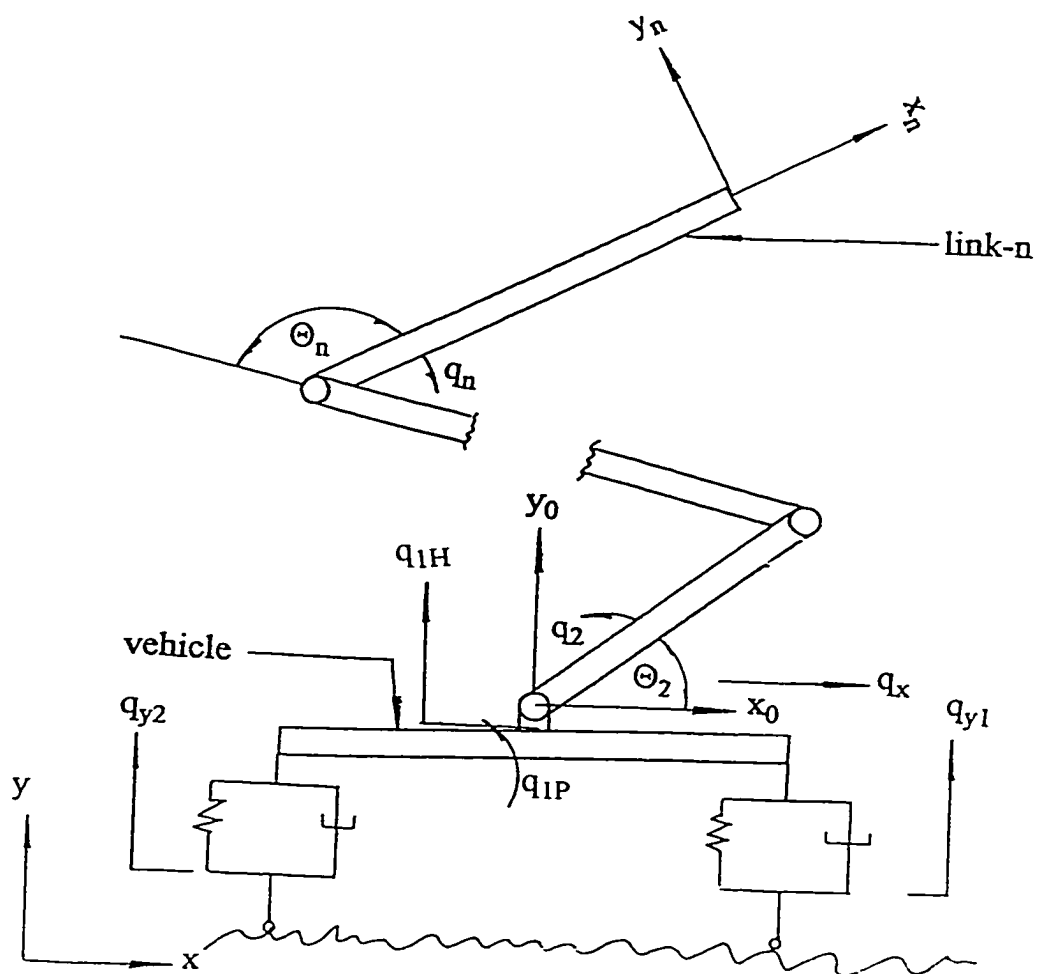


Figure 7.1 Model of a Multiple-Wheeled Mobile Manipulator

$\Theta_i$   $i$ -th kinematic configuration

$q_i$   $i$ -th elastic motion variable

## Chapter Eight

### MULTIPLE-WHEELED MOBILE MANIPULATOR, EXAMPLE

#### 8.1. Example: Two Link Manipulator

A two link manipulator mounted on two longitudinally aligned wheels is used to illustrate the ideas presented in Chapter seven (see Figure 8.1). The Lagrangian for the system  $L$  is given as

$$\begin{aligned}
 L = & \frac{1}{2} a_1 (\dot{q}_{1H} + \dot{q}_x)^2 + \frac{1}{2} I_2 \dot{q}_{1P}^2 + \frac{1}{2} a_2 (\dot{q}_{1P} + \dot{q}_2)^2 + \frac{1}{2} a_3 (\dot{q}_{1P} + \dot{q}_2 + \dot{q}_3)^2 \\
 & + a_4 (\dot{q}_2 + \dot{q}_{1P}) (\dot{q}_2 + \dot{q}_{1P} + \dot{q}_3) \cos(\Theta_3 + q_3) \\
 & + a_5 \dot{q}_{1H} (\dot{q}_2 + \dot{q}_{1P}) \cos(\Theta_2 + q_2 + q_{1P}) \\
 & + a_6 \dot{q}_{1H} (\dot{q}_{1P} + \dot{q}_2 + \dot{q}_3) \cos(\Theta_2 + \Theta_3 + q_{1P} + q_2 + q_3) \\
 & - a_5 \dot{q}_x (\dot{q}_2 + \dot{q}_{1P}) \sin(\Theta_2 + q_2 + q_{1P}) \\
 & - a_6 \dot{q}_x (\dot{q}_{1P} + \dot{q}_2 + \dot{q}_3) \sin(\Theta_2 + \Theta_3 + q_{1P} + q_2 + q_3) \\
 & - \frac{1}{2} k_1 (q_{1H} - q_{y1} + l_1 q_{1P})^2 - \frac{1}{2} k_2 (q_{1H} - q_{y2} - l_2 q_{1P})^2 - \frac{1}{2} k_3 q_2^2 - \frac{1}{2} k_4 q_3^2
 \end{aligned}
 \tag{8.1}$$

$$a_1 = m_2 + m_3 + m_4 \quad (8.2)$$

$$a_2 = I_3 + m_3(l_{c3})^2 + m_4(l_3)^2 \quad (8.3)$$

$$a_3 = I_4 + m_4(l_{c4})^2 \quad (8.4)$$

$$a_4 = m_4 l_3 l_{c4} \quad (8.5)$$

$$a_5 = m_3 l_{c3} + m_4 l_3 \quad (8.6)$$

$$a_6 = m_4 l_{c4} \quad (8.7)$$

The Rayleigh dissipation function  $R$  is given as

$$R = \frac{1}{2}c_1(\dot{q}_{1H} - \dot{q}_{y1} + l_1\dot{q}_{1P})^2 + \frac{1}{2}c_2(\dot{q}_{1H} - \dot{q}_{y2} - l_2\dot{q}_{1P})^2 + \frac{1}{2}c_3\dot{q}_2^2 + \frac{1}{2}c_4\dot{q}_3^2 \quad (8.8)$$

It is noted that the total length of the vehicle base  $l$  is given as

$$l = l_1 + l_2 \quad (8.9)$$

It is assumed that the vehicle (base) has uniform area and density so that

$$l_1 = l_2 = \frac{l}{2} \quad (8.10)$$

It is assumed further that the first link of the manipulator is attached to the center of gravity of the mobile base (vehicle). This center of gravity is at a distance  $\frac{l}{2}$  from the front and rear suspensions.  $m_2$  and  $I_2$  are the mass and moment of inertia of the vehicle about its center of gravity respectively;  $m_3$ ,  $m_4$  and  $I_3$ ,  $I_4$  are the mass and centroidal moment of inertia of the manipulator links respectively;  $l_3$ ,  $l_4$  and  $l_{c3}$ ,  $l_{c4}$  are lengths and distance along the links from the joints to the centroids of the manipulator links respectively; the stiffness and damping coefficients of the vehicle suspension are  $k_1$ ,  $k_2$  and  $c_1$ ,  $c_2$  respectively, while the stiffness and damping coefficients of the manipulator joints are  $k_3$ ,  $k_4$  and  $c_3$ ,  $c_4$  respectively. Using the Lagrange principle the equation of motions for the manipulator on an accelerating base and on a constant velocity base can be obtained respectively. The inertia matrix is

$$\mathbf{D} = \begin{bmatrix} D_{11} & D_{12} & D_{13} & D_{14} \\ D_{21} & D_{22} & D_{23} & D_{24} \\ D_{31} & D_{32} & D_{33} & D_{34} \\ D_{41} & D_{42} & D_{43} & D_{44} \end{bmatrix} \quad (8.11)$$

$$D_{11} = a_1 \quad (8.12)$$

$$D_{12} = a_5 \cos(\Theta_2) + a_6 \cos(\Theta_2 + \Theta_3) \quad (8.13)$$

$$D_{13} = a_5 \cos(\Theta_2) + a_6 \cos(\Theta_2 + \Theta_3) \quad (8.14)$$

$$D_{14} = a_6 \cos(\Theta_2 + \Theta_3) \quad (8.15)$$

$$D_{21} = a_5 \cos(\Theta_2) + a_6 \cos(\Theta_2 + \Theta_3) \quad (8.16)$$

$$D_{22} = I_2 + a_2 + a_3 + 2.0a_4 \cos(\Theta_3) \quad (8.17)$$

$$D_{23} = a_2 + a_3 + 2.0a_4 \cos(\Theta_3) \quad (8.18)$$

$$D_{24} = a_3 + a_4 \cos(\Theta_3) \quad (8.19)$$

$$D_{31} = a_5 \cos(\Theta_2) + a_6 \cos(\Theta_2 + \Theta_3) \quad (8.20)$$

$$D_{32} = a_2 + a_3 + 2.0a_4 \cos(\Theta_3) \quad (8.21)$$

$$D_{33} = a_2 + a_3 + 2.0a_4 \cos(\Theta_3) \quad (8.22)$$

$$D_{34} = a_3 + a_4 \cos(\Theta_3) \quad (8.23)$$

$$D_{41} = a_6 \cos(\Theta_2 + \Theta_3) \quad (8.24)$$

$$D_{42} = a_3 + a_4 \cos(\Theta_3) \quad (8.25)$$

$$D_{43} = a_3 + a_4 \cos(\Theta_3) \quad (8.26)$$

$$D_{44} = a_3 \quad (8.27)$$

The stiffness matrix is

$$\mathbf{K} = \begin{bmatrix} K_{11} & K_{12} & K_{13} & K_{14} \\ K_{21} & K_{22} & K_{23} & K_{24} \\ K_{31} & K_{32} & K_{33} & K_{34} \\ K_{41} & K_{42} & K_{43} & K_{44} \end{bmatrix} \quad (8.28)$$

$$K_{11} = k_1 + k_2 \quad (8.29)$$

$$K_{12} = k_1/l_1 - k_2/l_2 \quad (8.30)$$

$$K_{13} = 0 \quad (8.31)$$

$$K_{14} = 0 \quad (8.32)$$

$$K_{21} = k_1/l_1 - k_2/l_2 \quad (8.33)$$

$$K_{22} = k_2/l_2^2 + k_1/l_1^2 \quad (8.34)$$

$$K_{23} = 0 \quad (8.35)$$

$$K_{24} = 0 \quad (8.36)$$

$$K_{31} = 0 \quad (8.37)$$



$$K_{32} = 0 \quad (8.38)$$

$$K_{33} = k_3 \quad (8.39)$$

$$K_{34} = 0 \quad (8.40)$$

$$K_{41} = 0 \quad (8.41)$$

$$K_{42} = 0 \quad (8.42)$$

$$K_{43} = 0 \quad (8.43)$$

$$K_{44} = k_4 \quad (8.44)$$

The damping matrix is

$$\mathbf{C} = \begin{bmatrix} C_{11} & C_{12} & C_{13} & C_{14} \\ C_{21} & C_{22} & C_{23} & C_{24} \\ C_{31} & C_{32} & C_{33} & C_{34} \\ C_{41} & C_{42} & C_{43} & C_{44} \end{bmatrix} \quad (8.45)$$

$$C_{11} = c_1 + c_2 \quad (8.46)$$

$$C_{12} = c_1 l_1 - c_2 l_2 \quad (8.47)$$

$$C_{13} = 0 \quad (8.48)$$

$$C_{14} = 0 \quad (8.49)$$

$$C_{21} = c_1 l_1 - c_2 l_2 \quad (8.50)$$

$$C_{22} = c_2 l_2^2 + c_1 l_1^2 \quad (8.51)$$

$$C_{23} = 0 \quad (8.52)$$

$$C_{24} = 0 \quad (8.53)$$

$$C_{31} = 0 \quad (8.54)$$

$$C_{32} = 0 \quad (8.55)$$

$$C_{33} = c_3 \quad (8.56)$$

$$C_{34} = 0 \quad (8.57)$$

$$C_{41} = 0 \quad (8.58)$$

$$C_{42} = 0 \quad (8.59)$$

$$C_{43} = 0 \quad (8.60)$$

$$C_{44} = c_4 \quad (8.61)$$

The excitation vectors and their components are given below

$$\mathbf{f}_1 = \begin{bmatrix} k_1 \\ k_1/l_1 \\ 0 \\ 0 \end{bmatrix} \quad (8.62)$$

$$\mathbf{f}_2 = \begin{bmatrix} c_1 \\ c_1/l_1 \\ 0 \\ 0 \end{bmatrix} \quad (8.63)$$

$$\mathbf{f}_4 = \begin{bmatrix} k_2 \\ -k_2/l_2 \\ 0 \\ 0 \end{bmatrix} \quad (8.64)$$

$$\mathbf{f}_5 = \begin{bmatrix} c_2 \\ -c_2/l_2 \\ 0 \\ 0 \end{bmatrix} \quad (8.65)$$

$$\mathbf{f}_3 = \begin{bmatrix} 0 \\ a_5 \sin(\Theta_2) + a_6 \sin(\Theta_2 + \Theta_3) \\ a_5 \sin(\Theta_2) + a_6 \sin(\Theta_2 + \Theta_3) \\ a_6 \sin(\Theta_2 + \Theta_3) \end{bmatrix} \quad (8.66)$$

To generalize the results, a dimensionless time  $\bar{t}$  defined as in equation (4.1) is introduced and this leads to.

$$\bar{\mathbf{f}}_1 = \begin{bmatrix} 1 \\ l_1 \\ 0 \\ 0 \end{bmatrix} \quad (8.67)$$

$$\bar{\mathbf{f}}_2 = \begin{bmatrix} \bar{c}_1 \\ \bar{c}_1/l_1 \\ 0 \\ 0 \end{bmatrix} \quad (8.68)$$

$$\bar{\mathbf{f}}_4 = \begin{bmatrix} 1 \\ -l_2 \\ 0 \\ 0 \end{bmatrix} \quad (8.69)$$

$$\bar{\mathbf{f}}_5 = \begin{bmatrix} \bar{c}_2 \\ \bar{c}_2/l_2 \\ 0 \\ 0 \end{bmatrix} \quad (8.70)$$

$$\bar{\mathbf{f}}_3 = \begin{bmatrix} 0 \\ \bar{a}_5 \sin(\Theta_2) + \bar{a}_6 \sin(\Theta_2 + \Theta_3) \\ \bar{a}_5 \sin(\Theta_2) + \bar{a}_6 \sin(\Theta_2 + \Theta_3) \\ \bar{a}_6 \sin(\Theta_2 + \Theta_3) \end{bmatrix} \quad (8.71)$$

$$\bar{\mathbf{D}} = \frac{1}{a_1} \mathbf{D} \quad (8.72)$$

$$\bar{\mathbf{C}} = \frac{1}{\sqrt{a_1 k_1}} \mathbf{C} \quad (8.73)$$

$$\bar{\mathbf{K}} = \frac{1}{k_1} \mathbf{K} \quad (8.74)$$

$$\bar{c}_1 = \frac{c_1}{\sqrt{a_1 k_1}} \quad (8.75)$$

$$\bar{c}_2 = \frac{c_2}{\sqrt{a_1 k_1}} \quad (8.76)$$

$$\bar{a}_5 = \frac{a_5}{a_1} \quad (8.77)$$

$$\bar{a}_6 = \frac{a_6}{a_1} \quad (8.78)$$

The Jacobian matrix of the tip motion in the vehicle frame  $\mathbf{x}_0 = [x_0, y_0]^T$  is given as

$$\mathbf{J}_0 = \begin{bmatrix} J_{11} & J_{12} & J_{13} & J_{14} \\ J_{21} & J_{22} & J_{23} & J_{24} \end{bmatrix} \quad (8.79)$$

$$J_{11} = 0 \quad (8.80)$$

$$J_{12} = -l_3 \sin(\Theta_2) - l_4 \sin(\Theta_2 + \Theta_3) \quad (8.81)$$

$$J_{13} = -l_3 \sin(\Theta_2) - l_4 \sin(\Theta_2 + \Theta_3) \quad (8.82)$$

$$J_{14} = -l_4 \sin(\Theta_2 + \Theta_3) \quad (8.83)$$

$$J_{21} = 1 \quad (8.84)$$

$$J_{22} = l_3 \cos(\Theta_2) + l_4 \cos(\Theta_2 + \Theta_3) \quad (8.85)$$

$$J_{23} = l_3 \cos(\Theta_2) + l_4 \cos(\Theta_2 + \Theta_3) \quad (8.86)$$

$$J_{24} = l_4 \cos(\Theta_2 + \Theta_3) \quad (8.87)$$

## 8.2. Surface Profile Representation

The surface profile representation used in this Chapter has the same characteristic as that presented in Section 6.2. The system response is studied using numerical simulation and the procedure developed in Chapter seven.

### 8.3. Numerical Simulation

#### 8.3.1. Case 1. Manipulator on an Accelerating Mobile Base

##### INITIAL CONDITION

##### Stochastic Response:

It is assumed that the vehicle starts from rest with uniform horizontal acceleration. In order to initialize the Runge-Kuta integration routine for the stochastic response of equation (7.26) a set of initial values of the covariance matrix  $\mathbf{P}(0)$  entries is required. From the assumption of homogeneity of the surface profile, the variances of the suspension motion are  $E\{q_{y1}^2(\bar{t})\} = E\{q_{y2}^2(\bar{t})\} = \sigma^2$ . This implies  $P_{99}(0) = P_{1010}(0) = 1$ . Further, at  $\bar{t} = 0$ , there is no relative motion between the vehicle heave motion  $q_1$  and the suspension motion  $q_{y1}$  and  $q_{y2}$ , therefore,  $P_{11}(0) = P_{19}(0) = P_{99}(0) = P_{1010}(0) = P_{110}(0)$ . All other initial conditions are set to zero.

##### Deterministic Response:

To initiate the Runge-Kuta integration algorithm for the deterministic response, a set of initial values of the state  $\mathbf{z}(0)$  have to be provided. Since the state vector  $\mathbf{z}$  is normalized with the standard deviation of the surface profile  $\sigma$  and at time  $\bar{t} = 0$  there is no relative motion between the vehicle heave motion  $q_1$  and the suspension motion  $q_{y1}$  and  $q_{y2}$ , then  $z_1(0) = 1/\sigma$ . All other initial conditions are set to zero.

## 8.4. Results and Discussion

### 8.4.1. Case 1. Manipulator on an Accelerating Mobile Base

A program to simulate the deterministic and nonstationary random response of the tip motion of a two degree of freedom manipulator on an accelerating mobile base having two wheels was developed. The flow chart for the program is given in Figures 8.2 and 8.3. In this discussion, the term stochastic response refers to the major principal variance of the tip displacement, while the term deterministic response refers to the square of the magnitude of the tip deterministic displacement.

Sensitivity to Link Configuration: Figure 8.4 shows the sensitivity of the tip response to the changes of the manipulator configuration for  $\Theta_3 = 0^\circ$ ,  $\alpha = .45$ , and  $\ddot{q}_x = 1$ . It can be observed that the more perpendicular the manipulator structure to the excitation, the higher the response to that excitation. Thus, the highest stochastic response occurs at  $\Theta_2 = 0^\circ$ . At this configuration the links of the manipulator are perpendicular to the stochastic base excitations  $\dot{q}_{y1}(t)$ ,  $\dot{q}_{y2}(t)$ ,  $q_{y1}(t)$  and  $q_{y2}(t)$ . Also, at this configuration, the deterministic response is transient and depends only on the initial condition since the deterministic excitation vector  $f_3 = 0$ . The highest deterministic response occurs at  $\Theta_2 = 90^\circ$  when the deterministic excitation vector  $f_3$  reaches its maximum value. The stochastic response for  $\Theta_2 = 90^\circ$  and  $\Theta_3 = 0^\circ$  is that of the vehicle since the dynamic coupling terms between the vehicle (heave and pitch) motions and the links are zero ( $D_{13} = D_{31} = D_{14} = D_{41} = D_{23} = D_{32} = D_{24} = D_{42} = 0$ ); the vehicle moves with the links as a rigid body. Subsequent plots for the deterministic and stochastic responses are for the configurations of maximum responses.



Influence of Joint Stiffness: Figure 8.5 shows the influence of the relative magnitude of the suspension and links' stiffness on the responses. Increase in the vehicle stiffness for a fixed stiffness of the links leads to decreased stochastic response and increased deterministic response. But, increase in the links stiffness for a fixed value of the suspension stiffness leads to increased stochastic response and decreased deterministic response. At the beginning of motion, the deterministic and stochastic responses show little sensitivity to stiffness.

Sensitivity to System Damping: The sensitivity of the system response to damping is shown in Figure 8.6. It can be observed that both the deterministic and stochastic responses can be reduced by the presence of damping. But if only suspension damping is present, the stochastic response displays low sensitivity to damping. The deterministic response, on the other hand, shows high sensitivity to the suspension damping in the absence of the links damping and low sensitivity to the links damping in the absence of suspension damping. Further, at the beginning of motion both the deterministic and the stochastic responses show little sensitivity to damping.

Sensitivity to Manipulator's Length: The sensitivity of the manipulator response to the relative lengths of link-2 to link-1 is shown in Figure 8.7. The longer the terminal link (link-2) compared to link-1, the higher the value of the stochastic response. The stochastic response is more sensitive to the relative lengths of the links than the deterministic response.

Effect of Vehicle Acceleration and Surface Roughness Coefficient: Figure 8.8 indicates the effect of acceleration on the deterministic response. The deterministic response increases with the increase of the vehicle acceleration except for the configurations when  $f_5 = 0$  i.e. when the excitation has no effect. Figure 8.9 shows the effects of the vehicle acceleration and surface roughness on the stochastic response. At the beginning of motion, the stochastic response is not sensitive to either surface roughness or acceleration. As the motion continues, for low acceleration  $\ddot{q}_x = .3$ , it is noted that the higher the surface roughness coefficient the higher the maximum value of the stochastic response; also the response under this condition is smooth. On the other hand, for high acceleration  $\ddot{q}_x = 3.$ , the surface with high roughness coefficient  $\alpha = .9$  produces uneven response with quick rise. The maximum value of the response is also low under this condition. The surface with low roughness coefficient  $\alpha = .15$  produces a smooth stochastic response with a slow rise and a high maximum value.

#### **8.4.2. Case 2. Manipulator On a Constant Velocity Mobile Base**

A program to simulate the stationary random response of the tip motion of a flexible manipulator on a mobile base moving with constant velocity was developed. The flow chart for the program is given in Figure 8.10.

In the following discussion the term displacement refers to the major principal variance of the tip response. Figure 8.11 shows the sensitivities of the displacements and velocities to changes in the manipulator configuration  $\Theta_2$ . It is observed that the more perpendicular the manipulator structure to the excitation,

the higher the response. Thus, the highest response occurs at  $\Theta_2 = \Theta_3 = 0^\circ$ . At this configuration the links of the manipulator are perpendicular to the stochastic base excitations  $q_{1y}(t)$  and  $q_{2y}(t)$ .

The influence of the manipulator and the suspension damping on the displacement is shown in Figure 8.12. It is observed that the displacement can be reduced with the presence of damping. But if only the suspension damping is present, the response has low sensitivity to damping. On the other hand, if only the manipulator joints are damped the response is very sensitive to damping.

The influence of the relative lengths of link-1 to link-2 on the displacements and velocities is shown in Figure 8.13. It is noted that the longer the terminal link (link-2) compared to link-1, the higher the responses. Therefore, designing the links of the manipulator so that lower links are longer than the upper links will result in reduced stochastic vibration.

## 8.5. Summary and Concluding Remarks

In this chapter, the Lagrangian and the Rayleigh dissipation function for a two link manipulator on a two-wheels traction mobile manipulator has been developed. The Lagrange principle has been used to derive the equation of motion for the manipulator on an accelerating and a constant velocity mobile base. To generalize the results dimensionless time has been introduced. The ideas developed in Chapter seven have been used to study the system.

For the manipulator on an accelerating mobile base, sensitivity of the system responses to the manipulator configuration, the relative lengths of the links, stiffness, damping, vehicle acceleration, and surface roughness have been explored. Results indicate that the more perpendicular the manipulator to the excitation, the higher the response to that excitation. Thus, the highest stochastic response occurs at  $\Theta_2 = \Theta_3 = 0^\circ$  and the highest deterministic response occurs at  $\Theta_2 = 90^\circ$  and  $\Theta_3 = 0^\circ$ . Further, to minimize the stochastic vibration on the manipulator structure it can be concluded that the lower links of the manipulator should be longer than the upper links, the vehicle suspension stiffness should be high compared to the links' stiffness and the vehicle suspension damping is not sufficient, the links of the manipulator have to be damped.

For the manipulator on a base moving with constant velocity, a two link manipulator on a vehicle has been used to illustrate the principles. Influence of the system parameters on the maximum variance of response has been studied. It can be concluded that to minimize the stochastic vibration on the manipulator structure the lower links of the manipulator should be longer than the upper links. Further, the manipulator links as well as the suspension must be damped. In the next chapter a model for the identification of the dynamic parameters of mobile manipulators is developed.

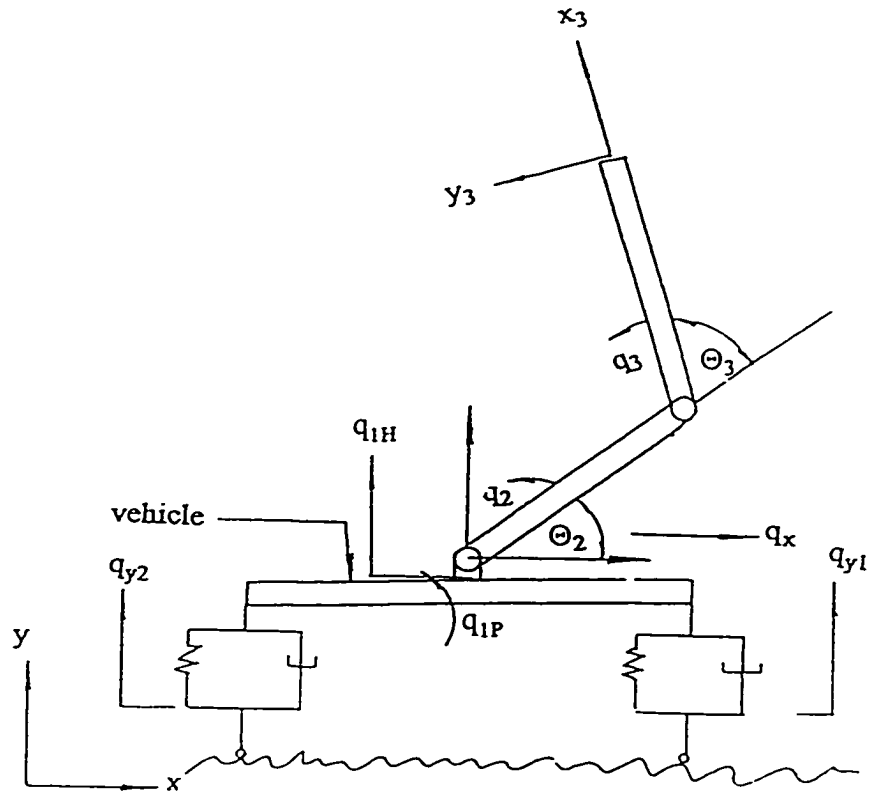


Figure 8.1. Model of a Two Link Two-Wheeled Mobile Manipulator

- $\Theta_i$  kinematic configuration of link  $i$
- $q_i$  elastic motion variable of link  $i$
- $q_x$  vehicles horizontal motion
- $(x,y)_1$  Cartesian coordinate frame attached to link 1

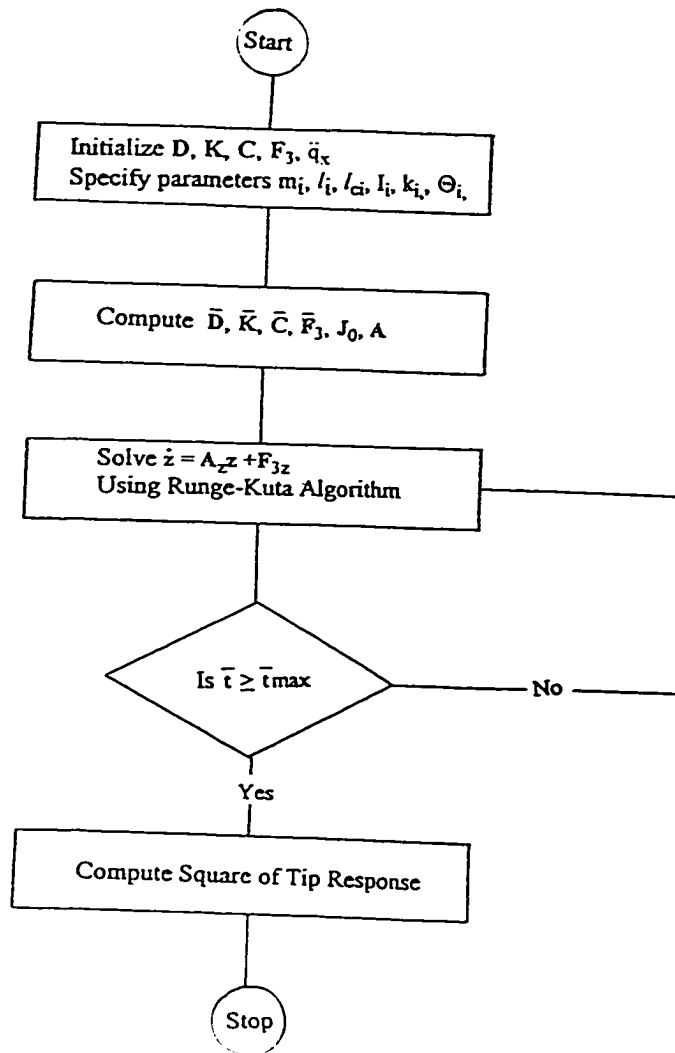


Figure 8.2. Flow Chart of the Program Used for Simulating the Deterministic Dynamics of a Two-Wheeled Mobile Manipulator.

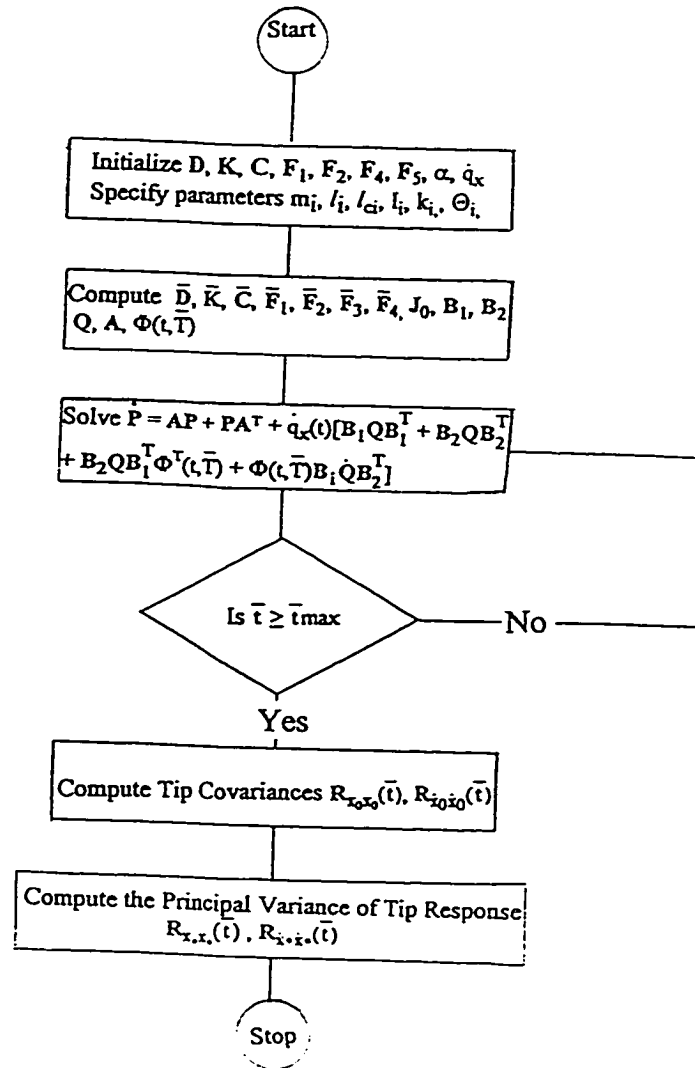
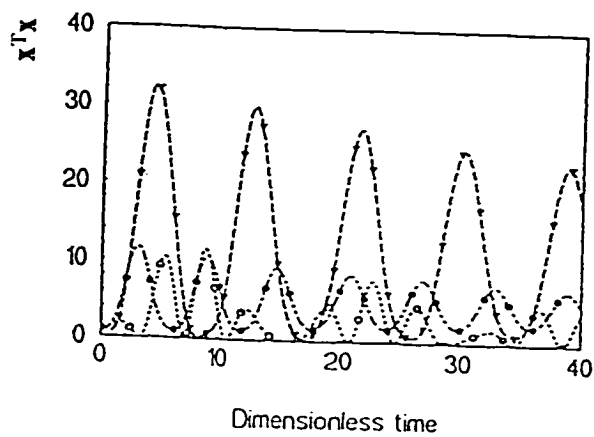
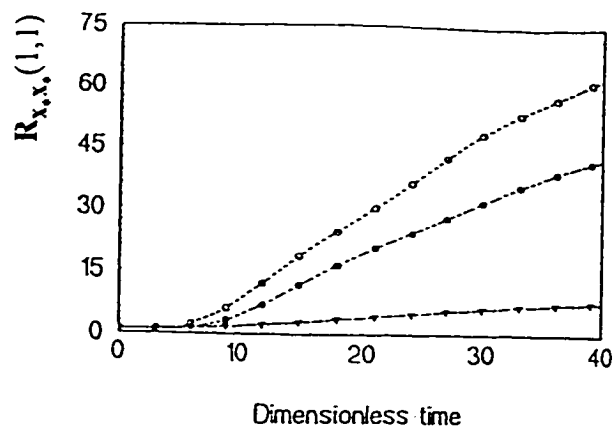


Figure 8.3. Flow Chart of the Program Used for Simulating the Nonstationary Stochastic Dynamics of a Two-Wheeled Mobile Manipulator.



- $\Theta_3 = 0^\circ$
- $\Theta_3 = 45^\circ$
- ▲····▲  $\Theta_3 = 90^\circ$

Figure 8.4. Sensitivity of the Principal Variance and the Square of the Deterministic Tip Response of a Two-wheeled Mobile Manipulator on an Accelerating base to Configuration Changes (a) Nonstationary Stochastic (b) Deterministic



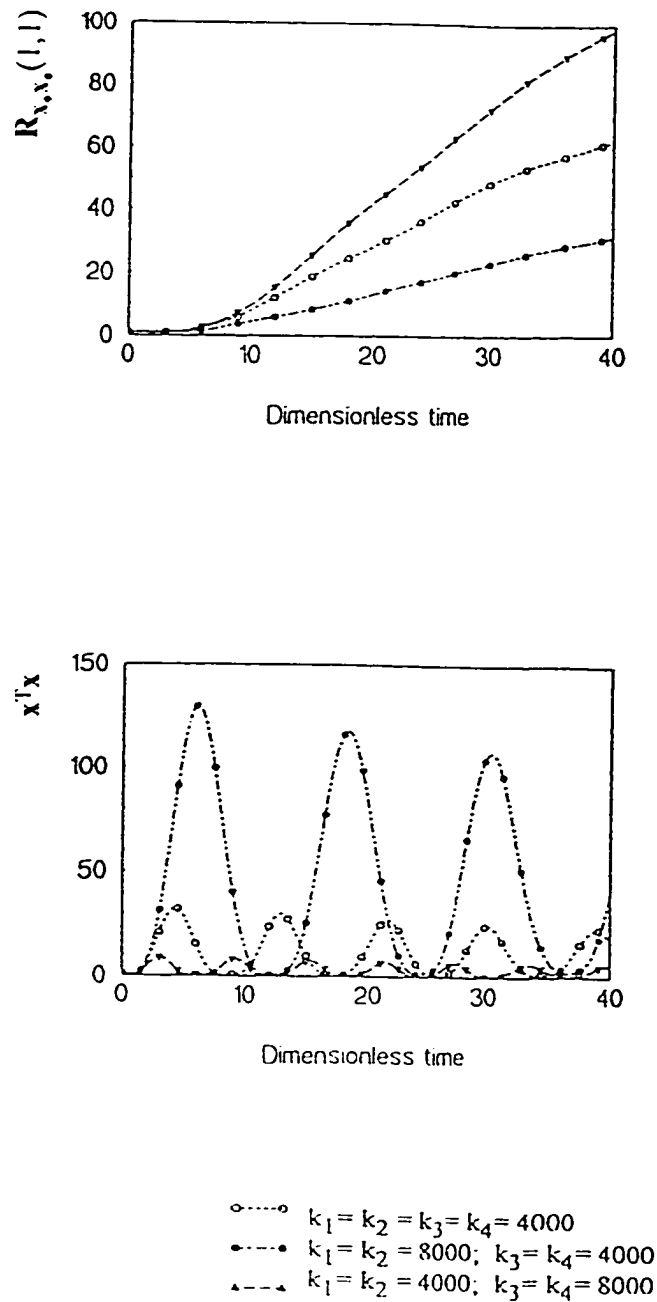
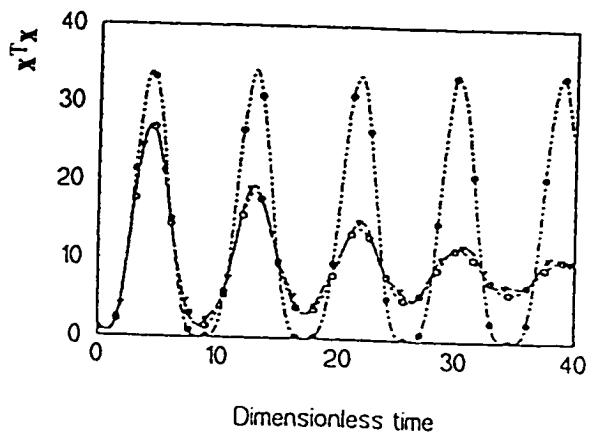
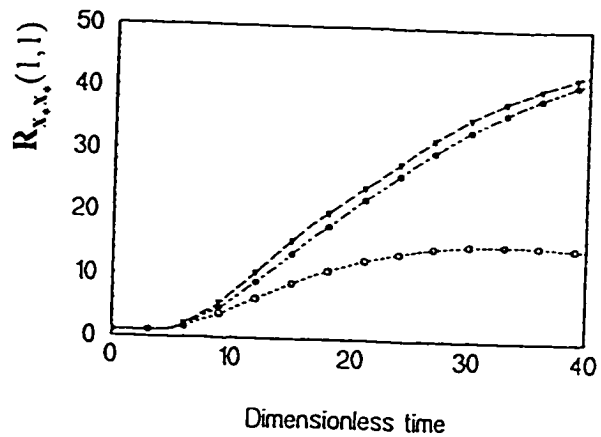
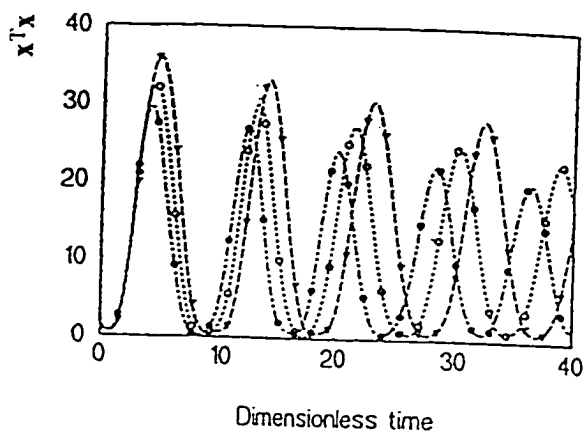
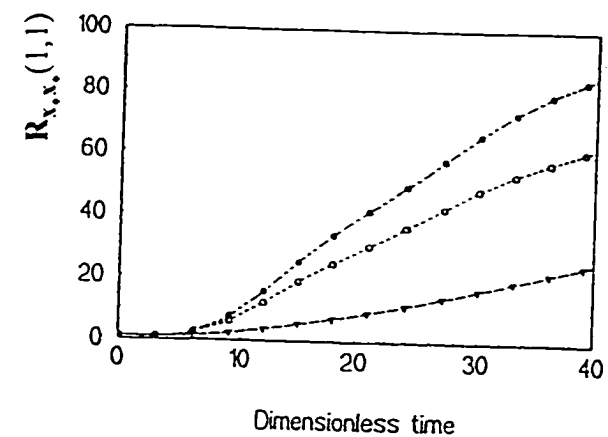


Figure 8.5. Influence of Joint Stiffness on the Principal Tip Displacement Variance and Square of the Deterministic Tip Response of a Two-wheeled Mobile Manipulator (a) Nonstationary Stochastic (b) Deterministic.



- $c_1 = c_2 = c_3 = c_4 = 50$
- △·····  $c_1 = c_2 = 50; c_3 = c_4 = 0$
- $c_1 = c_2 = 0; c_3 = c_4 = 50$

Figure 8.6. Influence of Damping on the Principal Tip Displacement Variance and Square of the Deterministic Tip Response of a Two-wheeled Mobile Manipulator (a) Nonstationary Stochastic (b) Deterministic.



- $l_1=l_2=1; l_3=l_4=2$
- ▲---▲  $l_1=l_2=1; l_3=2.5; l_4=1.5$
- $l_1=l_2=1; l_3=1.5; l_4=2.5$

Figure 8.7. Influence of Links Length on the Principal Tip Displacement Variance and Square of the Deterministic Tip Response of a Two-wheeled Mobile Manipulator (a) Nonstationary Stochastic (b) Deterministic.

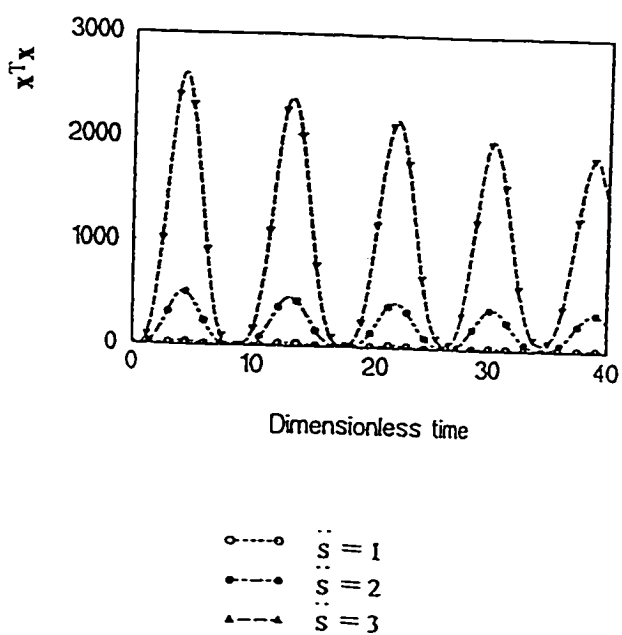


Figure 8.8. Effect of the Horizontal Base acceleration on the Square of the Deterministic Tip Response of a Two-wheeled Mobile Manipulator.

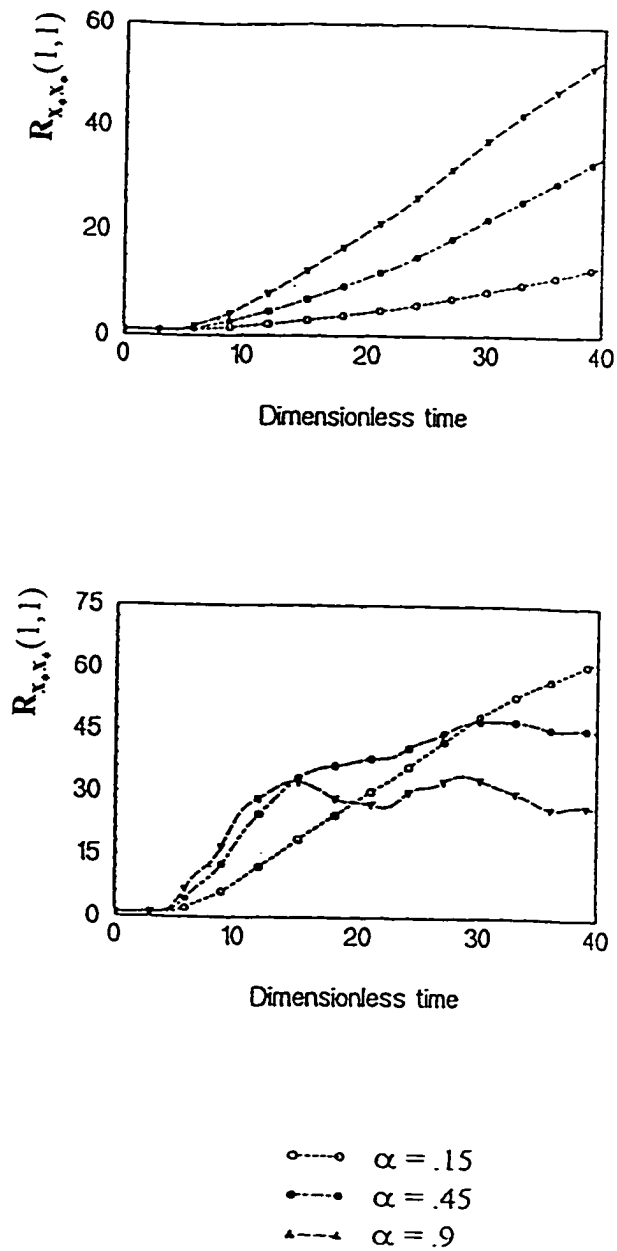


Figure 8.9. Effect of the Horizontal Base Acceleration and Surface Roughness Coefficient on the Principal Tip Displacement Variance of a Two-wheeled Mobile Manipulator. (a)  $\ddot{q}_x = .3$  (b)  $\ddot{q}_x = 3$ .

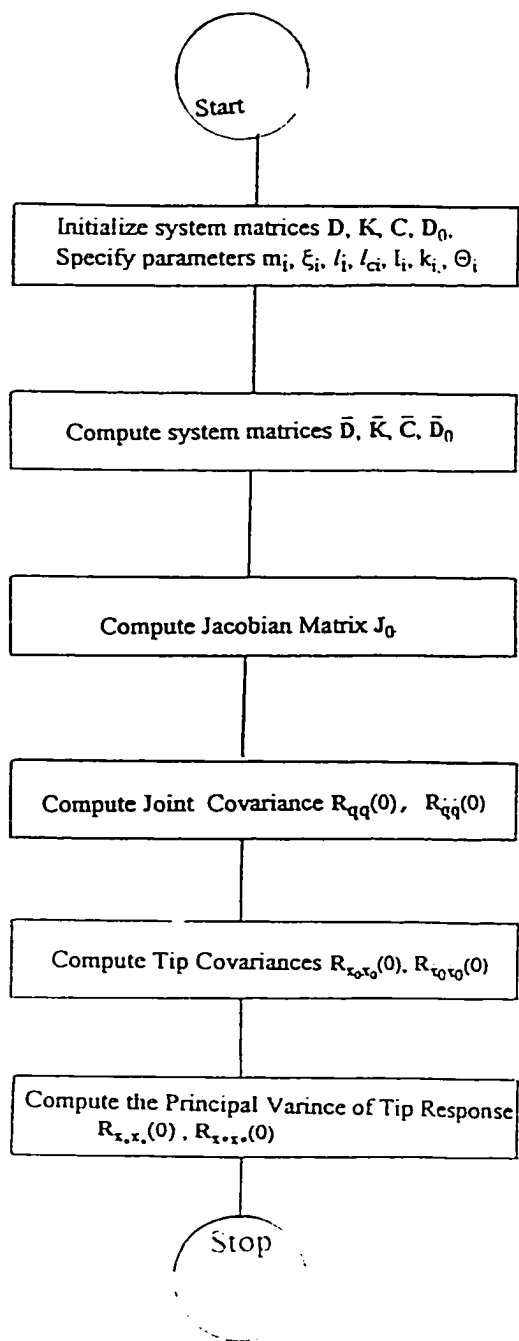


Figure 8.10. Flow Chart of the Program Used for Simulating the Stationary Stochastic Dynamics of a Two-Wheeled Mobile Manipulator Using the State Space approach.

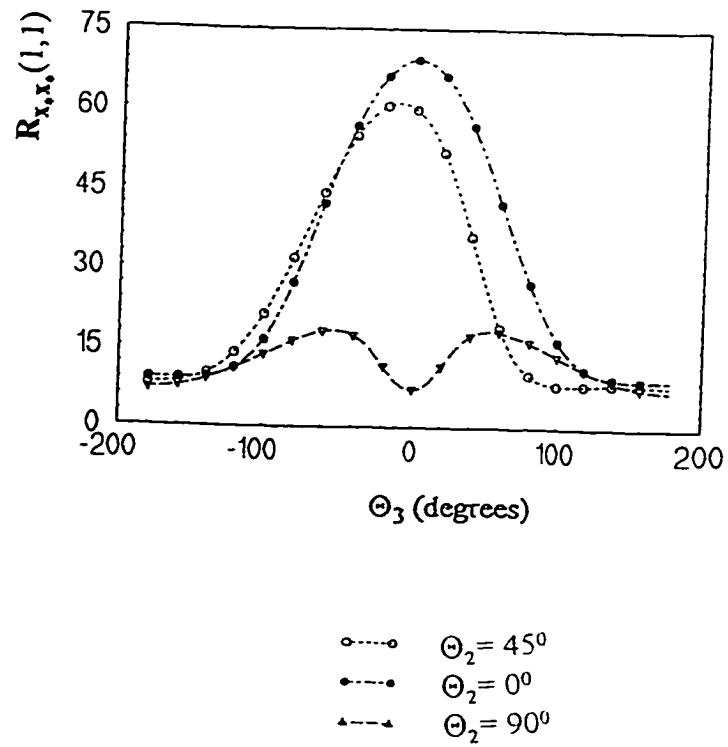


Figure 8.11. Sensitivity of the Stationary Principal Variance of a Constant Velocity Two-Wheeled Mobile Manipulator to Configuration Changes.

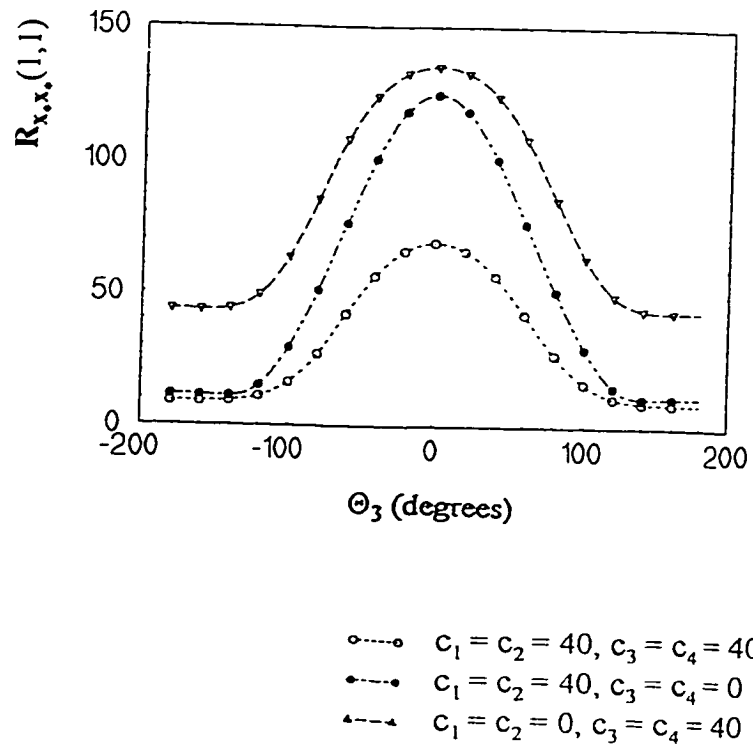


Figure 8.12. Effect of Damping on the Principal Tip Displacement Variance of a Two-wheeled Mobile Manipulator Moving with a Constant Base Velocity.



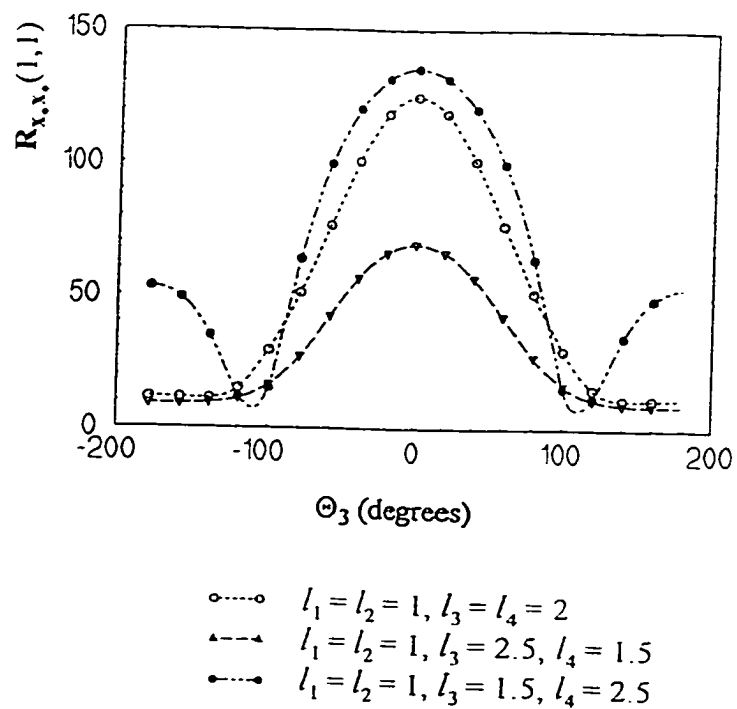


Figure 8.13. Sensitivity of the Principal Tip Displacement Variance of a Two-wheeled Mobile Manipulator Moving with a Constant Velocity to the Length of Links.

## **Chapter Nine**

# **IDENTIFICATION OF MOBILE MANIPULATORS, ANALYSIS**

### **9.1. Introduction**

This chapter contains an original contribution of the author. The originality is in the development and optimization of the identification model for the dynamic parameters of mobile manipulators. A selection and composition of known analytical tools such as least square and singular value decomposition have been used in the formulation.

### **9.2. Model Assumptions**

Consider an  $n$  degree of freedom mobile flexible manipulator modeled according to the general assumptions presented in Section 1.2. It is further assumed that; the nominal (design) values of the manipulator dynamic parameters are known and are close to their actual values; the geometric and kinematic parameters of the manipulator are known accurately. The goals of this chapter are twofold namely: to develop a mathematical model for estimating the discrepancies between the nominal and the actual values of the structural dynamic parameters of the manipulator links and joints, and to optimize the model in order to minimize

the number of measurements required for estimation. In this report the discrepancies between the design and the actual values of the dynamic parameters will be referred to as the dynamic parameter deviations.

To estimate the dynamic parameter deviations a series of measurements have to be made. If the motion of the manipulator tip is selected as the most critical (since this is easy to measure) then measurements should be carried out at manipulator kinematic configurations where small perturbations of the dynamic parameters have dominant effect on the amplitude of the tip oscillation. Also, system excitation should be such that the tip oscillations can be related to the dynamic parameter deviation. Before, this can be done a model has to be developed which relates the parameter deviations and the tip oscillation. Further, the model has to be optimized so that the parameter deviations can be identified with a small number of measurements. The optimization is in terms of the set of manipulator kinematic configurations chosen for measurements, and the excitation for measurement. The focus of this chapter, is therefore on the identifiability of the dynamic parameter deviations of mobile manipulators.

### 9.3. Equation of Motion

The equation of motion for the mobile manipulator is as follows

$$\mathbf{D}\ddot{\mathbf{q}}(t) + \mathbf{C}\dot{\mathbf{q}}(t) + \mathbf{K}\mathbf{q}(t) = \mathbf{F}(t) \quad (9.1)$$

where  $\mathbf{F}$  represents the base excitation vector. The joint motion  $\mathbf{q}$  is assumed to have the form

$$\mathbf{q} = \mathbf{Q}e^{-i\omega t} \quad (9.2)$$

where  $\mathbf{Q}$  is the amplitude of the small joint vibration. Also the excitation vector is assumed to be of the form

$$\mathbf{F}(t) = \mathbf{F}_0e^{-i\omega t} \quad (9.3)$$

where  $\mathbf{F}_0$  is the amplitude vector of the excitation. Substituting equations (9.3) and (9.2) into equation (9.1) and considering only the amplitude of the joint vibration and excitation results in the eigenvalue problem

$$(-\omega^2\mathbf{D} -i\omega\mathbf{C} + \mathbf{K})\mathbf{Q} = \mathbf{F}_0 \quad (9.4)$$

Equation (9.4) can be written as

$$\mathbf{Q} = (-\omega^2\mathbf{D} -i\omega\mathbf{C} + \mathbf{K})^{-1}\mathbf{F}_0 \quad (9.5)$$

Equation (9.5) gives the amplitude of the joint displacement  $\mathbf{Q}$  as a function of the system dynamic parameters -inertia, damping and stiffness parameters- and the amplitude of system excitation  $\mathbf{F}_0$ .

## 9.4. Identification Model

Since the amplitude of the joint motion  $\mathbf{Q}$  is small, it can be related to the amplitude of the manipulator tip motion  $\mathbf{x}$  by a Jacobian  $\mathbf{J}$

$$\mathbf{x} = \mathbf{J}\mathbf{Q} \quad (9.6)$$

where:

$$\mathbf{x} = [x, y, \alpha_z]^T \quad (9.7)$$

$x, y$ , are the linear amplitude components and  $\alpha_z$  is the rotational amplitude component of the tip displacement. Application of equation (9.5) in equation (9.6) gives

$$\mathbf{x} = \mathbf{J}(-\omega^2\mathbf{D} - i\omega\mathbf{C} + \mathbf{K})^{-1}\mathbf{F}_0 \quad (9.8)$$

The Jacobian matrix  $\mathbf{J}$  contains only the kinematic and geometric parameters of the system. It does not contain the dynamic parameters of the manipulator joints and links. A vector  $\boldsymbol{\varepsilon}$  containing the dynamic parameters of the manipulator can be formed. If a small perturbation  $\Delta\boldsymbol{\varepsilon}$  of the dynamic parameter vector takes place then the corresponding change in the amplitude of the tip oscillation vector  $d\mathbf{x}$  can be defined as

$$\begin{aligned} dx &= \frac{\partial x}{\partial \varepsilon} \Delta \varepsilon \\ &= \frac{\partial(\mathbf{JQ})}{\partial \varepsilon} \Delta \varepsilon \end{aligned} \quad (9.9)$$

Application of equation (9.8) in (9.9) leads to

$$dx = \mathbf{P} \Delta \varepsilon \quad (9.10)$$

where

$$\begin{aligned} \mathbf{P} = & \left[ -\mathbf{J}(-\omega^2 \mathbf{D} - i\omega \mathbf{C} + \mathbf{K})^{-1} \left( -\omega^2 \frac{\partial \mathbf{D}}{\partial \varepsilon} - i\omega \frac{\partial \mathbf{C}}{\partial \varepsilon} + \frac{\partial \mathbf{K}}{\partial \varepsilon} \right) (-\omega^2 \mathbf{D} - i\omega \mathbf{C} + \mathbf{K})^{-1} \mathbf{F}_0 \right. \\ & \left. + \mathbf{J}(-\omega^2 \mathbf{D} - i\omega \mathbf{C} + \mathbf{K})^{-1} \frac{\partial \mathbf{F}_0}{\partial \varepsilon} \right] \end{aligned} \quad (9.11)$$

Equations (9.10) and (9.11) constitute an identification model that can be used to estimate  $\Delta \varepsilon$ . The matrix  $\mathbf{P}$  will be referred to as the parameter propagation matrix. The propagation matrix indicates how the parameter perturbations  $\Delta \varepsilon$  contribute to the change of the amplitude of the tip oscillation  $dx$ . It can be observed that  $\mathbf{P}$  depends on:

1. The manipulator Jacobian  $\mathbf{J}$  i.e. the kinematic configuration  $\Theta$ ;
2. The dynamic parameters  $\mathbf{K}$ ,  $\mathbf{C}$  and  $\mathbf{D}$  and the parameter sensitivity  $\frac{\partial \mathbf{D}}{\partial \varepsilon}$ ,  $\frac{\partial \mathbf{C}}{\partial \varepsilon}$  and  $\frac{\partial \mathbf{K}}{\partial \varepsilon}$ ,
3. The location, and the parameter sensitivity of the amplitude of excitation  $\mathbf{F}_0$ .

When the nominal ( $N$ ) and the actual ( $I$ ) values of the parameter vector  $\varepsilon$  are used to estimate the amplitude of the tip oscillation equation (9.6) can be interpreted as follows

$$\mathbf{x}^N = \mathbf{x}^N(\varepsilon^N, \Theta, \mathbf{F}_0) \quad (9.12)$$

$$\mathbf{x}^I = \mathbf{x}^I(\varepsilon^I, \Theta, \mathbf{F}_0) \quad (9.13)$$

The actual values of the parameter vector  $\varepsilon^I$ , by definition, is given as

$$\varepsilon^I = \varepsilon^N \pm \Delta\varepsilon^I \quad (9.14)$$

The difference  $d\mathbf{x}$  between the actual amplitudes  $\mathbf{x}^I$  of the tip oscillation reflecting the actual values of the parameter  $\varepsilon$  and the nominal amplitude  $\mathbf{x}^N$  is defined as

$$d\mathbf{x} = \mathbf{x}^I - \mathbf{x}^N = \mathbf{x}^I(\varepsilon^N \pm \Delta\varepsilon^I, \Theta, \mathbf{F}_0) - \mathbf{x}^N(\varepsilon^N, \Theta, \mathbf{F}_0) \quad (9.15)$$

Equation (9.10) is a first order approximation of equation (9.15). The identification model of equation (9.10) can be used as long as the assumption that the parameter deviation vector  $\Delta\varepsilon$  is very small when compared to the nominal vector  $\varepsilon^N$ .

The aim of this chapter is to find a set of the manipulator configurations, and excitations that will assure the best estimates of the vector  $\Delta\varepsilon$ .

## 9.5. Estimation of the Dynamic Parameter Deviations

To estimate the parameter perturbation vector  $\Delta\varepsilon$  a series of measurements have to be taken for various configurations and excitations. In general, to reduce experimental cost, it is desired that the total number of configurations, and excitations being considered be as small as possible.

Assuming that the number of the elements of the vector  $\Delta\varepsilon$  is  $n$  and that the 3 components of the amplitude of the tip displacement are measured, then the total number of measurements  $m$  has to be  $m > n/3$  to assure unique solution for  $\Delta\varepsilon$ . For  $m$  measurements equation (9.10) can be written in the form

$$dX = P\Delta\varepsilon \quad (9.16)$$

where

$$dX = [dx_1^T, dx_2^T, dx_3^T, \dots, dx_m^T]^T \quad (9.17)$$

$$P = [P_1^T, P_2^T, P_3^T, \dots, P_m^T]^T \quad (9.18)$$

The  $3m \times 1$   $dX$  matrix and  $3m \times n$   $P$  matrix are collection vectors pertaining to individual  $m$  measurements.

In the following discussion it is assumed that there are no linearly dependent or unobservable parameters in the vector  $\Delta\varepsilon$  and no useful parameters have been excluded. The case of linearly dependent and unobservable parameter



will be discussed later. With the above assumption, singular value decomposition (Golub and Van Loan, 1990) of the matrix  $\mathbf{P}$  can be performed to obtain

$$\mathbf{P} = \mathbf{U}\mathbf{\Sigma}\mathbf{V}^H \quad (9.19)$$

The superscript H denotes complex conjugate (hermitian) transpose. The unitary matrices  $\mathbf{U}$  and  $\mathbf{V}$  are composed from  $3m \times 1$   $\mathbf{u}_i$  and  $n \times 1$   $\mathbf{v}_i$  vectors respectively i.e.

$$\mathbf{U} = [\mathbf{u}_1, \mathbf{u}_2, \dots, \mathbf{u}_{3m}] \quad (9.20)$$

$$\mathbf{V} = [\mathbf{v}_1, \mathbf{v}_2, \dots, \mathbf{v}_n] \quad (9.21)$$

The  $3m \times n$   $\mathbf{\Sigma}$  matrix is composed from an  $n \times n$  diagonal matrix  $\mathbf{\Sigma}_1$  and a  $(3m-n) \times n$  null  $\mathbf{0}$  matrix i.e.

$$\mathbf{\Sigma} = [\mathbf{\Sigma}_1, \mathbf{0}]^T \quad (9.22)$$

$$\mathbf{\Sigma}_1 = \text{diag}(\sigma_1, \sigma_2, \sigma_3, \dots, \sigma_n) \quad (9.23)$$

The components of  $\mathbf{\Sigma}_1$  are listed in a descending order and  $\sigma_1 \geq \sigma_2 \geq \sigma_3 \geq \dots \geq \sigma_n$  with  $\sigma_i > 0$ . Using the relations defined in equations (9.23), (9.21) and (9.20) then equation (9.16) can be written as

$$d\mathbf{X} = \sum_{i=1}^n \sigma_i \mathbf{v}_i^H \Delta \boldsymbol{\epsilon} \mathbf{u}_i \quad (9.24)$$

Since  $\mathbf{V}$  is an  $n \times n$  unitary matrix, its columns form a linearly independent set of vectors of rank  $n$ . The parameter deviation vector  $\Delta\boldsymbol{\varepsilon}$  has dimension  $n$  and can be expanded in terms of the elements of the columns of  $\mathbf{V}$  as

$$\Delta\boldsymbol{\varepsilon} = \sum_{i=1}^n \beta_i \mathbf{v}_i \quad (9.25)$$

where  $\beta_i$  are constant parameters to be determined. Application of equation (9.25) in equation (9.24) gives

$$\begin{aligned} dX &= \sum_{i=1}^n \sigma_i \beta_i \mathbf{v}_i^H \mathbf{v}_i \mathbf{u}_i \\ &= \sum_{i=1}^n \sigma_i \beta_i \mathbf{u}_i \\ &= [\sigma_1 \mathbf{u}_1, \dots, \sigma_n \mathbf{u}_n] [\beta_1, \beta_2, \dots, \beta_n]^T \end{aligned} \quad (9.26)$$

where  $\beta_i$  are the constant coefficients to be determined. The following simplifications can be used to determine  $\beta_i$ . Multiplication of both sides of equation (9.26) by the transpose of the complex conjugate of the unitary eigenvector  $\mathbf{u}_i^H$  leads to

$$\mathbf{u}_i^H dX = \mathbf{u}_i^H [\sigma_1 \mathbf{u}_1, \dots, \sigma_n \mathbf{u}_n] [\beta_1, \beta_2, \dots, \beta_n]^T \quad (9.27)$$

Noting that  $\mathbf{u}_i$  are unitary vectors the right hand side of equation (9.27) reduces to

$$\mathbf{u}_i^H [\sigma_1 \mathbf{u}_1, \dots, \sigma_n \mathbf{u}_n] [\beta_1, \beta_2, \dots, \beta_n]^T = \sigma_i \beta_i \delta_{ij} \quad (9.28)$$

where  $\delta_{ij}$  is the kronecker delta with property

$$\delta_{ij} = 1, \quad i = j, \quad \delta_{ij} = 0 \quad i \neq j \quad (9.29)$$

Substituting equation (9.29) in equation (9.27) leads to

$$\beta_i = \frac{\mathbf{u}_i^H d\mathbf{X}}{\sigma_i} \quad (9.30)$$

Application of equation (9.30) in (9.25) gives

$$\Delta\boldsymbol{\varepsilon} = \sum_{i=1}^n \frac{\mathbf{u}_i^H d\mathbf{X}}{\sigma_i} \mathbf{v}_i \quad (9.31)$$

## 9.6. Identifiability and Excitability of the Parameter Deviation Vector

Equation (9.31) can be defined as an  $n$ -dimensional ellipsoid in  $n$  ( $\mathbf{u}_i^H d\mathbf{X}$ ) coordinates when the perturbation vector  $\Delta\boldsymbol{\varepsilon}$  is bound by a norm of constant magnitude. Taking the 2-norm  $|\Delta\boldsymbol{\varepsilon}|^2 = \text{constant}$ , this ellipsoid can be expressed as

$$|\Delta\varepsilon|^2 = \sum_{i=1}^n \left( \frac{\mathbf{u}_i^H d\mathbf{X}}{\sigma_i} \right)^2 \quad (9.32)$$

Thus the shape and size of the ellipsoid are functions of the singular values ( $\sigma_i$ ,  $i = 1, 2, 3, \dots, n$ ) of the propagation matrix  $\mathbf{P}$ . When the volume of the ellipsoid is large then all components of the vector  $\Delta\varepsilon$  have significant contribution to changes in the amplitude of the tip oscillation  $d\mathbf{X}$ . The volume of this ellipsoid is proportional to the determinant of the matrix  $\mathbf{P}^H \mathbf{P}$  (Nakamura, 1991).  $\mathbf{P}^H \mathbf{P}$  can be expanded as

$$\begin{aligned} \mathbf{P}^H \mathbf{P} &= \mathbf{V} \Sigma^H \mathbf{U}^H \mathbf{U} \Sigma \mathbf{V}^H \\ &= \mathbf{V} \Sigma^H \Sigma \mathbf{V}^H \end{aligned} \quad (9.33)$$

where the unitary properties of  $\mathbf{U}$  has been utilized. Since  $\mathbf{V}$  is a unitary matrix, then

$$\det(\mathbf{V}) = \det(\mathbf{V}^H) = \pm 1 \quad (9.34)$$

Taking the determinant of equation (9.33) and utilizing the properties of the determinants then

$$\det(\mathbf{P}^H \mathbf{P}) = \det(\mathbf{V}) \det(\Sigma^H \Sigma) \det(\mathbf{V}^H) \quad (9.35)$$

Since  $\Sigma^H \Sigma$  is a diagonal matrix with the elements  $\sigma_1^2 \geq \sigma_2^2 \geq \sigma_3^2 \geq \dots \geq \sigma_n^2$  therefore

$$\det(\mathbf{P}^H \mathbf{P}) = \prod_{i=1}^n \sigma_i^2 \quad (9.36)$$

The identifiability measure for the parameter deviation ( $\mathbf{Id}$ ) is proposed as

$$\mathbf{Id} = \frac{1}{m} \sqrt[n]{\prod_{i=1}^n \sigma_i^2} \quad (9.37)$$

A scaling factor  $\frac{1}{m}$  ( $m$  -total number of measurements) has been used in the proposed index in order to account for the requirements that the number of measurements should be as small as possible. Equation (9.37) is very general, it can be used in many ways:

1. If the manipulator configuration is fixed while the excitation is varied then the index  $\mathbf{Id}$  serves as a measure of the effect of excitation on the identifiability of  $\Delta \epsilon$ . During an experiment, the system can be excited through any of the  $n$  joint coordinates  $q$ . It is most probable that the excitation will be executed through a motion  $q_0$  of the manipulator base. In that case the excitation vector  $\mathbf{F}$  will be of the form  $\mathbf{F} = -\omega^2 q_0 [D_{01}, D_{02}, \dots, D_{0n}]^T$ ; where  $D_{0i}$ ,  $i = 1, 2, \dots, n$  are dynamic coupling terms between the base motion and the joint coordinates  $q$ .  $D_{0i}$  are

functions of the inertia parameters of the links and the configurations of the manipulator.

2. If the excitation is fixed while the manipulator configuration is varied, then the index  $I_d$  provides a measure of the effect of the manipulator configuration on the identifiability of  $\Delta\epsilon$ .
3. If both the excitation and the configuration are varied then  $I_d$  provides a general measure of the identifiability of  $\Delta\epsilon$ .

It is important to point out that it has been assumed that all the elements of the perturbation vector  $\Delta\epsilon$  contribute to the discrepancies in the amplitude of the tip oscillation  $dX$  i.e. all of them are identifiable and linearly independent. But in practice, some of the elements of the vector  $\Delta\epsilon$  might not be observable from  $dX$ , in which case there is a need to isolate such elements and remove them from the vector  $\Delta\epsilon$ . This leads naturally into the problem of identification of the basis vector of perturbation.

The observable perturbation vector  $\Delta\epsilon^*$  becomes a subvector of  $\Delta\epsilon$ . A method is proposed for identification of  $\Delta\epsilon^*$ . The singular value decomposition of the parameter deviation matrix  $\mathbf{P}$  (equation 9.19) produced diagonal  $n \times n$   $\Sigma_1$  matrix. If the matrix  $\mathbf{P}$  has rank  $s$  ( $s < n$ ) then all the singular values of  $\mathbf{P}$   $\sigma_i$  ( $i = s+1, s+2, \dots, n$ ) will be very small. The rank  $s$  is the number of linearly independent columns of  $\mathbf{V}$  and the dimension of the identifiable elements of the

perturbation vector  $\Delta \boldsymbol{\varepsilon}^*$ . An individual identifiability index for the element of the perturbation vector  $\Delta \boldsymbol{\varepsilon}$  can be defined as the ratio

$$\kappa_i = \frac{\sigma_i}{\sigma_{i+1}} \quad (9.38)$$

If the rank of identifiable parameters equals  $s$ , then  $\sigma_{s+1}$  will be very small compared to  $\sigma_s$  and the ratio  $\kappa_s$  defined as  $\kappa_s = \frac{\sigma_s}{\sigma_{s+1}}$  will be very high compared

to  $\kappa_{s-1} = \frac{\sigma_{s-1}}{\sigma_s}$ .

## 9.7. Estimation Error and Improvement of Estimated Parameter

To assess the quality of the proposed identifiability indices (equations 9.38, 9.37) and the estimated parameters to be estimated the following measure is used. The relationship between the nominal value of the parameter vector  $\boldsymbol{\varepsilon}^N$ , its actual value  $\boldsymbol{\varepsilon}^A$ , and the estimated value  $\boldsymbol{\varepsilon}^E$  are defined as follows

$$\boldsymbol{\varepsilon}^A = \boldsymbol{\varepsilon}^N \pm \Delta \boldsymbol{\varepsilon}^A \quad (9.39)$$

$$\boldsymbol{\varepsilon}^E = \boldsymbol{\varepsilon}^N \pm \Delta \boldsymbol{\varepsilon}^E \quad (9.40)$$

Each element of the parameter vector can be normalized as

$$\epsilon_n = \frac{\epsilon}{\epsilon^A} \quad (9.41)$$

Therefore

$$\epsilon_n^E = \frac{\epsilon^E}{\epsilon^A} \quad (9.42)$$

The relative estimation error is defined as

$$\Delta\epsilon_n^{\text{error}} = \frac{\sum |\epsilon_n^E - \epsilon_n^A|}{\text{no. of parameters}} \quad (9.43)$$

Once the vector  $\epsilon^E$  is obtained it can then be used as the current values of the nominal parameter and the process of estimation repeated until  $\Delta\epsilon_n^{\text{error}}$  or  $\|dx\|_2$  (equation 9.18) is or tends to zero.

## 9.8. Practical Application of the Proposed Model

Apart from being used for estimation of the dynamic parameter deviation of terrestrial mobile manipulator, this model will be extremely useful for identifying the dynamic parameters of space manipulators. This is because many of the dynamic parameters of space manipulators cannot be verified on the ground because of the effect that gravity has on the manipulator structure.



Space manipulators are designed to be light because of the high cost involved in launching and maneuvering masses in space. Therefore, they are flexible. The in-orbit testing of space manipulators has to be limited to a very short time compared to ground base experiments. This is because of the high cost involved in any space operation. These constraints on space experiments pose very strict requirements for testing. It is therefore expedient that measurements are carried out at the best configurations and system excitations. By undertaking a computer study using the identifiability index defined in this chapter and the nominal parameter of space manipulators, configurations and types of excitations of high identifiability can be identified and used during in-orbit testing. This will minimize the cost of experiments in space. Further, it should be noted that although the system excitation has been restricted to the base due to the mobile manipulator nature of the study, the model which has been presented will still be applicable if the excitation is at other locations such as joints.

## **9.9. Summary and Concluding Remarks**

In this chapter a model has been developed for identifying the dynamic parameter deviations of mobile flexible manipulators. Practical interpretation has been given to the model. Further by utilizing the elliptic geometry, the model has been optimized in terms of the excitation, and the configuration used for measurement. The properties of singular value decomposition of matrices has been used to identify the rank space of the parameter deviation and to estimate the system dynamic parameter deviations. For the case of unidentifiable parameters, a

a technique has been developed on how to identify such parameters and eliminate them from the model. Practical application of the model for space experiments has been noted. In the next chapter numerical simulation is undertaken to illustrate the proposed model.

## Chapter Ten

### IDENTIFICATION OF MOBILE MANIPULATORS, EXAMPLE

#### 10.1. Example: Two Link Manipulator

The two link non-wheeled mobile manipulator (Figure 4.2) is used to illustrate the ideas presented in chapter nine. It is assumed that the joint damping is negligible and equal to zero. The dynamic parameter vector for the manipulator can be formed as

$$\varepsilon = \begin{bmatrix} m_1 \\ I_1 \\ l_{c1} \\ m_2 \\ I_2 \\ l_{c2} \\ k_1 \\ k_2 \end{bmatrix} \quad (10.1)$$

The deviation between the nominal values of these parameters and the actual values constitute the dynamic parameter deviation vector  $\Delta\varepsilon$ . Since a change in the inertia components of the dynamic parameters results in a change in the inertia terms  $a_1 - a_5$  (equations (4.26)- (4.30)), the dynamic parameter vector for the system under consideration is therefore chosen as

$$\boldsymbol{\varepsilon} = \begin{bmatrix} k_1 \\ k_2 \\ a_1 \\ a_2 \\ a_3 \\ a_4 \\ a_5 \end{bmatrix} \quad (10.2)$$

In this chapter the dynamic parameter deviation vectors are the deviations of the components of the vector given in equation (10.2). Since the excitation is through the base, the amplitude of the excitation vector  $\mathbf{F}_0$  is given as

$$\mathbf{F}_0 = \omega^2 Q_0 \mathbf{D}_y \quad (10.3)$$

where the components of the dynamic coupling vector  $\mathbf{D}_y$  are given in equations 4.42 and 4.43;  $\omega$  and  $Q_0$  are the frequency and amplitude of the excitation vectors respectively. The derivative of the tip motion coordinate with respect to the elements of the dynamic parameters  $\boldsymbol{\varepsilon}$  can be obtained using (9.10) as

Tip Motion derivative with respect to  $a_1$ :

$$\frac{\partial \mathbf{x}}{\partial a_1} = \mathbf{J} \frac{\partial \mathbf{Q}}{\partial a_1} \quad (10.4)$$

$\mathbf{J}$  is the Jacobian matrix given in equation (4.48) and

$$\frac{\partial \mathbf{Q}}{\partial a_1} = \frac{1}{\omega^2 (D_{11}D_{22} - D_{21}D_{12})^2} \begin{bmatrix} -D_{22}D_{22} & D_{12}D_{22} \\ D_{12}D_{22} & -D_{12}D_{12} \end{bmatrix} \mathbf{F}_0 \quad (10.5)$$

Tip Motion derivative with respect to  $a_2$ :

$$\frac{\partial \mathbf{x}}{\partial a_2} = \mathbf{J} \frac{\partial \mathbf{Q}}{\partial a_2} \mathbf{F}_0 \quad (10.6)$$

$$\frac{\partial \mathbf{Q}}{\partial a_2} = \frac{1}{\omega^2(D_{11}D_{22}-D_{21}D_{12})^2} \begin{bmatrix} -D_{12}D_{12}+2D_{22}D_{12} & -D_{11}D_{22}-D_{12}D_{12}+D_{12}D_{11} \\ -D_{11}D_{22}-D_{12}D_{12}+D_{12}D_{11} & -D_{11}D_{11}+2D_{22}D_{11} \end{bmatrix}$$

(10.7)

Tip Motion derivative with respect to  $a_3$ :

$$\frac{\partial \mathbf{x}}{\partial a_3} = \mathbf{J} \frac{\partial \mathbf{Q}}{\partial a_3} \mathbf{F}_0 \quad (10.8)$$

$$\frac{\partial \mathbf{Q}}{\partial a_3} = \frac{\cos(\Theta_2)}{\omega^2(D_{11}D_{22}-D_{21}D_{12})^2} \begin{bmatrix} 2D_{22}D_{12}-2D_{22}D_{22} & -D_{11}D_{22}-D_{12}D_{12}+2D_{12}D_{22} \\ -D_{11}D_{22}-D_{12}D_{12}+2D_{12}D_{22} & -D_{12}D_{12}+2D_{12}D_{11} \end{bmatrix}$$

(10.9)

Tip Motion derivative with respect to  $a_4$ :

$$\frac{\partial \mathbf{x}}{\partial a_4} = \mathbf{J} \frac{\partial \mathbf{Q}}{\partial a_4} \quad (10.10)$$

$$\frac{\partial \mathbf{Q}}{\partial a_4} = (-\mathbf{D} + \omega^2 \mathbf{K})^{-1} \begin{bmatrix} \cos(\Theta_1 + \Theta_2) \\ \cos(\Theta_1 + \Theta_2) \end{bmatrix} \quad (10.11)$$

Tip Motion derivative with respect to  $a_5$ :

$$\frac{\partial \mathbf{x}}{\partial a_5} = \mathbf{J} \frac{\partial \mathbf{Q}}{\partial a_5} \quad (10.12)$$

$$\frac{\partial \mathbf{Q}}{\partial a_4} = (-\mathbf{D} + \omega^2 \mathbf{K})^{-1} \begin{bmatrix} \cos \Theta_1 \\ 0 \end{bmatrix} \quad (10.13)$$

Tip Motion derivative with respect to  $k_1$ :

$$\frac{\partial \mathbf{x}}{\partial k_1} = \mathbf{J} \frac{\partial \mathbf{Q}}{\partial k_1} \quad (10.14)$$

$$\frac{\partial \mathbf{Q}}{\partial k_1} = \frac{1}{(K_{11}K_{22})^2} \begin{bmatrix} -K_{22} & 0 \\ 0 & 0 \end{bmatrix} \mathbf{F}_0 \quad (10.15)$$

Tip Motion derivative with respect to  $k_2$ :

$$\frac{\partial \mathbf{x}}{\partial k_2} = \mathbf{J} \frac{\partial \mathbf{Q}}{\partial k_2} \quad (10.16)$$

$$\frac{\partial \mathbf{Q}}{\partial k_2} = \frac{1}{(K_{11}K_{22})^2} \begin{bmatrix} 0 & 0 \\ 0 & -K_{11} \end{bmatrix} \mathbf{F}_0 \quad (10.17)$$

The dynamic parameter propagation matrix (equation 9.11) can be written as

$$\mathbf{P} = \mathbf{J} \begin{bmatrix} \frac{\partial \mathbf{Q}}{\partial k_1} & \frac{\partial \mathbf{Q}}{\partial k_2} & \frac{\partial \mathbf{Q}}{\partial a_1} & \frac{\partial \mathbf{Q}}{\partial a_2} & \frac{\partial \mathbf{Q}}{\partial a_3} & \frac{\partial \mathbf{Q}}{\partial a_4} & \frac{\partial \mathbf{Q}}{\partial a_5} \end{bmatrix} \quad (10.18)$$

and the parameter deviation vector is

$$\Delta \varepsilon = [\Delta k_1, \Delta k_2, \Delta a_1, \Delta a_2, \Delta a_3, \Delta a_4, \Delta a_5]^T \quad (10.19)$$

## 10.2. Numerical Simulation

Numerical simulation is undertaken to validate the proposed identification model (equation 9.33) and to verify the accuracy of the identifiability and excitability index (equations 9.41) and the usefulness of the individual parameter identifiability index (equation 9.43). The nominal values of the links dynamic parameters and the actual values used for simulation are given in Table 10.1. Table 10.2 shows the details of the configurations used for simulation. The 5 cases given in table 1 are excited through the manipulator base. Table 10.3 shows the values of the identifiability index  $I_d$ , the estimation error and the number of measurements done for the five cases. Tables 10.4a, 10.4b, 10.4c, 10.4d and 10.4e show the actual and the estimated values of the parameter deviation for the five cases considered. It is observed that configurations with high identifiability index result in better estimation of the parameter deviation vector; Further, it is seen that the number of measurements is not as important as the configuration used for estimation.

To explore the use of the individual parameter identifiability index  $\kappa_i$  Case 4 and Case 5 are reconsidered. Table 10.5 shows the individual parameter identifiability

index for the five cases. It can be seen from the table that only 5 parameters are identifiable in Case 4 and Case 5. A reduced model of dynamic parameter vector with five parameters is then used. The estimated and the actual values of the parameter obtained using the reduced model is shown in Table 10.6a and Table 10.6b. The identifiability indices and the estimation errors for the reduced model are shown in Table 10.7. It is noted that reduction of the dimension of the parameter deviation vector using individual identifiability index  $\kappa_i$  leads to improved estimation of the identifiable parameters.

### 10.3. Summary and Concluding Remarks

In this chapter, the procedures presented in chapter 9 for the estimation of the dynamic parameter of mobile manipulators has been verified using a two link non-wheeled mobile manipulator. The dynamic parameter vector for this case has been formed and the components of the dynamic parameter propagation matrix for the elements of the dynamic parameter vector have been derived. Numerical simulation has been undertaken to validate the models (equation 9.33, 9.41 and 9.43). It can be concluded that it is practical to use the introduced model (equation (9.33)) to compute the parameter deviations; the observability index  $I_d$  is a useful measure for evaluation of the effect of manipulator configuration on the identifiability of the parameters; the number of measurements used for estimation is not as important as the configuration; elimination of low sensitive parameters from the parameter deviation vector model  $\varepsilon$  using the individual identifiability index  $\kappa_i$  (equation (9.43)) leads to improve estimation of the high sensitive



parameters. A summary of the conclusions from the thesis and suggestions for future research are presented in the next chapter.

Table 10.1 Nominal and actual values of Parameters Used for Simulation

Parameter	Nominal Value	Actual Value	Unit
$k_1$	4596	4656	N/m
$k_2$	3215	3325	N/m
$m_1$	5.6	6.0	kg
$m_2$	3.5	3.9	kg
$I_1$	2.5	2.7	kgm <sup>2</sup>
$I_2$	1.9	2.2	kgm <sup>2</sup>
$l_{c1}$	0.35	0.45	m
$l_{c2}$	0.45	0.35	m
$l_1$	1.	1.	m
$l_2$	1.	1.	m

Table 10.2 Configuration Used for Simulation

Configuration Set	$\Theta_1$	$\Theta_2$
Case 1	0°	0°
	10°	45.5°
	0°	85.6°
	45°	135°
	115°	180°
Case 2	0°	90°
	170°	45.5°
	60°	177°
	45°	90°
	120°	160
	45°	45
Case 3	0°	90°
	170°	45.5°
	60°	177°
	45°	90°
	120°	160°
	45°	45°
	66°	204°
	130°	140°
	37°	53°

Case 4	0°	0°
	10°	45.5°
	0°	85.6°
	45°	135°
	115°	180°
	90°	90°
	90°	45.5°
	177°	60°
	90°	45°
	120°	160°
	45°	45°
Case 5	0°	90°
	90°	45.5°
	90°	180°
	270°	0°
	0°	270°
	45°	45°
	71°	199°
	185°	85°
	90°	10°
	0°	270°
	11°	79°
	20°	56°
	87°	42°

Table 10.3 Identifiability Index, Number of Measurements and Estimation Error for Case 1 to Case 5.

Case	Id	Number of Measurements	Estimation Error in %
1	3.25	15	8.58
2	2.86	18	14.87
3	1.94	27	17.02
4	0.67	33	280
5	0.08	39	225

Table 10.4a Actual and Estimated Parameters for Case 1

Parameter	Actual Value	Estimated Value
$\Delta k_1$	140	134.512
$\Delta k_2$	110	113.643
$\Delta a_1$	1.225	1.094
$\Delta a_2$	0.069	0.077
$\Delta a_3$	0.020	0.0195
$\Delta a_4$	0.020	0.0188
$\Delta a_5$	1.140	1.143

Table 10.4b Actual and Estimated Parameters for Case 2

Parameter	Actual Value	Estimated Value
$\Delta k_1$	140	125.18
$\Delta k_2$	110	97.54
$\Delta a_1$	1.225	0.987
$\Delta a_2$	0.069	0.076
$\Delta a_3$	0.02	0.0276
$\Delta a_4$	0.02	0.0177
$\Delta a_5$	1.14	1.176

Table 10.4c Actual and Estimated Parameters for Case 3

□ Parameter	Actual Value	Estimated Value
$\Delta k_1$	140	132.910
$\Delta k_2$	110	104.112
$\Delta a_1$	1.225	1.064
$\Delta a_2$	0.069	0.052
$\Delta a_3$	0.02	0.031
$\Delta a_4$	0.02	0.0197
$\Delta a_5$	1.14	1.151

Table 10.4d Actual and Estimated Parameters for Case 4

Parameter	Actual Value	Estimated Value
$\Delta k_1$	140	97.18
$\Delta k_2$	110	156.54
$\Delta a_1$	1.225	2.087
$\Delta a_2$	0.069	1.076
$\Delta a_3$	0.02	.05
$\Delta a_4$	0.02	.004
$\Delta a_5$	1.14	3.176

Table 10.4e Actual and Estimated Parameters for Case 5

Parameter	Actual Value	Estimated Value
$\Delta k_1$	140	85.9
$\Delta k_2$	110	170.2
$\Delta a_1$	1.225	3.087
$\Delta a_2$	0.069	0.566
$\Delta a_3$	0.02	0.052
$\Delta a_4$	0.02	0.0677
$\Delta a_5$	1.14	3.51

Table 10.5 Values of individual identifiability indices for Case 1 to Case 5

$\kappa_i$	Case 1	Case 2	Case 3	Case 4	Case 5
$\kappa_1$	3.51	3.43	4.15	4.87	3.56
$\kappa_2$	3.43	2.88	3.77	4.65	2.99
$\kappa_3$	3.99	2.96	3.98	5.12	3.87
$\kappa_4$	2.86	3.21	4.45	4.97	3.89
$\kappa_5$	3.04	2.79	3.22	276.93	543.0
$\kappa_6$	3.47	3.08	4.02	1.2	1.12

Table 10.6a Actual and Estimated Parameters for Case 6 (Case 4 Reduced Model)

Parameter	Actual Value	Estimated Value
$\Delta k_1$	140	129.8
$\Delta k_2$	110	96.59
$\Delta a_1$	1.225	1.387
$\Delta a_2$	0.069	0.066
$\Delta a_3$	0.02	0.014



Table 10.6b Actual and Estimated Parameters for Case 7(Case 5. Reduced Model)

Parameter	Actual Value	Estimated Value
$\Delta k_1$	140	155.19
$\Delta k_2$	110	107.73
$\Delta a_1$	1.225	1.087
$\Delta a_2$	0.069	0.081
$\Delta a_3$	0.02	0.021

Table 10.7 Identifiability Index, Number of Measurements and Estimation Error for the Case 6 and Case 7.

Case	Id	Number of Measurements	Estimation Error in %
1	1.95	33	13.41
2	2.06	39	9.3

## Chapter Eleven

# CONCLUSIONS

### 11.1. Final Remarks

The studies presented in the previous chapters lead to the following final remarks:

1. Mobile manipulators have been classified into two groups -the non-wheeled and the wheeled manipulators. The non-wheeled mobile manipulator has a base which is much larger than the manipulator structure therefore the dynamics of the manipulator does not affect the base dynamics. The wheeled mobile manipulator has a base mounted on wheels and the dynamics of the manipulator base is of the same order of magnitude as the manipulator therefore they are coupled with each other.
2. In non-wheeled mobile manipulators the base motion has been modeled as a random process. The response of both the joints and the tip of the manipulator have been studied as stationary and non-stationary random processes. Expressions for the covariance tensors of the stationary responses have been studied in the frequency domain using modal decomposition and the concept of power spectral density. State space variable concepts have been applied in the time domain to derive expressions for the nonstationary responses.

3. Single link and two-link manipulators have been used to illustrate the nonstationary and stationary joint and tip covariance responses of non-wheeled mobile manipulators. Closed form expressions for the response of the single-link have been developed.
4. Two models have been used to study wheeled locomotion: the so-called quarter-car model and the half-car model. A deterministic horizontal motion of the vehicle has been used to investigate the wheeled motion. The elastic response of the system, including motion of the vehicle, that results from the surface irregularity has been modeled as a stochastic process.
5. Two cases of horizontal vehicle motion have been explored: uniform and accelerated motions. The uniform motion produced purely stationary stochastic response while the accelerated motion produced nonstationary response in addition to a deterministic motion.
6. Expressions for the covariances of the tip and joint stationary response of wheeled mobile manipulators have been developed for the quarter-car model using two techniques: modal decomposition combined with the power spectral density method and the state space concept. Response from both methods have been shown to be practically the same. The state space concept however, has been recommended for practical applications because:
  - (i) it gives the displacement and the velocity covariances simultaneously;
  - (ii) it can accommodate non-proportional damping without computational complications;
  - (iii) it avoids complex contour integration.

(iv) it can also accommodate nonstationary responses.

The State Space representation has therefore been employed to study the tip and joint nonstationary covariance responses of wheeled mobile manipulators for the quarter-car and the half-car models.

7. Examples employing two link manipulators mounted on the vehicles have been explored. Sensitivity of the principal variance of the manipulator tip responses to system parameters have been investigated.
8. The Singular Value Decomposition technique has been used to derive procedures for computation of the optimal configurations and excitations for the estimation of the parameters. An algorithm for eliminating unobservable parameters has been presented. Examples and numerical simulations have been given to illustrate the ideas.

## **11.2. Major Contributions and Conclusions**

1. In the author's opinion, the thesis is the first reported attempt to systematically review the theoretical dynamics of mobile manipulators.
2. The thesis classifies mobile manipulators into two broad categories: non-wheeled and wheeled. Such classification streamlined the study and allowed systematic analysis of the system response.
3. The reported research includes the first known attempt of study of the random dynamics of flexible mobile manipulators.

4. The concept of the covariance tensor has been known in the field of multidimensional random process and adopted for the first time to the mobile manipulator dynamic analysis.
5. The concept of the principal variance of the manipulator tip motion has been introduced for the first time.
6. It has been shown that the principal variance of the tip motion is almost unidirectional and highly configuration dependent for all the mobile manipulator models and types of random motion studied.
7. The author has investigated the sensitivity of the manipulator tip response to system parameters and has suggested several design considerations to minimize the manipulator tip random response.
8. The suggestions relate to:
  - (i) selection of links length; the “lower” links should be longer than the “upper” links.
  - (ii) the relative magnitude of damping in the joints; the damping efforts should be concentrated in the “lower” joints.
  - (iii) the relative stiffness of the joints; the “lower” joints should be stiffer than the “upper” joints.
9. New computation models to identify the dynamic parameters of flexible mobile manipulators have been derived.

10. The author has introduced new optimization criteria which can be used to set the manipulator configuration and excitation for efficient testing.
11. For the two link manipulators on a non-wheeled mobile base it has been discovered that the manipulator has a family of configurations at which a mode reversal takes place. The mode reversal configurations has been characterized by the angle between the two links  $\Theta_2 = \pm 131.81^\circ$ . It was discovered that for the manipulator studied at these angles the covariance between the joint motion is zero since the joint motion is decoupled. Further, at the adjacent angles to the mode reversal angle the modal parameters of each modal vector change their direction with respect to each other because the covariance of the displacements changes sign.

### **11.3. Recommendations for Future Work**

The author believes that the study presented will lead to several promising research studies such as experimental validation of the unidirectional motion of the manipulator tip and experimental verification of the dynamic parameter identification model etc. From the results presented the following recommendations can be made for future research

1. The analysis of the stochastic responses of the manipulator joint motion did not include the small non-linearities inherent in the joint vibration of the manipulator. It is expected that inclusion of the kinematic non linearities will lead to studies of the large joint motion and to studies of the combination of vibration and the controlled large angle motion.

2. The random vibration analysis, in this study, has neglected the small varying nature of the kinematic configuration of the manipulator. This variation will invariably lead to parametric excitation (Liu, 1992) of the mobile manipulator small vibration. The stability and the response bounds of parametrically excited mobile manipulators under random excitation can be investigated.
3. The system parameters have been assumed to be deterministic while the excitation has been assumed stochastic. However, in some cases the parameters may vary in a stochastic way as well. There are reports on related topics [Wien and Sinha, 1984] and [Sinha and Wien 1989]; they were focused on stability under deterministic excitation. It will be worth investigating the stability and response bounds under stochastic excitation as well.
4. It has been illustrated in this thesis that the principal variance of the tip motion of the manipulator is unidirectional. An experimental study can be carried out to validate the findings.
5. The study of the stochastic responses of joint motion has been limited to planar manipulators. The analysis could be extended to spatial manipulators; for example the observed unidirectional nature of the tip response can be investigated.
6. Algorithms have been developed for dynamic testing of flexible manipulators and optimization of the configuration and excitations have been reported. These findings can be verified experimentally.

## REFERENCES

- Akpan, U. O. and Kujath, M. R., (1996a), Stochastic Response of Flexible Mobile Robotic Manipulator Structure. *International Journal of Computer and Structures*, 59(5):891-898.
- Akpan, U. O. and Kujath, M. R., (1996b), Nonstationary Random Response of a Flexible Mobile Robotic Manipulator. *ASME Journal of Dynamic Systems Measurements and Control* (accepted for publication, 5th March, 1996)
- Akpan, U. O. and Kujath, M. R., (1996c), Sensitivity of a Mobile Manipulator Response to System Parameters. *ASME Journal of Vibration and Acoustics* (accepted for publication, 9th Feb, 1996).
- Akpan, U. O. and Kujath, M. R., (1996d), Dynamics of Mobile Manipulator. *Mechanism and Machine Theory* (manuscript under review)
- Akpan, U. O. and Kujath, M. R., (1995a), Response Covariance of a Structure Mounted Atop a Vehicle. *Canadian Congress of Applied Mechanics, CANSAM 1995*.
- Akpan, U. O. and Kujath, M. R., (1995b), Nonstationary Random Response of a Vehicle with a Varying Structure. *International Journal of Vehicle Design*, 6(16):531-540.



- Anderson, G. L., (1985), Stability of a Manipulator with Resilient Joints. *Journal of Sound and Vibration*. 101(4): 463-480.
- Armstrong, B., Khatib, O and Burdick, J., (1986), The Explicit Dynamic Model and Inertial Parameters of the PUMA 560 Arm. *Proceedings of the 1986 IEEE International Conference on Robotics and Automation*. 510-518.
- Asada, H. and Slotine, J. J., (1986), Robot Analysis and Control. John Wiley and Sons, Inc. New York.
- Atkeson, C. G., An, C. H. and Hollerbach, J. M., (1990), Estimation of Inertia Parameters of Manipulator Loads and Links. *International Journal of Robotic Research*. 5(3): 101-119.
- Behi, Fariborz and Tesar, Delbert, (1991), Parameter Identification for Industrial Manipulators Using Experimental Modal Analysis. *IEEE Transactions on Robotics and Automation*. 7(5): 642-652.
- Bendat, J. S. and Piersol, A. G., (1986), Random Data, Analysis and Measurements Procedures. Second Edition, Revised and Expanded.
- Bogdanoff, J. L. and Citron, S. J., (1965), On the Stabilization of the Inverted Pendulum. *Developments in Mechanics*. 3(2): 3-15.

- Book, W. J., Maizza-Neto, O., and Whitney, D. E., (1975), Feedback Control of Two Beam, Two Joint System with Distributed Flexibility. *Journal of Dynamic Systems, Measurement and Control*. 97: 424-431.
- Book, W. J., (1984), Recursive Lagrangian Dynamics of Flexible Manipulator Arms. *International Journal Of Robotic Research*. 3: 87-101.
- Born, Jin-Hwan and Menq, Chia-Hsiang, (1991), Determination of Optimal Measurement Configurations for Robot Calibration Based on Observability Measure. *The International Journal of Robotics Research*. 10(1): 51 -63.
- Brooks, P. C. and Sharp, R. S, (1987), A Computational Procedure Based on Eigenvalue Sensitivity Theory Applicable to Linear System Design. *Journal of Sound and Vibration*. 114(1): 13-18.
- Caughey T. K. and Stumpf, H. J., (1961), Transient Response of a Dynamic System Under Random Excitation. *Transactions of American Society of Mechanical Engineers, Journal of Applied Mechanics*. 28:563-566.
- Chalhoub, N. G and Ulsoy, A. G., (1986), Dynamic Simulation of Leadscrew Driven Flexible Robot Arm and Controller. *Journal of Dynamic Systems, Measurements and Control*. 108:119-126.
- Chang, T. P. (1993) Dynamic Response of Space Structures under Random Excitation. *Computer and Structures*. 48:575-582.

- Chang, R. J. and Young, G. E., (1989), Prediction of Stationary Response of Robot Manipulators Under Stochastic Base and External Excitations--Statistical Linearization Approach. *Journal of Dynamic Systems, Measurements and Control*. 111: 426-432.
- Chen, J., Wang, C. B. and Yang, J. C. S., (1985), Robot Position Accuracy Improvement through Kinematic Parameter Identification. *Third Canadian CAD/CAM Robotics Conference*. Toronto, Ontario, Canada: 4.7-4.12.
- Choi, S. -B., Cheong, C. -C. and Shin, H. -C., (1995), Sliding Mode Control of Vibration in a Single-Link Flexible Arm with Parameter Variations. *Journal of Sound and Vibration*. 179(5): 737-748.
- Davidson, E. J. and Man, F. T. (1968), The Numerical Solution of  $AQ + QA = -C$ . *IEEE Transaction on Automatic Control*: 448-446.
- De Smet, M. , Liefoghe, Sas, P., Snoeys, R., (1989), Dynamic Analysis of Flexible Structures Using Component Mode Synthesis. *Journal of Applied Mechanics*. 56:875-880.
- De Wit, C. C. and Aubin, A., (1991), Robot Parameter Identification via Sequential Hybrid Estimation Algorithm. *Proceedings of the 1991 IEEE International Conference on Robotics and Automation*. Sacramento, California: 952-957.

- Denavit, J. and Hartenberg, R. S. (1955), A Kinematic Notation for Lower-Pair Mechanisms Based on Matrices. ASME Journal of Applied Mechanics:215-221.
- Dubowsky, S. and Vance, E. E., (1989), Planning Mobile Manipulator Motions Considering Vehicles Dynamic Stability Constraints. Proceedings IEEE International Conference on Robotics and Automation. Scottsdale, Az.
- Elosegui, P., (1994), Measurement of the Dynamic Model of a PUMA 560 Robot Using Experimental Modal Analysis. ASME Journal of Mechanical Design. 116: 75-79.
- Fugimore Y. and Lin, Y. K., (1973), Analysis of Airplane Response to Nonstationary Turbulence Including Wind Bending Flexibility. American Institute of Aeronautics and Astronautics Journal. 11:334-339.
- Golub, G. H. and Van Loan, C. F., (1990), Matrix Computation. John Hopkins, 2nd Edition.
- Gopal, M., (1989) Modern Control System Theory. Wiley Eastern, 2nd Edition.
- Hac. A., (1985), Suspension Optimization of a 2 DOF Vehicle Model Using Stochastic Optimal Control Technique. Journal of Sound and Vibration. 100(3): 343-357.

- Hammond, J. K., (1968), On the Response of Single and Multi-Degree of Freedom System to Nonstationary Random Excitations. *Journal of Sound and Vibration*. 7:393-416.
- Hammond, J. K. and Harrison, R. F., (1981), Nonstationary Response of Vehicles on Rough Ground- A State Space Approach. *Journal of Dynamic Systems, Measurements and Control* 103: 245-250.
- Harrison, R. F., (1981), The Nonstationary Response of Vehicles on Rough Ground. Unpublished Ph.D. Dissertation, University of Southampton.
- Hayati, S. A., (1983), Robot Arm Geometric Link Calibration. *Proceeding 22nd IEEE Conference on Decision and Control*. 1477-1483.
- Hedrick, J. K. and Firouztash, H., (1974), Covariance Propagation Equation Including Time Delay Inputs. *IEEE Transaction on Automatic Control*. 19(5): 587-589.
- Hootsmans, N. A. M., (1992), The Motion Control of Manipulators on Mobile Vehicles, Unpublished D. Sc. Dissertation, Massachusetts Institute of Technology.

- Hootsmans, N. A. M. and Dubowsky, S., (1991), Large Motion Control of Mobile Manipulators Including Vehicle Suspension Characteristics. Proceedings IEEE International Conference on Robotics and Automation. Sacramento, California. 2336-2341.
- Hoskins, R. F., (1979), Generalized Functions. John Wiley and Sons.
- Hsu, P., J. Hauser and Sastry, S., (1988), Dynamic Control of Redundant Manipulators. Proceedings American Control Conference (Boston). 2135-2139.
- Iwan, W.D. and Hou, Z. K. (1989), Explicit Solutions for the Response of Simple Systems Subjected to Nonstationary Random Excitation. Structural Safety. 6: 77-86.
- Jacobs, P. and Canny, J., (1989), Planning Smooth Paths for Mobile Robots. Proceedings IEEE International Conference on Robotics and Automation. Scottsdale, Az.
- Khalil, W, Gautier M. and Enguehard, C., (1991), Identifiable Parameters and Optimum Configurations for Robot Calibration. Robotica. 9: 63-70.

- Khatib, O. and Le Maitre, J. F., (1978), Dynamic Control of Manipulators Operating in a Complex Environment. Proceedings 3rd International CISM-IFTOMM Symposium. 267-282.
- Khosla, P. K. and Kanade, T., (1985), Parameter Identification of Robot Dynamics, Proceedings of the 1985 IEEE International Conference on Decision and Control. 1754-1760.
- Khosla, Pradeep K., (1988), Estimation of Robot Dynamic Parameters: Theory and Application. International Journal of Robotic and Automation. 3(1): 35-41.
- Kozin, F. and Bogdanoff, J. L., (1960), On the Statistical Analysis of the Motion of Some Simple, Two-dimensional Linear Vehicles, Moving on a Random Track. International Journal of Mechanical Science. 2: 168-178.
- Krishnamurthy, K., (1989), Dynamic Modeling of a Flexible Cylindrical Manipulator. Journal of Sound and Vibration. 132(1):143-154.
- Kujath, M. R. and Akpan, U. O., (1994a), Optimization of Dynamic Testing of Space Manipulators. Proceedings 12th International Modal Analysis Conference. Honolulu, Hawaii. 626 -632.
- Kujath M. R. and Akpan, U. O., (1994b), Dynamic Testing of Space Manipulators, Theory and Practice of Robots and Manipulator Proceedings

of Romansy 10: The tenth CISM-IFTOMM Symposium, Edited by A. Morecki, G. Bianchi and K. Jawork. 255-260.

Kujath, M. R. and Akpan, U. O., (1996b), Stochastic Vibration of a Mobile Manipulator. ASME Journal of Applied Mechanics (submitted for publication, 8th August, 1995).

Kujath, M. R. and Akpan, U. O., (1996a), Dynamic Response of the Manipulator Tip to Random Excitation. ASME Journal of Dynamic Systems Measurements and Control (accepted for publication, 6th, March, 1995 and to appear in vol. 118, September, 1996).

Kujath, M. R. and Akpan, U. O., (1995), Stochastic Dynamics of a Mobile Manipulator. Proceedings Ninth World Congress on the Theory of Machines and Mechanisms. 2132-2136.

Kujath, M. R., and Akpan, U. O., (1996c), Sensitivity of Manipulator Random Response to System Parameters. Journal of Sound and Vibration (submitted for publication, 3rd January, 1996)

Kumar, A. and Waldron, K. J., (1981), Numerical Plotting of Surfaces of Positioning Accuracy of Manipulators. Mechanism and Machine Theory. 14(4):361-368.

Lin. Y. K., (1967), Probabilistic Theory of Structural Dynamics. Krieger, Florida.



- Liu, Kefu, (1992), *Vibration of Linear Time Varying Systems*. Unpublished Ph.D. Thesis. Technical University of Nova Scotia.
- Mark, W. D., (1970), Spectral Analysis of the Convolution and Filtering of Nonstationary Stochastic Processes. *Journal of Sound and Vibration*. 11(1): 19-63.
- Masri, S. F., (1978), Response of a Multi-degree of Freedom System to Nonstationary Random Excitation. *Journal of Applied Mechanics*. 45:649-656.
- McKerrow, P. J., (1991), Introduction to Robotics. Addison Wesley.
- Meirovitch, Leonard, (1990), Dynamics and Control of Structures. John Wiley and Sons.
- Menq, Chia-Hsiang, Borm , Jin-Hwan and Lai, Jim Z., (1989), Identification and Observability Measure of a Basis Set of Error Parameters in Robot Calibration. *Journal Of Mechanisms, Transmissions and Automation in Design*. 111:513-518.
- Mooring, B. W., (1983), The Effect of Joint Axis Misalignment on Robot Position Accuracy. *Proceedings Computers in Engineering Conference and Exhibition*. 2: 151-155.

- Mukerjee, A. and Ballard, D. H., (1985), Self-calibration in Robot Manipulators. Proceedings IEEE Conference in Robotic and Automation. St Louis. MO. 1050-1057.
- Murray, M. R., Li, Z., Sastry, S. S., (1994), A Mathematical Introduction to Robotic Manipulation, CRC Press.
- Naganathan, G., and Soni, A. H., (1987), Coupling Effects of Kinematics and Flexibility in Manipulators. Kinematics of Robot Manipulators. Edited by J. M. McCarthy. MIT Press.
- Nakamura, Yoshihiko, (1991), Advanced Robotics Redundancy and Optimization. Addison Wesley Publishing Company.
- Newland, D. E., (1984), An Introduction to Random Vibration and Spectral Analysis. 2nd Edition, Longman Scientific and Technical.
- Nguyen, L. A. , Walker, I. D. and DeFigueiredo, R. J. P., (1992), Dynamic Control of Flexible, Kinematically Redundant Robot Manipulators. IEEE Transactions on Robotics and Automation. 8(6): 759-767.
- Priestley, M. B., (1967), Power Spectral Analysis of Nonstationary Random Process. Journal of Sound and Vibration. 6(1): 86-97.

- Rivin, Eugene I., (1987), Mechanical Design of Robots. McGraw-Hill Book Company.
- Rome, H. J., (1969), A Direct Solution to the Linear Variance Equation of a Time-Invariant Linear System. IEEE Transaction on Automatic Control: 592-593.
- Sasiadek, J. Z. and Srinivasan, R., (1989), Dynamic Modeling and Adaptive Control of a Single-Link Flexible Manipulator. AIAA Journal. 32(2):838-844.
- Seeger, G. and Leonard, W., (1989), Estimation of Rigid Body Models for a Six-Axis Manipulator with Geared Electric Drives. Proceedings IEEE International Conference on Robotics and Automation. Scottsdale, AZ. 1690-1695.
- Sharp, R. S. and Brooks, P. C., (1988), Sensitivities of Frequency Response Functions of Linear Dynamic Systems to Variation in Design Parameter Values. Journal of Sound and Vibration. 126(1):167-172.
- Shir-Kuan, Lin, (1995), Minimal Linear Combination of the Inertia Parameters of a Manipulator. IEEE Transaction on Robotics and Automation: 11(3):360-373.

- Singh, S. N. and Schy, A. A., (1986), Control of Elastic Robotic Systems by Nonlinear Inversion and Modal Damping. *Journal of Dynamic Systems, Measurements and Control*. 108: 180-189.
- Sinha, S. C. and Wiens, G. J., (1989), Response Bounds for Lumped Vibrational Systems with Time-dependent Parameters. *Journal of Sound and Vibration*, 132(1): 1-9.
- Smaili, Ahmad A., (1993), A Three-Node Finite Beam Element for Dynamic Analysis of Planar Manipulators with Flexible Joints. *Mechanism and Machine Theory*. 28(2):193-206
- Smith, P. G., (1971), Numerical Solution of the Matrix Equation  $AX + XA^T + B = 0$ . *IEEE Transaction on Automatic Control*. 278-279.
- Sobczyk, K. and Macvean, D. B., (1976), Nonstationary Random Vibrations of System Traveling With Variable Velocity. *Symposium on Stochastic Problems in Dynamics*, University of Southampton. Edited by B. L. Clarkson.
- Spanos, P-T. D., (1987), An Approach to Calculating Random Vibration Integrals. *Journal of Applied Mechanics*. 54: 409-413.
- Spong M. W. and Vidyasagar, M., (1989), Robot Dynamics and Control. John Wiley and Sons.

- Streit, D. A., Krousgrill, C. M. and Bajaj, A. K., (1989), Nonlinear Response of Flexible Robotic Manipulator Performing Repetitive Tasks. *Journal of Dynamic Systems, Measurements and Control*. 111:470-480.
- Streit, D. A., Krousgrill, C. M. and Bajaj, A. K., (1986), A Preliminary Investigation of the Dynamic Stability of Flexible Manipulators Performing Repetitive Tasks. *Journal of Dynamic Systems, Measurements and Control*. 108:206-214.
- Sunada, W. H. and Dubowsky, S., (1983), On the Dynamic Analysis and Behavior of Industrial Robotic Manipulators with Elastic Members. *Journal of Mechanisms, Transmission and Automation in Design*. 105:42-51.
- Thomson, W. T., (1988), Theory of Vibration with Applications. Prentice Hall, Third edition.
- To, C. W. S. and Wang, B., (1993), Time Dependent Response Statistics of Axisymmetric Shell Structures. *Journal of Sound and Vibration*. 164(3): 554-564.
- To, C. W. S. and Orisamolu, I. R. (1987), Response of Discretized Plates to Transversal and In-Plane Non-Stationary Random Excitations. *Journal of Sound and Vibration*. 114(3):481-494.

- To, C. W. S., (1982), Nonstationary Random Responses by the Theory of Evolutionary Spectra. *Journal of Sound and Vibration*. 83(2): 273-291.
- To, C. W. S., (1986), Response Statistics of Discretized Structures to Nonstationary Random Excitation. *Journal of Sound and Vibration*. 105(2): 217-231.
- To, C. W. S., (1984), Time Dependent Variance and Covariance of Responses of Structures to Nonstationary Random Excitation. *Journal of Sound and Vibration*. 89(1):135-156.
- Turcic, D. A and Midha, A., (1984), Generalized Equations of Motion for the Dynamic Analysis of Elastic Mechanism Systems. *Journal of Dynamic Systems, Measurements and Control*. 106: 243-248.
- Usono, P. B., Nadira, N. and Mahil, S. S., (1986), A Finite Element/Lagrange Approach to Modeling Lightweight Flexible Manipulators. *Journal of Dynamic Systems, Measurements and Control*. 108:198-205.
- Veitschegger, W. K. and Wu, C. H., (1987), A Method for Calibrating and Compensating Robot Kinematic Errors. *Proceedings IEEE International Conference on Robotic and Automation*. 1: 39-44.
- Virchis, V. J, and Robsin, J. D., (1971), Response of Accelerating Vehicle to Random Road Undulation. *Journal of Sound and Vibration*. 18(3): 243-427.

- Walker, I. D., (1990), The Use of Kinematic Redundancy in Reducing Impact and Contact Forces. Proceedings IEEE International Conference on Robotic and Automation. Cincinnati, OH. 434-439.
- Whitney, D. E , C. Lozinski, A. and Rourke, J. M., (1984), Industrial Robot Calibration Method and Results. Proceedings International Computer in Engineering Conference and Exhibition. 1: 92-100.
- Wiens, G. J. and Sinha, S. C., (1984), On the Application of Liapunov's Direct Method to Discrete Dynamic Systems with Stochastic Parameters. Journal of Sound and Vibration. 94(1): 19-31.
- Wu, C. H., (1983a), The Kinematic Error Model for the Design of Robot Manipulator. American Control Conference. San Francisco, CA.
- Wu, C. H., (1983b), A CAD Tool for the Kinematic Design of Robot Manipulator. International Conference on Advanced Automation. Taipei, Taiwan Republic of China.
- Wu, C. H., (1984), A Kinematic CAD Tool for the Design and Control of Robot Manipulator. International Journal of Robotic Research. 3(1).

- Wung, Chih-Dao and Kiureghian, Armen Der, (1989), Computer- Assisted Learning System for Stochastic Dynamic Analysis of Structures Part I (Theory and Development).
- Xia, Jack Zhijie and Menq, Chia-Hsiang, (1993), Real Time Estimation of Elastic Deformation for End-Point Tracking Control of Flexible Two Link Manipulators. *Journal of Dynamic Systems, Measurements and Control*. 115:385-393.
- Yadav, D. and Nigam, N. C., (1978), Ground Induced Nonstationary Response of Vehicle. *Journal of Sound and Vibration*. 61(1): 117-126.
- Yang, C. Y., (1986), Random Vibration of structures. John Wiley and Sons Inter Science.
- Yoshikawa, T., (1985), Analysis and Control of Robot Manipulators with Redundancy. *Robotics Research First International Symposium* Brady and Paul Eds. Cambridge MA. MIT Press. 735-747.
- Yuan, B. S , W. J. Book, Huggins, J. D., (1993), Dynamics of Flexible Manipulator Arms: Alternative Derivation, Verification and Characteristics for Control. *Journal of Dynamic Systems, Measurements and Control* 115:394-404.



Yun-Hui, L. and Suguru, A., (1991), Proposal Tangent Graph and Extended Tangent Graph for Path Planning of Mobile Robots. Proceedings IEEE International Conference on Robotics and Automation. Sacramento California. 312 - 317.

Zadeh, L. A. and Desoer, C. A., (1963), Linear System Theory. McGraw-Hill Book Co.

## Appendix A

### FUNDAMENTALS OF RANDOM PROCESS

#### A1. Terminology of Stochastic Process

System excitations or responses can be deterministic or stochastic (see Figures A.1. and A.2. for illustration). In this discussion, the word process is used to denote either excitation or response. For a deterministic process mathematical expressions to determine the instantaneous value of the process at any time  $t$  can be written. However, this is not the case for a random process. Statistical methods and probability theories have to be used. Consider the stochastic process shown in Figure A.2. In spite of the irregular nature of the process some degree of statistical regularities can be found. Averaging procedures can be applied to establish gross characteristics of the process.

In any statistical method, however, a large amount of data is necessary to establish reliability. To establish useful statistics of the random process of a manipulator hundreds of records of the type shown in Figure A.3 may be required.

Realization: Each record is called a realization.

Ensemble: This is the total collections of records.

### A1.1. Probability Structure of Random Processes

Let the random process  $X$  at time  $t_i$  be  $X_i$  i.e.

$$X(t_i) = X_i \quad (\text{A.1})$$

#### Probability Distribution Function (CDF) $P_{X_i}(x_i)$

It is defined as the probability that the value of the random process  $X_i$  is less or equal to some number  $x_i$  i.e.

$$P_{X_i} = P\{X_i \leq x_i\} \quad (\text{A.2})$$

where  $P\{\cdot\}$  -probability that

#### Probability Density Function (PDF) $p_{X_i}$

$$p_{X_i}(x_i) = \frac{\partial P_{X_i}}{\partial X_i} \quad (\text{A.3})$$

#### Probability Structure of a Random Process at n different times $t_1, t_2, \dots, t_n$

##### Joint Probability Distribution Function (JCDF) $P_{X_1, X_2, \dots, X_n}$

$$P_{X_1, X_2, \dots, X_n} = P\{X_1 \leq x_1 \cap X_2 \leq x_2 \cap \dots \cap X_n \leq x_n\} \quad (\text{A.4})$$

##### Joint Probability Density Function $p_{X_1, X_2, \dots, X_n}$

$$p_{X_1, X_2, \dots, X_n} = \frac{\partial P_{X_1, X_2, \dots, X_n}}{\partial X_1 \partial X_2 \dots \partial X_n} \quad (\text{A.5})$$

## A1.2. Statistical Properties of a Random Process

### First Order Moment (Mean Function)

It is defined as

$$\mu_X(t_i) = E\{X(t_i)\} = \int_{-\infty}^{\infty} X_i p_{X_i}(x_i) dX_i \quad (\text{A.6})$$

where  $E\{\cdot\}$  is the expectation operator.

### Second Order Moment (Autocorrelation Function) $R_{XX}(t_i, t_j)$

$$R_{XX}(t_i, t_j) = E\{X_i X_j\} = \int_{-\infty}^{\infty} \int_{-\infty}^{\infty} X_i X_j p_{X_i X_j}(x_i, x_j) dX_i dX_j \quad (\text{A.7})$$

### Autocovariance function (Second Order Central Moment) $C_{XX}(t_i, t_j)$

$$\begin{aligned} C_{XX}(t_i, t_j) &= E\{[X_i - \mu_i(t_i)][X_j - \mu_j(t_j)]\} \\ &= \int_{-\infty}^{\infty} \int_{-\infty}^{\infty} [X_i - \mu_X(t_i)][X_j - \mu_X(t_j)] p_{X_i X_j} dX_i dX_j \\ &= R_{XX}(t_i, t_j) - \mu_X(t_i)\mu_X(t_j) \end{aligned} \quad (\text{A.8})$$

when  $t_i = t_j = t$ , equation (A.8) reduces to the variance function  $\sigma_{XX}(t)$  given as

$$\sigma_{XX}(t) = R_{XX}(t) - \mu^2(t) \quad (\text{A.9})$$

### A1.3. Statistical Properties of Two Random Processes

In this section the statistical properties of two different random processes  $X$  and  $Y$  and their definitions are summarized

Cross correlation Function  $R_{XY}(t_i t_j)$

$$R_{XY}(t_i t_j) = E\{X_i Y_j\} = \int_{-\infty}^{\infty} \int_{-\infty}^{\infty} X_i Y_j p_{X_i Y_j} dX_i dY_j \quad (\text{A.10})$$

Cross covariance function  $C_{XY}(t_i t_j)$

$$\begin{aligned} C_{XY}(t_i t_j) &= E\{[X_i - \mu_X(t_i)][Y_j - \mu_Y(t_j)]\} \\ &= \int_{-\infty}^{\infty} \int_{-\infty}^{\infty} [X_i - \mu_X(t_i)][Y_j - \mu_Y(t_j)] p_{X_i Y_j} dX_i dY_j \\ &= R_{XY}(t_i t_j) - \mu_X(t_i)\mu_Y(t_j) \end{aligned} \quad (\text{A.11})$$

when  $t_i = t_j = t$ , equation (A.11) reduces to the Covariance function  $C_{XY}(t)$  given as

$$C_{XY}(t) = R_{XY}(t) - \mu_X(t)\mu_Y(t) \quad (\text{A.12})$$

It is noted that in all the above statistical operations, the expectations have been taken across the ensemble of the random processes.

## **A2. Definitions of Nonstationary and Stationary Random Processes**

### Nonstationary Random Process

A random process  $X$  is said to be nonstationary or non-homogenous if all the orders of the probability density function (PDF) vary with time  $t$ .

### Stationary Random Process

A random process  $X$  is said to be stationary or homogenous if all the orders of the probability density function (PDF) are invariant under arbitrary translation of time  $t$ .

### Statistical Properties of Stationary Random Processes

1.  $\mu_X(t) = \mu_X = \text{constant}$
2.  $C_{XX}(tt) = \sigma_{XX}(t) = \text{constant}$
3.  $R_{XX}(t_i t_j) = R_{XX}(t_i - t_j) = R_{XX}(\tau)$
4.  $C_{XY}(t_i t_j) = C_{XY}(t_i - t_j) = C_{XY}(\tau)$

where  $\tau$  is the time lag  $t_i - t_j$ . In practice only very few or a single realization is obtained. To simplify analysis, the concept of weakly stationary random process is usually introduced.

Weakly Stationary or Ergodic Random Process:

This is a special case of a stationary random process in which the statistical properties of the ensemble are the same as those taken over a single realization. Figure A.4 summarizes the various types of excitations or processes that a system can experience.

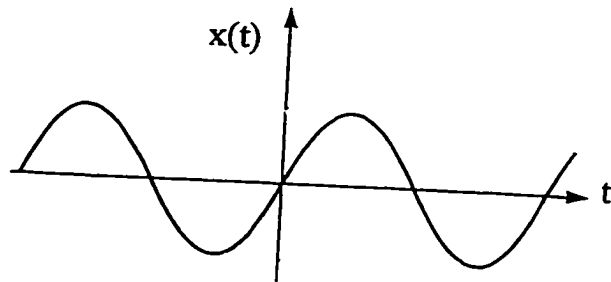


Figure A.1. Sample of A Deterministic Process



Figure A.2 Realization of a Random Process



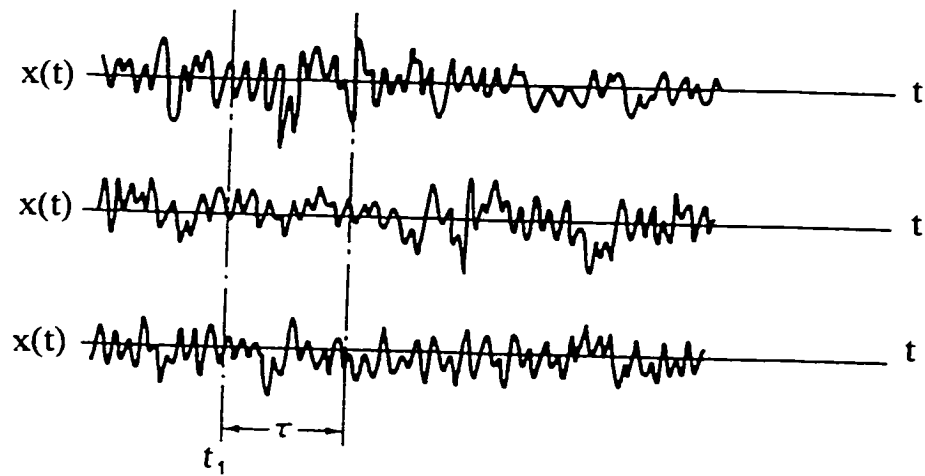


Figure A.3 Records of Realization of a Random Process

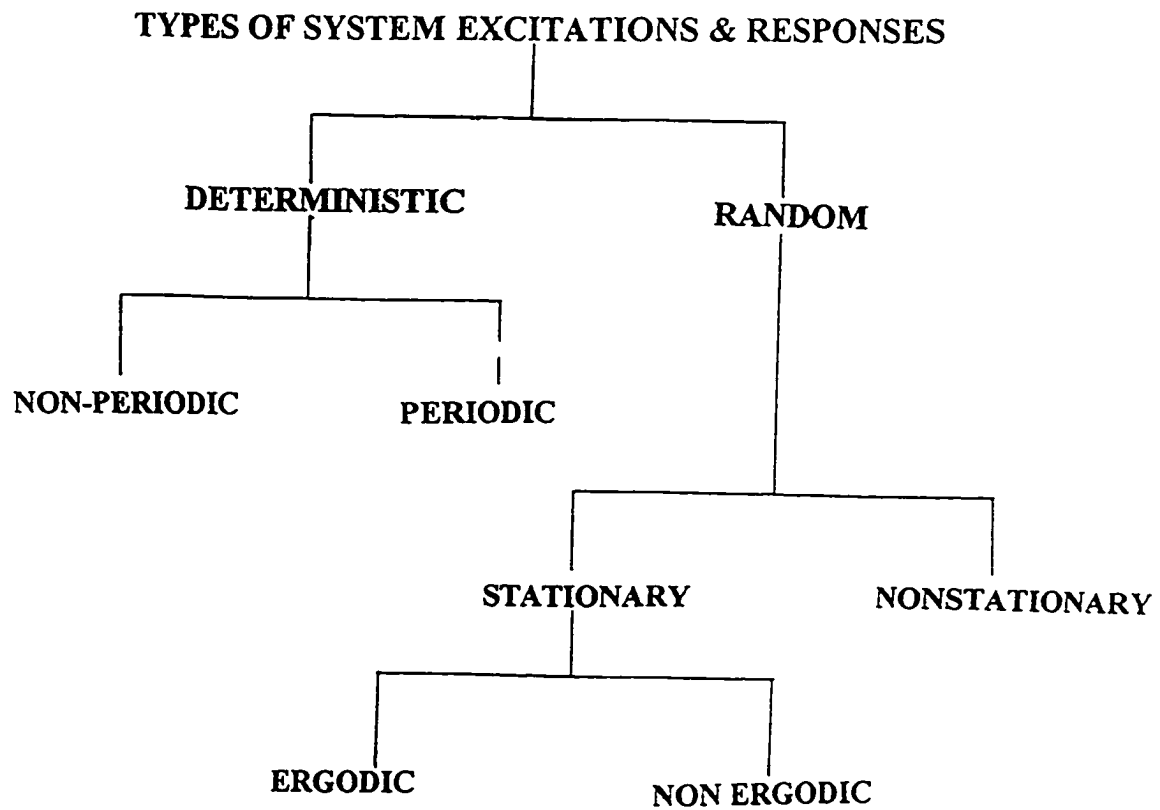


Figure A.4 Classifications of Processes

## Appendix B

### LONG DERIVATIONS OF EQUATIONS OF MOTION

#### B1. Introduction

To simplify the expression derived in this appendix, all second and higher order terms in the elements of the equation of motion involving the small joint motion  $q_i$ , or  $\dot{q}_i$   $i = 1, 2, \dots, n$  are neglected since their values are very small. Also for the small coordinate  $q_i$  the following approximate relations have been implicitly used in the derivations

$$\cos(q_i + q_{i+1}) = 1, \quad \sin(q_i + q_{i+1}) \approx q_i + q_{i+1} \quad (\text{B.1})$$

$$\cos(\Theta_i + q_i + \Theta_{i+1} + q_{i+1}) = \cos(\Theta_i + \Theta_{i+1}) - (q_i + q_{i+1})\sin(\Theta_i + \Theta_{i+1}) \quad (\text{B.2})$$

$$\sin(\Theta_i + q_i + \Theta_{i+1} + q_{i+1}) = \sin(\Theta_i + \Theta_{i+1}) + (q_i + q_{i+1})\cos(\Theta_i) \quad (\text{B.3})$$

It is noted that equations (B.1) to (B.3) apply for any  $i = 1, 2, \dots, n$  and the number of terms  $n$  can be reduced or increased.

#### B2. Two Link Non-Wheeled Mobile Manipulator

The Lagrangian and the Rayleigh dissipation function for the two-link non-wheeled mobile manipulator are given in equations (4.24) and (4.31)

respectively. The derivative of the Lagrangian function with respect to the time derivative of base velocity  $\dot{q}_y$  is

$$\frac{\partial L}{\partial \dot{q}_y} = a_0 \dot{q}_y + a_4 \dot{q}_1 \cos(\Theta_1) + a_5 (\dot{q}_1 + \dot{q}_2) \cos(\Theta_1 + \Theta_2) \quad (\text{B.4})$$

$$\frac{d}{dt} \left( \frac{\partial L}{\partial \dot{q}_y} \right) = a_0 \ddot{q}_y + a_4 \ddot{q}_1 \cos(\Theta_1) + a_5 (\ddot{q}_1 + \ddot{q}_2) \cos(\Theta_1 + \Theta_2) \quad (\text{B.5})$$

Consideration of the joint motion coordinate  $q_1$  leads to

$$\begin{aligned} \frac{\partial L}{\partial \dot{q}_1} = & a_1 \dot{q}_1 + a_2 (\dot{q}_1 + \dot{q}_2) + a_3 (\dot{q}_1 + \dot{q}_2) \cos(\Theta_2) + a_3 \dot{q}_1 \cos(\Theta_2) \\ & + a_4 \dot{q}_y \cos(\Theta_1) + a_5 \dot{q}_y \cos(\Theta_1 + \Theta_2) \end{aligned} \quad (\text{B.6})$$

$$\begin{aligned} \frac{d}{dt} \left( \frac{\partial L}{\partial \dot{q}_1} \right) = & a_1 \ddot{q}_1 + a_2 (\ddot{q}_1 + \ddot{q}_2) + a_3 (\ddot{q}_1 + \ddot{q}_2) \cos(\Theta_2) + a_3 \ddot{q}_1 \cos(\Theta_2) \\ & + a_4 \ddot{q}_y \cos(\Theta_1) + a_5 \ddot{q}_y \cos(\Theta_1 + \Theta_2) \end{aligned} \quad (\text{B.7})$$

$$\frac{\partial L}{\partial q_1} = -k_1 q_1 \quad (\text{B.8})$$

$$\frac{\partial R}{\partial \dot{q}_1} = -c_1 \dot{q}_1 \quad (\text{B.9})$$

Similarly for the joint motion coordinate  $q_2$  we have

$$\frac{d}{dt} \left( \frac{\partial L}{\partial \dot{q}_2} \right) = a_2 (\ddot{q}_1 + \ddot{q}_2) + a_3 \ddot{q}_1 \cos(\Theta_2) + a_5 \ddot{q}_y \cos(\Theta_1 + \Theta_2) \quad (\text{B.10})$$

$$\frac{\partial L}{\partial q_1} = -k_2 q_2 \quad (\text{B.11})$$

$$\frac{\partial R}{\partial \dot{q}_2} = -c_2 \dot{q}_2 \quad (\text{B.12})$$

Since the base motion  $q_1$  is known (see equations 4.4 and 4.7) then equations (B.5) is not required. Assembling of equations (B.7) to (B.12) in matrix-vector form gives the system's equation of motion (equation (3.7)).

### B3. Two-Link Wheeled Mobile Manipulator

The Kinetic Energy and the Rayleigh dissipation function for the two-link wheeled mobile manipulator are given in equations (6.1) and (6.9) respectively. The Lagrangian for the system can be found using equations (2.3), (6.1) and (6.8). The derivative of the Lagrangian function with respect to the motion  $\dot{q}_x$  is

$$\frac{\partial L}{\partial \dot{q}_x} = a_1 \dot{q}_x - a_5 \dot{q}_2 \sin(\Theta_2) - a_6 (\dot{q}_2 + \dot{q}_3) \sin(\Theta_2 + \Theta_3) \quad (\text{B.13})$$

$$\frac{d}{dt} \left( \frac{\partial L}{\partial \dot{q}_x} \right) = a_1 \ddot{q}_x - a_5 \ddot{q}_2 \sin(\Theta_2) - a_6 (\ddot{q}_2 + \ddot{q}_3) \sin(\Theta_2 + \Theta_3) \quad (\text{B.14})$$

Considering the vehicle motion coordinate  $q_1$

$$\frac{d}{dt}\left(\frac{\partial L}{\partial \dot{q}_1}\right) = a_1 \ddot{q}_1 + a_5 \ddot{q}_2 \cos(\Theta_2) + a_6 (\ddot{q}_2 + \ddot{q}_3) \cos(\Theta_2 + \Theta_3) \quad (\text{B.15})$$

$$\frac{\partial L}{\partial q_1} = -k_1 q_1 + k_1 q_y \quad (\text{B.16})$$

$$\frac{\partial R}{\partial \dot{q}_1} = -c_1 \dot{q}_1 + c_1 \dot{q}_y \quad (\text{B.17})$$

Considering the manipulator joint coordinate  $q_2$

$$\begin{aligned} \frac{d}{dt}\left(\frac{\partial L}{\partial \dot{q}_2}\right) &= a_2 \ddot{q}_2 + a_3 (\ddot{q}_2 + \ddot{q}_3) + a_4 (\ddot{q}_2 + \ddot{q}_3) \cos(\Theta_3) + a_4 \ddot{q}_2 \cos(\Theta_3) \\ &\quad + a_5 \ddot{q}_1 \cos(\Theta_2) + a_6 \ddot{q}_1 \cos(\Theta_2 + \Theta_3) \\ &\quad - a_5 \ddot{q}_x \sin(\Theta_2) - a_6 \ddot{q}_x \sin(\Theta_2 + \Theta_3) \end{aligned} \quad (\text{B.18})$$

$$\frac{\partial L}{\partial q_2} = -k_2 q_2 \quad (\text{B.19})$$

$$\frac{\partial R}{\partial \dot{q}_2} = -c_2 \dot{q}_2 \quad (\text{B.20})$$

Considering the manipulator joint coordinate  $q_3$

$$\begin{aligned} \frac{d}{dt}\left(\frac{\partial L}{\partial \dot{q}_3}\right) &= a_3 (\ddot{q}_2 + \ddot{q}_3) + a_4 \ddot{q}_2 \cos(\Theta_3) + a_6 \ddot{q}_1 \cos(\Theta_2 + \Theta_3) \\ &\quad - a_6 \ddot{s} \sin(\Theta_2 + \Theta_3) \end{aligned} \quad (\text{B.21})$$

$$\frac{\partial L}{\partial q_3} = -k_3 q_3 \quad (\text{B.22})$$

$$\frac{\partial R}{\partial \dot{q}_3} = -c_3 \dot{q}_3 \quad (\text{B.23})$$

Since the base motion  $q_x$  is known then equations (B14) can be ignored. Assembling of equations (B.15) to (B.23) in matrix-vector form gives the system's equation of motion (equation (5.1)).

#### B4. Two-Link Two-Wheeled Mobile Manipulator

The Lagrangian and the Rayleigh dissipation function for the two-link manipulator on a two-wheel mobile base are given in equations 8.1 and 8.8 respectively. The derivative of the Lagrangian function with respect to the time derivative of vehicle motion  $\dot{q}_x$  is

$$\frac{\partial L}{\partial \dot{q}_x} = a_1 \dot{q}_x - a_6 (\dot{q}_{1P} + \dot{q}_2) \sin(\Theta_2) - a_6 (\dot{q}_{1P} + \dot{q}_2 + \dot{q}_3) \sin(\Theta_2 + \Theta_3) \quad (\text{B.24})$$

$$\frac{d}{dt} \left( \frac{\partial L}{\partial \dot{q}_x} \right) = a_1 \ddot{q}_x - a_6 (\ddot{q}_{1P} + \ddot{q}_2) \sin(\Theta_2) - a_6 (\ddot{q}_{1P} + \ddot{q}_2 + \ddot{q}_3) \sin(\Theta_2 + \Theta_3) \quad (\text{B.25})$$

Considering the vehicle motion coordinate  $q_1$

$$\frac{d}{dt} \left( \frac{\partial L}{\partial \dot{q}_{1H}} \right) = a_1 \ddot{q}_{1H} + a_5 (\ddot{q}_{1P} + \ddot{q}_2) \cos(\Theta_2) + a_6 (\ddot{q}_{1P} + \ddot{q}_2 + \ddot{q}_3) \cos(\Theta_2 + \Theta_3)$$

(B.26)

$$\frac{\partial L}{\partial q_1} = -k_1 (q_{1H} - q_{y1} - l_1 q_{1P}) - k_2 (q_{1H} - q_{y2} + l_2 q_{1P}) \quad (\text{B.27})$$

$$\frac{\partial R}{\partial \dot{q}_1} = -c_1 (\dot{q}_1 - \dot{q}_{y1} - l_1 \dot{q}_{1P}) - c_2 (\dot{q}_1 - \dot{q}_{y1} + l_2 \dot{q}_{1P}) \quad (\text{B.28})$$

Considering the vehicle motion coordinate  $q_{1P}$

$$\begin{aligned} \frac{d}{dt} \left( \frac{\partial L}{\partial \dot{q}_{1P}} \right) &= I_2 \ddot{q}_{1P} + a_2 (\ddot{q}_{1P} + \ddot{q}_2) + a_3 (\ddot{q}_{1P} + \ddot{q}_2 + \ddot{q}_3) + a_4 (\ddot{q}_{1P} + \ddot{q}_2) \cos(\Theta_3) \\ &+ a_4 (\ddot{q}_{1P} + \ddot{q}_2 + \ddot{q}_3) \cos(\Theta_3) + a_5 \ddot{q}_{1H} \cos(\Theta_2) + a_6 \ddot{q}_{1H} \cos(\Theta_2 + \Theta_3) \\ &- a_5 \ddot{q}_x \sin(\Theta_2) - a_6 \ddot{q}_x \sin(\Theta_2 + \Theta_3) \end{aligned} \quad (\text{B.29})$$

$$\frac{\partial L}{\partial q_{1P}} = l_1 k_1 (q_{1H} - q_{y1} - l_1 q_{1P}) - k_2 l_2 (q_{1H} - q_{y2} + l_2 q_{1P}) \quad (\text{B.30})$$

$$\frac{\partial R}{\partial \dot{q}_{1P}} = l_1 c_1 (\dot{q}_{1H} - \dot{q}_{y1} - l_1 \dot{q}_{1P}) - l_2 c_2 (\dot{q}_{1H} - \dot{q}_{y1} + l_2 \dot{q}_{1P}) \quad (\text{B.31})$$

Considering the manipulator joint coordinate  $q_2$

$$\frac{d}{dt} \left( \frac{\partial L}{\partial \dot{q}_2} \right) = a_2 (\ddot{q}_{1P} + \ddot{q}_2) + a_3 (\ddot{q}_{1P} + \ddot{q}_2 + \ddot{q}_3) + a_4 (\ddot{q}_{1P} + \ddot{q}_2) \cos(\Theta_3)$$



$$\begin{aligned}
& + a_4(\ddot{q}_{1P} + \ddot{q}_2 + \ddot{q}_3)\cos(\Theta_3) + a_5 \ddot{q}_{1H} \cos(\Theta_2) + a_6 \ddot{q}_{1H} \cos(\Theta_2 + \Theta_3) \\
& - a_5 \ddot{q}_x \sin(\Theta_2) - a_6 \ddot{q}_x \sin(\Theta_2 + \Theta_3)
\end{aligned} \tag{B.32}$$

$$\frac{\partial L}{\partial q_2} = -k_3 q_2 \tag{B.33}$$

$$\frac{\partial R}{\partial \dot{q}_2} = -c_3 \dot{q}_2 \tag{B.34}$$

Considering the manipulator joint coordinate  $q_3$

$$\begin{aligned}
\frac{d}{dt}\left(\frac{\partial L}{\partial \dot{q}_3}\right) &= a_3(\ddot{q}_{1P} + \ddot{q}_2 + \ddot{q}_3) + a_4(\ddot{q}_{1P} + \ddot{q}_2)\cos(\Theta_3) \\
& + a_6 \ddot{q}_{1H} \cos(\Theta_2 + \Theta_3) - a_6 \ddot{q}_x \sin(\Theta_2 + \Theta_3)
\end{aligned} \tag{B.35}$$

$$\frac{\partial L}{\partial q_3} = -k_4 q_3 \tag{B.36}$$

$$\frac{\partial R}{\partial \dot{q}_3} = -c_4 \dot{q}_3 \tag{B.37}$$

Since the vehicle motion  $q_x$  is known then equations (B.25) can be ignored. Assembling the elements of equations (B.26) to (B.37) in a vector matrix form leads to equation (7.1).

## Appendix C

### DERIVATION OF ROTATION AND JACOBIAN MATRICES

#### C1. Introduction

In this appendix, elements of the Rotation matrices and the manipulator Jacobians used in computing the tip responses in the various coordinate systems are derived using the Denavit Hartenburg Homogenous transformation. The approach employed for flexible manipulators is similar to that used in Mackerrow (1991). and Spong and Vidyasagar (1989) for rigid manipulators.

#### C2. Non-Wheeled Mobile Manipulator

##### C2.1 Single-link Manipulator

The homogenous transformation matrix  $T_0^1$  of the manipulator is given as

$$T_0^1 = \begin{bmatrix} \mathbf{Rot}_0^1 & \mathbf{d}_0^1 \\ \mathbf{0} & 1 \end{bmatrix} \quad (C.1)$$

$$\mathbf{Rot}_0^1 = \begin{bmatrix} \cos(\Theta_1 + q_1) & -\sin(\Theta_1 + q_1) & 0 \\ \sin(\Theta_1 + q_1) & \cos(\Theta_1 + q_1) & 0 \\ 0 & 0 & 1 \end{bmatrix} \quad (C.2)$$

$$\mathbf{d}_0^1 = \begin{bmatrix} l_1 \cos(\Theta_1 + q_1) \\ l_1 \sin(\Theta_1 + q_1) \\ 0 \end{bmatrix} \quad (\text{C.3})$$

The matrix  $\mathbf{Rot}_0^1$  is the rotation matrix of the manipulator tip with respect to the base frame, while the vector  $\mathbf{d}_0^1$  is the position vector of the manipulator tip with respect to the base frame. Note that  $q_1 = \Delta\Theta_1$  and only small motion  $\mathbf{q} = \Delta\Theta_1$  has taken place at the joint.

### C2.1.1 Jacobian Matrix in the Base Frame

The manipulator Jacobian matrix  $\mathbf{J}_0$  with respect to the base frame can be obtained using equation (2.14) as

$$\dot{\mathbf{d}}_0^1 = \mathbf{J}_0 \dot{\mathbf{q}} \quad (\text{C.4})$$

$$\mathbf{J}_0 = \frac{\partial \mathbf{d}_0^1}{\partial \mathbf{q}} = \frac{\partial \mathbf{d}_0^1}{\partial q_1} \quad (\text{C.5})$$

$$\mathbf{J}_0 = \begin{bmatrix} J_{11} \\ J_{21} \end{bmatrix} \quad (\text{C.6})$$

$$J_{11} = -l_1 \sin(\Theta_1 + q_1) \quad (\text{C.7})$$

$$J_{21} = l_1 \cos(\Theta_1 + q_1) \quad (\text{C.8})$$

Since the joint motion  $q_1$  is small then

$$\Theta_1 + q_1 \approx \Theta_1 \quad (\text{C.9})$$

Application of equation (C.9) to equations (C.7) and (C.8) lead to equation (4.13). It is now shown that the Jacobian matrix  $J_0$  can also be applied to small displacement of the tip. Multiplication of equation (C.4) by a small change in time  $\Delta t$  leads to

$$\dot{\mathbf{d}}_0^1 \Delta t = \mathbf{J}_0 \dot{\mathbf{q}} \Delta t \quad (\text{C.10})$$

Equation (C.10) can be written as

$$\Delta \mathbf{d}_0^1 = \mathbf{J}_0 \mathbf{q} \quad (\text{C.11})$$

where  $\Delta \mathbf{d}_0^1$  is the small displacement of the position of the manipulator tip as seen in the base frame due to a small displacement at the joint  $\mathbf{q}$ . In particular, in this report the vector  $\Delta \mathbf{d}_0^1$  is denoted by  $\mathbf{x}_0$ . It is noted that the vector  $\mathbf{x}_0$  represents a change in the position vector of the manipulator tip as seen in the base frame due to the small displacement of the joint  $\mathbf{q}$ .

### C2.1.2 Transformation of Jacobian Matrix Between Cartesian Frames

Equation (C.4) gives the relationship between the manipulator tip velocity as seen in the base frame  $\dot{\mathbf{d}}_0^1$  and the manipulator joint motion velocity  $\dot{\mathbf{q}}$ . The rotation of the tip cartesian frame as seen in the base cartesian frame is given by equation (C.2). Since velocity is a free vector (vectors which can be positioned anywhere in space without loss or change of meaning provided the magnitude and direction are

preserved i.e. the action of a free vector is not confined to a unique line). it can be transformed from one cartesian frame to another, by premultiplication with a rotation matrix. This is because the relative locations of the origins of the two cartesian frames is not important with a free vector (Mackerrow, 1990). Application of this property to (C.4) give the velocity of the manipulator tip motion in the  $i$ -th cartesian frame as

$$\mathbf{Rot}_0^i \dot{\mathbf{d}}_0^1 = \dot{\mathbf{d}}_i^1 = \mathbf{Rot}_0^i \mathbf{J}_0 \dot{\mathbf{q}} = \mathbf{J}_i \dot{\mathbf{q}} \quad (\text{C.12})$$

Comparison of the coefficients in equation (C.12) gives

$$\mathbf{J}_i = \mathbf{Rot}_0^i \mathbf{J}_0 \quad (\text{C.13})$$

where  $\mathbf{J}_i$  is defined as the manipulator Jacobian matrix in the  $i$ -th Cartesian frame. Similar reasoning can be applied to compute the small change in displacement  $\Delta \mathbf{d}_0^1$  in the  $i$ th Cartesian frame..

## C2.2. Two-Link Manipulator

The homogenous transformation matrix  $\mathbf{T}_0^2$  of the manipulator is given as

$$\mathbf{T}_0^2 = \begin{bmatrix} \mathbf{Rot}_0^2 & \mathbf{d}_0^2 \\ \mathbf{0} & 1 \end{bmatrix} \quad (\text{C.14})$$

$$\mathbf{Rot}_0^2 = \begin{bmatrix} \cos(\Theta_1 + \Theta_2 + q_1 + q_2) & -\sin(\Theta_1 + \Theta_2 + q_1 + q_2) & 0 \\ \sin(\Theta_1 + \Theta_2 + q_1 + q_2) & \cos(\Theta_1 + \Theta_2 + q_1 + q_2) & 0 \\ 0 & 0 & 1 \end{bmatrix} \quad (\text{C.15})$$

$$\mathbf{d}_0^2 = \begin{bmatrix} l_1 \cos(\Theta_1 + q_1) + l_2 \cos(\Theta_1 + \Theta_2 + q_1 + q_2) \\ l_1 \sin(\Theta_1 + q_1) + l_2 \sin(\Theta_1 + \Theta_2 + q_1 + q_2) \\ 0 \end{bmatrix} \quad (\text{C.16})$$

The matrix  $\mathbf{Rot}_0^2$  is the rotation matrix of the manipulator tip with respect to the Cartesian base frame, while the vector  $\mathbf{d}_0^2$  is the position vector of the manipulator tip with respect to the base frame. Note that  $q_1 = \Delta\Theta_1$  and  $q_2 = \Delta\Theta_2$  and only small motion  $\mathbf{q} = [\Delta\Theta_1, \Delta\Theta_2]^T = [q_1, q_2]^T$  has taken place at the joint.

### C2.2.1 Jacobian Matrix in the Base Frame

The manipulator Jacobian matrix  $\mathbf{J}_0$  with respect to the base frame can be obtained using equation (2.14) as

$$\dot{\mathbf{d}}_0^2 = \mathbf{J}_0 \dot{\mathbf{q}} \quad (\text{C.17})$$

$$\mathbf{J}_0 = \frac{\partial \mathbf{d}_0^2}{\partial \mathbf{q}} \quad (\text{C.18})$$

$$\mathbf{J}_0 = \begin{bmatrix} J_{11} & J_{12} \\ J_{21} & J_{22} \end{bmatrix} \quad (\text{C.19})$$

$$J_{11} = -l_1 \sin(\Theta_1 + q_1) - l_2 \sin(\Theta_1 + q_1 + \Theta_2 + q_2) \quad (\text{C.20})$$

$$J_{12} = -l_2 \sin(\Theta_1 + q_1 + \Theta_2 + q_2) \quad (\text{C.21})$$

$$J_{21} = l_1 \cos(\Theta_1 + q_1) + l_2 \cos(\Theta_1 + q_1 + \Theta_2 + q_2) \quad (\text{C.22})$$

$$J_{22} = l_2 \cos(\Theta_1 + q_1 + \Theta_2 + q_2) \quad (\text{C.23})$$

Since the joints motion  $q_1$  and  $q_2$  are very small motion , then

$$\Theta_1 + q_1 \approx \Theta_1 \quad \Theta_2 + q_2 \approx \Theta_2 \quad (\text{C.24})$$

Application of equation (C.24) to equations (C.23), (C.22), (C.21) and (C.20) lead to equations (4.49), (4.50), (4.51) and (4.52). Using the reasoning advanced in Section C2.1 and multiplication of equation (C.17) by a small change in time  $\Delta t$ , leads to

$$\dot{\mathbf{d}}_0^2 \Delta t = \mathbf{J}_0 \dot{\mathbf{q}} \Delta t = \Delta \mathbf{d}_0^2 = \mathbf{J}_0 \mathbf{q} \quad (\text{C.25})$$

where  $\Delta \mathbf{d}_0^2$  is the small displacement of the position of the manipulator tip in the base frame due to a small displacement at the joint  $\mathbf{q}$ .

### C3. Wheeled Mobile Manipulator

#### C3.1 Two-Link Manipulator

The homogenous transformation matrix  $\mathbf{T}_0^3$  of the manipulator is given as

$$\mathbf{T}_0^3 = \begin{bmatrix} \mathbf{Rot}_0^3 & \mathbf{d}_0^3 \\ \mathbf{0} & 1 \end{bmatrix} \quad (\text{C.26})$$

$$\mathbf{Rot}_0^3 = \begin{bmatrix} \cos(\Theta_2 + \Theta_3 + q_2 + q_3) & -\sin(\Theta_2 + \Theta_3 + q_2 + q_3) & 0 \\ \sin(\Theta_2 + \Theta_3 + q_2 + q_3) & \cos(\Theta_2 + \Theta_3 + q_2 + q_3) & 0 \\ 0 & 0 & 1 \end{bmatrix} \quad (\text{C.27})$$

$$\mathbf{d}_0^3 = \begin{bmatrix} l_2 \cos(\Theta_2 + q_2) + l_3 \cos(\Theta_2 + \Theta_3 + q_2 + q_3) \\ q_1 + l_2 \sin(\Theta_2 + q_2) + l_3 \sin(\Theta_2 + \Theta_3 + q_2 + q_3) \\ 0 \end{bmatrix} \quad (\text{C.28})$$

The matrix  $\mathbf{Rot}_0^3$  is the rotation matrix of the manipulator tip with respect to the vehicle frame (which is moving in the horizontal direction), while the vector  $\mathbf{d}_0^3$  is the position vector of the manipulator tip with respect to the vehicle frame  $\mathbf{d}_0^3$ . Note that  $q_1 = \Delta\Theta_1$ ,  $q_2 = \Delta\Theta_2$  and  $q_3 = \Delta\Theta_3$  and only small motion  $\mathbf{q} = [\Delta\Theta_1, \Delta\Theta_2, \Delta\Theta_3]^T = [q_1, q_2, q_3]^T$  has taken place at the joint.



### C3.1.1 Jacobian Matrix in the Vehicle Frame

The manipulator Jacobian matrix  $\mathbf{J}_0$  with respect to the base frame can be obtained using equation (2.14) as

$$\dot{\mathbf{d}}_0^3 = \mathbf{J}_0 \dot{\mathbf{q}} \quad (\text{C.29})$$

$$\mathbf{J}_0 = \frac{\partial \mathbf{d}_0^3}{\partial \mathbf{q}} \quad (\text{C.30})$$

$$\mathbf{J}_0 = \begin{bmatrix} J_{11} & J_{12} & J_{13} \\ J_{21} & J_{22} & J_{23} \end{bmatrix} \quad (\text{C.31})$$

$$J_{11} = 0 \quad (\text{C.32})$$

$$J_{12} = -l_2 \sin(\Theta_2 + q_2) - l_3 \sin(\Theta_2 + q_2 + \Theta_3 + q_3) \quad (\text{C.33})$$

$$J_{13} = -l_3 \sin(\Theta_2 + q_2 + \Theta_3 + q_3) \quad (\text{C.34})$$

$$J_{21} = 1 \quad (\text{C.35})$$

$$J_{22} = l_2 \cos(\Theta_2 + q_2) + l_3 \cos(\Theta_2 + q_2 + \Theta_3 + q_3) \quad (\text{C.36})$$

$$J_{23} = l_3 \cos(\Theta_2 + q_2 + \Theta_3 + q_3) \quad (\text{C.37})$$

Since  $q_1$ ,  $q_2$  and  $q_3$  are very small motion , then

$$\Theta_2 + q_2 \approx \Theta_2 \quad \Theta_3 + q_3 \approx \Theta_3 \quad (\text{C.38})$$

Application of equation (C.39) to equations (C.38), (C.37), (C.36), (C.35), (C.34) and (C.33) lead to equations (6.43), (6.44), (6.45), (6.46), (6.47) and (6.48). Further

$$\dot{\mathbf{d}}_0^3 \Delta t = \mathbf{J}_0 \dot{\mathbf{q}} \Delta t = \Delta \mathbf{d}_0^3 = \mathbf{J}_0 \mathbf{q} \quad (\text{C.39})$$

where  $\Delta \mathbf{d}_0^3$  is the small displacement of the position of the manipulator tip in the vehicle due to a small displacement at the joint.

## C4. Two-Wheeled Mobile Manipulator

### C4.1 Two-Link Manipulator

The homogenous transformation matrix  $\mathbf{T}_0^3$  of the manipulator is given as

$$\mathbf{T}_0^3 = \begin{bmatrix} \mathbf{Rot}_0^3 & \mathbf{d}_0^3 \\ \mathbf{0} & 1 \end{bmatrix} \quad (\text{C.40})$$

$$\mathbf{Rot}_0^3 = \begin{bmatrix} \cos(\Theta_2 + \Theta_3 + q_{1P} + q_2 + q_3) & -\sin(\Theta_2 + \Theta_3 + q_{1P} + q_2 + q_3) & 0 \\ \sin(\Theta_2 + \Theta_3 + q_{1P} + q_2 + q_3) & \cos(\Theta_2 + \Theta_3 + q_{1P} + q_2 + q_3) & 0 \\ 0 & 0 & 1 \end{bmatrix} \quad (\text{C.41})$$

$$\mathbf{d}_0^3 = \begin{bmatrix} l_3 \cos(\Theta_2 + q_{1P} + q_2) + l_4 \cos(\Theta_2 + \Theta_3 + q_{1P} + q_2 + q_3) \\ q_{1H} + l_3 \sin(\Theta_2 + q_{1P} + q_2) + l_4 \sin(\Theta_2 + \Theta_3 + q_{1P} + q_2 + q_3) \\ 0 \end{bmatrix} \quad (\text{C.42})$$

The matrix  $\mathbf{Rot}_0^3$  is the rotation matrix of the manipulator tip motion with respect to the vehicle frame (which is moving in the horizontal direction), while the vector  $\mathbf{d}_0^3$  is the position vector of the manipulator tip with respect to the vehicle frame  $\mathbf{d}_0^3$ . Note  $q_{1H} = \Delta\Theta_1$ ,  $q_{1P} = \Delta\Theta_2$ ,  $q_2 = \Delta\Theta_2$  and  $q_3 = \Delta\Theta_3$  and only small motion  $\mathbf{q} = [\Delta\Theta_1, \Delta\Theta_2, \Delta\Theta_2, \Delta\Theta_3]^T = [q_{1H}, q_{1P}, q_2, q_3]^T$  has taken place at the joint.

#### C4.1.1 Jacobian Matrix in the Vehicle Frame

The manipulator Jacobian matrix  $\mathbf{J}_0$  with respect to the base frame can be obtained using equation (2.14) as

$$\dot{\mathbf{d}}_0^3 = \mathbf{J}_0 \dot{\mathbf{q}} \quad (\text{C.43})$$

$$\mathbf{J}_0 = \frac{\partial \mathbf{d}_0^3}{\partial \mathbf{q}} \quad (\text{C.44})$$

$$\mathbf{J}_0 = \begin{bmatrix} J_{11} & J_{12} & J_{13} & J_{14} \\ J_{21} & J_{22} & J_{23} & J_{24} \end{bmatrix} \quad (\text{C.45})$$

$$J_{11} = 0 \quad (\text{C.46})$$

$$J_{12} = -l_3 \sin(\Theta_2 + q_2 + q_{1P}) - l_4 \sin(\Theta_2 + q_{1P} + q_2 + \Theta_3 + q_3) \quad (\text{C.47})$$

$$J_{13} = -l_3 \sin(\Theta_2 + q_2 + q_{1P}) - l_4 \sin(\Theta_2 + q_{1P} + q_2 + \Theta_3 + q_3) \quad (\text{C.48})$$

$$J_{14} = -l_4 \sin(\Theta_2 + q_{1P} + q_2 + \Theta_3 + q_3) \quad (\text{C.49})$$

$$J_{21} = 1 \quad (\text{C.50})$$

$$J_{22} = l_3 \cos(\Theta_2 + q_2 + q_{1P}) + l_4 \cos(\Theta_2 + q_{1P} + q_2 + \Theta_3 + q_3) \quad (\text{C.51})$$

$$J_{23} = l_3 \cos(\Theta_2 + q_2 + q_{1P}) + l_4 \cos(\Theta_2 + q_{1P} + q_2 + \Theta_3 + q_3) \quad (\text{C.52})$$

$$J_{24} = l_4 \cos(\Theta_2 + q_{1P} + q_2 + \Theta_3 + q_3) \quad (\text{C.53})$$

Since  $q_{1P}$ ,  $q_2$ , and  $q_3$  are very small motion, then

$$\Theta_2 + q_{1P} + q_2 \approx \Theta_2 \quad \Theta_3 + q_3 \approx \Theta_3 \quad (\text{C.54})$$

Application of equation (C.58) to equations (C.57), (C.56), (C.55), (C.54), (C.53), (C.52), (C51), and (C50) lead to equations (8.80), (8.81), (8.82), (8.83), (8.84), (8.85), (8.86), (8.87). Further

$$\dot{\mathbf{d}}_0^3 \Delta t = \mathbf{J}_0 \dot{\mathbf{q}} \Delta t = \Delta \mathbf{d}_0^3 = \mathbf{J}_0 \mathbf{q} \quad (\text{C.55})$$

where  $\Delta \mathbf{d}_0^3$  is the small displacement of the position of the manipulator tip in the vehicle due to a small displacement at the joint.

## Appendix D

### CONTOUR INTEGRALS USED FOR THE STATIONARY RESPONSES

#### D1. Introduction

To compute the elements of the covariance tensors of the joint displacements and velocities for the stationary random responses of the non-wheeled and the wheeled mobile manipulators (see Sections 3.41 and 5.5.2.2) a number of complex contour integration associated with the different modes of vibrations of the manipulator have to be carried out. It is only after this has been done that appropriate transformations can be applied to obtain the joint and tip responses (Section 3.5). In the following discussions expressions for the covariances of the modal responses associated with the random function used in the illustrative examples of chapters four and six are derived. For simplicity of presentation the same notations are used to denote the modes of vibration of non-wheeled and wheeled mobile manipulators. For clarity of presentation some of the common notations used are stated upfront.

#### D1.1 Common Notations

- $\omega$  natural frequency term
- $\omega_r$  natural frequency of mode  $r$
- $i = \sqrt{-1}$
- $\xi_r$  damping factor of mode  $r$
- $Res(.)$  residue of .

$Re(.)$  real part of .

Other symbols and expressions are defined as they are encountered or at the end of the appendix.

## D2. Non-Wheeled Mobile Manipulator

### D2.1 Covariance of Modal Responses

The power spectrum representation of the excitation used is given in equation (4.4). Equation (4.4) can be normalized by the intensity of the white noise  $S_{0y}$ . To compute the modal responses the integral of the term  $H_r H_k^*$  given in equation (3.35) for modes  $r$  and  $k$  have to be evaluated since it appears implicitly in equation (3.36). The two integrals in equation (3.36) are  $\int_{-\infty}^{\infty} H_r H_r^* d\omega$  and  $\int_{-\infty}^{\infty} H_r H_k^* d\omega$ .

Further, for the velocity responses (equation 3.37) the two integrals which have to be evaluated are  $\int_{-\infty}^{\infty} \omega^2 H_r H_r^* d\omega$  and  $\int_{-\infty}^{\infty} \omega^2 H_r H_k^* d\omega$ .

$$\text{Evaluation of } \int_{-\infty}^{\infty} H_r H_r^* d\omega = \int_{-\infty}^{\infty} F_1(\omega) d\omega$$

where

$$F_1(\omega) = \frac{1}{(\omega_r^2 - \omega^2)^2 + (2\xi_r \omega_r \omega)^2} \quad (\text{D.1})$$

Using the residue theorem to evaluate the integral leads to

$$\int_{-\infty}^{\infty} F_1(\omega) d\omega = 2\pi i \sum \text{Res}(F_1(\omega)) \quad (\text{D.2})$$

The function  $F_1(\omega)$  has 4 poles but only two of them lie in the region of integration. These are

$$\omega_{r1} = (\sqrt{1-\xi_r^2} + i\xi_r)\omega_r \quad (D.3)$$

$$\omega_{r2} = (-\sqrt{1-\xi_r^2} + i\xi_r)\omega_r \quad (D.4)$$

$$\begin{aligned} Res(\omega_{r1}) &= \lim_{\omega \rightarrow \omega_{r1}} \{(\omega - \omega_{r1})F_1(\omega)\} \\ &= \frac{1}{8i\xi_r\omega_r^3 \sqrt{1-\xi_r^2} (\sqrt{1-\xi_r^2} + i\xi_r)} \end{aligned} \quad (D.5)$$

$$\begin{aligned} Res(\omega_{r2}) &= \lim_{\omega \rightarrow \omega_{r2}} \{(\omega - \omega_{r2})F_1(\omega)\} \\ &= \frac{1}{8i\xi_r\omega_r^3 \sqrt{1-\xi_r^2} (\sqrt{1-\xi_r^2} - i\xi_r)} \end{aligned} \quad (D.6)$$

Application of equations (D.5) and (D.6) in (D.2) gives

$$\int_{-\infty}^{\infty} F_1(\omega) d\omega = \int_{-\infty}^{\infty} H_r H_r^* d\omega = \frac{\pi}{2\xi_r\omega_r^3} \quad (D.7)$$

Evaluation of  $\int_{-\infty}^{\infty} H_r H_k^* d\omega$

Using the residue theorem then

$$\int_{-\infty}^{\infty} H_r H_k^* d\omega = 2 \int_{-\infty}^{\infty} F_2(\omega) d\omega = 4\pi i \Sigma Res(F_2(\omega)) \quad (D.8)$$

where

$$\begin{aligned} F_2(\omega) &= Re(H_r H_k^*) \\ &= \frac{(\omega_r^2 - \omega^2)(\omega_k^2 - \omega^2) + 4\xi_r \xi_k \omega_r \omega_k \omega^2}{[(\omega_r^2 - \omega^2)^2 + (2\xi_r \omega_r \omega)^2][(\omega_k^2 - \omega^2)^2 + (2\xi_k \omega_k \omega)^2]} \end{aligned} \quad (D.9)$$



The function  $F_2(\omega)$  has eight poles but only four of them lie in the region of integration. These are

$$\omega_{r1} = (\sqrt{1-\xi_r^2} + i\xi_r)\omega_r \quad (D.10)$$

$$\omega_{r2} = (-\sqrt{1-\xi_r^2} + i\xi_r)\omega_r \quad (D.11)$$

$$\omega_{k1} = (\sqrt{1-\xi_k^2} + i\xi_k)\omega_k \quad (D.12)$$

$$\omega_{k2} = (-\sqrt{1-\xi_k^2} + i\xi_k)\omega_k \quad (D.13)$$

Consideration of the poles associated with mode  $r$  lead to

$$\begin{aligned} Res(\omega_{r1}) &= \lim_{\omega \rightarrow \omega_{r1}} \{(\omega - \omega_{r1})F_2(\omega)\} \\ &= \frac{D_{1r} - iD_{2r}}{K_r(P_{1r} + iP_{2r})} \end{aligned} \quad (D.14)$$

$$\begin{aligned} Res(\omega_{r2}) &= \lim_{\omega \rightarrow \omega_{r2}} \{(\omega - \omega_{r2})F_2(\omega)\} \\ &= \frac{D_{1r} + iD_{2r}}{K_r(P_{1r} - iP_{2r})} \end{aligned} \quad (D.15)$$

the terms  $D_{1r}$ ,  $D_{2r}$ ,  $P_{1r}$ ,  $P_{2r}$  and  $K_r$  are defined at the end of this Appendix.

Therefore

$$Res(\omega_{r1}) + Res(\omega_{r2}) = \frac{2(P_{1r}D_{1r} - P_{2r}D_{2r})}{K_r(P_{1r}^2 + P_{2r}^2)} \quad (D.16)$$

Similarly by interchanging the subscript  $r$  with  $k$  the residues associated with mode  $k$  is obtained as

$$Res(\omega_{k1}) + Res(\omega_{k2}) = \frac{2(P_{1k}D_{1k} - P_{2k}D_{2k})}{K_k(P_{1k}^2 + P_{2k}^2)} \quad (D.17)$$

Application of equations (D.17) and (D.16) in (D.8) and substituting for  $K_r$  and  $K_k$  leads to

$$\int_{-\infty}^{\infty} H_r H_k^* d\omega = \frac{\pi(P_{1r}D_{1r} - P_{2r}D_{2r})}{\xi_r \omega_r^3 \sqrt{1-\xi_r^2}(P_{1r}^2 + P_{2r}^2)} + \frac{\pi(P_{1k}D_{1k} - P_{2k}D_{2k})}{\xi_k \omega_k^3 \sqrt{1-\xi_k^2}(P_{1k}^2 + P_{2k}^2)} \quad (D.18)$$

Equations (D.18) and (D.7) are used implicitly in equation (3.36).

Evaluation of  $\int_{-\infty}^{\infty} \omega^2 H_r H_r^* d\omega = \int_{-\infty}^{\infty} F_3(\omega) d\omega$

where

$$F_3(\omega) = \omega^2 (H_r H_r^*) = \frac{\omega^2}{(\omega_r^2 - \omega^2)^2 + (2\xi_r \omega_r \omega)^2} \quad (D.19)$$

Using the residue theorem then

$$\int_{-\infty}^{\infty} F_3(\omega) d\omega = 2\pi i \sum Res(F_3(\omega)) \quad (D.20)$$

The function  $F_3(\omega)$  has the same poles as  $F_1(\omega)$  and the two poles that are in the region of integration are given in equations (D.3) and (D.4). Therefore

$$\begin{aligned} Res(\omega_{r1}) &= \lim_{\omega \rightarrow \omega_{r1}} \{(\omega - \omega_{r1}) F_3(\omega)\} \\ &= \frac{(\sqrt{1-\xi_r^2} + i\xi_r)^2}{8i\xi_r \omega_r \sqrt{1-\xi_r^2} (\sqrt{1-\xi_r^2} + i\xi_r)} \end{aligned} \quad (D.21)$$

$$\begin{aligned}
Res(\omega_{r2}) &= \lim_{\omega \rightarrow \omega_{r2}} \{(\omega - \omega_{r2})F_3(\omega)\} \\
&= \frac{(\sqrt{1-\xi_r^2} - i\xi_r)^2}{8i\xi_r\omega_r \sqrt{1-\xi_r^2} (\sqrt{1-\xi_r^2} - i\xi_r)}
\end{aligned} \tag{D.22}$$

Application of equations (D.21) and (D.22) in equation (D.20) gives

$$\int_{-\infty}^{\infty} \omega^2 H_r H_r^* d\omega = \frac{\pi}{2\xi_r\omega_r} \tag{D.23}$$

Evaluation of  $\int_{-\infty}^{\infty} \omega^2 H_r H_k^* d\omega$

Using the residue theorem then

$$\int_{-\infty}^{\infty} \omega^2 H_r H_k^* d\omega = 2 \int_{-\infty}^{\infty} F_4(\omega) d\omega = 4\pi i \sum Res(F_4(\omega)) \tag{D.24}$$

where

$$\begin{aligned}
F_4(\omega) &= Re(\omega^2 H_r H_k^*) \\
&= \frac{\omega^2 [(\omega_r^2 - \omega^2)(\omega_k^2 - \omega^2) + 4\xi_r \xi_k \omega_r \omega_k \omega^2]}{[(\omega_r^2 - \omega^2)^2 + (2\xi_r \omega_r \omega)^2][(\omega_k^2 - \omega^2)^2 + (2\xi_k \omega_k \omega)^2]}
\end{aligned} \tag{D.25}$$

The function  $F_4(\omega)$  has the same poles as  $F_2(\omega)$  and the four poles that are in the region of integration are given in equations (D.10), (D.11), (D.12) and (D.13)

Considering the poles associated with mode r lead to

$$\begin{aligned}
Res(\omega_{r1}) &= \lim_{\omega \rightarrow \omega_{r1}} \{(\omega - \omega_{r1})F_4(\omega)\} \\
&= \frac{(\Pi_{1r} + i\Pi_{2r})\omega_r^2}{K_r(P_{1r} + iP_{2r})}
\end{aligned} \tag{D.26}$$

$$\begin{aligned}
Res(\omega_{r2}) &= \lim_{\omega \rightarrow \omega_{r2}} \{(\omega - \omega_{r2})F_4(\omega)\} \\
&= \frac{(\Pi_{1r} - i\Pi_{2r})\omega_r^2}{K_r(P_{1r} - iP_{2r})}
\end{aligned} \tag{D.27}$$

Therefore

$$Res(\omega_{r1}) + Res(\omega_{r2}) = \frac{2(\Pi_{1r}P_{1r} - \Pi_{2r}P_{2r})\omega_r^2}{K_r(P_{1r}^2 + P_{2r}^2)} \tag{D.28}$$

Similarly by interchanging the subscript r with k the residues associated with mode k are

$$Res(\omega_{k1}) + Res(\omega_{k2}) = \frac{2(\Pi_{1k}P_{1k} + \Pi_{2k}P_{2k})\omega_k^2}{K_k(P_{1k}^2 + P_{2k}^2)} \tag{D.29}$$

Application of equations (D.28) and (D.29) in (D.24) and substituting for  $K_r$  and  $K_k$  (see the end of chapter for definition of symbols) gives

$$\int_{-x}^{\infty} \omega^2 H_r H_k^* d\omega = \frac{\pi(\Pi_{1r}P_{1r} + \Pi_{2r}P_{2r})}{\xi_r \omega_r \sqrt{1 - \xi_r^2 (P_{1r}^2 + P_{2r}^2)}} + \frac{\pi(\Pi_{1k}P_{1k} + \Pi_{2k}P_{2k})}{\xi_k \omega_k \sqrt{1 - \xi_k^2 (P_{1k}^2 + P_{2k}^2)}} \tag{D.30}$$

Equations (D.23) and (D.30) are used implicitly in equation (3.37).

## D3. Wheeled Mobile Manipulator

### D3.1 Covariance of Modal Responses

The power spectrum representation of the excitation used is given in equation (6.53) and (6.54). Equation (6.53) can be normalized by the variance of the surface irregularities  $\sigma^2$ . To compute the modal displacement responses the integral of the terms:

$$(a) S_{q_y q_y}(\omega) H_r H_k^* = \frac{\sigma^2 \alpha \dot{q}_x}{\pi(\omega^2 + \alpha^2 \dot{q}_x^2)} H_r H_k^*$$

$$(b) S_{q_y q_y}(\omega) H_r H_k^* = \omega^2 S_{q_y q_y}(\omega) H_r H_k^* = \frac{\sigma^2 \omega^2 \alpha \dot{q}_x}{\pi(\omega^2 + \alpha^2 \dot{q}_x^2)} H_r H_k^*$$

given in equation (5.36) have to be evaluated for modes  $r$  and  $k$  since they appear implicitly in the equation (5.37). Further, for the velocity responses (equation 5.38) the integral of the terms:

$$(c) \omega^2 S_{q_y q_y}(\omega) H_r H_k^*$$

$$(d) \omega^2 S_{\dot{q}_y \dot{q}_y}(\omega) H_r H_k^*$$

have to be evaluated. Since equations (b) and (c) are identical then six integrals (with two associated with each equation) have to be evaluated.

$$\text{Evaluation of } \int_{-\infty}^{\infty} S_{q_y q_y}(\omega) H_r H_k^* d\omega = \int_{-\infty}^{\infty} \frac{\sigma^2 \alpha \dot{q}_x}{\pi(\omega^2 + \alpha^2 \dot{q}_x^2)} H_r H_k^* d\omega = \frac{\sigma^2 \alpha \dot{q}_x}{\pi} \int_{-\infty}^{\infty} F_5(\omega) d\omega$$

where

$$F_5(\omega) = \frac{1}{[(\omega^2 + \alpha^2 \dot{q}_x^2)][(\omega_r^2 - \omega^2)^2 + (2\xi_r \omega_r \omega)^2]} \quad (D.31)$$

Using the residue theorem to evaluate the integral leads to

$$\frac{\sigma^2 \alpha \dot{q}_x}{\pi} \int_{-\infty}^{\infty} F_5(\omega) d\omega = \frac{\sigma^2 \alpha \dot{q}_x}{\pi} 2\pi i \sum \text{Res}(F_5(\omega)) \quad (D.32)$$

The function  $F_5(\omega)$  has 6 poles but only three of them lie in the region of integration. These are

$$\omega_{r1} = (-\sqrt{1-\xi_r^2} + i\xi_r)\omega_r \quad (\text{D.33})$$

$$\omega_{r2} = (\sqrt{1-\xi_r^2} + i\xi_r)\omega_r \quad (\text{D.34})$$

$$\omega_q = i\alpha\dot{q}_x \quad (\text{D.35})$$

$$\begin{aligned} \text{Res}(\omega_{r1}) &= \lim_{\omega \rightarrow \omega_{r1}} \{(\omega - \omega_{r1})F_5(\omega)\} \\ &= \frac{1}{8i\xi_r\omega_r^3 \sqrt{1-\xi_r^2} (T_{1r} - iT_{2r})} \end{aligned} \quad (\text{D.36})$$

$$\begin{aligned} \text{Res}(\omega_{r2}) &= \lim_{\omega \rightarrow \omega_{r2}} \{(\omega - \omega_{r2})F_5(\omega)\} \\ &= \frac{1}{8i\xi_r\omega_r^3 \sqrt{1-\xi_r^2} (T_{1r} + iT_{2r})} \end{aligned} \quad (\text{D.37})$$

$$\text{Res}(\omega_q) = \lim_{\omega \rightarrow \omega_q} \{(\omega - \omega_q)F_5(\omega)\} = \frac{1}{2i\alpha\dot{q}_x U_r} \quad (\text{D.38})$$

$$\begin{aligned} \text{Res}(\omega_{r1}) + \text{Res}(\omega_{r2}) + \text{Res}(\omega_q) &= \frac{T_{1r}}{4i\xi_r\omega_r^3 \sqrt{1-\xi_r^2} (T_{1r}^2 + T_{2r}^2)} + \frac{1}{2i\alpha\dot{q}_x U_r} \\ & \quad (\text{D.39}) \end{aligned}$$

Therefore

$$\int_{-\infty}^{\infty} \frac{\sigma^2 \alpha \dot{q}_x}{\pi(\omega^2 + \alpha^2 \dot{q}_x^2)} H_r H_r^* d\omega = \frac{\sigma^2 \alpha \dot{q}_x T_{1r}}{2\xi_r \omega_r^3 \sqrt{1-\xi_r^2} (T_{1r}^2 + T_{2r}^2)} + \frac{\sigma^2}{U_r} \quad (\text{D.40})$$

$$\text{Evaluation of } \int_{-\infty}^{\infty} S_{q_y q_x}(\omega) H_r H_k^* d\omega = \int_{-\infty}^{\infty} \frac{\sigma^2 \alpha \dot{q}_x}{\pi(\omega^2 + \alpha^2 \dot{q}_x^2)} H_r H_k^* d\omega$$

Using the residue theorem then

$$\int_{-\infty}^{\infty} \frac{\sigma^2 \alpha \dot{q}_x}{\pi(\omega^2 + \alpha^2 \dot{q}_x^2)} H_r H_k^* = \frac{2\sigma^2 \alpha \dot{q}_x}{\pi} \int_{-\infty}^{\infty} F_6(\omega) d\omega = \frac{2\sigma^2 \alpha \dot{q}_x}{\pi} 2\pi i \Sigma \text{Res}(F_6(\omega)) \quad (\text{D.41})$$

where

$$F_6(\omega) = \frac{[(\omega_r^2 - \omega^2)(\omega_k^2 - \omega^2) + 4\xi_r \xi_k \omega_r \omega \omega^2]}{(\omega^2 + \alpha^2 \dot{q}_x^2)[(\omega_r^2 - \omega^2)^2 + (2\xi_r \omega_r \omega)^2][(\omega_k^2 - \omega^2)^2 + (2\xi_k \omega_k \omega)^2]} \quad (\text{D.42})$$

The function  $F_6(\omega)$  has ten poles but only five of them lie in the region of integration. These are

$$\omega_{r1} = (\sqrt{1 - \xi_r^2} + i\xi_r)\omega_r \quad (\text{D.43})$$

$$\omega_{r2} = (-\sqrt{1 - \xi_r^2} + i\xi_r)\omega_r \quad (\text{D.44})$$

$$\omega_q = i\alpha \dot{q}_x \quad (\text{D.45})$$

$$\omega_{k1} = (\sqrt{1 - \xi_k^2} + i\xi_k)\omega_k \quad (\text{D.46})$$

$$\omega_{k2} = (-\sqrt{1 - \xi_k^2} + i\xi_k)\omega_k \quad (\text{D.47})$$

$$\text{Res}(\omega_{r1}) = \lim_{\omega \rightarrow \omega_{r1}} \{(\omega - \omega_{r1})F_6(\omega)\}$$

$$= \frac{D_{1r} - iD_{2r}}{K_r(W_{1r} + iW_{2r})} \quad (\text{D.48})$$

$$\begin{aligned}
Res(\omega_{r2}) &= \lim_{\omega \rightarrow \omega_{r2}} \{(\omega - \omega_{r2})F_6(\omega)\} \\
&= \frac{D_{1r} + iD_{2r}}{K_r(W_{1r} - iW_{2r})}
\end{aligned} \tag{D.49}$$

$$Res(\omega_{r1}) + Res(\omega_{r2}) = \frac{2(W_{1r}D_{1r} - W_{2r}D_{2r})}{K_r(W_{1r}^2 + W_{2r}^2)} \tag{D.50}$$

Similarly the residues associated with mode k are

$$Res(\omega_{k1}) + Res(\omega_{k2}) = \frac{2(W_{1k}D_{1k} - W_{2k}D_{2k})}{K_k(W_{1k}^2 + W_{2k}^2)} \tag{D.51}$$

And the residues associated  $\omega_q$  is

$$\begin{aligned}
Res(\omega_q) &= \lim_{\omega \rightarrow \omega_q} \{(\omega - \omega_q)F_6(\omega)\} \\
&= \frac{Y_{rk}}{2i\alpha\dot{q}_x U_r U_k}
\end{aligned} \tag{D.52}$$

Therefore

$$\begin{aligned}
&\int_{-\infty}^{\infty} \frac{\sigma^2 \alpha \dot{q}_x}{\pi(\omega^2 + \alpha^2 \dot{q}_x^2)} H_r H_k^* \\
&= \sigma^2 \alpha \dot{q}_x \left[ \frac{D_{1r} W_{1r} + D_{2r} W_{2r}}{\xi_r \omega_r^3 \sqrt{1 - \xi_r^2 (W_{1r}^2 + W_{2r}^2)}} + \frac{D_{1k} W_{1k} + D_{2k} W_{2k}}{\xi_k \omega_k^3 \sqrt{1 - \xi_k^2 (W_{1k}^2 + W_{2k}^2)}} + \frac{2Y_{rk}}{\alpha \dot{q}_x U_r U_k} \right]
\end{aligned} \tag{D.53}$$

Evaluation of  $\int_{-\infty}^{\infty} \omega^2 S_{q_y q_y}(\omega) H_r H_r^* d\omega = \int_{-\infty}^{\infty} \frac{\sigma^2 \alpha \dot{q}_x}{\pi(\omega^2 + \alpha^2 \dot{q}_x^2)} \omega^2 H_r H_r^* d\omega = \frac{\sigma^2 \alpha \dot{q}_x}{\pi} \int_{-\infty}^{\infty} F_7(\omega) d\omega$

where



$$F_7(\omega) = \frac{\omega^2}{[(\omega^2 + \alpha^2 \dot{q}_x^2)][(\omega_r^2 - \omega^2)^2 + (2\xi_r \omega_r \omega)^2]} \quad (D.54)$$

Using the residue theorem then

$$\frac{\sigma^2 \alpha \dot{q}_x}{\pi} \int_{-\infty}^{\infty} F_7(\omega) d\omega = \frac{\sigma^2 \alpha \dot{q}_x}{\pi} 2\pi i \Sigma \text{Res}(F_7(\omega)) \quad (D.55)$$

The function  $F_7(\omega)$  has the same poles as  $F_5(\omega)$ . Using the poles specified in equations (D.33), (D.34), (D.35) lead to

$$\begin{aligned} \sqrt{1 - \xi_k^2} + i\xi_k \omega_k \text{Res}(\omega_{r1}) &= \lim_{\omega \rightarrow \omega_{r1}} \{(\omega - \omega_{r1}) F_7(\omega)\} \\ \sqrt{1 - \xi_k^2} + i\xi_k \omega_k &= \frac{\lambda_{1r} - i\lambda_{2r}}{8i\xi_r \omega_r^3 \sqrt{1 - \xi_r^2} (T_{1r} - iT_{2r})} \end{aligned} \quad (D.56)$$

$$\begin{aligned} \text{Res}(\omega_{r2}) &= \lim_{\omega \rightarrow \omega_{r2}} \{(\omega - \omega_{r2}) F_7(\omega)\} \\ &= \frac{\lambda_{1r} + i\lambda_{2r}}{8i\xi_r \omega_r^3 \sqrt{1 - \xi_r^2} (T_{1r} + iT_{2r})} \end{aligned} \quad (D.57)$$

$$\text{Res}(\omega_q) = \lim_{\omega \rightarrow \omega_q} \{(\omega - \omega_q) F_7(\omega)\} = -\frac{\alpha \dot{q}_x}{2iU_r} \quad (D.58)$$

$$\text{Res}(\omega_{r1}) + \text{Res}(\omega_{r2}) + \text{Res}(\omega_q) = \frac{\lambda_{1r} T_{1r} + \lambda_{2r} T_{2r}}{4i\xi_r \omega_r^3 \sqrt{1 - \xi_r^2} (T_{1r}^2 + T_{2r}^2)} - \frac{\alpha \dot{q}_x}{2U_r} \quad (D.59)$$

Therefore

$$\int_{-\infty}^{\infty} \omega^2 S_{q_y q_y}(\omega) H_r H_r^* d\omega = \sigma^2 \alpha \dot{q}_x \left[ \frac{\lambda_{1r} T_{1r} + \lambda_{2r} T_{2r}}{2\xi_r \omega_r^3 \sqrt{1 - \xi_r^2} (T_{1r}^2 + T_{2r}^2)} - \frac{\alpha \dot{q}_x}{U_r} \right] \quad (D.60)$$

$$\text{Evaluation of } \int_{-\infty}^{\infty} \omega^2 S_{q_y, q_y}(\omega) H_r H_k^* d\omega = \int_{-\infty}^{\infty} \frac{\sigma^2 \alpha \dot{q}_x}{\pi(\omega^2 + \alpha^2 \dot{q}_x^2)} \omega^2 H_r H_k^* d\omega = \frac{\sigma^2 \alpha \dot{q}_x}{\pi} \int_{-\infty}^{\infty} F_8(\omega) d\omega$$

where

$$F_8(\omega) = \frac{\omega^2 [(\omega_r^2 - \omega^2)(\omega_k^2 - \omega^2) + 4\zeta_r \zeta_k \omega_k \omega^2]}{(\omega^2 + \alpha^2 \dot{q}_x^2) [(\omega_r^2 - \omega^2)^2 + (2\zeta_r \omega_r \omega)^2] [(\omega_k^2 - \omega^2)^2 + (2\zeta_k \omega_k \omega)^2]} \quad (D.61)$$

Using the residue theorem leads to

$$\frac{2\sigma^2 \alpha \dot{q}_x}{\pi} \int_{-\infty}^{\infty} F_8(\omega) d\omega = \frac{2\sigma^2 \alpha \dot{q}_x}{\pi} 2\pi i \sum \text{Res}(F_8(\omega)) \quad (D.62)$$

The function  $F_8(\omega)$  has the same poles as  $F_6(\omega)$ . Using the poles given in equations (D.43), (D.44), (D.45), (D.46) and (D.47) lead to

$$\begin{aligned} \text{Res}(\omega_{r1}) &= \lim_{\omega \rightarrow \omega_{r1}} \{(\omega - \omega_{r1}) F_8(\omega)\} \\ &= \frac{Q_{1r} + iQ_{2r}}{K_r(W_{1r} + iW_{2r})} \end{aligned} \quad (D.63)$$

$$\begin{aligned} \text{Res}(\omega_{r2}) &= \lim_{\omega \rightarrow \omega_{r2}} \{(\omega - \omega_{r2}) F_8(\omega)\} \\ &= \frac{Q_{1r} - iQ_{2r}}{K_r(W_{1r} - iW_{2r})} \end{aligned} \quad (D.64)$$

$$\text{Res}(\omega_{r1}) + \text{Res}(\omega_{r2}) = \frac{2(W_{1r}Q_{1r} + W_{2r}Q_{2r})}{K_r(W_{1r}^2 + W_{2r}^2)} \quad (D.65)$$

Similarly by interchanging the subscript r and k we have

$$Res(\omega_{k1}) + Res(\omega_{k2}) = \frac{2(W_{1k}Q_{1k} + W_{2k}Q_{2k})}{K_k(W_{1k}^2 + W_{2k}^2)} \quad (D.66)$$

$$Res(\omega_q) = \lim_{\omega \rightarrow \omega_q} \{(\omega - \omega_q)F_8(\omega)\} = -\frac{Y_{rk}\alpha\dot{q}_x}{2iU_r U_k} \quad (D.67)$$

Therefore

$$\begin{aligned} & \int_{-\infty}^{\infty} \omega^2 S_{q_y q_y}(\omega) H_r H_k^* d\omega \\ &= \sigma^2 \alpha \dot{q}_x \left[ \frac{Q_{1r} W_{1r} + Q_{2r} W_{2r}}{\xi_r \omega_r^3 \sqrt{1 - \xi_r^2 (W_{1r}^2 + W_{2r}^2)}} + \frac{Q_{1k} W_{1k} + Q_{2k} W_{2k}}{\xi_k \omega_k^3 \sqrt{1 - \xi_k^2 (W_{1k}^2 + W_{2k}^2)}} - \frac{2\alpha \dot{q}_x Y_{rk}}{U_r U_k} \right] \end{aligned} \quad (D.68)$$

Equations (D.68), (D.60), (D.53) and (D.40) are used implicitly in equation (5.37).

$$\text{Evaluation of } \int_{-\infty}^{\infty} \omega^2 S_{q_y q_y}(\omega) H_r H_r^* d\omega = \int_{-\infty}^{\infty} \frac{\sigma^2 \alpha \dot{q}_x}{\pi(\omega^2 + \alpha^2 \dot{q}_x^2)} \omega^4 H_r H_r^* d\omega = \frac{\sigma^2 \alpha \dot{q}_x}{\pi} \int_{-\infty}^{\infty} F_9(\omega) d\omega$$

where

$$F_9(\omega) = \frac{\omega^4}{[(\omega^2 + \alpha^2 \dot{q}_x^2)][(\omega_r^2 - \omega^2)^2 + (2\xi_r \omega_r \omega)^2]} \quad (D.69)$$

Using the residue theorem then

$$\frac{\sigma^2 \alpha \dot{q}_x}{\pi} \int_{-\infty}^{\infty} F_9(\omega) d\omega = \frac{\sigma^2 \alpha \dot{q}_x}{\pi} 2\pi i \Sigma Res(F_9(\omega)) \quad (D.70)$$

The function  $F_9(\omega)$  has the same poles as  $F_7(\omega)$ . Using the poles specified in equations (D.33), (D.34), (D.35) lead to

$$\begin{aligned}
Res(\omega_{r1}) &= \lim_{\omega \rightarrow \omega_{r1}} \{(\omega - \omega_{r1})F_9(\omega)\} \\
&= \frac{E_{1r} - iE_{2r}}{8i\xi_r \omega_r^3 \sqrt{1 - \xi_r^2} (T_{1r} - iT_{2r})} \quad (D.71)
\end{aligned}$$

$$\begin{aligned}
Res(\omega_{r2}) &= \lim_{\omega \rightarrow \omega_{r2}} \{(\omega - \omega_{r2})F_9(\omega)\} \\
&= \frac{E_{1r} + iE_{2r}}{8i\xi_r \omega_r^3 \sqrt{1 - \xi_r^2} (T_{1r} + iT_{2r})} \quad (D.72)
\end{aligned}$$

$$Res(\omega_q) = \lim_{\omega \rightarrow \omega_q} \{(\omega - \omega_q)F_9(\omega)\} = \frac{\alpha^3 \dot{q}_x^3}{2iU_r} \quad (D.73)$$

$$Res(\omega_{r1}) + Res(\omega_{r2}) + Res(\omega_q) = \frac{E_{1r}T_{1r} + E_{2r}T_{2r}}{4i\xi_r \omega_r^3 \sqrt{1 - \xi_r^2} (T_{1r}^2 + T_{2r}^2)} - \frac{\alpha \dot{q}_x}{2U_r} \quad (D.74)$$

Therefore

$$\int_{-\infty}^{\infty} \omega^2 S_{\dot{q}_y \dot{q}_y}(\omega) H_r H_r^* d\omega = \sigma^2 \alpha \dot{q}_x \left[ \frac{E_{1r}T_{1r} + E_{2r}T_{2r}}{2\xi_r \omega_r^3 \sqrt{1 - \xi_r^2} (T_{1r}^2 + T_{2r}^2)} + \frac{\alpha^3 \dot{q}_x^3}{U_r} \right] \quad (D.75)$$

Evaluation of  $\int_{-\infty}^{\infty} \omega^2 S_{\dot{q}_y \dot{q}_y}(\omega) H_r H_k^* d\omega = \int_{-\infty}^{\infty} \frac{\sigma^2 \alpha \dot{q}_x}{\pi(\omega^2 + \alpha^2 \dot{q}_x^2)} \omega^4 H_r H_k^* d\omega = \frac{\sigma^2 \alpha \dot{q}_x}{\pi} \int_{-\infty}^{\infty} F_{10}(\omega) d\omega$

where

$$F_{10}(\omega) = \frac{\omega^4 [(\omega_r^2 - \omega^2)(\omega_k^2 - \omega^2) + 4\xi_r \xi_k \omega_k \omega_r \omega^2]}{(\omega^2 + \alpha^2 \dot{q}_x^2) [(\omega_r^2 - \omega^2)^2 + (2\xi_r \omega_r \omega)^2] [(\omega_k^2 - \omega^2)^2 + (2\xi_k \omega_k \omega)^2]} \quad (D.76)$$

Using the residue theorem then

$$\frac{2\sigma^2\alpha\dot{q}_x}{\pi} \int_{-x}^x F_{10}(\omega) d\omega = \frac{2\sigma^2\alpha\dot{q}_x}{\pi} 2\pi i \Sigma Res(F_{10}(\omega)) \quad (D.77)$$

The function  $F_{10}(\omega)$  has the same poles as  $F_g(\omega)$ . Using the poles given in equations (D.43), (D.44), (D.45), (D.46) and (D.47) leads to

$$\begin{aligned} Res(\omega_{r1}) &= \lim_{\omega \rightarrow \omega_{r1}} \{(\omega - \omega_{r1})F_{10}(\omega)\} \\ &= \frac{V_{1r} + iV_{2r}}{K_r(W_{1r} + iW_{2r})} \end{aligned} \quad (D.78)$$

$$\begin{aligned} Res(\omega_{r2}) &= \lim_{\omega \rightarrow \omega_{r2}} \{(\omega - \omega_{r2})F_{10}(\omega)\} \\ &= \frac{V_{1r} - iV_{2r}}{K_r(W_{1r} - iW_{2r})} \end{aligned} \quad (D.79)$$

$$Res(\omega_{r1}) + Res(\omega_{r2}) = \frac{2(W_{1r}V_{1r} + W_{2r}V_{2r})}{K_r(W_{1r}^2 + W_{2r}^2)} \quad (D.80)$$

Similarly by interchanging the subscript r and k we have

$$Res(\omega_{k1}) + Res(\omega_{k2}) = \frac{2(W_{1k}V_{1k} + W_{2k}V_{2k})}{K_k(W_{1k}^2 + W_{2k}^2)} \quad (D.81)$$

$$Res(\omega_q) = \lim_{\omega \rightarrow \omega_q} \{(\omega - \omega_q)F_{10}(\omega)\} = \frac{Y_{rk}\alpha^3\dot{q}_x^3}{2iU_rU_k} \quad (D.82)$$

Therefore

$$\int_{-x}^x \omega^2 S_{q_y, q_y}(\omega) H_r H_k^* d\omega =$$

$$= \sigma^2 \alpha \dot{q}_x \left[ \frac{V_{1r} W_{1r} + V_{2r} W_{2r}}{\xi_r \omega_r^3 \sqrt{1 - \xi_r^2 (W_{1r}^2 + W_{2r}^2)}} + \frac{V_{1k} W_{1k} + V_{2k} W_{2k}}{\xi_k \omega_s^3 \sqrt{1 - \xi_k^2 (W_{1k}^2 + W_{2k}^2)}} + \frac{2\alpha^3 \dot{q}_x^3 Y_{rk}}{U_r U_k} \right] \quad (D.83)$$

Equations (D.68), (D.60), (D.84) and (D.73) are used implicitly in equation (5.38).

#### D4. Definitions of Symbols Used Appendix D.

$$D_{1r} = 2(\xi_r \omega_r)^2 (\omega_k^2 - \omega_r^2 + 2\xi_r^2 \omega_r^2) - (2\xi_r \omega_r^2 \sqrt{1 - \xi_r^2})^2 + 4\xi_r \xi_k \omega_r^3 \omega_k (1 - 2\xi_r^2) \quad (D.84)$$

$$D_{2r} = 2\xi_r \omega_r^2 \sqrt{1 - \xi_r^2} (\omega_k^2 - \omega_r^2 + 2\xi_r^2 \omega_r^2) + 4(\xi_r \omega_r)^2 \xi_r \omega_r^2 \sqrt{1 - \xi_r^2} - 8\xi_r^2 \xi_k \omega_r^3 \omega_k \sqrt{1 - \xi_r^2} \quad (D.85)$$

$$E_{1r} = (1 - 8\xi_r^2 + 8\xi_r^4) \omega_r^4 \quad (D.86)$$

$$E_{2r} = 4\omega_r^4 \xi_r \sqrt{1 - \xi_r^2} (1 - 2\xi_r^2) \quad (D.87)$$

$$K_r = 8i \xi_r \omega_r^3 \sqrt{1 - \xi_r^2} \quad (D.88)$$

$$P_{1r} = \sqrt{1 - \xi_r^2} [(\omega_k^2 - \omega_r^2 + 2\xi_r^2 \omega_r^2) \omega_k^2 - \omega_r^2 + 2\xi_r^2 \omega_r^2 - (2\xi_r \omega_r^2 \sqrt{1 - \xi_r^2})^2 + 4\xi_k^2 \omega_r^2 \omega_k^2 (1 - 2\xi_r^2)] - 8\xi_r^2 \xi_k \omega_r^2 \omega_k^2 \sqrt{1 - \xi_r^2} - 4(\xi_r^2 \omega_r^2 \sqrt{1 - \xi_r^2}) (\omega_k^2 - \omega_r^2 + 2\xi_r^2 \omega_r^2) \quad (D.89)$$

$$P_{2r} = \sqrt{1 - \xi_r^2} [8\xi_r \xi_k \omega_r^2 \omega_k^2 \sqrt{1 - \xi_r^2} - 4(\xi_r \omega_r^2 \sqrt{1 - \xi_r^2}) (\omega_k^2 - \omega_r^2 + 2\xi_r^2 \omega_r^2)]$$

$$+ \xi_r [(\omega_k^2 - \omega_r^2 + 2\xi_r^2 \omega_r^2) \omega_k^2 - \omega_r^2 + 2\xi_r^2 \omega_r^2 - (2\xi_r \omega_r^2 \sqrt{1-\xi_r^2})^2 + 4\xi_k^2 \omega_r^2 \omega_k^2 (1-2\xi_r^2)] \quad (\text{D.90})$$

$$Q_{1r} = [\omega_r^2 - 2\omega_r^2 \xi_r][2(\xi_r \omega_r)^2 (\omega_k^2 - \omega_r^2 + 2\xi_r^2 \omega_r^2) - (2\xi_r \omega_r^2 \sqrt{1-\xi_r^2})^2 + 4\xi_r \xi_k \omega_r^3 \omega_k (1-2\xi_r^2)] + [2\xi_r \omega_r^2 \sqrt{1-\xi_r^2}][2\xi_r \omega_r^2 \sqrt{1-\xi_r^2} (\omega_k^2 - \omega_r^2 + 2\xi_r^2 \omega_r^2) - 4(\xi_r \omega_r)^2 \xi_r \omega_r^2 \sqrt{1-\xi_r^2} - 8\xi_r^2 \xi_k \omega_r^3 \omega_k \sqrt{1-\xi_r^2}] \quad (\text{D.91})$$

$$Q_{2r} = [2\xi_r \omega_r^2 \sqrt{1-\xi_r^2}][2(\xi_r \omega_r)^2 (\omega_k^2 - \omega_r^2 + 2\xi_r^2 \omega_r^2) - (2\xi_r \omega_r^2 \sqrt{1-\xi_r^2})^2 + 4\xi_r \xi_k \omega_r^3 \omega_k (1-2\xi_r^2)] - [\omega_r^2 - 2\omega_r^2 \xi_r][2\xi_r \omega_r^2 \sqrt{1-\xi_r^2} (\omega_k^2 - \omega_r^2 + 2\xi_r^2 \omega_r^2) + 4(\xi_r \omega_r)^2 \xi_r \omega_r^2 \sqrt{1-\xi_r^2} - 8\xi_r^2 \xi_k \omega_r^3 \omega_k \sqrt{1-\xi_r^2}] \quad (\text{D.92})$$

$$T_{1r} = (\omega_r^2 - 2\xi_r \omega_r^2 + \alpha^2 \dot{q}_x^2) \sqrt{1-\xi_r^2} - 2\omega_r^2 \xi_r^2 \sqrt{1-\xi_r^2} \quad (\text{D.93})$$

$$T_{2r} = (2\omega_r^2 \xi_r \sqrt{1-\xi_r^2}) \sqrt{1-\xi_r^2} + (\omega_r^2 - 2\xi_r \omega_r^2 + \alpha^2 \dot{q}_x^2) \xi_r \quad (\text{D.94})$$

$$U_r = (\omega_r^2 + \alpha^2 \dot{q}_x^2)^2 - (2\xi_r \alpha \dot{q}_x \omega_r)^2 \quad (\text{D.95})$$

$$V_{1r} = [(1 - 8\xi_r^2 + 8\xi_r^4) \omega_r^4][2(\xi_r \omega_r)^2 (\omega_k^2 - \omega_r^2 + 2\xi_r^2 \omega_r^2) - (2\xi_r \omega_r^2 \sqrt{1-\xi_r^2})^2 + 4\xi_r \xi_k \omega_r^3 \omega_k (1-2\xi_r^2)] + [4\omega_r^4 \xi_r \sqrt{1-\xi_r^2} (1-2\xi_r^2)][2\xi_r \omega_r^2 \sqrt{1-\xi_r^2} (\omega_k^2 - \omega_r^2 + 2\xi_r^2 \omega_r^2) + 2\xi_r^2 \omega_r^2 + 4(\xi_r \omega_r)^2 \xi_r \omega_r^2 \sqrt{1-\xi_r^2} - 8\xi_r^2 \xi_k \omega_r^3 \omega_k \sqrt{1-\xi_r^2}] \quad (\text{D.96})$$

$$V_{2r} = [4\omega_r^4 \xi_r \sqrt{1-\xi_r^2} (1-2\xi_r^2)][2(\xi_r \omega_r)^2 (\omega_k^2 - \omega_r^2 + 2\xi_r^2 \omega_r^2) - (2\xi_r \omega_r^2 \sqrt{1-\xi_r^2})^2 + 4\xi_r \xi_k \omega_r^3 \omega_k (1-2\xi_r^2)] - (1 - 8\xi_r^2 + 8\xi_r^4) \omega_r^4 [2\xi_r \omega_r^2 \sqrt{1-\xi_r^2} (\omega_k^2 - \omega_r^2 + 2\xi_r^2 \omega_r^2) + 4(\xi_r \omega_r)^2 \xi_r \omega_r^2 \sqrt{1-\xi_r^2} - 8\xi_r^2 \xi_k \omega_r^3 \omega_k \sqrt{1-\xi_r^2}] \quad (\text{D.97})$$

$$\begin{aligned}
W_{1r} = & (\omega_r^2 - 2\xi_r\omega_r^2 + \alpha^2 \dot{q}_x^2) [\sqrt{1-\xi_r^2} [(\omega_k^2 - \omega_r^2 + 2\xi_r^2\omega_r^2)\omega_k^2 - \omega_r^2 + 2\xi_r^2\omega_r^2 - \\
& (2\xi_r\omega_r^2\sqrt{1-\xi_r^2})^2 + 4\xi_k^2\omega_r^2\omega_k^2(1-2\xi_r^2)] - 8\xi_r^2\xi_k^2\omega_r^2\omega_k^2\sqrt{1-\xi_r^2} - 4(\xi_r^2\omega_r^2\sqrt{1-\xi_r^2} \\
& )(\omega_k^2 - \omega_r^2 + 2\xi_r^2\omega_r^2)] - (2\omega_r^2\xi_r\sqrt{1-\xi_r^2}) [\sqrt{1-\xi_r^2} [8\xi_r\xi_k^2\omega_r^2\omega_k^2\sqrt{1-\xi_r^2} - \\
& 4(\xi_r\omega_r^2\sqrt{1-\xi_r^2})(\omega_k^2 - \omega_r^2 + 2\xi_r^2\omega_r^2)] + \xi_r [(\omega_k^2 - \omega_r^2 + 2\xi_r^2\omega_r^2)\omega_k^2 - \omega_r^2 + \\
& 2\xi_r^2\omega_r^2 - (2\xi_r\omega_r^2\sqrt{1-\xi_r^2})^2 + 4\xi_k^2\omega_r^2\omega_k^2(1-2\xi_r^2)]] \quad (D.98)
\end{aligned}$$

$$\begin{aligned}
W_{2r} = & (2\omega_r^2\xi_r\sqrt{1-\xi_r^2}) [\sqrt{1-\xi_r^2} [(\omega_k^2 - \omega_r^2 + 2\xi_r^2\omega_r^2)\omega_k^2 - \omega_r^2 + 2\xi_r^2\omega_r^2 - (2\xi_r\omega_r^2 \\
& \sqrt{1-\xi_r^2})^2 + 4\xi_k^2\omega_r^2\omega_k^2(1-2\xi_r^2)] - 8\xi_r^2\xi_k^2\omega_r^2\omega_k^2\sqrt{1-\xi_r^2} - 4(\xi_r^2\omega_r^2\sqrt{1-\xi_r^2})(\omega_k^2 \\
& - \omega_r^2 + 2\xi_r^2\omega_r^2)] + (\omega_r^2 - 2\xi_r\omega_r^2 + \alpha^2 \dot{q}_x^2) [\sqrt{1-\xi_r^2} [8\xi_r\xi_k^2\omega_r^2\omega_k^2\sqrt{1-\xi_r^2} - \\
& 4(\xi_r\omega_r^2\sqrt{1-\xi_r^2})(\omega_k^2 - \omega_r^2 + 2\xi_r^2\omega_r^2)] + \xi_r [(\omega_k^2 - \omega_r^2 + 2\xi_r^2\omega_r^2)\omega_k^2 - \omega_r^2 + \\
& 2\xi_r^2\omega_r^2 - (2\xi_r\omega_r^2\sqrt{1-\xi_r^2})^2 + 4\xi_k^2\omega_r^2\omega_k^2(1-2\xi_r^2)]] \quad (D.99)
\end{aligned}$$

$$Y_{rk} = (\omega_k^2 - \alpha^2 \dot{q}_x^2)(\omega_r^2 - \alpha^2 \dot{q}_x^2) - 4\xi_k\xi_r\omega_r\omega_k\alpha^2\dot{q}_x^2 \quad (D.100)$$

$$\lambda_{1r} = \omega_r^2 - 2\omega_r^2\xi_r \quad (D.101)$$

$$\lambda_{2r} = 2\xi_r\omega_r^2\sqrt{1-\xi_r^2} \quad (D.102)$$

$$\begin{aligned}
\Pi_{1r} = & (1-2\xi_r)[2(\xi_r\omega_r)^2(\omega_k^2 - \omega_r^2 + 2\xi_r^2\omega_r^2) - (2\xi_r\omega_r^2\sqrt{1-\xi_r^2})^2 + 4\xi_r\xi_k\omega_r^3\omega_k(1-2\xi_r^2)] \\
& + (2\xi_r\sqrt{1-\xi_r^2})[2\xi_r\omega_r^2\sqrt{1-\xi_r^2}(\omega_k^2 - \omega_r^2 + 2\xi_r^2\omega_r^2) + 4(\xi_r\omega_r)^2\xi_r\omega_r^2\sqrt{1-\xi_r^2} \\
& - 8\xi_r^2\xi_k\omega_r^3\omega_k\sqrt{1-\xi_r^2}] \quad (D.103)
\end{aligned}$$



$$\begin{aligned}
\Pi_{2r} = & (2\xi_r \sqrt{1-\xi_r^2}) [2(\xi_r \omega_r)^2 (\omega_k^2 - \omega_r^2 + 2\xi_r^2 \omega_r^2) - (2\xi_r \omega_r^2 \sqrt{1-\xi_r^2})^2 + 4\xi_r \xi_k \omega_r^3 \omega_k \\
& (1-2\xi_r^2)] - (1-2\xi_r) [2\xi_r \omega_r^2 \sqrt{1-\xi_r^2} (\omega_k^2 - \omega_r^2 + 2\xi_r^2 \omega_r^2) + 4(\xi_r \omega_r)^2 \xi_r \omega_r^2 \\
& \sqrt{1-\xi_r^2} - 8\xi_r^2 \xi_k \omega_r^3 \omega_k \sqrt{1-\xi_r^2}] \quad (D.104)
\end{aligned}$$

## Appendix E

### SPECIAL INTEGRALS USED FOR THE NONSTATIONARY RESPONSE

The following integrals apply to section 3.4.2. Specifically the integrals are applicable to the modulating functions of equation (4.5). The integrals are obtained using Beyer (1987).

$$\int e^{at} \sin(bt) \cos(ct) dt = \frac{e^{at} [a \sin((b-c)t) - (b-c) \cos((b-c)t)]}{2[a^2 + (b-c)^2]} + \frac{e^{at} [a \sin((b+c)t) - (b+c) \cos((b+c)t)]}{2[a^2 + (b+c)^2]} \quad (\text{E.1})$$

$$\int e^{at} \sin(bt) \sin(ct) dt = \frac{e^{at} [(b-c) \sin((b-c)t) + a \cos((b-c)t)]}{2[a^2 + (b-c)^2]} - \frac{e^{at} [(b+c) \sin((b+c)t) + a \cos((b+c)t)]}{2[a^2 + (b+c)^2]} \quad (\text{E.2})$$

$$\int e^{at} \cos(bt) \cos(ct) dt = \frac{e^{at} [(b-c) \sin((b-c)t) + a \cos((b-c)t)]}{2[a^2 + (b-c)^2]} + \frac{e^{at} [(b+c) \sin((b+c)t) + a \cos((b+c)t)]}{2[a^2 + (b+c)^2]} \quad (\text{E.3})$$

where  $a$ ,  $b$  and  $c$  are some constants and in particular  $c$  is associated with the damped natural frequency of the modes  $\omega_d$  while,  $a$  and  $b$  are associated with the  $\omega_d$  of the mode and the parameters  $\alpha_1$ ,  $\alpha_2$  of the excitation.

## Appendix F

### SOME PROPERTIES OF THE DIRAC DELTA FUNCTION

#### F1. The Delta Function Under a Change of Variable

The delta function is usually considered as the derivative of the unit step function i.e.

$$\delta(t) = \frac{d}{dt} u(t) = \begin{cases} +\infty & t = 0 \\ 0 & \text{elsewhere} \end{cases} \quad (\text{F.1})$$

In the more general case for  $\delta(f)$  where  $f = f(t)$ , one may write by the product rule of differentiation

$$\delta(f) = \frac{d}{df} u(f) = \frac{d}{dt} u(f(t)) \frac{dt}{df} = \frac{\frac{d}{dt} u(f(t))}{\frac{df}{dt}} \quad (\text{F.2})$$

Now, if  $f(t)$  has simple zeros at  $t = t_i$  and making use of the equivalence that

$$\begin{aligned} u(f(t)) &= u(t - t_i); & f \text{ monotonically increasing} \\ &= u(t_i - t); & f \text{ monotonically decreasing} \end{aligned} \quad (\text{F.3})$$

gives

$$\begin{aligned} \frac{d}{dt} u(f(t)) &= \frac{d}{dt} u(t - t_i) = \delta(t - t_i) && \text{f monotonically increasing} \\ \text{or} &&& \\ \frac{d}{dt} u(f(t)) &= \frac{d}{dt} u(t - t_i) = \delta(t_i - t) && \text{f monotonically decreasing} \end{aligned} \quad (\text{F.4})$$

but, since  $\delta$  is regarded as an even function then

$$\delta(t - t_i) = \delta(t_i - t) \quad (\text{F.5})$$

Using equation (F.4) in (F.1) yields

$$\delta(f(t)) = \frac{\delta(t - t_i)}{|f'(t_i)|} \quad (\text{F.6})$$

The derivative in the denominator is associated with  $f_i$  since when the expression in equation (F.6) is multiplied by a testing function,  $r(t)$ , say, and integrated over an appropriate range i.e. if  $a < t_i < b$  one may write

$$\int_a^b r(t) \delta(f(t)) dt = \int_a^b r(t) \frac{\delta(t - t_i)}{|f'(t_i)|} dt = \frac{r(t_i)}{|f'(t_i)|} \quad (\text{F.7})$$

## F2. The Delta Function Occurring at the Limit of Integration

As stated before the delta function is an even function having the property

$$\int_a^b r(t)\delta(t - t_i)dt = r(t_i); \quad a < t_i < b$$

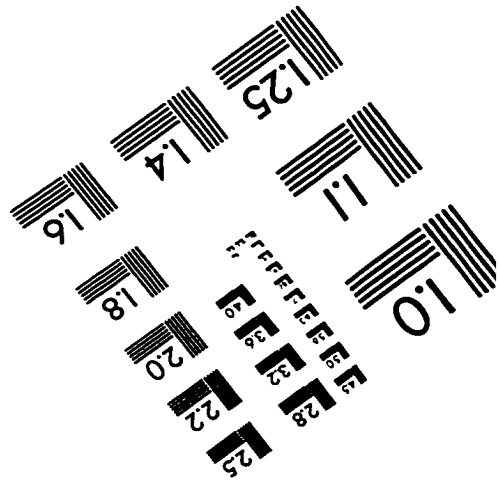
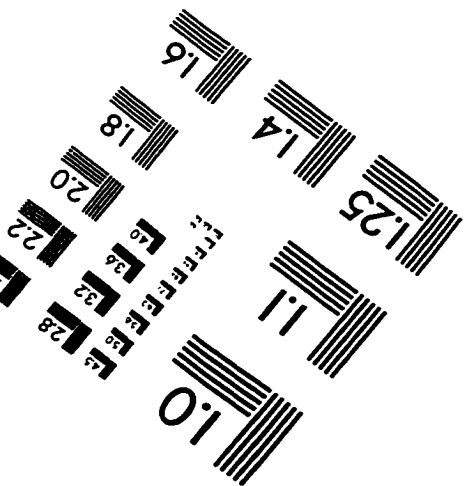
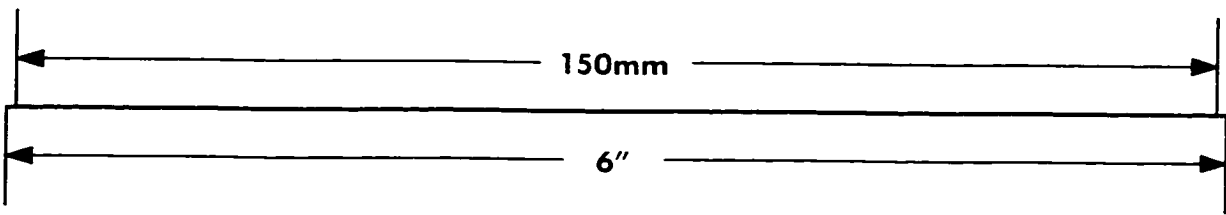
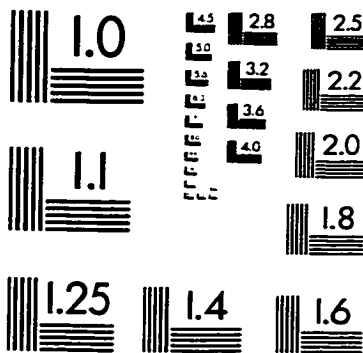
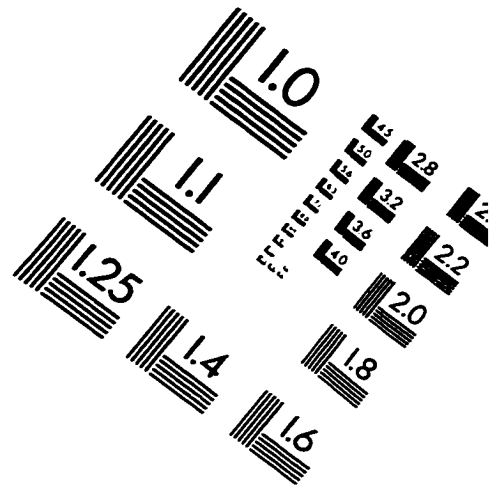
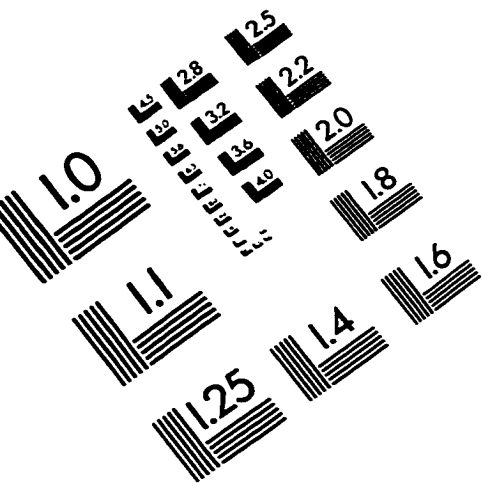
$$=0 \quad \text{otherwise}$$
(F.8)

Therefore if the zero of the argument of the delta function lies either at a or b, half of the contribution of the integrand will be lost due to this even property i.e.

$$\int_a^b r(t)\delta(t - t_i)dt = \frac{1}{2}r(a)$$
(F.9)

This is a common definition and it is employed in this thesis. (see for example Gopal, (1989)).

# IMAGE EVALUATION TEST TARGET (QA-3)



**APPLIED IMAGE, Inc**  
 1653 East Main Street  
 Rochester, NY 14609 USA  
 Phone: 716/482-0300  
 Fax: 716/288-5989

© 1993, Applied Image, Inc., All Rights Reserved